THE DISSERTATION COMMITTEE FOR SHIH-FAN JANG CERTIFIES THAT THIS IS THE APPROVED VERSION OF THE FOLLOWING DISSERTATION:

DEVELOPMENT OF A LOWER INTESTINE TARGETING MUCOADHESIVE PLATFORM OF ORAL DRUG DELIVERY

Committee:

Robert O. Williams, III Supervisor

Jason T. McConville, Co-Supervisor

James W. McGinity

Alan B. Combs

Laura J. Suggs

DEVELOPMENT OF A LOWER INTESTINE TARGETING MUCOADHESIVE PLATFORM OF ORAL DRUG DELIVERY

by

SHIH-FAN JANG, B.S.

DISSERTATION

Presented to the Faculty of the Graduate School of

The University of Texas at Austin

in Partial Fulfillment

of the Requirements

for the Degree of

DOCTOR OF PHILOSOPHY

THE UNIVERSITY OF TEXAS AT AUSTIN

MAY 2013

Dedication

To my family for their unconditional love and support.

Acknowledgements

This successful dissertation was conducted during my Ph.D. years at The University of Texas at Austin. By that time, I have experienced and worked with a number of people whose contribution in assorted ways to this dissertation. It is an honor for me to convey my gratitude to them all in my humble acknowledgement.

First and foremost, I wish to express my appreciation and gratitude to my advisor, Dr. Jason T. McConville for offering this research opportunity. His patience, encouragement and enthusiastic guidance have been unbelievably helpful and motivational. Without his mentoring and knowledge, I never would have accomplished this major milestone in my life.

Besides my advisor, I would also like to express my sincere gratitude to my dissertation committee members, Dr. James W. McGinity, Dr. Robert O. Williams, III, Dr. Alan B. Combs and Dr. Laura J. Suggs. Their insights and constructive comments on my work have been greatly appreciated and improved the quality of this dissertation.

I would also like to acknowledge the faculty and staff in the College of Pharmacy. In particular, I would like to convey thanks to Dr. Salomon A. Stavchansky for always being kind and supportive. I would also like to express my thanks to Ms. Mickie Sheppard and Stephanie Crouch for their incredible help and facilitating my graduate career. I would like to extend my thanks to Ms. Yolanda Abasta, Mr. James Baker, Mr. Joe D. Adcock, Ms. Joyce McClendon and Mr. Jay Hamman for their valuable assistance and support.

I would also like to thank my fellow graduate students for their friendship, generosity, assistance and guidance. In particular, I would like to thank Dr. Yoen Ju

Son, Dr. Sumalee Thitinan, Dr. Thiago Carvalho, Dr. Javier O. Morales, Mrs. Simone Raffa Carvalho, Dr. Ashkan Yazdi and Mrs. Ping Du for all of their assistance and invaluable scientific discussion and for all the fun we have had in the last four years. I would also like to express my special thanks to Dr. Sumalee who became my lab-mate and has been a great friend for me. Many thanks also to all of the past and present graduate students: Dr. Dorothea Sauer, Dr. Caroline Bruce, Ms. Loni Coots, Dr. Sandra Schilling, Dr. Wei Yang, Dr. Jim DiNunzio, Dr. Alan Watts, Dr. Nicole Nelson, Dr. Kevin O'Donnell, Dr. Stephanie Bosselmann, Mr. Bo Lang, Dr. Hélène Dugas, Dr. Justin Hughey, Mr. Ryan C. Bennet, Mr. Justin Keen, Mr. Yi-Bo Wang, Mr. John Yang, Mr. Ju Du, Dr. Letty Rodriguez, Ms. Xinran Li, Mr. Michael Sandoval, Mr. Amit Kumar, Dr. Jin Huk Choi, Dr. Joseph Dekker, and many others.

I would also like to acknowledge with tremendous and deep thanks Dr. Man-Fong Cheng and Dr. Piyanuch Wonganan for their assistance and mentorship throughout the years.

I am extremely fortunate in having Shih-Syuan (Elaine) Lin, my girlfriend, also Mr. Keng-Ming Chang, Dr. Ming-Cheng Hsu, Mr. Wei-Chen Lu, Mr. Chun Jung Chen, Mr. Kevin Tung, Mr. Chihhao Chen, and Mr. Stephen Wong as my best friends. I am truly appreciative for their endless friendship, encouragement and support.

Last but definitely not least, I would like to express my deepest love and appreciation to my beloved parents and brother for their unconditional unending love and support throughout my life.

DEVELOPMENT OF A LOWER INTESTINE TARGETING MUCOADHESIVE PLATFORM OF ORAL DRUG DELIVERY

SHIH-FAN JANG, PH.D.
The University of Texas at Austin, 2013

Supervisors: Robert O. Williams, III, and Jason T. McConville

Our goal was to develop a mucoadhesive, oral vaccination delivery platform designed to target Peyer's patches at ileum. In order to achieve this, we prepared poly (methyl methacrylate) (PMMA) particles of various sizes using W/O/W emulsification solvent evaporation and surface polymerization methods. We then coated and employed mucoadhesive polymers into the carrier system to enhance the residence time in the targeted site. Also we developed our own *in vitro* mucoadhesion testing ramp as an evaluation tool. Finally, nano- and micro-structured particles were manufactured as two different oral vaccine delivery systems (Solid Lipid Nanoparticles, SLNs; and Protein Coated Microcrystals, PCMC). After the model antigen, bovine serum albumin (BSA) was loaded into the SLNs or PCMC; mucoadhesive polymers were then incorporated and formulated the mixture into pellets. The pellets were then layered with an enteric coating, which was composed of a mixture of Eudragit® FS 30 D/Eudragit® L 30 D-55 for ileum targeted delivery. The *in vitro* mucoadhesion test ramp was capable of investigating the mucoadhesive properties of tablets and pellets, providing a rank order for study. Most important of all, it was anticipated that this might reduce the burden of testing animals for

future proposed mucoadhesive studies. Microcapsules/beads of specific size were manufactured reproducibly by solvent evaporation and surface polymerization. Although we could not specify the cut-off size at the pyloric sphincter in mice, we concluded that the cut-off size at the pyloric sphincter in rats was approximately 2.5-3 mm, which was supported by both the biodistribution data and the direct image results from scintigraphy scanning. Moreover, we found that the particle size significantly alters the gastric emptying time in both rodent models. The small microcapsules/beads were hindered in the folds of the stomach (size 50-100μm for mice and size 0.5-1 mm for rats) and emptied the slowest, followed by the large particles, then the medium particles. Finally, PCMC and SLNs we manufactured were suitable carriers for protein API, such as BSA. These particles were of fitting size for M cell uptake, which would possibly induce mucosal immune responses. Therefore, an antigen containing PCMC and SLNs might be suitable platforms for oral vaccination.

Table of Contents

List of Tables

List of Figures

Chapter 1: Introduction

1.1 Background and Significances

Immunization against microbial infections has been regarded as one of the most cost effective methods. Currently, the parenteral route is the most prevalent route of vaccine delivery. This route is effective against pathogens invading via the systemic route, but less efficient against mucosal infections. The antibodies elicited by systemic immunity do not extend to mucosal or serosal sites, which are also the major entry sites for invading pathogens. Mucosal vaccination has been shown to generate both mucosal and systemic immune responses in both animal and human models, and therefore could be considered to demonstrate a more effective protection. Oral vaccination is potentially cost efficient, with good patient compliance, and have much more physicochemical stability (compared to injection vaccines) during storage and transportation. However, the oral route for mucosal vaccination has not reportedly been successful in presenting antigens to the body, mainly due to the environmental issues of the GI tract before presentation to the immune-responsive M-cells (at Peyer's patches). Recent research has suggested that targeted microparticle and/or nanoparticle-based vaccines could potentially be used to negate some of the issues associated with mucosal delivery. These particles (e.g. PLGA, PLA, enteric-coating polymers, alginates, and chitosans) have been shown to improve cell uptake, and act as adjuvants to promote a stronger immune response while being targeted to the appropriate tissues. This review covers a wide range of multiparticulate-based drug delivery systems that have recently been investigated for oral vaccination use.

1.2 Current vaccination solutions

Presently, most vaccines are attenuated vaccines administrated via systemic routes (the parenteral route) [1]. However, there are several drawbacks, including patient compliance, side effects, storage/transportation issues (refrigeration required) and sterilization [2]. Although vaccination via injection can induce effective systemic immune responses against infective virus and bacteria, parenterally administered vaccines are not generally effective for induction of a mucosal immune response [3]. Table 1.1 comparatively summarizes some general advantages and disadvantages of parenteral, nasal, and oral vaccination [4] routes.

Table 1.1: Comparison of oral vaccines versus parenteral/nasal vaccines

	Parental	Nasal	Oral
Delivery	Injection, professionally trained personnel required	Designed delivery device required	Direct ingestion, most patient compliance
Adminstration site	Cells and tissues in circulation	Mucosal surface	Mucosal surface
Delivery risk	Possible infection at the injection sites (contaminated needles/syringes)	Minimal, no needles/syringes needed	Minimal, no needles/syringes needed
Adjuvent	Various adjuvant (aluminum, most widely used)	Mucosal adjuvant required	Mucosal adjuvant required
Antien dose required	Low	Medium (Efficient transfer across nasal epithelium required)	High (Digestion and insufficient uptake in the gastrointestinal tract; can be possible overcome by successful encapsulation/targeted delivery
Induced immune response	Potent systemic antibody and T cell (IgG)	Mucosal and systemic antibody/T cell, may induces tolerance (both IgG and IgA))	Mucosal and systemic antibody/T cell, may induces oral tolerance (both IgG and IgA))
Current clinical use	Extensive	Limited number of clinical trials	Extensive use for live-attenuated vaccines and limited number of clinical trials of subunit oral vaccines
Cost	High (due to sterile equipment/storage and medical personnel required)	Medium	Low

In some cases, antibodies induced via parenteral routes are not accessible to mucosal surfaces, which are the primary sites for most infectious pathogens. Among the induced antibodies, those produced by humoral immune responses at the mucosal surfaces are of importance in fighting against pathogens [5]. Intranasal (IN) vaccination

has recently been widely studied for its advantages of generating both local and systemic immunity. IN administration is needle-free, non-invasive, painless, and most importantly, does not require sterile preparation and can be self-administered. Moreover, the large surface area of the nasal cavity and the presence of microvilli have been suggested to further enhance the possible therapeutic effect of vaccines [6]. However, despite these potential advantages, a high mucosal clearance rate in the nasal cavity is a key issue. Therefore, mucoadhesive polymers have been investigated in many studies to improve the residence time of the vaccine and increase efficacy. Among these polymers, chitosan is the most widely studied, while other polymers include Carbopol®, hyaluronic acid, and N-trimethyl chitosan chloride (TMC) [7].

Oral vaccination, potentially an ideal vaccination route since both mucosal and systemic immune responses can be provoked via the stimulation of mucosally-situated IgA and IgG plasmacyte precursors [8]. The oral route is attractive for vaccination because the GI tract of a human has over 300 m2 of mucosal surface containing immune inductive tissue, such as the intraepithelial lymphocytes and lymphoid follicles at the laminar propria and Peyer's patches, known as the gut associated lymphoid tissues (GALT). Live-attenuated oral poliovirus vaccine (OPV) was developed and licensed in 1961, and due to its ease of administration OPV is widely used in the world for elimination of wild-type poliovirus transmission [9]. As most pathogens invade their host through their digestive tract, immunization with live-attenuated vaccines actually mimics natural infections of the antigen. In fact, these result in the induction of local secretory immunoglobulin A (sIgA) and the reduction of virus shedding of from the

intestine; while an intramuscular or intravenous injection vaccine can only induce serum antibodies, rather than inducing secretory IgA. sIgA derives from monomeric IgA and becomes dimerized by complexing with secretory component (SC, an epithelial glycoprotein) associated with the epithelial cell [10]. At least 80% of the antibodies are produced locally in the gut lamina propria (mainly IgA) [11]. Nearly 3 grams of dimeric IgA is produced and translocated to the gut lumen everyday as sIgA, which is more than the total daily production amount of IgG in an average human subject [12]. sIgA highlights the importance of the defense of mucosal infections by the fact that most pathogens/antigens are encountered by the mucous membrane. It was well known that sIgA in breast milk showed promising protection for the neonates against cholera, enterotoxic Escherichia coli and Campylobacter infections, especially in third-world countries [13]. However, efficacy of orally administered vaccines is generally low due to degradation of the delivered antigen in the gastrointestinal (GI) tract, and low antigen uptake by the gut associated lymphoid tissue (GALT, part of the mucosal-associated lymphoid tissues (MALT)) [14]. In order to reach immune component cells located in the epithelium, lamina propria, or beneath the basal membrane, penetration of the intestinal epithelial barrier is required of an oral vaccine. To achieve that, a suitable carrier system is necessary for an oral vaccine. These carriers can be microspheres of synthetic polymers (such as, PLGA, and polyacryl starch) [15], natural polymers (such as chitosan, and alginate) [16], or liposomes [5]. It is proven that particles with sizes below 10 μm can be taken up by the M-cells in the Peyer's patches and transported through the intestinal epithelial barrier [17]. The uptake antigens are then transported to the regional lymphoid

tissues, processed, and stimulate antigen specific B lymphocytes in the germinal centres of follicles located beneath domes (Figure 1.1) [18]. In spite of the significant barriers to protein/peptide-based vaccine delivery in the gastrointestinal tract, oral delivery continues to be the most intensively studied for these macromolecules delivery. The advantages of oral vaccination over traditional vaccine injection are obvious, these include: (a) Ease of administration without sterile needles/syringe, as well as well-trained professionals, (b) ease of transportation and storage, since oral vaccines are relatively more stable than injection vaccine and are less susceptible to contaminations, (c) mass immunization can be achieved, (d) large patient acceptability (good patient compliance), (e) reduction in the risk of infection at the injected site, compared to parental vaccines (i.e. Human immunodeficiency Virus and Hepatitis B infections in developing countries) [19], and (f) induction in both mucosal and systemic immune responses. While most vaccines are administered through parental route, there are several vaccines that have been developed for oral administration. These include cholera vaccine (bacterial vaccine), typhoid vaccine (bacterial vaccine), polio vaccine (viral vaccine), and rotavirus vaccine (viral vaccine). These vaccines are based on killed/inactivated or live-attenuated pathogens and are able to generate both cellular and humoral immune responses. However, vaccines based on killed/inactivated whole organisms can only induce a weaker immunity and therefore, a large dose, or a multiple dosing regiment, is required [20]. Lately, research has focused on using purified sub-units of bacteria or virus as a vaccine. Due to the nature of these new vaccines (mostly protein, peptide, or DNA-based macromolecules), these macromolecules are highly susceptible to gastric acid and are of

low permeability to the mucus membrane in the GI tract [21]. Therefore, a combination of using biopharmaceutical macromolecules and polymeric carrier has been widely investigated in recent years [22-24]. On one hand, these polymeric particles act as adjuvants to the immune response by themselves, and are able to enhance the induction of immunity [25]. On the other hand, polymeric particles/carriers provide protection to the biopharmaceutical macromolecules against degradation and inactivation in the GI tract. Several researchers have also pointed out the enhanced transmucosal transport of biopharmaceutical macromolecules in the presence of polymeric particles/carriers [23].

Figure 1.1: Illustration of pathogens/antigens sampling by M-cells. (1) M cell uptake antigens via phagocytosis and translocate the antigens to the lumen side of intestine. (2) Invaded antigens or bacteria. (3) An antigen being delivered to antigen presenting cells. (4) Dendritic cell. (5) Enterocytes.

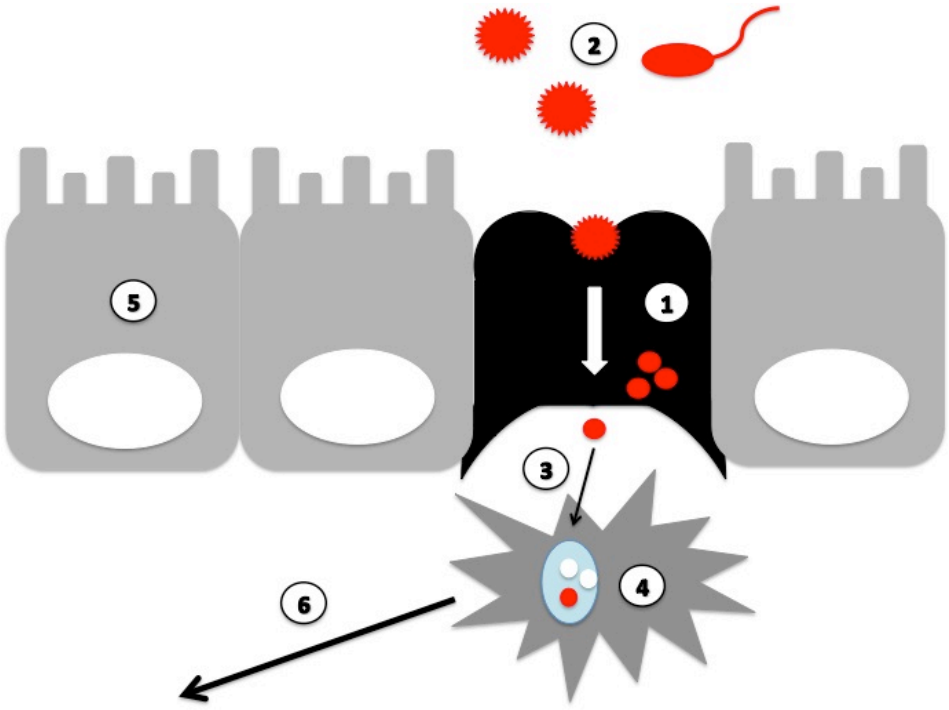

1.3 Mucosal immune system

The increased availability of new protein and peptide-based drugs and antigens offers new approaches for treatment against diseases. However, protein/peptide-based drugs are macromolecules that are inherently susceptible to loss of both their native structure (enzymatic digestion and/or hydrolysis induced by gastric acid) and conformation. Additionally, these macromolecules have a short half-life (normally in a few hours) and are prone to rapid clearance in the liver and other body tissues. Due to the large molecular weight (normally > 3,000 Da) and the hydrophilic nature of protein/peptide-based drugs, these macromolecules generally have low bioavailability (<1%) and short a half-life (<30 minutes). Therefore, a carrier-mediate drug delivery system with high drug encapsulation efficiency and high biocompatibility is required to improve the bioavailability of these protein/peptide-based drugs and provide possible administration via alternative routes (e.g., oral, nasal, and pulmonary).

As indicated, the major reason for using a mucosal route of vaccination is that most infections affect or start at a mucosal surface. Mucosal infection is the major cause of death for those aged of 5 years, with approximately 10 million child mortalities annually [10]. By provoking both mucosal and systemic immunity, a more pronounced and long-term effect can be achieved by mucosal vaccination. In fact, the mucosal immune system provides two layers of adaptive anti-inflammatory defensive mechanisms: (1) the immune exclusion, and (2) and oral tolerance. The first mechanism is majorly provided by sIgA antibodies to restrict the epithelial contact and penetration of invaded pathogens and other potentially defective antigens (Figure 1.2), while the latter strategy is to prevent

overreaction against innocuous luminal antigens (i.e. various food proteins), which is dependent mainly on the development of regulatory T cells (Treg) [10].

Figure 1.2: Mechanism of Peyer's patches mediated mucosal immune responses at gut associated lymphoid tissue (GALT). (1) Invaded pathogens (i.e. antigens and bacteria). (2) An antigen being uptake by M cell and presented to a dendritic cell. (3) Activation of B-lymphocytes. (4) Activation of T cells in the mesenteric lymph nodes (induced by the dendritic cells) (5) Matured B cell with pathogen-specific sIgA. (6) Pathogen-specific sIgA and T cells entered the bloodstream and sent back to the infected mucosal membrane. (7) Interaction of pathogen-specific sIgA against pathogens.

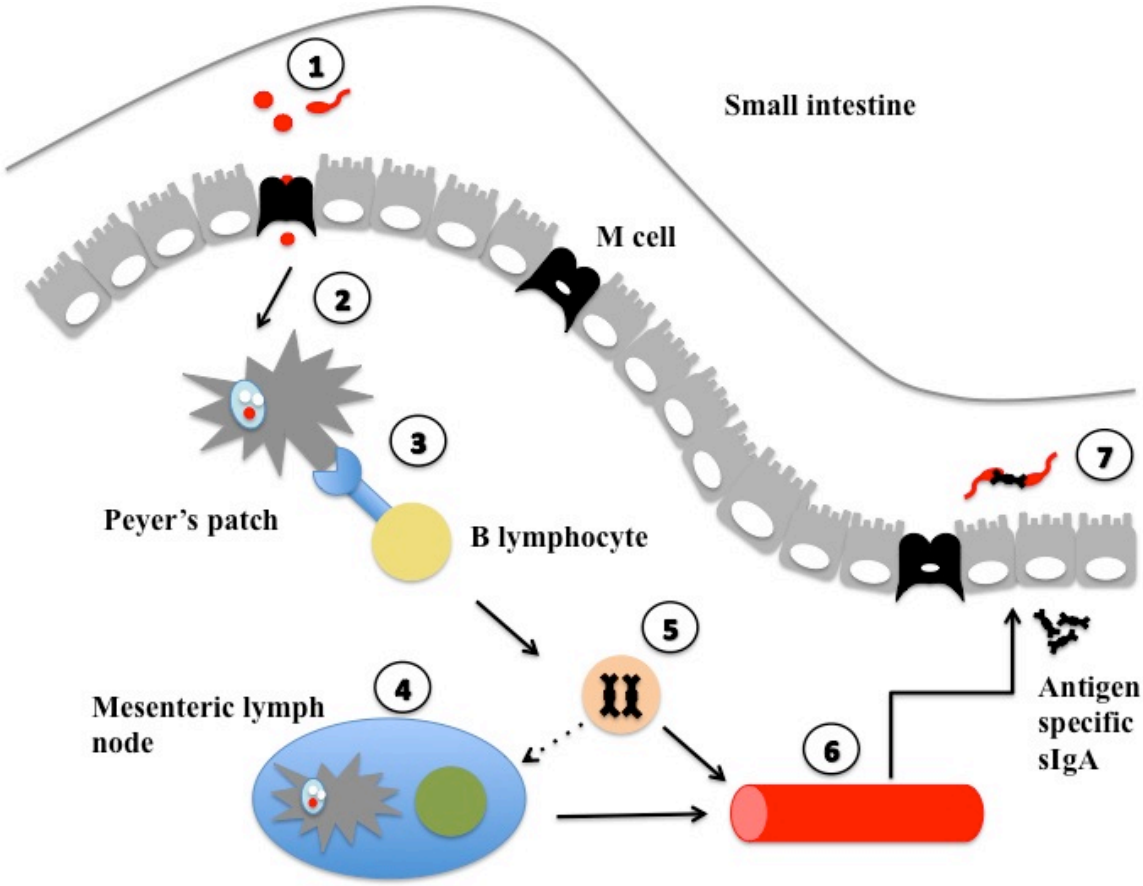

Table 1.2 lists currently available vaccines against mucosal infections [26]. About 70% of the body's immune system is found in the digestive tract. GALT is made up of several types of lymphoid tissue that store immune cells (such as T and B lymphocytes),

with Peyer's patches as the major sites of GALT. Therefore, Peyer's patches, which are present mainly in the lower ileum, become the primary target for oral vaccines. Physiologically, the intestinal epithelium overlying the Peyer's patches is specialized to allow the transport of pathogens by M-cells into the lymphoid tissue [27]. Vaccination via GALT differs from the injection route as it has a higher capacity and can provide a diversified immune response, including both cellular and humoral components, as well as a local and systemic response [15]. Attenuated vaccines are themselves not an ideal vaccination method; however, there are several issues, such as adverse effect (e.g. fever, fatigue), and the requirement for refrigerated storage and transportation. Consequently, subunit vaccines, which are manufactured from antigenic components of infectious organisms, have gained popularity. Unfortunately, when administered orally, these subunit vaccines show poor immunogenicity, low GI tract absorption and low GALT uptake. Moreover, the amount of antigens required for oral immunization is far more than those for parenteral administration (via systemic immunity) [28]. To increase immunogenicity of oral subunit vaccines, some adjuvant systems are proposed, including bacterial toxins and their derivatives (e.g. Cholera toxin, bacterial pili protein and lectins), CPG containing DNA (bacterial DNA contains unmethylated-CpG dinucleotide), cytokines and chemokines, DNA vaccines, micro- and nano-particulates (e.g. PLA, PLGA, polystyrene and polymethyl methacrylate), liposomes and lipopeptides (attachment of synthetic or bacterial lipids to peptide antigens) [29, 30]. Among these methods, the multiparticulate systems (micro- or nanoparticles) are able to protect the

loaded antigens from gastric damage and are able to control the release of loaded antigen as well.

Table 1.2: Internationally licensed vaccines against mucosal infections

Vaccine	Delivery route	Trade name
Polio (live-attenuated polio virus)	Oral	Various
Cholera (Cholera toxin B subunit/inactivated *V. cholera* whole cells)	Oral	Dukoral (SBL Vaccine)
Typhoid (Vi polysaccharide)	Subcutaneous/ intramuscular	TyphimVi (Aventis)
Ty21 (live-attenuated vaccine)	Oral	Vivotif (Bernam SSVI)
Rotavirus (live-attenuated monovalent human rotavirus strain)	Oral	RotaRix
Influenza (live-attenuated cold-adapted influenza virus reassortant strains)	Nasal	FluMist (MedImmune)
Diarrhea (live-attenuated vaccine, ACE527)	Oral	Phase Ⅲ
Dysentery (live-attenuated vaccine, Shigella infection, CVD 1208S)	Oral	Phase Ⅱa
Anthrax (live-attenuated Anthrax vaccine and subunit vaccine)	Oral	Pre-clinical
Peptic ulcer, gastric cancer (Killed/inactivated)	Oral	Phase Ⅰ

1.4 Peyer's patches

In most cases, mucosal immunity is expressed in the gut region [31] (about 80% of the body's activated B cells present in the intestinal mucosa). The organized mucosa-associated lymphoid tissues (O-MALT) occur throughout the gastrointestinal tract and consist of lymphoid follicles are arranged as solitary follicles or as clusters forming distinct structures such as the Peyer's patches (PP), the major inductive site for both

humoral and cell-mediated immunity [19] and appendix. Gut-associated lymphoid tissues (GALT) are responsible for the production of secretory immunoglobins. The epithelium over-lying the lymphoid follicles is termed the follicle associated epithelium (FAE) and is distinguished from the intestinal epithelium at other sites by the presence of the specialized antigen sampling membranous epithelial cells (also called microfold cells and M cells). In the intestine, induction and regulation of mucosal immune responses are taken place primarily in Peyer's patches. Peyer's patches are the inductive sites for immune surveillance (regulation of antigen (Ag)-specific IgA Ab responses following oral immunization) [32], and are optimal sites of uptake for those drugs that need to be delivered to the intestinal lymph (drugs that undergo extensive first pass metabolism) [33]. Peyer's patches have high transcytotic capability and are able to transport a broad range of substances, including bacteria, viruses, antigens and particles from the intestinal lumen to the underlying lymphoid tissues. The number and location of PP varies between species, however, the basic physiological pattern is similar [34]. In humans, PP tend to increase in size and number with increasing age. Generally, the ileum contains more PP than the jejunum, while the duodenum contains very few PP [35]. Pathogens enter GI tract are wither taken up by M cells or dendritic cells (DCs). M cells sample these antigens and forward them to the antigen presenting cells (APCs), including macrophages and antigen carrying dendritic cells. M cells of the PP non-selectively transport macromolecules, particles and microorganisms [36]. Neutra and co-workers pointed out that lectins and polycations that adhere to glycoconjugates on the luminal membranes of M cells are endocytosed via deep, clathrin-coated pits from the inter-microfold domains

of M cell surface. M-cells uptake and transport particles from the lumen site of the GI tract and subsequently present them to underlying follicles [30]. The basement membrane beneath the M cells contains pores approximately 3 μm in diameter. The unique pore structure, reportedly key in facilitating antigen-cell interactions during the immune response [35]. Moreover, M cells represent the most efficient cell type for intestinal absorption of biologically active agents administered in particulate form. Particle interaction with M cells is greatly influenced by the surface properties of both the cells (which exhibit species associated variations) and the particles. The level of targeting to M cells of particles can be modified by, types of polymer used, size of the particles, ligand-modification of the particle surface, hydrophobicity, and surface charge [37]. The immune response to Staphylococcus enterotoxin B was studied in mice using PLGA microspheres. Particles less than 5 μm were effectively taken up by the PPs and dissembled to the mesenteric lymph nodes as well as the spleen, which corresponded to induction of enterotoxin-specific IgM and IgG antibodies (humoral immune response). In contrast, particles between 5-10 μm have been shown to remain in the PP for 35 days, while particles above 10 μm were shown to be taken up by the PP [38]. In addition, hydrophobic polymeric microparticles (polystyrene, polymethylmethacrylate and polyhydroxybutrate) showed more efficiency for uptake than hydrophilic particles [33]. In order to illustrate particle sampling by M cells, Beier and co-workers investigated the kinetics of particle uptake in the domes of Peyer's patches. A suspension of Saccharomyces cerevisiae was injected into the gut lumen of anesthetized mini-pigs; the

position of yeast cells in the tissue was determined after 1, 2.5, 4, and 24 hours using fluorescence light and thin-section electron microscopy. 30% of the yeast cells were found to be trafficking at the intercellular space of the epithelium during the first hour post-administration. After 4 hours, 70% of the yeast cells were completely translocated through the basal membrane and taken up by the phagocytes surrounding the PP [39].

1.5 Oral Vaccination Delivery Platforms

Using micro- or nanoparticles as drug delivery carriers has been widely studied in the past 20-30 years. Recently, research has focused on utilizing these micro- or nanoparticles for mucosal vaccination (i.e. nasal and oral vaccination) due to the following advantages: (1) Micro- or nanoparticulate vaccines can be delivered and distributed more efficiently at the targeted site, (2) due to the nature of their nano-structured size, nanoparticles can be more efficiently sampled by the M cells, as well as dendritic cells by endocytosis/phagocytosis, (3) the particles can act as adjuvant by themselves and help induce enhanced immune responses. One of the major challenges of oral vaccination is avoidance of an immune tolerance. This issue could be avoided by encapsulating vaccine antigen into small particles. Efficient and enhanced uptake of particulate antigen by M cells in the Peyer's patches by phagocytosis has been observed, while only minimal antigen uptake (through pinocytosis) was found in the solution form. Nonetheless, protein antigens taken up as particles are more potent in activating antigen presenting cells (APCs) than soluble antigens. Orally delivered particulate vaccines were found to be uptake by M-cells in the Peyer's patches of the intestine. After being processed by APCs (i.e. dendritic cells and macrophages that reside in the Peyer's

patches) and elicit both T cell and B cell-mediated immune response. Table 1.3 lists recently developed multiparticulates-based oral vaccination delivery systems.

Table 1.3: Recent multiparticulates-based delivery systems developed for oral vaccination

*Active Pharmaceutical Ingredient

Platform	API* or model antigen	Manufacturing Method	Particle size	Loading capacity (%)	Encapsulation Efficiency (%)
PLA and PLGA micro-, nanospheres [48]	Rotavirus	W/O/W double emulsification solvent evaporation	Varied, 2-8 μm and/or 250-500 nm		Varied, 25-55%
PLA-PEG-PLA (PELA) microspheres [51]	*H. pylori* lysates	W/O/W double emulsification solvent evaporation	3.20-4.05 μm	5.06-5.40%	74.9-82.2%
Chitosan–bile salt microparticles [53]	Adenoviral vectors	Ionotropic coacervation of	10-80 μm	-	>80%
N-trimethyl chitosan nanoparticles [64]	BSA and Urease	Ionic gelation	300-500 nm	10-45%	81-95%
Alginate-coated chitosan microparticles [68]	BSA	Ionic crosslinking and layer-by-layer coating	~1 μm	6%	40%-60%
Alginate-coated chitosan nanoparticles [69]	Hepatitis B surface antigen (HBsAg)	Ionic crosslinking and coating	300-600 nm	2.57%	86%
Alginate microparticles [70]	Plasmid DNA	W/O emulsification solvent evaporation	45 μm	-	~72%
Lioposomes [77]	Recombinant Ag85A-DNA (*Mycobacterium* antigen)	-	-	-	-
Chitosan-coated liposomes and polyplex loaded (PPL) liposomes [79]	Plasmid DNA, pRc/CMV-HBs	Reverse-phase evaporation; thin film method	50-550 nm	>80%	-
Bilosomes [82]	Haemagglutinin antigen (HA)	Homogenization	50-250 nm	-	~50%

Table 1.3 (continued)

Platform	API* or model antigen	Manufacturing Method	Particle size	Loading capacity (%)	Encapsulation Efficiency (%)
Bilosomes [84]	Influenza A antigen	Homogenization	10-100, or 60-350 nm	-	~50%
Starch microparticles [87]	Human serum albumin (HSA) and recombinant cholera toxin B subunit (rCTB)	Polymerization	-	-	-
Bilosome, CTB conjugated [95]	BSA	Lipid cast film method	100-120 nm	-	~20%

1.5.1 PLGA and PLA-based micro- and nanoparticles

In the past few decades, biodegradable polymers (i.e. poly (lactic-co-glycolic acid and polylactic acid) have been widely invested in various dosage forms, such as oral, nasal, and pulmonary drug delivery systems. Biodegradable polymers provide sustained release of entrapped antigen/drugs and could be degraded in the body and then are eliminated from the body [40]. Biodegradable polymer-based particles can be sampled by M cells and dendritic cells via phagocytosis. in addition, researchers have demonstrated that phagocytosis can become more efficient with increasing polymer hydrophobicity [41]. Therefore, biodegradable polymers, such as poly (lactic-co-glycolic acid) and polylactic acid, have been utilized for mucosal vaccination research for the past two decades. PLGA is a copolymer synthesized by random ring-opening co-polymerization of two different monomers, glycolic acid and lactic acid. Based on its biodegradability and high biocompatibility [42], PLGA is approved by FDA and commonly used in

pharmaceutical industry, especially being uses in microencapsulation [43, 44]. PLA is another widely used biodegradable copolymers manufactured by ring-opening polymerization of lactide lactic acid and lactide. Delivery of PLGA, PLA has been investigated in numerous dosage forms, including nasal [45], pulmonary [46] and oral [47] drug/antigen delivery. Nayak et al. prepared rotavirus (strain SA11) encapsulated with polylactide (PLA) and polylactide-co-glycolide (PLGA) microspheres using a W/O/W solvent evaporation technique. Microspheres sized 2-8 μm were obtained by sonication during the primary emulsion and homogenization during the secondary emulsion process, whereas nanoparticles sized 250-500 nm were formed when sonication was used during both primary and secondary emulsion processes. The encapsulation efficiency of the PLA and PLGA particles was seen to vary between 25-55% depended on the composition of the formulations. With BSA as a stabilizer (to prevent antigen degradation in the emulsification process), PLA microspheres in a size range between 1-3 μm showed approximately 45% encapsulation efficiency. Only about 30 – 35% burst release of antigen was shown in this particular PLA formulation, followed by a sustained release of antigen in subsequent weeks. Furthermore, a single dose oral inoculation (20 μg) of antigen encapsulated PLA microparticles to Swiss Webster mice elicited significantly higher ($p < 0.05$) IgA (>5 fold rise in IgA titer) and IgG (>4 fold rise in IgG titer) antibody titer, compared to the control group. In addition, while antibody titers in mice inoculated with soluble antigen were increased after immunization, a declining of antibody titers was observed shorty after initial elevation. However, mice inoculation

with antigen loaded PLA microspheres showed significantly improved ($p < 0.05$) long-lasting IgA and IgG antibody titer. Therefore, the results from Nayak and co-workers illustrated that PLA microspheres could be a useful polymeric microparticulated oral vaccine delivery platform for rotavirus, since the PLA microspheres were of ideal particle size (less than 5 μm) for mucosal vaccination and most importantly, both systemic and mucosal immune responses could be elicited and sustained for up to 3 months [48].

Although not fully described *in vivo*, a study has pointed out that the degraded products (lactic acid and glycolic acid) of PLA and PLGA form a local acidic environment, which might result in acidic hydrolysis of the carrying antigen (or protein/peptide-based drug) [49]. Therefore, copolymerization of hydrophilic polyethylene glycol (PEG) with PLA and/or PLGA has been developed for micro- or nanoparticle-based drug delivery systems [46, 50]. Ren and coworkers synthesized triblock copolymers (PELA) by incorporated PEG into PLA (PLA : PEG w/w ratio = 95:5). Helicobacter pylori (HP) lysate was encapsulated into PELA microspheres using a W/O/W double emulsification solvent evaporation method. The final products were seized between 3.20-4.05 μm in diameter and the loading capacity and encapsulation efficiency of HP was approximately 5% and 80%, respectively. Adding hydrophilic PEG into the PLEA copolymer enhanced the entrapment of water-soluble bacteria lysates and led to the high encapsulation efficiency. In order to evaluate particle distribution in the GI tract, the microspheres were first orally administered to miniature pig (sus scorfa domestica). After three days, most of the particles were found in the gastric region of the

animal, while the majority of the microspheres were shown at the intestine by CT scan after 15 days. When HP loaded microspheres were orally inoculated into BALB/c mice (at three immunization doses of 0, 1, and 2 weeks, followed by a booster immunization at week 7), a significantly elevated ($p < 0.05$) sIgA was in the saliva, compared to the mice immunized with soluble antigens. Furthermore, one week after the booster immunization, the specific sIgA-ASCs (Antibody secretory cells), IgG-ASCs, and gut sIgA in oral microspheres inoculated mice were also significantly increased ($p<0.05$), compared to both mice immunized with soluble antigen and the control group [51]. Therefore, PELA microparticles could be another useful platform for protein/peptide-based API and are capable of delivering antigens to the intestine and elicit both mucosal and systemic immunity.

1.5.2 pH-sensitive enteric coating polymer-based microparticles

Recently, adenoviral vectors (AdV) have been widely used for as a vector for gene delivery and expression of foreign proteins for vaccination. The reason why AdV are attractive for vaccine delivery to mucosal surfaces is that most of AdV serotypes invade through these surfaces, followed by replication of themselves in mucosal sites of the digestive tracts [52]. Unfortunately, the strong mucosal immune responses elicited by AdV could actually degrade the vaccine and reduce the efficacy of the AdV vaccines [53]. Therefore, polymeric particles micro- or nanoparticles have been introduced to enhance mucosal immunity.

Eudragits®, pH-sensitive acrylic co-polymers manufactured by Evonik Industries AG, are commonly used in varies oral dosage forms as enteric coating material against

gastric degradation [54]. These acrylic co-polymer products pH-sensitive and various grades of Eudragit® dissolve at certain pH range. Therefore, targeted delivery of oral dosage forms to specific pH region along GI tract could be achieved by utilizing an appropriate grade of Eudragit®. Hypromellose acetate succinate (HPMCAS, also known as hydroxypropyl methylcellulose acetate succinate) is a cellulose ester, which is also typically used as an enteric coating agent for solid dosage forms in the pharmaceutical industry [55]. Tawde and co-workers incorporated whole cell lysate of murine ovarian cancer cell line (ID8, a source antigen that correlates closely to human ovarian cancer cell) into Eudragit® FS 30D and HPMCAS-based microparticles using a Buchi B-191 Mini Spray Drier. In order to target the microparticles to M cells at the Peyer's patches, an M cell-specific ligand, Aleuria aurantia lectin (AAL) was used in the formulation. The obtained microparticles made of Eudragit® FS 30D were approximately 1.6 μm in diameter with an encapsulation efficiency of about 92%. Microparticles were administered to C57BL/c mice via oral gavage to evaluate the vaccine efficacy using a challenge with live tumor cells (back injection of tumor cells). Three weeks after the tumor challenge, the vaccinated mice showed significant ($p < 0.05$) retardation of tumor volume compared to non-vaccinated animals. A significantly elevated ($p < 0.05$) serum IgG level was observed in vaccinated mice, in comparison to non-vaccinated animals. Additionally, CD8+ T-cells, CD4+ T-cells and B-cells in various lymphatic organs were increased in vaccinated mice. Therefore, orally delivered, whole cell lysate entrapped microparticles made of enteric polymers are of potential in triggering humoral as well as cellular immune response in the mice model [56]. Such vaccine could be a potential

treatment for patients with residual tumor in the future, although further studies are required to test the stability of the vaccine.

1.5.3 Chitosan-based micro- and nanoparticles

Chitosan, a natural hydrophilic polysaccharide is generally obtained by partial deacetylation of chitin from the hard exoskeleton of crustacean (i.e. crab, lobster, and shrimp). Chitosan is regarded as biocompatible and biodegradable by lysozymes and chitinases produced by macrophages in human bodies [57]. Chitosan can enhance tight junction permeability [58] and shows strong mucoadhesive properties in numerous studies [59, 60]. Additionally, chitosan is able to interact with negatively charged mucus membrane of gastrointestinal tract due to its positive net charge [61]. Lameiro et al. encapsulated adenoviral vectors by the method of ionotropic complexation of chitosan chains with bile salts. The encapsulation efficiency was over 80%, while using sodium deoxycholate as counter-anion and poloxamer 188 (Pluronic F68) as surfactant. The obtained microparticles were then inoculated directly into 293 and Caco-2 cells. 24 hours after viral inoculation, the microparticles were detected to be spread up to 30–40% of the total cells in the monolayer. Furthermore, encapsulation in chitosan-bile salt containing microparticles was capable of protecting the adenovirus from low pH medium (used in the *in vitro* dissolution test), and delaying adenovirus release after cell contact (due to the mucoadhesive property of chitosan) [53]. Overall, chitosan-bile salts microparticles showed protection for the encapsulated AdV in a cell model; however, further *in vivo* studies are required to verify whether these formulations are of good properties for future mucosal adenovirus delivery. However, it has been pointed out that chitosan loses its

mucoadhesive, as well as penetration enhancing property under acidic conditions due to deprotonation [62]. N-trimethyl chitosan (TMC) has drawn attention in recent research due to its solubility in water over a wide pH range. In addition, this modified chitosan is of absorption enhancing property even in neutral or basic pH environment [63]. Chen et al. manufactured TMC nanoparticles by ionic gelation using fluorescein isothiocyanate labeled BSA (FITC-BSA) and Urase as a model protein vaccine. The TMC nanoparticles obtained were sized between 300-500 nm with approximately 80% (FITC-BSA)-95% (Urease) encapsulation efficiency and 10% (FITC-BSA)-45% (Urease) loading capacity. From the permeability test in Caco-2 cell monolayer, significantly ($p < 0.05$) higher permeation efficiency was observed in TMC nanoparticles, compared to the control group (about 1.4 fold increase). Furthermore, after oral inoculation of TMC nanoparticles, both serum IgG and gut sIgA were significantly elevated ($p < 0.05$) in the mice, compared to the antibodies amount in Urease solution administered animals and the control group. On the other hand, mice subcutaneously injected with TMC nanoparticles showed only significantly increase ($p < 0.05$) serum IgG, but not secretory IgA. This indicated that TMC nanoparticles are of potential in eliciting both systemic and mucosal immunity, and could be a better vesicle as an oral vaccine, compared to subcutaneously injection vaccine [64].

1.5.4 Alginates-based micro- and nanoparticles

Although chitosan is generally regarded as of mucoadhesive (due to its innate positive charge) and permeation enhancing (though tight junction) properties as previously described, it is only soluble in acidic conditions (pKa 5.6). Therefore, chitosan

may be deprotonated in physiological fluid and lose its mucoadhesive and permeation enhancing capability [65]. Therefore, one solution for this issue is to use a negatively charged material, such as sodium alginate, to coat/protect the acid-sensitive chitosan by electrostatic interactions. Alginates are anionic polysaccharides obtained from the cell wall of brown algae. In the pharmaceutical industry, alginates are used in a wide variety of applications as thickeners, stabilizers, and gelling agents. Alginates have mucoadhesive properties and have been investigated in various oral delivery formulations [66, 67]. Li et al. first manufactured chitosan microparticles via ionic gelation. The prepared colloidal chitosan solution was then incubated with BSA solution to form protein loaded microparticles. Sodium alginates were then coated onto the chitosan microparticles in a layer-by-layer manner. The particle size of manufactured microparticles with and without alginate coating was approximately 1300 nm and 400 nm, respectively. BSA encapsulation efficiency was dependent on the initial protein concentration. The highest encapsulation efficiency (EE) was achieved (60%) at a BSA concentration of 2 mg/mL, while EE dropped greatly to less than 30% when BSA concentration was over 2 mg/mL. In addition, due to the competitive absorption between BSA and alginate onto the surface of the chitosan microparticles, BSA loading capacity was the highest (about 90%) at 1:1 alginates/chitosan (w/w) ratio, and was less than 40% at 4:1 alginates/chitosan ratio. However, microparticles prepared at 4:1 alginates/chitosan ratio showed the best stability due to the inversed positive zeta potential obtained from alginates coating (from -28mv to +27 mv) [68]. From Li's results, alginate-coated chitosan microparticles appeared to be a suitable vehicle for oral protein delivery, the

alginates were able to protect the entrapped BSA from acid degradation, as well as provide control over the release of BSA. However, a further investigation in an animal model would be required to evaluate the performance of this formulation in a *in vivo*. In another study, Borges and co-workers prepared alginate-coated chitosan nanoparticles by a similar method, while recombinant hepatitis B surface antigen (HBsAg) was loaded as the model antigen, with or without a potent adjuvant, oligodeoxynucleotides containing immunostimulatory CpG motifs (CpG-ODN). The size of coated nanoparticles was in a range between 300-600 nm, with encapsulation efficiency and loading capacity of approximately 2.5% and 85%, respectively. From their results, the loaded HBsAg maintained their integrity after the manufacturing process (evaluated by SDS-PAGE), as well as after an *in vitro* dissolution test (in pH7.4 phosphate buffer solution). After coating, nanoparticles containing both HBsAg and CpG-ODN or only HBsAg were administered into BALB/c mice via oral gavage. Both formulations showed significantly elevated ($p < 0.05$) percentage of CD4+ T-lymphocytes expressing CD69 (a cell membrane receptor expressed on B and T lymphocytes, and was commonly used as a parameter in vaccination studies) in the mice spleen, which suggested these formulations were able to elicit cellular immune responses. Furthermore, both formulations induced a significantly proliferated IL-2 and IFN-γ production, which resulted in the presence of serum IgG and sIgA in the gut of the mice [69]. Alginate-coated chitosan particles have been demonstrated as a possible platform for future oral vaccine delivery. However, a burst release of encapsulated antigen from alginate-coated chitosan nanoparticles was found in simulated gastric fluid (pH 1.2), therefore, further protection is certainly

necessary to control the release of entrapped antigen and prevent its release in the gastric region.

Nograles and co-workers produced alginate microspheres using water-in-oil (W/O) emulsification technique. The average particle size of alginate microspheres was about 45 μm. Plasmid DNA (pDNA) with fluorescent protein reporter gene (GFP), pVAX-GFP, was encapsulated into the alginate microspheres at encapsulation efficiency of approximately 72%. The pVAX-GFP loaded alginate microparticles showed a significantly increased ($p < 0.05$) release under basic conditions, compared to acidic conditions. This was due to the shrinkage of alginate microspheres in acidic environment while the swelling of these microparticles in basic conditions. The pVAX-GFP loaded-microspheres were inoculated into BALB/c mice via oral gavage to monitor the biodistribusion of GFP in the intestine. After inoculation, GFP protein was detected in the mice intestinal cells within 24 to 48 hours [70]. Therefore, alginate microparticles were able to protect and deliver DNA to the intestine for gene expression, which implied alginate microparticles of potential for future oral vaccination using recombinant DNA.

1.6 Lipid based micro- and nanoparticles

1.6.1 Liposomes based micro- and nanoparticles

DNA vaccines have recently been conducted as a potential new generation of vaccine for humans. DNA vaccines are generally considered as being potentially safer and more stable at room temperature (compared to live-attenuated vaccines), cheaper to produce, and easy to manufacture [71]. Manipulating DNA into a particulate delivery

system potentially renders DNA useful for mucosal immunization, by which it is possible to stimulate both humoral and cell-mediated responses. Additionally, increasing evidence has shown that DNA vaccination at the mucosal site is of better performance to that at peripheral sites in generating immune response against a number of infectious agents, including viruses and bacteria [72, 73]. This is partially explained by the observation that memory T and B cells induced upon mucosal vaccination acquire mucosa-homing receptors and preferentially accumulated at the mucosal site of induction. However, mechanisms that lead to elicit activation of memory T and B cells are still to be determined. Liposomes have been widely investigated for antigens and genes delivery via different routes [74, 75] due to their properties of high biocompatibility and biodegradability. Cationic liposomes can also act as adjuvants and improve the expression of the plasmid DNA or recombinant DNA encapsulated inside. Liposomes can be uptake by endocytosis absorption sites. In addition, several studies in the past decade have suggested that liposomes fused with the plasma membrane and mediated the entry of DNA into the cell compartment [76]. Wang et al. encapsulated recombinant Ag85A (coded for *mycobacterium* antigen 85A, one of the protein ingredients secreted by *Mycobacterium tuberculosis bovis*) in liposomes, followed by oral inoculation of the liposomes to C57BL/c mice (three does in at a bi-weekly interval). Immunofluorescent staining was performed to detect Ag85A antigen in intestine cells, M cells and dendritic cells in the mice intestine. For mice inoculated with recombinant DNA-loaded liposomes, Ag85A antigen was expressed and detectable at both M cells and dendritic cells in the mice intestine (especially in M cells), compared to no Ag85A expression in the control

group. This suggests that M cells indeed, take a crucial role in sampling antigen continuing vesicles and translocate these vesicles to the dendritic cells afterward. In addition, from the results of an *in vivo Mycobacterium tuberculosis* challenge test (in a BALB/c mice model), sIgA level was significantly ($p < 0.05$) elevated after immunization, compared to the control group. This provides proof that oral vaccination of recombinant DNA-loaded liposomes is able to elicit mucosal immunity in the mice model. Additionally, Ag85A antigen was intensively expressed in the basolateral compartment of epithelium, rather than expressed in the apical membrane of intestinal epithelial cells. This implied that the basolateral compartment of intestine epithelium plays an important role in initiating Ag85A-specific immune response, while the full mechanism is still unknown [77].

Nevertheless, plasmid DNA is susceptible to gastric pH and enzymatic degradation. Therefore, a chitosan –plasmid polyplex, namely polyplex, was introduced for that it is regarded as of the capability in providing protection of the DNA from nuclease degradation and a mucoadhesive property that permits a sustained interaction between the encapsulated materials and the membrane epithelia [78]. Channarong et al. prepared chitosan coated plasmid DNA (pRc/CMV-HBs) loaded liposomes and polyplex (chitosan-plasmid DNA complex) loaded liposomes (PPLs) using phosphatidylcholine/cholesterol as the main lipid component (w/w ratio: 5:4) for oral DNA vaccination. The main size of all pRc/CMV-HBs loaded liposomes were between 60 to 500 nm in diameter; while the size of polyplex ranged between 350 to 550 nm, dependent on the chitosan content. The loading efficiency of pRc/CMV-HBs was over

80%. After the manufacturing process, plasmid DNA was found stable in both SGF (1 hour at 37 ℃) and SIF (2 hour at 37 ℃), which implied protection imparted by the liposome/polyplex. To further evaluate whether the chitosan-coated liposomes and PLLs were of potential as oral gene delivery systems, each formulation that carrying pEGFP-C2 was investigated in BALB/c mice via intragastric inoculation (single dose inoculation). After 24 hours, both chitosan-coated liposomes and PLLs were detected at the upper part of duodenum and the signal of PPLs was found throughout the intestine. This higher potential for oral DNA delivery of chitosan-coated PLL was due to the increase in permanent positive surface charges that enhanced the internalization of the DNA, as well as the prevention of enzymatic degradation [79].

1.6.2 Bilosomes-based micro- nanoparticles

Although lipid-based carrier platforms have been recently investigated for oral vaccination, it has been pointed out that these lipid-based vehicles (such as liposomes) are susceptible to bile salts and enzymatic degradation in the GI tract [80]. Therefore, a relatively stable (in the GI tract) lipid-based carrier is required for future oral drug/vaccination delivery. A colloidal delivery system consisting of bilosomes, similar to niosomes (nonionic surfactant base vesicles), but with have incorporated bile salts into the vesicular lipid bilayer membrane. Bilosomes are made of naturally occurring lipids, which makes them highly biocompatible. In addition, the bilosomes components have also been shown to possess inherent adjuvant properties when associated with antigen [81]. Singh et al. prepared BSA loaded bilosomes by lipid cast film method. The

manufactured bilosomes were then chemically conjugated with Cholera toxin B sub-unit (CTB) to enhance the affinity of the formulation toward M cells at Peyer's patches. In their study, bilosomes manufactured were stable at 5 and 20 mM bile salt concentration (average bile salt concentration in health humans), as well as in simulated gastric fluid and in simulated intestinal fluid. The average particle size of bilosomes was between 100 to 120 nm in diameter, with BSA encapsulation efficiency (%) of about 30%. CTB anchored bilosomes (BSA loaded) was orally administered to BALB/c mice as a single primary inoculation and a three-primary inoculation (in three consecutive days) and compared to a single subcutaneous (SC) immunization. A single dose of oral CTB conjugated bilosomes was able to generate almost equivalent immune response (serum IgG), compared to subcutaneous immunization of the same antigen (along with Freund's adjuvant). Additionally, CTB anchored bilosomes was able to elicit an mucosal immune system response, since significantly increased (compared to SC BSA and non-CTB conjugated BSA loaded bilosomes) ($p < 0.05$) fractions of specific IgA against BSA to total IgA levels in intestinal, salivary and vaginal secretions of the inoculated mice was found. In another study, haemagglutinin antigen (HA) was entrapped into a bilosome vesicle (BV) system and inoculated to BALB/c mice as a lipid based oral delivery system by Mann and co-workers. The mean particle size of these bilosomes was about 50 to 250 nm in diameter and of an antigen loading of approximately 50%. Three BV systems were prepared using homogenization methods: (1) Unilamella (BV1), (2) Double lipid group (BV2), (3) Double protein group (BV3). Three weeks after treatment, both BV1 and BV3 showed significantly ($p = 0.012$ and $p = 0.009$, respectively) higher IgG1 titer, compared

to the control group. On the other hand, IgA titer was significantly higher after three weeks for BV1 ($p = 0.05$), and after four weeks for BV2 ($p = 0.03$) and after 2, 3 and 4 weeks for BV3 ($p = 0.05$, 0.05 and 0.05 respectively), compared to the untreated controls. Therefore, only BV3 (comprised of a double protein to lipid ratio) was able to induce both mucosal and systemic responses and could be possible applied for future oral vaccine development [82]. From previous studies, small lipid vesicle formulations (< 100 nm) induce Th2 responses while large vesicles (> 200 nm) induce Th1 biased responses to entrapped antigen following subcutaneous administration [83]. Although the exact mechanism underlying this immune response is not yet fully understood, Mann and co-workers also demonstrated that it is possible to polarize the immune response to entrapped antigen via oral vaccination with different sized vesicles (bilosomes). While small vesicles (Z-average diameter 250 nm) induce a Th_2 response, a mixed population of small and larger vesicles (Z-average diameter 980 nm) promotes a significant Th_1 bias as measured by IgG_2a and IFN-γ production (using influenza A entrapped bilosomes in a ferret model). These results implied that an oral vaccine formulation could be modified physically to adapt resultant Th biased immune responses after inoculation [84].

1.6.3 Niosomes-based micro- and nanoparticles

Liposomes were widely investigated as a vehicle for oral vaccine delivery in the past few decades. However, liposomes are found susceptible to gastrointestinal environment (i.e. stability issues in gastric or intestinal fluid, bile salt caused dissolution)

and enzymatic degradation. Therefore, modified lipid-based vesicles niosomes were developed to provide a greater stability over traditional liposomes. A niosome is a non-ionic surfactant-based liposome. Niosomes are closed bilayer vesicles formed by non-ionic amphiphiles. It has been stated that niosomes are of strong adjuvant property and have good penetrating capability. Furthermore, since niosomes were composed of non-ionic surfactant, they are generally regarded to have better stability and can be easily stored, compared to liposomes. Jain and co-workers developed an oral vaccination delivery niosomes made of cholesterol, stearylamine and sorbitan monstearate [85]. Plasmid DNA, pRc/CMV-HBs (coded for the small proteins of the hepatitis B virus, HBsAg) was encapsulated into the niosomes by using a reverse phase evaporation method. The manufactured niosomes were further coated with a modified polysaccharide o-palmitoyl mannan (OPM) in order to protect the niosomes against bile salt caused dissolution in the GI tract, as well as targeting the mannose receptors expressed on macrophages and dendritic cells present in the vicinity of Peyer's patches. In the immunization experiment, OPM-coated niosomes were orally administered to BALB/c mice and compared to mice administered with equivalent amount of naked plasmid DNA or recombinant HBsAg via intramuscular injection (a 2-time inoculation in two weeks). The size of plain niosomes and OPM-coated niosomes were approximately 2.3 μm and 2.5 μm, respectively, while the encapsulation efficiency of plasmid-DNA was found to be about 63% and 61%, respectively for plain and OPM coated niosomes, respectively. However, the stability of plain niosomes showed 45–50% DNA loss after 1 hour in both SGF SIF, while about 25–30% DNA loss was found in OPM-coated niosomes under the

same condition. This suggested that OPM coating was able to prevent the disruption of niosomes and reduce the degradation of encapsulated DNA. Nevertheless, all mice inoculated with oral niosomes were seropositive (>1 mIU/ml) in 2 weeks. It was suggested that antibody levels in the vaccinated mice were more than sufficient (>10 mIU/ml) to get seroprotection against hepatitis B. Additionally, OPM coated niosomes generated a significantly higher anti-HBsAg IgG ($p < 0.05$), compared to plain niosomes. On the other hand, OPM-coated niosomes elicited mucosal immune response, while negligible IgA amount was found on intramuscular administration of naked plasmid DNA or recombinant protein vaccine. This is in concordance to the general agreement that parenterally administered vaccines lack the ability to elicit mucosal immune system, while oral vaccination could stimulate both mucosal and systemic immunity. Furthermore, a strong cell mediated immune response (significantly higher level of both IL-2 and IFN-γ elicited) was observed in mice administered with intramuscular naked DNA and oral OPM-coated niosomes. Therefore, OPM coated niosomes could be another lipid-based vehicle as DNA vaccine carrier and adjuvant for future oral vaccination delivery [85].

1.7 Polyacryl starch-based microparticles

Polyacryl starch microparticles are able to be taken up by follicle-associated epithelium (FAE) in the Peyer's patches and elicit both local and systemic immunity [86]. Stertman et al. prepared polyacryl starch microparticles by polymerization. Two model

antigens, human serum albumin (HAS) and recombinant cholera toxin B subunit (rCTB) were encapsulated into the microparticles. The final formulations were orally administered into BALB/c mice via oral gavage. When rCTB was conjugated to polyacryl starch, they were taken up over both the FAE and the villus epithelium, while HAS conjugated microparticles were only taken up over FAE. When HSA and rCTB were conjugated together to the polyacryl starch microparticles and orally administered to the mice, both the HSA- and rCTB-specific responses were elicited quantitatively (elevated serum IgM/IgG and fecal s-IgA level. The results from Stertman and co-workers indicated that only Peyer's patches mediated particle uptake decided the immune responses after oral administration, and polyacryl starch was of strong adjuvant capacity and was able to elicit both systemic and mucosal immune responses [87].

1.8 Targeted Delivery to Peyer's Patches (M Cells)

While M cells are present at a low density along gastrointestinal tract, specific targeting of M cells could possibly enhance particle sampling by the M cells [88]. Although there is limited information available for specific markers of human M cells targeting, several studies have been conducted with drug delivery systems that target β1 integrins that are overexpressed at the apical pole of human M cells [89]. Ovalbumin (OVA) was encapsulated into PLGA nanoparticles using W/O/W solvent evaporation technique by Fievez and co-workers. To further target the formulation directly to human M cells, four different ligands (15% w/w) [RGD oligopeptides, RGD peptidomimetic (RGDp), LDV derivative (LDVd) and LDV peptidomimetic (LDVp)] were grafted onto the PEG chain of PCL-PEG (15% w/w) co-polymer and incorporated into PLGA

nanoparticles (70% w/w) and tested for *in vitro* transport in human enterocytes (Caco-2 cells) and human follicle-associated epithelium (Raji cells), as well as *in vivo* mucosal/cellular immunity in BALB/c mice. All ligand-grafted PLGA nanoparticles were sized between 220 to 260 nm and the loading efficiency (%) of OVA was between 15-19%. Both RGD- and RGDp-nanoparticles showed significantly higher uptake across the mono- (Caco-2 cells) and co-culture (Caco-2 cells and Raji cells), compared to the non-targeted nanoparticles ($p < 0.05$). Additionally, after 60 minutes incubation, both RGD and LDVd labeled PLGA nanoparticles showed doubled internalization by J774 macrophages cells *in vitro*, compared to non-targeted nanoparticles. When the PLGA nanoparticles were administered directly to the mice duodenum via gavage, both RGDp and LDVd labeled nanoparticles elicited significantly ($p < 0.05$) higher production of IgG, compared to the mice administered non-targeted OVA via IM injection. Moreover, all the targeted-nanoparticles were able to induce a cellular immune response, as shown by the production of IGN-γ in the splenocytes (BALB/c mice study). Lastly, OVA encapsulated RGD- and RGDp-nanoparticles were able to target specifically to β1 integrins at the surface of M cells and enhanced particle uptake of M cells, which could successfully lead to the induction of cellular immunity against OVA [20].

Aleuria aurantia lectin (AAL) has been validated as an M-cell targeting agent in a previous study [90]. Chablani and co-workers developed an M-cell targeting (use ALL as the ligand) microparticles-based oral vaccine via spray drying and used BSA as the model antigen. The microparticles were composed of Eudragit® FS 30D, hydroxyl propyl methyl cellulose acetate succinate (HPMCAS), and BSA in a ratio of 1:1:1 (by weight).

The obtained particles were approximately 1.5 μm in diameter with about 70% encapsulation efficiency. M-cell targeting/uptake of the microparticles was evaluated in-situ on excised mice intestines. Peyer's patches (PP) containing intestinal segments showed higher uptake of particles by lymphoid tissues. On the other hand, no fluorescence was detected in villi area indicating no particle uptake. Since follicle associated epithelium covering the PP is composed of M-cells, particles translocating the epithelium are possibly only mediated by M-cells sampling. Therefore, such enhanced M cell uptake can be attributed to the presence of AAL ligand as previously discussed [90]. BSA-loaded microparticles (with rhodamin-123 as a fluorescence dye) were also orally inoculated into C57BL/6 mice. These enteric polymer-based microparticles showed a prolonged BSA release over 8 hours. Furthermore, 8 hours after immunization, fluorescent-labeled microparticles were found in the Peyer's patches of the mice intestine [91], which implied that an oral delivery platform composed of pH-sensitive enteric polymer and M-cell targeting ligand, AAL could be of potential in oral vaccination, however, additional immunity responses followed by vaccination must be further studies.

The phage display technique (expression of a foreign peptide sequences by transfection a set of genetically recombinant bacteriophages) is a validate method to find interacting peptide ligands to certain targets [92]. Additionally, identification of homing peptide ligands targeting various organs or tissues, such as, M cells have been investigated in previous studies [93]. Yoo et al. developed a M-cell targeted oral vaccine composed of chitosan nanoparticles and M-cell homing peptide that was coded by a phage clone encoding CKSTHPLSC (CKS9) sequence. The manufacturing chitosan

nanoparticles were sized approximately 225 nm in diameter and labeled with fluorescence dye. Transcytotic efficiency of the nanoparticles (CKS9-CNs) to the M cells *in vitro* and Peyer's patch targeting properties *in vivo* were evaluated by *in vitro* transcytosis assay and closed ileal loop assay, respectively. From the *in vitro* transcytosis assay performed in Caco-2 cells at 37 °C, the amount of translocated nanoparticles across M-cell layer was significantly ($p < 0.05$) increased, compared to the amount that was observed under 4 °C. In addition, the high transcytosis was regained once the incubation temperature was elevated back to 37 °C. Since M cells are specialized cells which are able to sample antigens via transcytosis, the temperature-dependent change of particle translocation efficiency found in Yoo's study indicated that the translocation was mediated by transcytosis through the M cells, rather than by simple diffusion through intercellular spaces. Furthermore, both the chitosan nanoparticles, CKS9-CNs and chitosan nanoparticles alone (CNs), showed similar amounts of particle translocation across Caco-2 cell layers without any significance at the begging of the *in vitro* test. However, transcytosis CKS9-CNs increased gradually over time. After 3 hours, the accumulated amount of CKS9-CNs across the cell layer was about 1.5-fold higher than CNs, which illustrated that CKS9-CNs were taken up by M cells in a more efficient manner, compared to CNs. This efficient sampling by M cells was as a result from the incorporation of M cell-homing peptide. On the other hand, the targeting property of CKS9-CNs to Peyer's patches was also monitored *in vivo* (closed ileal loop incubation). And similarly to the *in vitro* M cell results, CKS9 promoted the affinity of chitosan nanoparticles to Peyer's patches in rat small intestine under the demonstration of confocal

scanning microscopy. Moreover, CKS9-CNs injected into closed ileal loop were specifically localized within FAE layer Peyer's patches, where located the most abundant M cells, in contrast to CNs without targeting ligands [94]. These M-cell targeted formulations we discussed earlier were summarized in Table 1.4.

Table 1.4: Recent M cell/Peyer's patches targeted delivery systems for oral drug delivery/oral vaccination

Delivery platform	API[1]	Ligand	Target	Manufacturing method	Size (nm)	EE %[2]	Test model
PLGA[3] nanoparticles [20]	Ovalbumin	RGD[4], RGDp,[5] LDVd[6], LDVp[7],	β1 (Human M cells)	W/O/W[8] solvent evaporation	200-280	15-20	Human Caco-2 cell line, Human lymphoma Raji B line, BALB/c mice
Enteric polymer-based microparticles [56]	Whole cell lysate of a murine ovarian cancer cell line, ID8	Aleuria aurantia lectin (AAL)	M cells	Spray-drying	~1600	~92	C57BL/6
Niosomes [85]	Plasmid DNA, pRc/CMV-HBs (codded for HBsAg)	O-palmitoyl mannan	Macrophages and dendritic cells at Peyer's patches	Reverse phase evaporation	2300-2500	~60	BALB/c mice
Enteric polymer-based microparticles [91]	BSA	Aleuria aurantia lectin (AAL)	M cells	Spray-drying	1500	66-78	C57BL/6
Chitosan nanoparticles [94]	M cell homing peptide CKS9 (CKSTHPLSC)	CKS9	M cells	Ionic gelation and chemical conjugation	~220 nm	-	Caco-2 cells and rat ileal loop

1.9 Mucoadhesion

Mucus is a complex viscous adherent secretion synthesized by specialized goblet cells in the columnar epithelium, that line all of organs exposed to an external environment. Mucus serves many functions, including lubrication for the passage of objects, maintenance of a hydrated layer over the epithelium, acting as a barrier to pathogens and noxious substances, and being as a permeable gel layer for the exchange of gases and nutrients with the underlying epithelium. Mucus is also the first barrier by which nutrients and drugs must interact and diffuse through in order to be absorbed and gain access to the circulatory system, as well as their subsequent target organs [95]. Physically, mucus is composed of about 90-95% water, and 5-10% mucins. Mucins are a family of polydispersable molecules with high molecular mass and a high proportion of covalently bound oligosaccharide side chains, which afford high resistance to the effects of acid and digestive enzymes. In mammals, mucins typically contain fructose, galactose, N-acetylglucosamine, N-acetylgalactosamine, and sialic acid, together with small amounts of sulfate, and mannose [96].

Mucoadhesion is a process by which mucoadhesive polymers contact and attach on to the mucus membrane (Figure 1.3).

Figure 1.3: Mechanisms of mucoadhesion process: (A) Wetting and swelling; (B) Entanglement; (C) Bond formation.

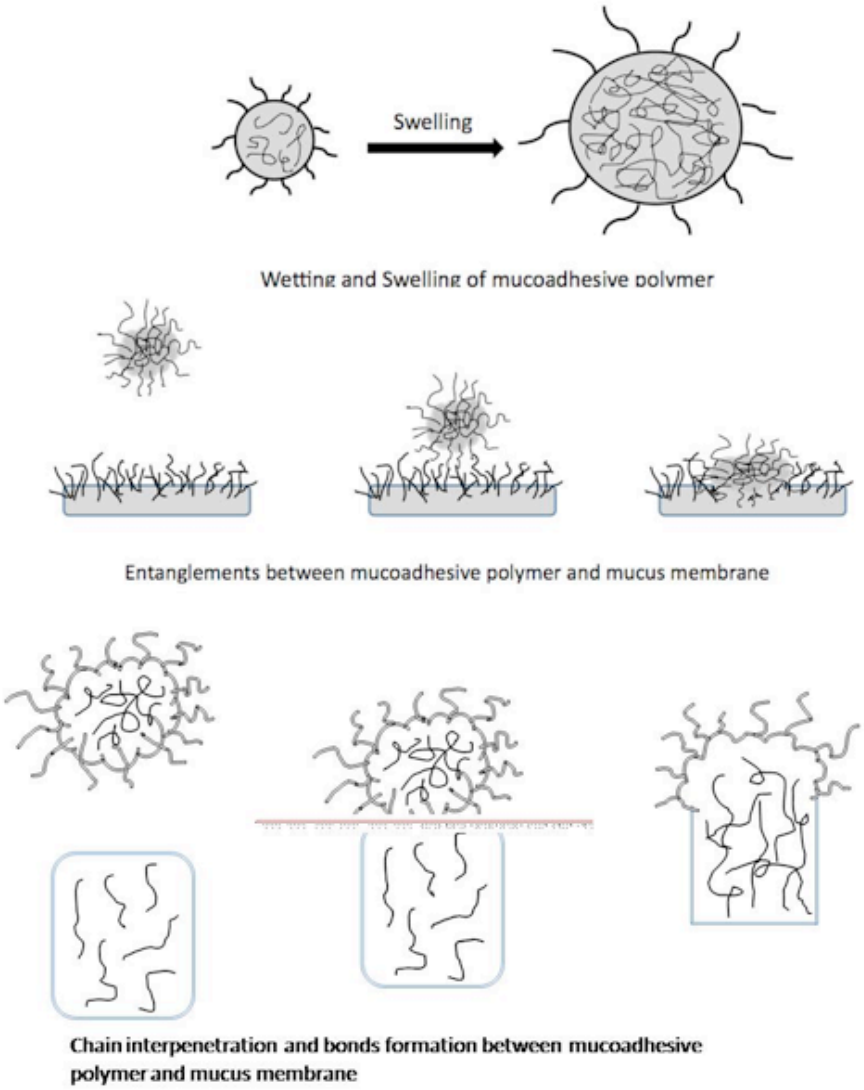

Mucoadhesive polymers get swollen once they are soaked and wetted in the physiological environment. Swelling of the polymers provides an outward force and help the polymers approach the mucus membrane. Once the polymers get contact with the mucus membrane, the swelling force further act as a "pushing force" which enhances the following steps of mucoadhesion process. After mucoadhesive polymers and mucus

membrane make contact, the polymer chains and glycoprotein chains of the mucus membrane start to entangle. The entanglement process pulls the two substances closer and closer, which finally, lead to the last process of mucoadhesion, the bonds formation between the mucoadhesive polymers and mucus membrane. These chemical bonds can be hydrogen bonds, electrostatic forces or even covalent bonds. These bonds/interaction provide an increased residence time at the attached site. The increased residence time can possibly lead to higher absorption and bioavailability of a dosed drug. Therefore, numerous studies have been focusing on incorporating mucoadhesive polymers into different formulations, such as buccal, nasal and oral dosage forms to enhance the bioavailability by virtue of an increased residence time at the sites of absorption. Both natural and synthetic polymers can be utilized as a mucoadhesive agent. The most well-known and recently investigated mucoadhesive materials are chitosan [97], alginate [98], carbomers [99], polycarbophil [100], pectin [101], and some thiolated derivatives of mucoadhesive polymers (e.g. thiolated chitosan) [102].

1.10 *In vitro* mucoadhesion test

In the past 20 years, several methods have been developed and used to determine the mucoadhesive properties of different dosage forms. The oligosaccharide chains of mucins are attached to the protein core and carry negative charges (due to the sialic acid and sulfates moieties). Therefore, a material that carries positive charges (such as chitosan) is generally considered to be of mucoadhesive property (due to the electrostatic interactions between the material and mucus membrane). Zeta potential is used to represent the electrokinetic potential in colloidal systems Zeta potential not only

determines the electrostatic interactions between dispersed particles, but also serves as an important parameter in characterizing the properties of dispersion systems affected by this electrical phenomenon. Whether electrostatic interactions between a mucoadhesive polymer and mucus membrane play a decisive role in mucoadhesion, therefore, zeta potential measurements of polymer dispersions can be used to predict the mucoadhesive properties of the polymer [103]. Alternately, other methods have been developed to predict bioadhesion/mucoadhesion, including tensile strength tests [104], dynamic techniques [105], and everted-gut sac method [106]. In a tensile strength study, one side of a testing sample is fixed on a stage of a tensile meter, while the other side is contacting with the mucus membrane or gut tissues from an animal (usually mice or rats). Briefly, a tensile strength test is typically used to evaluate the adhesion force of a testing formulation/material. The adhesion force is generally represented as maximum detachment force (the maximum force required to separate the testing sample and the mucus membrane) and work of adhesion (the total area-under-the-curve from the force versus time curve during the adhesion test). Everted gut is another widely used method for evaluating mucoadhesion property of a sample. Everted gut method is especially useful in testing small particles, such as microspheres and small pellets. Briefly, guts from a mouse (or a rat) is freshly excised, everted and cut into 5-10 cm length sacs before test. In one method, testing samples (in a suspension form) are filled into the sac and then submerged into an aqueous medium. In the other method, the samples are dispersed into an aqueous medium first, followed by placing the everted sac into the same medium. After certain period of time, the amount of samples retaining on the everted sac is

quantified and the mucoadhesion property of the sample can then be determined. Dynamic method is another technique for evaluating mucoadhesive property. In this method, a freshly excised gut is placed onto a tilted surface. The gut is continuously flushed over by an aqueous testing medium from the upper end of the tilted surface. The testing samples are then placed onto the gut and mucoadhesion property can be easily determined by observation of the movement of the particles on the gut during the whole process.

However, among these testing methods, only the dynamic method can access the duration of adhesion. Moreover, the dynamic method reflects real-state adhesion performance since both adhesion strengths and zeta-potential measurements are indirect methods for mucoadhesion evaluation [107]. The dynamic method attempts to mimic *in vivo* conditions in terms of temperature, humidity, and liquid flow, and aims to extract information about the influence of a range of parameters on the mucoadhesion process. In addition, the dynamic method is able to evaluate the percent retention of an applied sample on a mucosal surface over time [105], which makes it unique from the traditional adhesion strength test.

1.11 ***Conclusions***

Numerous multiparticulate-based drug delivery systems have been developed in the past two decades for oral vaccination. These formulations showed prominently enhanced immune responses in both systemic and mucosal pathways. Evidence from both *in vitro* cell model and *in vivo* mice studies suggested that olymeric (i.e. PLGA, PLA, and chitosans) micro- and/or nanoparticles of particle sizes less than 10 μm in diameter can

be taken up by M cells in Peyer's patches via phagocytosis and pinocytosis. The particles were then translocated to the lumen side of the gut and elicit a series of immune responses afterward (i.e. secretion of sIgA in the gut and production of serum IgG). However, in spite of these promising *in vitro* and *in vivo* results obtained so far in various multiparticulate-based oral vaccines, the translation of these formulations into the real clinical case still has many challenges. Such as how to scale-up the batch size of the oral vaccines for massive administration, the stability of the formulation, the amount of antigens required to elicit adequate immunity in a real human body, as well as controlling the release of antigen (or the antigen-loaded particles) at the right time to the targeted site.

1.12 Reference

1. Schultz-Cherry, S. and J.C. Jones, Influenza Vaccines: The Good, the Bad, and the Eggs, in Advances in Virus Research, Vol 77, K. Maramorosch, A.J. Shatkin, and F.A. Murphy, Editors. 2010, Elsevier Academic Press Inc: San Diego. p. 63-84.

2. Giudice, E.L. and J.D. Campbell, Needle-free vaccine delivery. Advanced Drug Delivery Reviews, 2006. 58(1): p. 68-89.

3. Kunisawa, J., et al., Characterization of mucoadhesive microspheres for the induction of mucosal and systemic immune responses. Vaccine, 2000. 19(4-5): p. 589-594.

4. Ryan, E.J., L.M. Daly, and K.H.G. Mills, Immunomodulators and delivery systems for vaccination by mucosal routes. Trends in Biotechnology, 2001. 19(8): p. 293-304.

5. Venkatesan, N. and S.P. Vyas, Polysaccharide coated liposomes for oral immunization - development and characterization. International Journal of Pharmaceutics, 2000. 203(1-2): p. 169-177.

6. Kang, M.L., C.S. Cho, and H.S. Yoo, Application of chitosan microspheres for nasal delivery of vaccines. Biotechnology Advances, 2009. 27(6): p. 857-865.

7. Alpar, H.O., et al., Biodegradable mucoadhesive particulates for nasal and pulmonary antigen and DNA delivery. Advanced Drug Delivery Reviews, 2005. 57(3): p. 411-430.

8. Heritage, P.L., et al., Oral administration of polymer-grafted starch microparticles activates gut-associated lymphocytes and primes mice for a subsequent systemic antigen challenge. Vaccine, 1998. 16(20): p. 2010-2017.

9. Hird, T.R. and N.C. Grassly, Systematic Review of Mucosal Immunity Induced by Oral and Inactivated Poliovirus Vaccines against Virus Shedding following Oral Poliovirus Challenge. Plos Pathogens, 2012. 8(4).

10. Brandtzaeg, P., Mucosal Immunity: Induction, Dissemination, and Effector Functions. Scandinavian Journal of Immunology, 2009. 70(6): p. 505-515.

11. Brandtzaeg, P., MOLECULAR AND CELLULAR ASPECTS OF THE SECRETORY IMMUNOGLOBULIN SYSTEM. Apmis, 1995. 103(1): p. 1-19.

12. Faubion, W.A. and C. Fiocchi, Gut immunity and inflammatory bowel disease, in Pediatric Inflammatory Bowel Disease. 2008, Springer US. p. 15.

13. Hanson, L.A., et al., Breast-feeding, a complex support system for the offspring. Pediatrics International, 2002. 44(4): p. 347-352.

14. Mishra, N., et al., Recent advances in mucosal delivery of vaccines: role of mucoadhesive/biodegradable polymeric carriers. Expert Opinion on Therapeutic Patents, 2010. 20(5): p. 661-679.

15. Wikingsson, L.D. and I. Sjoholm, Polyacryl starch microparticles as adjuvant in oral immunisation, inducing mucosal and systemic immune responses in mice. Vaccine, 2002. 20(27-28): p. 3355-3363.

16. Li, X.Y., et al., Chitosan-alginate microcapsules for oral delivery of egg yolk immunoglobulin (IgY): Effects of chitosan concentration. Applied Biochemistry and Biotechnology, 2009. 159(3): p. 778-787.

17. Tabata, Y., Y. Inoue, and Y. Ikada, Size effect on systemic and mucosal immune responses induced by oral administration of biodegradable microspheres. Vaccine, 1996. 14(17-18): p. 1677-1685.

18. Mitragotri, S., Immunization without needles. Nature Reviews Immunology, 2005. 5(12): p. 905-916.

19. Jain, S., et al., Nanocarriers for Transmucosal Vaccine Delivery. Current Nanoscience, 2011. 7(2): p. 160-177.

20. Fievez, V., et al., Targeting nanoparticles to M cells with non-peptidic ligands for oral vaccination. European Journal of Pharmaceutics and Biopharmaceutics, 2009. 73(1): p. 16-24.

21. Salamat-Miller, N. and T.P. Johnston, Current strategies used to enhance the paracellular transport of therapeutic polypeptides across the intestinal epithelium. International Journal of Pharmaceutics, 2005. 294(1-2): p. 201-216.

22. Hu, Y., T.M. Yang, and X.M. Hu, Novel polysaccharides-based nanoparticle carriers prepared by polyelectrolyte complexation for protein drug delivery. Polymer Bulletin, 2012. 68(4): p. 1183-1199.

23. Oyarzun-Ampuero, F.A., et al., Chitosan-coated lipid nanocarriers for therapeutic applications. Journal of Drug Delivery Science and Technology, 2010. 20(4): p. 259-265.

24. Rajapaksa, T.E., et al., Claudin 4-targeted protein incorporated into PLGA nanoparticles can mediate M cell targeted delivery. Journal of Controlled Release, 2010. 142(2): p. 196-205.

25. Berner, V.K., M.E. Sura, and K.W. Hunter, Conjugation of protein antigen to microparticulate beta-glucan from Saccharomyces cerevisiae: a new adjuvant for intradermal and oral immunizations. Applied Microbiology and Biotechnology, 2008. 80(6): p. 1053-1061.

26. Holmgren, J. and C. Czerkinsky, Mucosal immunity and vaccines. Nature Medicine, 2005. 11(4): p. S45-S53.

27. van der Lubben, I.M., et al., Chitosan microparticles for mucosal vaccination against diphtheria: oral and nasal efficacy studies in mice. Vaccine, 2003. 21(13-14): p. 1400-1408.

28. Deaizpurua, H.J. and G.J. Russelljones, Oral vaccination - Identification of classes of proteins that provoke an immune-response upon oral-feeding. Journal of Experimental Medicine, 1988. 167(2): p. 440-451.

29. Moyle, P.M., et al., Mucosal immunisation: Adjuvants and delivery systems. Current Drug Delivery, 2004. 1(4): p. 385-396.

30. Shalaby, W.S.W., Development of oral vaccines to stimulate mucosal and systemic immunity - Barriers and novel strategies. Clinical Immunology and Immunopathology, 1995. 74(2): p. 127-134.

31. Spahn, T.W. and T. Kucharzik, Modulating the intestinal immune system: the role of lymphotoxin and GALT organs. Gut, 2004. 53(3): p. 456-465.

32. Hashizume, T., et al., Peyer's patches are required for intestinal immunoglobulin A responses to Salmonella spp. Infection and Immunity, 2008. 76(3): p. 927-934.

33. Hussain, N., V. Jaitley, and A.T. Florence, Recent advances in the understanding of uptake of microparticulates across the gastrointestinal lymphatics. Advanced Drug Delivery Reviews, 2001. 50(1-2): p. 107-142.

34. Kararli, T.T., Comparison of the gastrointestinal anatomy, physiology, and biochemistry of humans and commonly used laboratory-animals. Biopharmaceutics & Drug Disposition, 1995. 16(5): p. 351-380.

35. Yeh, P.Y., H. Ellens, and P.L. Smith, Physiological considerations in the design of particulate dosage forms for oral vaccine delivery. Advanced Drug Delivery Reviews, 1998. 34(2-3): p. 123-133.

36. Neutra, M.R., et al., Transport of membrane-bound macromolecules by m-cells in follicle-associated epithelium of rabbit Peyer's patch. Cell and Tissue Research, 1987. 247(3): p. 537-546.

37. Bhattacharjee, S., et al., Cytotoxicity and cellular uptake of tri-block copolymer nanoparticles with different size and surface characteristics. Particle and Fibre Toxicology, 2012. 9.

38. Eldridge, J.H., et al., Controlled vaccine release in the gut-associated lymphoid-tissues .1. Orally-administered biodegradable microspheres target the Peyer's patches. Journal of Controlled Release, 1990. 11(1-3): p. 205-214.

39. Beier, R. and A. Gebert, Kinetics of particle uptake in the domes of Peyer's patches. American Journal of Physiology-Gastrointestinal and Liver Physiology, 1998. 275(1): p. G130-G137.

40. Dewit, M.A. and E.R. Gillies, A Cascade Biodegradable Polymer Based on Alternating Cyclization and Elimination Reactions. Journal of the American Chemical Society, 2009. 131(51): p. 18327-18334.

41. Prior, S., et al., *In vitro* phagocytosis and monocyte-macrophage activation with poly(lactide) and poly(lactide-co-glycolide) microspheres. European Journal of Pharmaceutical Sciences, 2002. 15(2): p. 197-207.

42. Severino, P., et al., Biodegradable Synthetic Polymers: Raw-Materials and Production Methods of Microparticles for Drug Delivery and Controlled Release. Polimeros-Ciencia E Tecnologia, 2011. 21(4): p. 286-292.

43. Della Porta, G., et al., Bacteria microencapsulation in PLGA microdevices by supercritical emulsion extraction. Journal of Supercritical Fluids, 2012. 63: p. 1-7.

44. Mata, E., et al., Enhancing immunogenicity to PLGA microparticulate systems by incorporation of alginate and RGD-modified alginate. European Journal of Pharmaceutical Sciences, 2011. 44(1-2): p. 32-40.

45. Mainardes, R.M., N.M. Khalil, and M.P.D. Gremiao, Intranasal delivery of zidovudine by PLA and PLA-PEG blend nanoparticles. International Journal of Pharmaceutics, 2010. 395(1-2): p. 266-271.

46. Takami, T. and Y. Murakami, Development of PEG-PLA/PLGA microparticles for pulmonary drug delivery prepared by a novel emulsification technique assisted with amphiphilic block copolymers. Colloids and Surfaces B-Biointerfaces, 2011. 87(2): p. 433-438.

47. Liu, M.X., et al., Anti-inflammatory effects of triptolide loaded poly(D,L-lactic acid) nanoparticles on adjuvant-induced arthritis in rats. Journal of Ethnopharmacology, 2005. 97(2): p. 219-225.

48. Nayak, B., et al., Formulation, characterization and evaluation of rotavirus encapsulated PLA and PLGA particles for oral vaccination. Journal of Microencapsulation, 2009. 26(2): p. 154-165.

49. Huang, Y.Y., T.W. Chung, and T.W. Tzeng, A method using biodegradable polylactides polyethylene glycol for drug release with reduced initial burst. International Journal of Pharmaceutics, 1999. 182(1): p. 93-100.

50. Sunoqrot, S., et al., Temporal Control over Cellular Targeting through Hybridization of Folate-targeted Dendrimers and PEG-PLA Nanoparticles. Biomacromolecules, 2012. 13(4): p. 1223-1230.

51. Ren, J.M., et al., PELA microspheres loaded H-pylori lysates and their mucosal immune response. World Journal of Gastroenterology, 2002. 8(6): p. 1098-1102.

52. Mercier, G.T., et al., Oral immunization of rhesus macaques with adenoviral HIV vaccines using enteric-coated capsules. Vaccine, 2007. 25(52): p. 8687-8701.

53. Lameiro, M.H., et al., Encapsulation of adenoviral vectors into chitosan-bile salt microparticles for mucosal vaccination. Journal of Biotechnology, 2006. 126(2): p. 152-162.

54. Cui, F.D., et al., Preparation and *in vitro* evaluation of pH, time-based and enzyme-degradable pellets for colonic drug delivery. Drug Development and Industrial Pharmacy, 2007. 33(9): p. 999-1007.

55. Okhamafe, A.O., et al., Modulation of protein release from chitosan-alginate microcapsules using the pH-sensitive polymer hydroxypropyl methylcellulose acetate succinate. Journal of Microencapsulation, 1996. 13(5): p. 497-508.

56. Tawde, S.A., et al., Formulation and evaluation of oral microparticulate ovarian cancer vaccines. Vaccine, 2012. 30(38): p. 5675-5681.

57. Muzzarelli, R.A.A., Human enzymatic activities related to the therapeutic administration of chitin derivatives. Cellular and Molecular Life Sciences, 1997. 53(2): p. 131-140.

58. Hsu, L.W., et al., Elucidating the signaling mechanism of an epithelial tight-junction opening induced by chitosan. Biomaterials, 2012. 33(26): p. 6254-6263.

59. Meng, J.N., T.F. Sturgis, and B.B.C. Youan, Engineering tenofovir loaded chitosan nanoparticles to maximize microbicide mucoadhesion. European Journal of Pharmaceutical Sciences, 2011. 44(1-2): p. 57-67.

60. Sandri, G., et al., The role of chitosan as a mucoadhesive agent in mucosal drug delivery. Journal of Drug Delivery Science and Technology, 2012. 22(4): p. 275-284.

61. He, P., S.S. Davis, and L. Illum, *In vitro* evaluation of the mucoadhesive properties of chitosan microspheres. International Journal of Pharmaceutics, 1998. 166(1): p. 75-88.

62. Kotze, A.F., et al., Chitosan for enhanced intestinal permeability: Prospects for derivatives soluble in neutral and basic environments. European Journal of Pharmaceutical Sciences, 1999. 7(2): p. 145-151.

63. Baudner, B.C., et al., Modulation of immune response to group C meningococcal conjugate vaccine given intranasally to mice together with the LTK63 mucosal adjuvant and the trimethyl chitosan delivery system. Journal of Infectious Diseases, 2004. 189(5): p. 828-832.

64. Chen, F., et al., *In vitro* and *in vivo* study of N-trimethyl chitosan nanoparticles for oral protein delivery. International Journal of Pharmaceutics, 2008. 349(1-2): p. 226-233.

65. Tsai, M.L., et al., The storage stability of chitosan/tripolyphosphate nanoparticles in a phosphate buffer. Carbohydrate Polymers, 2011. 84(2): p. 756-761.

66. Coppi, G. and V. Iannuccelli, Alginate/chitosan microparticles for tamoxifen delivery to the lymphatic system. International Journal of Pharmaceutics, 2009. 367(1-2): p. 127-132.

67. Patil, S.B. and K.K. Sawant, Development, optimization and *in vitro* evaluation of alginate mucoadhesive microspheres of carvedilol for nasal delivery. Journal of Microencapsulation, 2009. 26(5): p. 432-443.

68. Li, X.Y., et al., Preparation of alginate coated chitosan microparticles for vaccine delivery. Bmc Biotechnology, 2008. 8.

69. Borges, O., et al., Evaluation of the immune response following a short oral vaccination schedule with hepatitis B antigen encapsulated into alginate-coated chitosan nanoparticles. European Journal of Pharmaceutical Sciences, 2007. 32(4-5): p. 278-290.

70. Nograles, N., et al., Formation and characterization of pDNA-loaded alginate microspheres for oral administration in mice. Journal of Bioscience and Bioengineering, 2012. 113(2): p. 133-140.

71. Longbottom, D. and M. Livingstone, Vaccination against chlamydial infections of man and animals. Veterinary Journal, 2006. 171(2): p. 263-275.

72. Kuklin, N., et al., Induction of mucosal immunity against herpes simplex virus by plasmid DNA immunization. Journal of Virology, 1997. 71(4): p. 8.

73. Kaneko, H., et al., Oral DNA vaccination promotes mucosal and systemiciImmune responses to HIV envelope glycoprotein. Viology, 2000. 267(1): p. 9.

74. Garnier, B., et al., Development of a Platform of Antibody-Presenting Liposomes. Biointerphases, 2012. 7(1-4).

75. Swaminathan, J. and C. Ehrhardt, Liposomal delivery of proteins and peptides. Expert Opinion on Drug Delivery, 2012. 9(12): p. 1489-1503.

76. Tamaddon, A.M., F. Hosseini-Shirazi, and H.R. Moghimi, Preparation of oligodeoxynucleotide encapsulated cationic liposomes and release study with models of cellular membranes. Daru-Journal of Pharmaceutical Sciences, 2007. 15(2): p. 61-70.

77. Wang, D.A., et al., Liposomal oral DNA vaccine (mycobacterium DNA) elicits immune response. Vaccine, 2010. 28(18): p. 3134-3142.

78. Ko, Y.T. and U. Bickel, Liposome-Encapsulated Polyethylenimine/Oligonucleotide Polyplexes Prepared by Reverse-Phase Evaporation Technique. Aaps Pharmscitech, 2012. 13(2): p. 373-378.

79. Channarong, S., et al., Development and Evaluation of Chitosan-Coated Liposomes for Oral DNA Vaccine: The Improvement of Peyer's Patch Targeting Using a Polyplex-Loaded Liposomes. Aaps Pharmscitech, 2011. 12(1): p. 192-200.

80. Ouadahi, S., et al., Liposomal formulations for oral immunotherapy: In-vitro stability in synthetic intestinal media and in-vivo efficacy in the mouse. Journal of Drug Targeting, 1998. 5(5): p. 365-378.

81. Flower, D.R. and Y. Perrie, Immunomic Discovery of Adjuvants and Candidate Subunit Vaccines: Springer.

82. Mann, J.F.S., et al., Optimisation of a lipid based oral delivery system containing A/Panama influenza haemagglutinin. Vaccine, 2004. 22(19): p. 2425-2429.

83. Brewer, J.M., et al., Lipid vesicle size determines the Th1 or Th2 response to entrapped antigen. Journal of Immunology, 1998. 161(8): p. 4000-4007.

84. Mann, J.F.S., et al., Lipid vesicle size of an oral influenza vaccine delivery vehicle influences the Th1/Th2 bias in the immune response and protection against infection. Vaccine, 2009. 27(27): p. 3643-3649.

85. Jain, S., et al., Mannosylated niosomes as adjuvant-carrier system for oral genetic immunization against Hepatitis B. Immunology Letters, 2005. 101(1): p. 41-49.

86. Larhed, A., et al., Starch microparticles as oral vaccine adjuvant: Antigen-dependent uptake in mouse intestinal mucosa. Journal of Drug Targeting, 2004. 12(5): p. 289-296.

87. Stertman, L., E. Lundgren, and I. Sjoholm, Starch microparticles as a vaccine adjuvant: Only uptake in Peyer's patches decides the profile of the immune response. Vaccine, 2006. 24(17): p. 3661-3668.

88. Devriendt, B., et al., Crossing the barrier: Targeting epithelial receptors for enhanced oral vaccine delivery. Journal of Controlled Release, 2012. 160(3): p. 431-439.

89. Gullberg, E., et al., Identification of cell adhesion molecules in the human follicle-associated epithelium that improve nanoparticle uptake into the Peyer's patches. Journal of Pharmacology and Experimental Therapeutics, 2006. 319(2): p. 632-639.

90. D'Souza, B., et al., Oral microparticulate vaccine for melanoma using M-cell targeting. Journal of Drug Targeting, 2012. 20(2): p. 166-173.

91. Chablani, L., S.A. Tawde, and M.J. D'Souza, Spray-dried microparticles: a potential vehicle for oral delivery of vaccines. Journal of Microencapsulation, 2012. 29(4): p. 388-397.

92. Smith, G.P., FILAMENTOUS FUSION PHAGE - NOVEL EXPRESSION VECTORS THAT DISPLAY CLONED ANTIGENS ON THE VIRION SURFACE. Science, 1985. 228(4705): p. 1315-1317.

93. Arap, M.A., Phage display technology - Applications and innovations. Genetics and Molecular Biology, 2005. 28(1): p. 1-9.

94. Yoo, M.K., et al., Targeted delivery of chitosan nanoparticles to Peyer's patch using M cell-homing peptide selected by phage display technique. Biomaterials, 2010. 31(30): p. 7738-7747.

95. Singh, P., et al., Cholera toxin B subunit conjugated bile salt stabilized vesicles (bilosomes) for oral immunization. International Journal of Pharmaceutics, 2004. 278(2): p. 379-390.

96. Lycke, N., Recent progress in mucosal vaccine development: potential and limitations. Nature Reviews Immunology, 2012. 12(8): p. 592-605.

95. Venkatesan, N. and S.P. Vyas, Polysaccharide coated liposomes for oral immunization - development and characterization. International Journal of Pharmaceutics, 2000. 203(1-2): p. 169-177.

96. Kang, M.L., C.S. Cho, and H.S. Yoo, Application of chitosan microspheres for nasal delivery of vaccines. Biotechnology Advances, 2009. 27(6): p. 857-865.

97. Alpar, H.O., et al., Biodegradable mucoadhesive particulates for nasal and pulmonary antigen and DNA delivery. Advanced Drug Delivery Reviews, 2005. 57(3): p. 411-430.

98. Heritage, P.L., et al., Oral administration of polymer-grafted starch microparticles activates gut-associated lymphocytes and primes mice for a subsequent systemic antigen challenge. Vaccine, 1998. 16(20): p. 2010-2017.

99. Wikingsson, L.D. and I. Sjoholm, Polyacryl starch microparticles as adjuvant in oral immunisation, inducing mucosal and systemic immune responses in mice. Vaccine, 2002. 20(27-28): p. 3355-3363.

100. Li, X.-Y., et al., Chitosan-alginate microcapsules for oral delivery of egg yolk immunoglobulin (IgY): Effects of chitosan concentration. Applied Biochemistry and Biotechnology, 2009. 159(3): p. 778-787.

101. Tabata, Y., Y. Inoue, and Y. Ikada, Size effect on systemic and mucosal immune responses induced by oral administration of biodegradable microspheres. Vaccine, 1996. 14(17-18): p. 1677-1685.

102. Holmgren, J. and C. Czerkinsky, Mucosal immunity and vaccines. Nature Medicine, 2005. 11(4): p. S45-S53.

103. Van der Lubben, I.M., et al., Chitosan microparticles for mucosal vaccination against diphtheria: oral and nasal efficacy studies in mice. Vaccine, 2003. 21(13-14): p. 1400-1408.

104. De Aizpurua, H.J. and G.J. Russell-Jones, Oral vaccination identification of classes of proteins that provoke an immune response upon oral feeding. Journal of Experimental Medicine, 1988. 167(2): p. 440-451.

105. Moyle, P.M., et al., Mucosal immunisation: Adjuvants and delivery systems. Current Drug Delivery, 2004. 1(4): p. 385-396.

106. Shalaby, W.S.W., Development of oral vaccines to stimulate mucosal and systemic immunity - barriers and novel strategies. Clinical Immunology and Immunopathology, 1995. 74(2): p. 127-134.

107. Hashizume, T., et al., Peyer's patches are required for intestinal immunoglobulin A responses to Salmonella spp. Infection and Immunity, 2008. 76(3): p. 927-934.

Chapter 2: Research Outline

2.1 Overall Objective

Most currently available vaccines require intravenous (i.v.) or subcutaneous (s.c.) delivery of antigens. Over the past 20 years, numerous studies have assessed the potential of orally delivered antigens on the induction of mucosal and systemic immune responses. In addition, mucosal delivery is the only vaccination route to induce effective B cell class switching and the development of secretory IgA-producing plasma cells. Moreover, mucosal vaccination (delivered via oral or nasal route) has many advantages, including no need for sterile needles, a reduced need for trained personnel, and the ability of inducing both mucosal and systematic immunity. However, the major challenge of oral vaccination is the harsh environment of the gastrointestinal tract and the possibility of orally delivered soluble antigens inducing tolerance rather than immunity. Therefore, protection of the antigens or utilization of a carrier system is required. Our goal is to develop a mucoadhesive, oral delivery platform that could be targeted to the ileum. In order to achieve that, we started by developing a multiparticulate drug/protein delivery platform. Solid Lipid Nanoparticles, SLNs and Protein Coated Microcrystals, PCMCs were manufactured by W/O/W double emulsification solvent evaporation and direct precipitation, respectively. Numerous materials (i.e. lipid matrix, surfactants, protein carrier, and solvent) and manufacturing parameters were investigated to optimize the production of SLNs and PCMCs. The desired size of all these particles was below 5 micrometer in diameter (for M cell uptake). Drug loading capacity % under varied

manufacturing conditions was also evaluated. After the model antigen, bovine serum albumin (BSA) was loaded into the SLNs or PCMCs; mucoadhesive polymers are incorporated and formulated the mixture into pellets. In order to target the formulated pellets to the ileum (where most of the Peyer's patches located), the pellets are then layered with an enteric coating, which is composed of a mixture of Eudragit® FS 30D/Eudragit® L30D-55. In addition, since an increased residence time of a given formulation at the targeted site tends to enhance both absorption and bioavailability of a drug, our second goal was to employ mucoadhesive polymers into the developed platform. To do so, we must first be able evaluate mucoadhesion property *in vitro*. Therefore, we developed our own *in vitro* mucoadhesion testing ramp as an evaluation tool as one of our objectives. Adhesion properties of matrix tablet and pellets (made of potentially mucoadhesive polymers, Methocel® K4M, Carbopol® 934, chitosan, and sodium alginate) were investigated using our testing device. The objective for developing this *in vitro* biorelavent mucoadhesion test ramp was to reduce the use of live animals or excised animal tissues, which was in concord with the 3R's (Replacement, Refinement and Reduction) of animal welfare.

Last but not least, since the main thrust of this project was to manufacture a mucoadhesive multiparticulate platform, which was of potential as an oral vaccination delivery system targeted to the Peyer's patches at the ileum. We planned to develop a suitable animal model using small rodents (i.e. mice and rats). However, the gastric emptying cut-off size was unclear in these small rodents. Therefore, we prepared inert PMMA particles of varied size range (3 different ranges for ICR mice, and 3 different

ranges for SD rats) and labeled them with Tc-99^{m} for scintigraphy studies. The scintiscans were monitored and the gastric emptying cut-off, as well as the emptying rate of different sized particles could be evaluated. After the gastric emptying cut-off was determined, a suitable platform with appropriate particle size could be designed for these small rodents in the future.

2.2 Supporting Objectives

2.2.1 Manufacturing and evaluating mucoadhesive oral vaccine delivery systems composed of solid lipid nanoparticles (SLNs)

The objective of this study was to prepare a nano-sized antigen carrying system composed of solid lipid nanoparticles (SLNs) with bovine serum albumin (BSA) as the model antigen. SLNs were design to target to the ileum and uptake at Peyer's patches. To further enhance the contact time of the delivery system at the epithelium (at ileum), mucoadhesive polymers, Methocel® K4M and Methocel® E15, were incorporated into the platform. The mixture was granulated and spheronized into pellets (1-1.5 mm in diameter). The pellets were then enteric coated to prevent from gastric damage. We presume these nano-structured particles would be released through diffusion from the lipid matric after reaching the ileum and would be taken up by M cells at the Peyer's patches, which will ultimately induce both mucosal and systematic immune response.

2.2.3 Manufacturing and evaluating mucoadhesive oral vaccine delivery systems composed of protein coated microcrystal (PCMC)

In order to assure robustness and reproducibility of the multiple dose platforms, various mucosal immunity is stimulated by administration of antigen directly on the mucosal site where an infection occurs. Antigen is processed by mucosa-associated lymphoid tissue (MALT) in inductive sites where plasma cell precursors are induced. Gut

associated lymphoid tissue (GALT) is one of the major MALT. Peyer's Patches of GALT are responsible for antigen uptake. Peyer's patches are collections of lymphoid tissue containing B and T lymphocytes, as well as macrophages. Antigens are taken up via endocytosis by the Microfold cells (M cells) at the Peyer's patches. Particles less than 5 μm may be transferred to the draining lymph nodes and spleen to stimulate both a mucosal and systemic immune response after uptake by the M cells. Therefore, the aim if this study was to prepare two nano- and microstructured antigen carrying system composed protein coated microcrystals (PCMC) with bovine serum albumin (BSA) as the model antigen. PCMC were design to target to the ileum and uptake at Peyer's patches. To further enhance the contact time of the delivery system at the epithelium (at ileum), mucoadhesive polymers, Methocel® K4M and Methocel® E15, were incorporated into the platform. The mixture was granulated and spheronized into pellets (1-1.5 mm in diameter). The pellets were then enteric coated to prevent from gastric damage. We presume these micro-structured particles would be released through erosion after reaching the ileum and will be taken up by M cells at the Peyer's patches, which will ultimately induce both mucosal and systematic immune response.

2.2.3 Development of a novel *in vitro* mucoadhesion evaluation method

One of the main potential advantages of mucoadhesive dosage forms is to increase retention time and enhance bioavailability. Several feasible methods have been developed to evaluate mucoadhesive polymer containing formulations using *in vitro* studies. However, all the methods introduced have required freshly excised tissue or part of the gastrointestinal tract from live animals. Laws that mandate replacement alternatives, reduction alternatives, and refinement alternatives (the Three Rs) in scientific research have been passed in the United Kingdom, Germany, the Netherlands,

the United States, and the European Union over the past decade. Therefore, our major concern in Specific Aim 1 is to perform an easily controlled, reproducible and straightforward *in vitro* estimation for mucoadhesion study, while avoiding the need to sacrifice animals we developed our own method by using an agar/mucin mixture as our testing platform for adhesion tests, which is in concord with "Replacement alternatives" in the Three Rs for the animal welfare.

2.2.4 Evaluating the gastric emptying size at the pyloric sphincter in rodent models (mice/rats)

Particle size can significantly alter the gastric emptying time. As the major testing animals for biological and pharmaceutical studies, the gastric emptying size at the pyloric sphincter (the maximum size or cut-off size of the particles that can pass through the gastric) of mice and rats is not validated. Therefore, our goal in Specific Aim 2 is using gamma scinitigraphy to evaluate the cut-off size of pyloric sphincter in mice and rats via inert, non-swellable and non-digestible polymethyl methacrylate (PMMA) microspheres, which can possibly provide accurate information for future oral delivery formulation studies in these rodent models.

Chapter 3: Development of an Oral Vaccine Delivery Platform using Solid Lipid Nanoparticles

Abstract

Introduction: Recently, targeted delivery to Peyer's patches has been widely investigated as a possible solution for oral vaccination delivery system. The major advantage of oral vaccination is that it can generate both mucosal and systemic immune response. Moreover, oral vaccination can improve patient compliance, compared to traditional vaccination via injections. Methods: Bovine serum albumin (BSA) was used as the model antigen for the production of solid lipid nanoparticles (SLNs) via W/O/W double emulsification. SLNs particles were controlled at size below 500 nm. SLNs were then formulated into pellets using wet-granulation/spheronization techniques. Finally, the pellets were coated with enteric coat(s) to protect them from gastric fluid and assure drug release occurred at pH above 7.2 (ileum targeting). To further enhance the residence time of the formulation at the targeted site, mucoadhesive polymers, Methocel K4M, was tailed into the formulation. Results: In the present study, all SLNs were manufactured with particle size less than 7 micrometers. To produce SLNs less than 500 nm, Gelucire® 50/13 was used as the lipid matrix with lecithin as the surfactant. The encapsulation efficiency % of BSA was slightly less than 10%, due to the high water solubility of BSA. BSA was entrapped in the lipid matrix and sustain released through diffusion. Only about 60% of BSA release in 2 hours in pH 7.2 phosphate buffer. The BSA/SLNs was successfully tailed into 1-2 mm pellets by wet-granulation/spheronization. After coated with a double-layered enteric coating using a mixture of Eudragit® L 30 D-55 and

Eudragit® F S 30 D, no BSA released at gastric condition for at least 2 hours, followed by about 60% of BSA released in 2 hours after pH was adjusted to 7.2 from 1.2, which confirmed that the formation was proper for ileum targeted delivery. Finally, mucoadhesive polymer, Methocel® K4M (5%, w/w) was incorporated into the pellets to enhance the residence time of the pellets after they reach ileum. Conclusions: SLNs could be a suitable platform for oral vaccination delivery system, for that the particle size of SLNs could be controlled below 500 nm. With proper enteric coating, BSA/SLNs loaded pellets could be manufactured for ileum targeted delivery.

3.1 Introduction

Globally, vaccination is estimated to save approximately 3 million lives every year unfortunately; however, 3 million lives are still lost to vaccine-preventable diseases. One contributing factor to that lack of vaccine availability is due to their inherent thermal instability, which results in the wastage of half of all supplied vaccines worldwide [1]. Vaccine wastage is especially acute in developing countries; however, improper storage has also been reported in temperate countries and in the developed world [2, 3].

Most pathogenic microorganisms infect via mucosal surfaces [4]. In order to protect against such pathogens, induction of the mucosal immune response is required as the critical first-line defense mechanism [4]. An antigen itself, when orally administered, cannot maintain its integrity through the acidic gastric contents, and subsequently can't be taken up by a suitable lumen enterocyte [5]. However, when the antigens are loaded into specific carriers (e.g. biodegradable polymers, such as PLG and PLGA), it has been demonstrated that these antigens can be uptake and transported over the barrier by M-

cells in Peyer's patches [6, 7]. Uptake by these cells is ideally suited to particles sized less than 5 μm in diameter [8]. Peyer's patches are a collection of organized lymphoid tissues lining the intestinal tract, which are the most important units of gut-associated lymphoid tissues (GALT). Peyer's patches are the primary induction sites for mucosal immunity, which regulates IgA immunity against antigens that enter via the oral route [9].

Although most of the currently available vaccines are administered via injection, there are several drawbacks, which including patience compliance, higher cost, and the necessary requirement of low temperature during storage and transportation [10, 11]. Importantly, it has been reported that most of the antibodies induced following the parenteral administration of vaccines cannot reach mucosal surfaces where pathogenic infections take place [12]. Therefore, oral vaccination is considered an attractive alternative to the standard route of administration and it has generated much research interest [13, 14]. Oral vaccination is potentially a patient compliant and efficient way of inducing both mucosal and systemic immunity. In addition, a local effect of secretory IgA (sIgA) that are induced at the mucosal sites can further prevent attachment of bacteria and viruses to mucosa, and neutralize viruses and toxins than can damage the host cells [15].

Microencapsulation and nano-encapsulation techniques can involve coating and isolating bioactive substances in envelopes of protective materials until such time as their activity is needed (after reaching the specific site, e.g. ileum, or colon [16, 17]). These particulates carrier systems include polymeric hydrogels [18], nanoparticles/microspheres

[19-21], and lipid-based drug delivery systems (e.g. fat emulsions [22], liposomes [23, 24], and solid lipid nanoparticles (SLN) [25]. Unlike most polymeric microsphere and nanoparticle systems, SLN production techniques do not require potentially toxic organic solvents, which generally, have deleterious effect on protein or peptides (e.g. deformation of the protein structure, degradation of the protein). Both hydrophilic and lipophilic drugs can be loaded into SLNs. The lipid matrix of SLNs not only protects the loaded labile ingredients, but also can modulate drug release [26]. In addition, the lipophilic nature of the lipid carrier itself may exhibit certain absorption promoting effects [27, 28].

In order to enhance the oral bioavailability of poor-soluble drugs and/or protein (peptides), a prolonged residence time is required [29]. Mucoadhesive materials are able to adhere onto the mucus membrane at the gastrointestinal tract, which contributes to an increased absorption, due to the prolonged residence time [30, 31]. Therefore, a nano- or microstructured, mucoadhesive multiparticulate drug delivery system could consequently lead to higher efficiency. In this research we describe the development of multiparticulate oral vaccine delivery systems consisting of suitable mucoadhesive polymers with a layered enteric coating that is intended to be suitable for ileum-targeted delivery.

3.2 Materials and methods

3.2.1 Materials

Bovine serum albumin and soybean lecithin was purchased from Spectrum Chemicals Ltd. (Gardena, CA, USA). Ethyl acetate, methylene chloride, isopropyl acetate, and propyl acetate were obtained from Fisher Scientific International (Hampton, NH, USA). Gelucire® 44/14, Gelucire® 50/13, Compritol® 888 ATO, and Precirol® ATO

5 were kindly provided by Gattefosse Corporation (Paramus, NJ, USA). Pluronic® F68 and Pluronic® F127 was kindly provided by BASF Corporation (Florham Park, NJ, USA). Eudragit® FS 30 D, Eudragit® S-100, and Eudragit® L 30 D-55 were kindly donated from Evonik Degussa Corporation (Parsippany, NJ, USA). Avicel® PH101 was kindly donated by FMC Corporation (Philadelphia, Pennsylvania, USA). A Bradford protein assay kit was purchased from Bio-Rad Laboratories (Hercules, CA, USA). All the chemicals and solvents used were of analytical grade.

3.2.2 Methods

3.2.2.1 Selection of solid lipids

Due to the hydrophilic nature of BSA, W/O/W double emulsification was selected to prepare solid lipid particles in the study. A number of preliminary experiments are conducted in order to select the most appropriate conditions for nanoparticle formation. Physicochemical data of the selected solvent is listed in Table 3.1.

Table 3.1: Physicochemical and toxicity properties of solvents used in W/O/W preparation

Solvent	**bp (°C)**	**Water solubility (20°C)**	**DL_{50} (rat, mg/kg**
Ethyl acetate	76	150.4	5620
Methylene chloride	40	13.4	1600
Isopropyl acetate	88	30.9	6750
Propyl acetate	101	18.9	9370

Solubility of the employed lipids in different solvents will be investigated. Briefly, 0.1 ml of milli-Q water (inner aqueous phase) are added to a 1 mL solvent containing 100 mg of lipid and surfactant (oil phase). This mixture was dispersed with an ultrasonic probe to form a W/O emulsion. A double emulsion W/O/W is formed after addition of different volumes of the outer aqueous phase to the previous W/O emulsion followed by

another sonication cycle. This double emulsion was then diluted to 10 mL. The solvent was then evaporated with continuous stirring. The influence of variables, including the volume of the outer aqueous phase, types of surfactant, and surfactant concentration on the particle size distribution of nanoparticle suspensions was evaluated. After determination of the optimal manufacturing conditions, the physicochemical properties of nanoparticles were then characterized (Section 3.2.2.3).

3.2.2.2 Preparation of BSA loaded solid lipid nanoparticles

BSA-loaded SLNs were prepared by W/O/W double emulsion–solvent evaporation technique as previously described (Section 2.2.1). The composition and manufacturing conditions of SLNs were listed in Table 3.2. Briefly, 25 mg BSA was dissolved in 1 mL milli-Q water. The protein solution was emulsified in 5 mL solvent containing 500 mg dissolved lipid with an emulsifier (soy bean lecithin) using probe sonication over an ice bath. The resulting emulsion was further emulsified into an additional surfactant solution comprised of 2% Pluronic® F68, followed by further sonication using the condition previously described for the formation of a W/O/W double emulsion. The organic solvent in the double emulsion was eliminated by evaporation with continuous stirring for 3–5 hours. The nanoparticles were collected by centrifugation at 12,000 rpm for 30 minutes at 4 □C, and washed three times with distilled water. The SLNs were suspended in 5 mL distilled water and lyophilized for 24 hours. The control nanoparticles were prepared in the same way except 1 mL milli-Q water was used instead of 1 mL protein solution.

Table 3.2: The composition and manufacturing condition and labeling of SLNs.

SLNs #	Lipid matrix	Surfactant	BSA added	Sonication power (w)	Sonication Time (sec)
SLNs 1	Gelucire® 50/13, 500mg	Lecithin, 25mg	25mg	20	30
SLNs 2	Gelucire® 50/13, 500mg	Lecithin, 25mg	25mg	50	30
SLNs 3	Gelucire® 50/13, 500mg	Lecithin, 25mg	25mg	80	30
SLNs 4	Gelucire® 50/13, 1000mg	Lecithin, 50mg	50mg	50	30
SLNs 5	Gelucire® 50/13, 250mg	Lecithin, 12.5mg	12.5mg	50	30
SLNs 6	Gelucire® 50/13, 250mg	Lecithin, 25mg	12.5mg	50	30
SLNs 7	Compritol 888®, 500mg	Lecithin, 25mg	25mg	50	30
SLNs 8	Preciol ATO® 5, 500mg	Lecithin, 25mg	25mg	50	30

3.2.2.3 Physicochemical characteristics of SLNs

3.2.2.3.1 Particle size distribution

The size of the nanoparticles, (as well as the particle size distribution of each formulation) was measured using a Zetasizer Nano ZS by photon correlation spectroscopy (PCS) ((Malvern Instruments Ltd, Worcestershire, UK).

3.2.2.3.2 Zeta potential

SLNs were re-suspended in milli-Q water. Zeta potential of the nanoparticles was investigated using a Zetasizer Nano ZS by Laser Doppler Anemometry (Malvern Instruments Ltd, Worcestershire, UK).

3.2.2.4 BSA loading capacity of SLNs

The content of BSA in nanoparticles was determined indirectly by measuring the protein that was not encapsulated. The concentration of protein in the aqueous phase was determined by Bradford Assay. The encapsulation efficiency was calculated by formula (1):

$$EE\,(\%) = \frac{\text{wt. of protein used} - \text{wt. of free protein}}{\text{wt. of protein used}} \times 100 \quad (1)$$

3.2.2.5 In vitro release of antigen loaded SLNs

Loaded SLNs were isolated from non-encapsulated BSA by ultracentrifugation (85,000 rpm) and re-suspension in PBS. Particles were incubated for 24 hour at 37□C. At time intervals of 1, 2, 4, and 24 hours, a sample aliquot was collected and ultracentrifugated for 1 hour at 85,000 rpm. BSA content in the supernatant was determined by Bradford Assay.

3.2.2.6 Pellets manufacturing

Optimization of the pellet formulations was done using an easily detectable marker drug, theophylline via extrusion/spheronization technique [32]. Detailed pellet compositions were listed in Table 3.3. Briefly, SLNs were re-suspended with milli-Q water. SLN suspensions were pre-blended with MCC (Avicel® PH 101), and lactose (Total weight of mixture: 250 mg) for 5 minutes as the filler. A mucoadhesive polymer solution (Methocel® K4M and Methocel® E15) was added into the mixture and granulated for another 5 minutes. The mixture was then transferred into a Luwa Benchtop Granulator (LCI Corporation, Charlotte, NC, USA) and extruded into granules. The resultant granules were then transferred into a Caleva, Model 250 bench-top spheronizer (Caleva Process Solutions Ltd., Sturminster Newton UK) and spheronized into pellets.

The pellets were dried in oven overnight at 40℃and stored in a desiccator at room temperature prior to further testing. Pellets in the size range of 1.0-1.5 mm were used in subsequent studies.

Table 3.3: Composition of pellets

*For BSA (PCMC) loaded pellets, the compositions of pellet 1-4 are exactly the same, except that the API was replaced by BSA/PCMC

Pellet #	API: Theophylline, w/w	Avicel® PH 101, w/w	Kollidon® CL, w/w	Lactose, w/w	Methocel®, K4M, w/w	Methocel®, E15, w/w
Pellet 1	10%	40%	0%	50%	0%	0%
Pellet 2	10%	40%	10%	40%	0%	0%
Pellet 3	10%	40%	10%	30%	0%	10%
Pellet 4	10%	40%	10%	35%	5%	0%

3.2.2.7 Enteric coating of pellets

After manufacturing, the pellets were further coated with an enteric coat (a mixture of Eudragit® FS 30 D/Eudragit® L 30 D-55 to affect the release profile) using fluid-bed coating method [32]. The composition the three different enteric coating solution compositions were listed in Table 3.4.

Table 3.4: Composition of enteric coating solutions

Enteric coating 1	Eudragit LD30-55			Eudragit FS 30 D			TEC *			Polysorbate 80 (33% w/w aq.) **			Glyceryl Monostearate		
Coating solution	Total (g)	Dry (g)	/100g	Total (g)	Dry (g)	/100g	Total (g)	Dry (g)	% w/w	Total (g)	Dry (g)	% w/w	Total (g)	Dry (g)	/100g
	21.2	6.4		32	9.6		1.3	1.3	20	1.6	0.5	3.1	1.3	1.3	8.1

Enteric coating 2	Eudragit LD30-55			TEC			Citric Acid			Talc		
Inner coating solution (neutralized to pH 5.6)	Total (g)	Dry (g)	/100g	Total (g)	Dry (g)	% w/w	Total (g)	Dry (g)	% w/w	Total (g)	Dry (g)	% w/w
	21.0	6.3		0.32	0.32	5	0.95	0.95	15	3.1	3.1	50
Outer coating solution	Eudragit LD30-55			TEC			Talc					
	Total (g)	Dry (g)	/100g	Total (g)	Dry (g)	% w/w	Total (g)	Dry (g)	% w/w			
	41.67	12.5		1.25	1.25	10	6.25	6.25	50			

Enteric coating 3	Eudragit LD30-55			TEC			Citric Acid			Talc					
Inner coating solution (neutralized to pH 5.6)	Total (g)	Dry (g)	/100g	Total (g)	Dry (g)	% w/w	Total (g)	Dry (g)	% w/w	Total (g)	Dry (g)	% w.w			
	21.0	6.3		0.32	0.32	5	0.95	0.95	15	3.1	3.1	50			
Outer coating solution	Eudragit LD30-55			Eudragit FS 30 D			TEC			Polysorbate 80 (33% w/w aq.)			Glyceryl Monostearate		
	Total (g)	Dry (g)	/100g	Total (g)	Dry (g)	/100g	Total (g)	Dry (g)	% w/w	Total (g)	Dry (g)	% w/w	Total (g)	Dry (g)	% w/w
	21.2	6.4		32	9.6		1.3	1.3	20	1.6	0.5	3.1	1.3	1.3	8.1

*: w/w % ratio related to polymer content.

**: w/w % ratio related to polymer content.

Briefly, the pellets were put in the coating chamber of Strea-1 (Aeromatic-Fielder, Bubendorf, Switzerland) fluidized-bed coater (bottom set-up and a Wurster column). The operating conditions were set as follows: atomized air pressure; 2 bar; outlet air temperature: 30℃. The coating dispersion was stirred continuously during spraying. After coating, the pellets were dried in the bed at the same temperature for 10 minutes and then put in an oven at 40℃ for 2 hours. The target weight gains after coating were 5%, 10%, and 20% (w/w). After the coating conditions were optimized using theophylline-based pellets, BSA loaded SLNs suspension was introduced into the final pellet formulations to replace theophylline as the API. Briefly, BSA loaded SLNs were re-suspended in milli-Q water and used as the binder solution in the wet-granulation/pelletization process as previously described. After manufacturing, BCA/PCMC containing pellets were enteric coated in the exactly same manner as we coated the theophylline pellets.

3.2.2.8 In vitro release of BSA loaded pellets

BSA release from coated pellets was determined using a USP Ⅱ dissolution apparatus [33]. Pellets were added to 900 mL 0.1N HCl (pH 1.2) at 37 °C. The paddle speed was set at 100 rpm. At each time point (10, 30, 60, 90, and 120 min), a 5 mL sample was taken and the same volume of simulated gastric fluid was replaced. After 2 hours, the dissolution medium was replaced with 900 mL phosphate buffers (pH 7.2). Additional samples were taken at 3, 4, and 5 hours. Samples were analyzed by Bradford assay according to Bradford [34]. Dissolution tests were repeated six times for all formulations and the release profile of BSA was evaluated.

3.2.3 Statistics

All results were shown as mean ± standard deviation (N=6). Analysis of variance (ANOVA), Turkey's HSD or Wilcoxon test is used to evaluate the results via JMP 7.0 software (JMP, Cary, NC, USA). $p < 0.05$ was considered to be a significant difference.

3.3. Results and discussion

3.3.1. Physicochemical characteristics of SLNs

After manufacturing, particle size of each formulation of the SLNs was measured by photon correlation spectroscopy (PCS) using Malvern Zetasizer Nano ZS. Particle size (Z-average), polydispersity index (PSD), and zeta-potential were obtained and listed in Table 3.5. In order to obtain a SLN formulations with a smaller particle size (less than 500 nm) and narrower particle size distribution, several different factors were controlled over the manufacturing process, including the type of lipid matrix (Gelucire® 44/14, Gelucire® 50/13, Compritol® 888 ATO, and Precirol® ATO 5), amount of surfactant (lecithin), sonication power, as well as duration of sonication. From the results, only Gelucire® 50/13 was suitable under our SLNs manufacturing protocol. Gelucire® 44/14

emulsified and solidified rapidly once in contact with the ice bath during the sonication process; therefore, was not able to generate SLNs in this case. On the other hand, Compritol® 888 ATO, and Precirol® ATO 5) dissolved well in the solvent, DCM, as Gelucire® 50/13 (Z-average, less than 200 nm), however, the particles created by these two lipid matrix were significantly larger than Gelucire® 50/13 based SLNs ($p<0.05$, Z-average of Compritol® 888 ATO, Precirol® ATO 5, and Gelucire® 50/13 based SLNs was around 3000, 6000, and 190 nm, respectively) (Table 3.5). Therefore, Gelucire® 50/13 was chosen as the final lipid matrix for SLN preparation in the subsequent studies.

Table 3.5: Particle size, PSD, zeta-potential, and encapsulation efficiency % of manufactured SLNs. * N=6, Mean value ± Stdev

SLNs #	Particle size (nm) *	Polydispersity index, PSD*	Zeta-potential (mV)*	Encapsulation %
SLNs 1	269.2 ± 32.4	0.362 ± 0.05	-24.0 ± 1.2	11.12 ± 0.46
SLNs 2	184.5 ± 25.3	0.249 ± 0.03	-24.7 ± 2.3	9.14 ± 0.21
SLNs 3	271.9 ± 51.3	0.363 ± 0.06	-27.2 ± 3.5	12.24 ± 0.36
SLNs 4	579.1 ± 63.1	0.431 ± 0.04	-26.5 ± 2.6	18.62 ± 0.63
SLNs 5	520.8 ± 45.3	0.567 ± 0.1	-32.2 ± 3.2	15.24 ± 0.51
SLNs 6	503.9 ± 41.5	0.463 ± 0.07	-33.7 ± 3.4	13.98 ± 0.62
SLNs 7	3036 ± 625.3	0.331 ± 0.04	-34.1 ± 2.5	22.32 ± 5.41
SLNs 8	6070 ± 1354.6	1.00 ± 0.24	-32.2 ± 2.4	25.64 ± 8.62

In addition, we speculated that the intensity (power) and duration (time) of the sonication process would affect the formation of SLNs and alter the size and encapsulation efficiency % of SLN products. Under a lower sonication intensity of 20 watt (Z-average, approx. 270 nm), SLNs were significantly larger ($p<0.05$), compared those prepared at a power of 50 watt (Z-average, approx. 185 nm). However, when the power was further increased to 80 watt, the particle size was not further reduced (Z-

average, approx. 270 nm). This might due to the instability of SLNs during the emulsification process for that the force applied was too strong. Therefore, we set the sonication intensity at 50 watt and the duration of sonication at 30 seconds using ice to prevent damage or degradation of the BSA. While both particle size and PSD were altered by the intensity of sonication process, zeta-potential was only affected by the type and the amount of lipid matrix that was incorporated into the formulations. With the same amount of lipid matrix used, SLNs composed of Gelucire® 50/13 showed significantly lower zeta-potential ($p<0.05$), compared to Compritol® 888 ATO and Precirol® ATO 5 containing SLNs. However, this was because that the particles generated by both Compritol® 888 ATO and Precirol® ATO 5 were significantly larger than particles generated by Gelucire® 50/13, therefore, more lipid matrix was presented in the formulation, which resulted in a higher negative charge on the surface of SLNs. Due to the high solubility of BSA, the encapsulation efficiency % after SLN manufacturing via W/O/W double emulsification was low. The majority of BSA remains in the aqueous phase during the sonication process, or is partitioned back into the aqueous phase during the solvent-evaporation process. Both of these factors can contribute to the poor encapsulation efficiency. Under our preparation method, the encapsulation efficiency % was affected largely by the size of SLNs, rather than the type lipid matrix, or sonication intensity. Encapsulation efficiency increased with increasing particle size, since more BSA was entrapped in the SLNs. However, one primary goal was to manufacture SLNs with particle size between less than 500 nm and with lower particle size distribution. Based on the results we found, the final optimized SLNs formulation was composed of Gelucire® 50/13 as the lipid matrix. The ratio of Gelucire® 50/13 : Lecithin : BSA was controlled at 20 : 1 : 1, while the sonication process was controlled at 50 watt for duration of 30 seconds on an ice bath.

3.3.2 *In vitro* release of antigen loaded SLNs

After manufacturing, BSA loaded SLNs (Gelucire® 50/13) were weighed and placed in 20 mL vials for a modified dissolution test, in pH 7.2 phosphate buffer as previously described (Section 2.2.5). The BSA release profile (accumulated release %) was shown in Figure 3.1. Almost 50% of BSA released in the first hour of dissolution, while about 75% of BSA released in 2 hours. Approximately 15% of BSA was still entrapped in the lipid matrix up to at least 12 hours. BSA showed complete release in 48 hours.

Figure 3.1: Dissolution of BSA loaded SLNs with Gelucire® 50/13 as lipid matric in pH 7.2 phosphate buffer. * N=6, Mean value ± Stdev

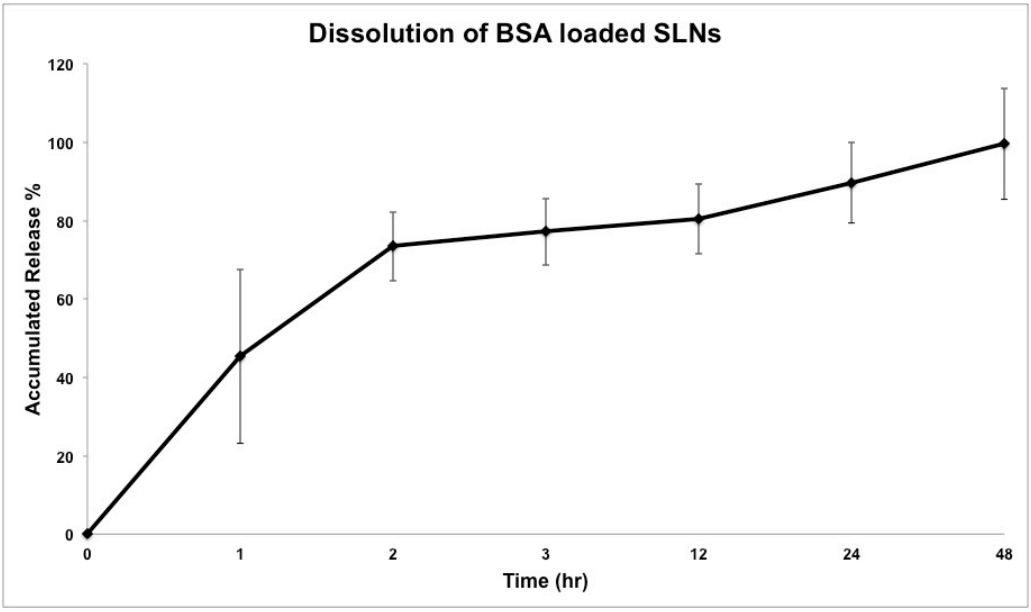

3.3.3 Pellets production

Granulation/pelletization is widely used in oral drug delivery systems [35, 36]. Compared to dry-granulation direct compression (tablets), wet-granulation is more cost-effective, since it can be processed using much less expensive equipment. In addition,

wet-granulation improves free-flowing properties, homogeneity of the powder ingredients, provides better compressibility, and reduces dust during the processing. In a wet-granulation process, the pharmaceutical active ingredient can be either a dry substance or, be dissolved in a medium as a binder solution, which increases the possibility of optimizing a formulation based on the physicochemical property of its API, compared to direct compression. After wet-granulation, the granules can be further processed for direct compression, or extruded before pelletization. In general, pellets offer the well-known benefits of more uniform release and reproducibility of the formulation. This is due to the *in vivo* dispersion of a multiparticulate system, and the gastrointestinal transit in human body. While the gastric emptying transit time of a single solid tablet might range from 30 minutes to a couple hours, the dispersion of a multiparticulate system starts from the gastric and provide a more reproducible overall transit time. Furthermore, wet-granulation/pelletization can be easily scaled-up for industrial manufacturing. In order to produce a more easily handled formation, as well as reducing possible damage during the manufacturing process to the acid labile BSA, Eudragit® S-100 coated PCMC was formulated into the pellets using wet-granulation/pelletization techniques. Eudragit® S-100 coated PCMCs were re-suspended in IPA and used as a binder during the wet-granulation process. MCC (Avicel® PH 101) was used as the filler since it has a well-known advantage of forming an easy moist granulated mass, and generating strong granules on drying.. Since the objective of the study was to design an oral vaccination delivery platform using a multiparticulate system, BSA loaded SLNs were required to release promptly after reaching ileum. To achieve more rapid release Kollidon® CL was added during the wet-granulation/pelletization process to act as a as superdisintegrant. Furthermore, in order to control the release time of BSA loaded SLNs, and synchronize this to the regional position of the GI tract, three

different enteric coating mixtures were evaluated using the easily detectable drug theophylline.

3.3.4 Enteric coating of pellets

The GI tract is a very hostile environment, with regions of lower and higher pH, high enzymatic activity, and lipid solubilizing ability. For ileum targeted drug delivery, it is necessary to traverse an extended section of the lumen whilst not experiencing lost efficacy. A pH solubility dependent coating is effective and well described in the literature [37, 38]. These drug delivery systems utilize polymeric carriers that are insoluble in the low pH media of the upper gastrointestinal tract, but dissolve at a higher, near neutral pH of the distal gut. Such polymers will begin to dissolve in the ileum and as such are more appropriately defined as the materials for ileum targeting. The pH-dependent approach for ileum drug delivery is based on the pH differences along the gastrointestinal tract with values increasing from about 1 to 2.5 in the stomach through 6.6 in the proximal small bowel to a peak of about 7.5 in the terminal ileum [39]. The mean gastric residence time is considered to be 0.25–2 hours and small intestinal residence time between 3 and 4 hours [40]. These conditions are valid for single solid dosage forms and for fasting state of patients. One of the major concerns for this study was to make protein antigens (BSA) release rapidly after the delivery system reached ileum. Therefore, Kollidon® CL was included into the pellets to act as a superdisintegrant. Without superdisintegrant, less than 10% of drug was released at 30 minutes; and only about 45% of the drug was released in 1 hour at pH 7.2 (pellet 1, Figure 3.2). With 10% w/w Kollidon® CL, more than 95% of the drug was released at 30 minutes; and the drug release was completely in less than one hour in pH 7.2 (pellet 2, Figure 3.2). This is potentially appropriate for an ileum targeted oral vaccination delivery system, since once

the pellets reached ileum, all antigens could be released promptly once triggered, rather than passing the targeted site to release in the large bowel. We assumed that with the mucoadhesive polymers, the pellets would adhere onto the targeted site after wetted, which would prevent the pellets from emptying out ileum before drug release [41, 42]. Therefore, mucoadhesive polymer, Methocel® E15 or K4M was included into the fast-disintegrating pellets. However, from the results, with 10% Methocel® E15, only less than 25% of the drug was released in 30 minutes at pH 7.2 (pellet 3, Figure 3.2), while nearly 60% of the drug was released in 30 minutes, when 5% Methocel® K4M was used (pellet 4, Figure 3.2). The release rate of drug was hindered, because of the gel formation of HPMC, which formed a matrix system and controlled the drug release through a combination of diffusion/erosion [43].

Figure 3.2: Dissolution of enteric coated pellets (API: theophylline): Non-coated pellets.
* N=6, Mean value ± Stdev

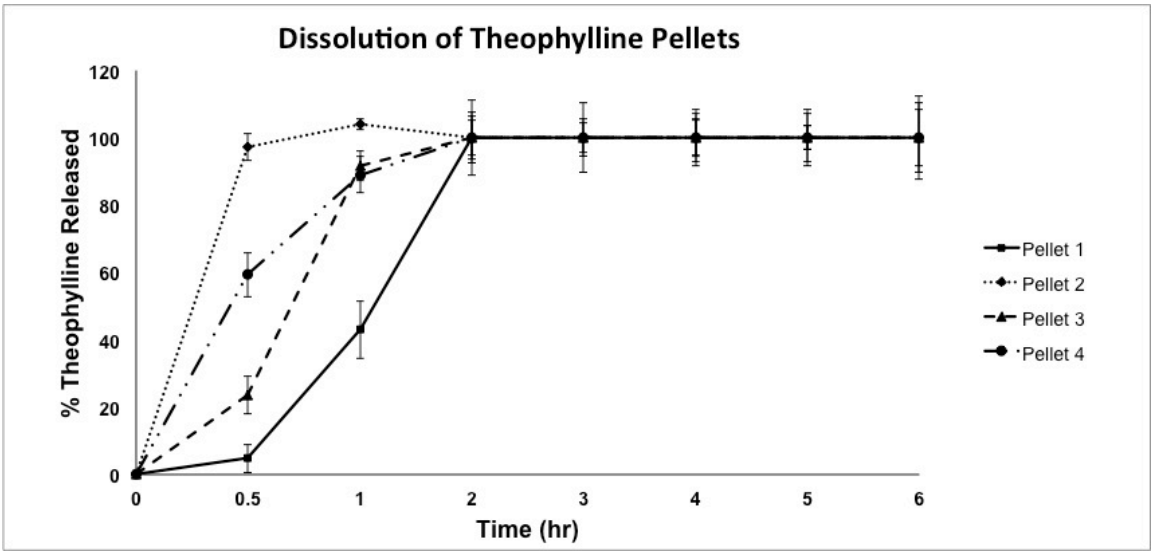

In order to protect the pellets from the stomach, the pellets were adequately coated with suitable enteric coat(s). The focus was to control drug to release at pH > 7.2

(in accordance with the physiological conditions found in the ileum). Eudragit® L and S polymers enable targeting specific areas of the intestine. Eudragit® L 30 D-55 dissolves at pH above 5.5, which is advantageous for drug delivery at the upper intestine [44]; while Eudragit® FS 30D polymer dissolves at pH above 7.0 and is suitable for drug delivery to colon area [45]. The objective was to both prevent drug being released/damaged at gastric pH and prevent drug release along the proximal intestine, followed by a rapid release at ileum. To achieve this, three enteric coating layers were combined in the final formulation. In coating solution 1, a single layer of a mixture of Eudragit® L 30 D-55 and Eudragit® F S 30D (w/w ratio: 2:3) was coated onto the pellets. No drug was found to release for up to 2 hours at pH 1.2, regardless of the amount (weight-gained, % w/w) of enteric coating applied. When applying only 5 % w/w (weight-gained) Eudragit® L 30 D-55 coating to the pellets (including 10% w/w superdisintegrant, Kollidon® CL), more than 90% of the drug released in just one hour after adjusting the pH from 1.2 to 7.2. Nonetheless, after the enteric coating applied increased to 10% w/w (weight-gained), approximately 20% of the drug released at 2 hours, and 90% at 3 hours after adjusting the pH from 1.2 to 7.2 (Figure 3.3). However, without the superdisintegrant, Kollidon® CL, no drug released for up to 2 hours after adjusting the pH from 1.2 to 7.2, while nearly 90% of the drug released at 3 hours, regardless enteric coating level (either 5% or 10%) (Figure 3.3).

Figure 3.3: Dissolution of enteric coated pellets (API: theophylline), Coating solution 1.
* N=6, Mean value ± Stdev

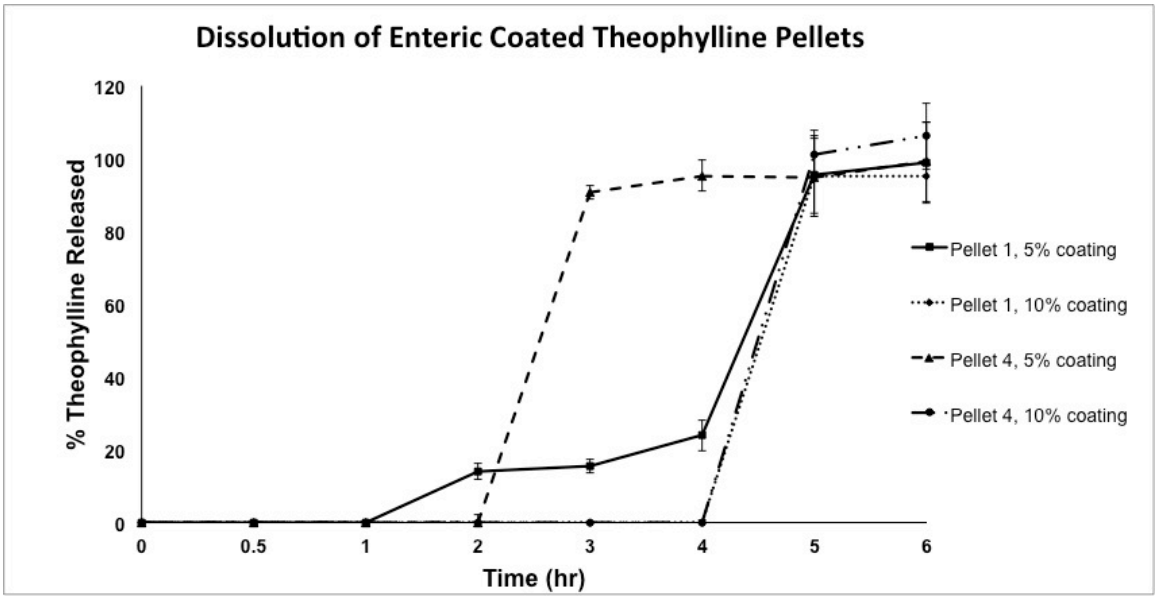

In this study, the second type of enteric coating was comprised of a double-layer enteric coat. The inner coat was composed of Eudragit® L 30 D-55 (neutralized with a pH of 5.6 in the enteric coating suspension). Neutralizing the inner coat would help the rapid release of coated drug, since part of the Eudragit® L 30 D-55 was dissolved during the preparation process of the coating solution. The outer coat was composed of Eudragit® F S 30D as with enteric coating solution 1. With 10% (w/w of the total weight of a pellet) superdisintegrant (Kollidon® CL), nearly 90% of the drug released in less than one hour after the pH was adjusted from 1.2 to 7.2, regardless of the coating level (Figure 3.4). Without Kollidon® CL, about 5% (w/w of the total weight of a pellet) of the drug released with either 5% or 10% (weight-gained, w/w) of the outer coat applied (with 5% w/w weight-gained inner coat) in 2 hours at pH 1.2, which showed non-successful enteric coating under gastric condition.

Figure 3.4: Dissolution of enteric coated pellets (API: theophylline): Coating solution 2.
* N=6, Mean value ± Stdev

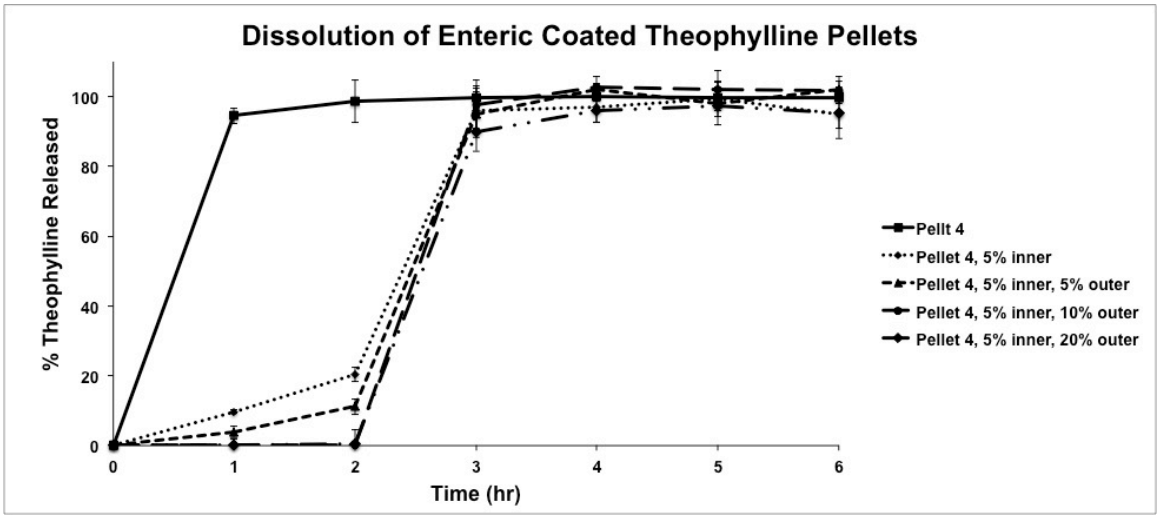

Without Kollidon® CL, about 5% (w/w of the total weight of a pellet) of the drug released with either 5% or 10% (weight-gained, w/w) of the outer coat applied (with 5% w/w weight-gained inner coat) in 2 hours at pH 1.2, which showed non-successful enteric coating under gastric condition. When the outer coat was increased to 20%, no drug released under gastric condition for up to 2 hours, however, more than 90% of the drug released in less than 2 hours after the pH was adjusted from 1.2 to 7.2 (Figure 3.5), which could not be considered as suitable for ileum targeting, as most of the drug would be likely to be released prior to reaching the ileum. The results demonstrated that the pre-neutralization showed a more rapid release of the drug, once the outer enteric coating layer had dissolved; however, the drug released too early and would not be suitable for ileum targeting.

Figure 3.5: Dissolution of enteric coated pellets (API: theophylline, without disintegrant), Coating solution 2. * N=6, Mean value ± Stdev

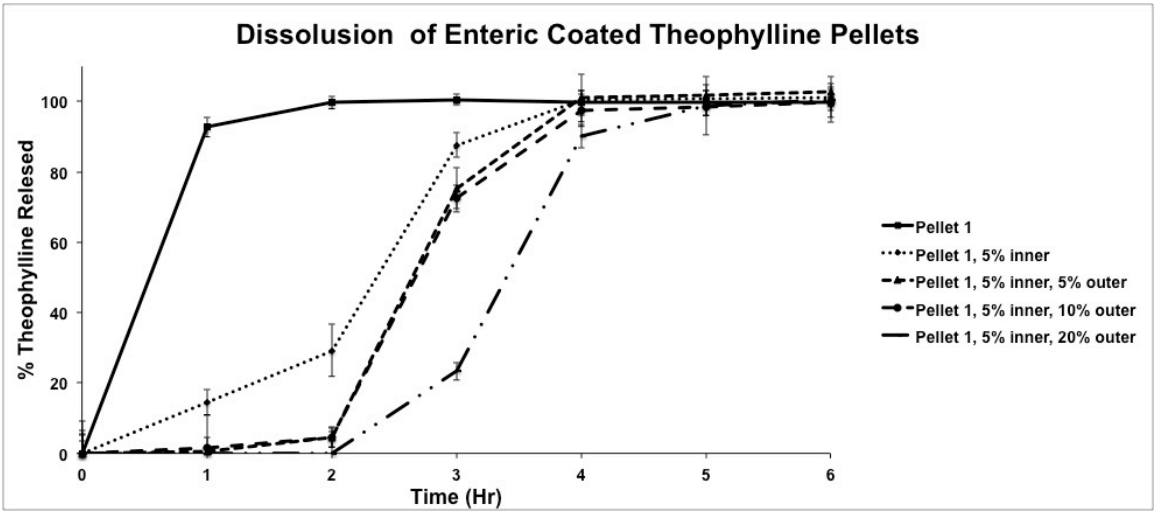

Finally, a third enteric coating solution composed of a modified (from the second type of enteric coating solution) outer layer was prepared. The outer coat was replaced with a mixture of 1:4 w/w ratio of Eudragit® L 30 D-55 and Eudragit® F S 30D, compared to enteric coating solution 2. With 10% (w/w of the total weight of a pellet) superdisintegrant (Kollidon® CL) and 10% (w/w, weight-gained) outer enteric coating (5% w/w, weight-gained inner coat), no drug released for up to 2 hours at pH 1.2 (Figure 3.6). However, more than 50% of the drug released in one hour after the pH was adjusted from 1.2 to 7.2. Nevertheless, after the outer coat was increased to 20% (w/w, weight-gained), the drug was prevented from releasing for one hour after the pH was adjusted from 1.2 to 7.2, followed by about 90% of the drug release in the subsequent hour. This indicates a suitable profile for a potential ileum targeted formulation, since the drug was well-protected against gastric conditions, and could be further protected for about another

hour at pH above 7 (paralleling the transit time from duodenum to the ileum), followed by prompt release of the drug in less than an hour (Figure 3.6).

Figure 3.6: Dissolution of enteric coated pellets (API: theophylline), Coating solution 3. * N=6, Mean value ± Stdev

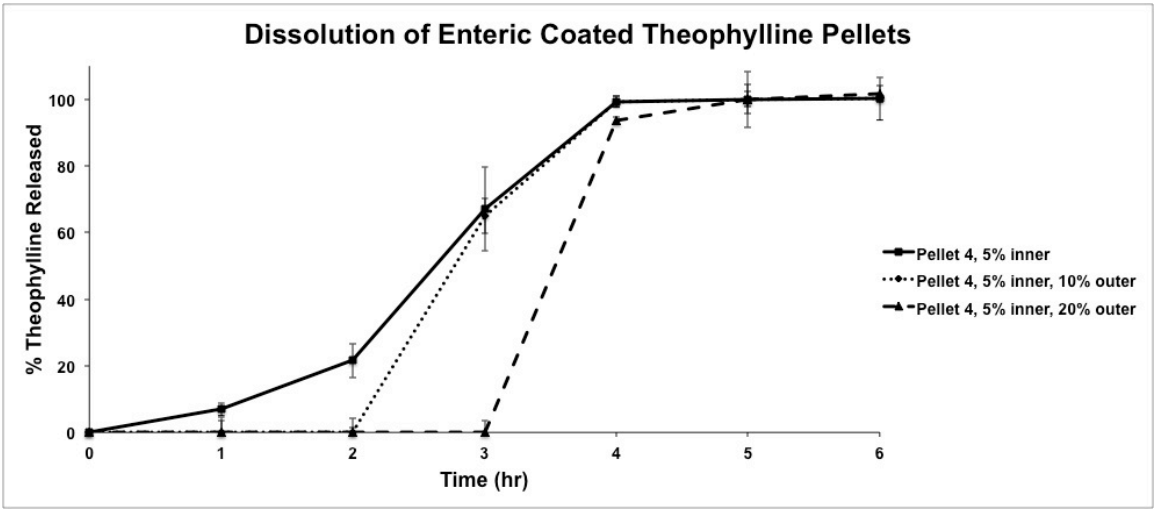

3.3.5 *In vitro* release of BSA/SLNs loaded pellets

When loaded with BSA the results from pellets coated with enteric coating solution 1 and 2 were similar as what we found before when theophylline was used as a marker drug. Pellets coated with enteric coating solution 1 were able to prevent BSA release for more than 2 hours after the dissolution medium was converted to pH 7.2 from pH 1.2 at a coating level of 20% w/w, however, this transit time was too long, and would possible resulted in drug release in the colon area. Additionally, pellets coated with enteric coating solution 2 also not fitting to the targeting goal, since almost all BSA released in less than one hour after the dissolution medium was converted to pH 7.2 from pH 1.2, regardless of the weight-gain added with the enteric coating. These results were again in accordance with what we found in our previous theophylline loaded pellets. BSA/SLNs loaded

pellets (with 5% Methocel® K4M) coated with a double-layer enteric coating (enteric coating 3, 5% w/w weight-gained inner coat and 20% w/w weight-gained outer coat) were suitable for ileum targeted delivery, since no BSA release was found at low pH for at least 2 hours. After the pH was adjusted from 1.2 to 7.2, less than 5% of BSA released after at 3 hours, but a prompt release of BSA occurred in the subsequent hour (up to 60% of BSA released) (Figure 3.7). This was in concordance with gastrointestinal transit from stomach to ileum at fasted state as previously described.

Figure 3.7: Dissolution of enteric coated pellets (loaded with BSA/SLNs): (A) Non-coated pellets; (B) Coating solution 3, 5% inner coat and 10% outer coat; (C) Coating solution 3, 5% inner coat and 20% outer coat. * N=6, Mean value ± Stdev

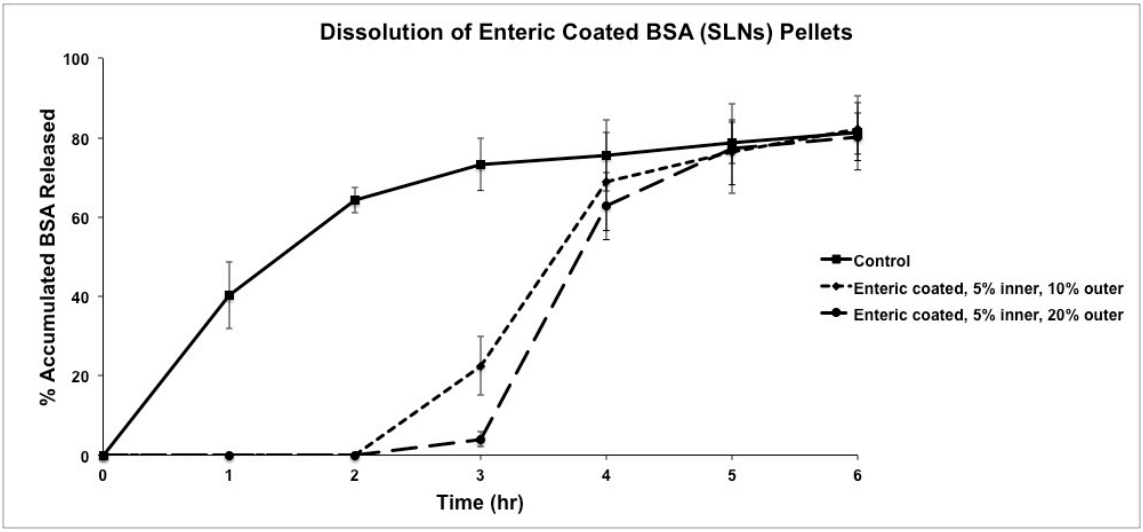

3.4. Conclusions

Nano-particulates platforms can be appropriate for oral protein/peptide drug delivery. However, the acid labile pharmaceutical active ingredients must be well-protected to avoid deactivation/damage in the gastric. In this study, BSA was successfully loaded into SLNs with Gelucire 50/13 as the lipid matrix using a double emulsification

method. The manufacturing process was optimized by screening various parameters (i.e. type of lipid matrix, type of surfactant, sonication speed, and sonication power). In summary, the particle size of SLNs manufactured was proper for oral vaccination delivery systems. The manufactured BSA loaded SLNs were then successfully incorporated into pellets as a potential platform for oral delivery. Furthermore, our study provided proof that with a suitable (a double-layered enteric coating (Eudragit® L 30 D-55 and Eudragit® F S 30D) enteric coating, the release of BSA/SLNs loaded pellets could be well-controlled across the pH range and time that is appropriate for targeted delivery to ileum. In addition, the pH sensitive, well-targeted system we developed could act as a potential platform for a variety of payloads related to protein/peptide or even antigen delivery to the ileum in the future. Nonetheless, further improvement on the enteric coating property is required to help stabilize the platform for long-term storage processes.

3.5 Reference

1. Barder, O. Vaccines for Development. 2006; Available from: http://www.cgdev.org/files/7366_file_Vaccines2.pdf

2. Murdan, S., et al., Immobilisation of vaccines onto micro-crystals for enhanced thermal stability. International Journal of Pharmaceutics, 2005. 296(1-2): p. 117-121.

3. Okeke, I.N., A. Lamikanra, and R. Edelman, Socioeconomic and behavioral factors leading to acquired bacterial resistance to antibiotics in developing countries. Emerging Infectious Diseases, 1999. 5(1): p. 18-27.

4. Kunisawa, J., et al., Characterization of mucoadhesive microspheres for the induction of mucosal and systemic immune responses. Vaccine, 2000. 19(4-5): p. 589-594.

5. Zhou, F. and M.R. Neutra, Antigen delivery to mucosa-associated lymphoid tissues using liposomes as a carrier. Bioscience Reports, 2002. 22(2): p. 355-369.

6. McClean, S., et al., Binding and uptake of biodegradable poly-DL-lactide micro- and nanoparticles in intestinal epithelia. European Journal of Pharmaceutical Sciences, 1998. 6(2): p. 153-163.

7. Torche, A.M., et al., *Ex vivo* and *in situ* PLGA microspheres uptake by pig ileal Peyer's patch segment. International Journal of Pharmaceutics, 2000. 201(1): p. 15-27.

8. Wikingsson, L.D. and I. Sjoholm, Polyacryl starch microparticles as adjuvant in oral immunisation, inducing mucosal and systemic immune responses in mice. Vaccine, 2002. 20(27-28): p. 3355-3363.

9. Hashizume, T., et al., Peyer's patches are required for intestinal immunoglobulin A responses to Salmonella spp. Infection and Immunity, 2008. 76(3): p. 927-934.

10. Bell, K.N., et al., Risk factors for improper vaccine storage and handling in private provider offices. Pediatrics, 2001. 107(6): p. art. no.-e100.

11. Centers for Disease, C. and Prevention, Guidelines for maintaining and managing the vaccine cold chain. MMWR. Morbidity and mortality weekly report, 2003. 52(42): p. 1023-5.

12. Chalmers, W.S.K., Overview of new vaccines and technologies. Veterinary Microbiology, 2006. 117(1): p. 25-31.

13. Challacombe, S.J., et al., Enhanced secretory iga and systemic igg antibody-responses after oral immunization with biodegradable microparticles containing antigen. Immunology, 1992. 76(1): p. 164-168.

14. Maloy, K.J., et al., induction of mucosal and systemic immune-responses by immunization with ovalbumin entrapped in poly(lactide-co-glycolide) microparticles. Immunology, 1994. 81(4): p. 661-667.

15. Bowersock, T.L., et al., Oral vaccination with alginate microsphere systems. Journal of Controlled Release, 1996. 39(2-3): p. 209-220.

16. Gavini, E., et al., Development of solid nanoparticles based on hydroxypropyl-beta-cyclodextrin aimed for the colonic transmucosal delivery of diclofenac sodium. Journal of Pharmacy and Pharmacology, 2011. 63(4): p. 472-482.

17. Krishnamachari, Y., P. Madan, and S.S. Lin, Development of pH- and time-dependent oral microparticles to optimize budesonide delivery to ileum and colon. International Journal of Pharmaceutics, 2007. 338(1-2): p. 238-247.

18. Peppas, N.A., K.M. Wood, and J.O. Blanchette, Hydrogels for oral delivery of therapeutic proteins. Expert Opinion on Biological Therapy, 2004. 4(6): p. 881-887.

19. Ahire, V.J., et al., Chitosan microparticles as oral delivery system for tetanus toxoid. Drug Development and Industrial Pharmacy, 2007. 33(10): p. 1112-1124.

20. Yin, L.C., et al., Drug permeability and mucoadhesion properties of thiolated trimethyl chitosan nanoparticles in oral insulin delivery. Biomaterials, 2009. 30(29): p. 5691-5700.

21. Dupeyron, D., et al., Protein Delivery by Enteric Copolymer Nanoparticles. Journal of Dispersion Science and Technology, 2009. 30(8): p. 1188-1194.

22. Perlman, M.E., et al., Development of a self-emulsifying formulation that reduces the food effect for torcetrapib. International Journal of Pharmaceutics, 2008. 351(1-2): p. 15-22.

23. Werle, M. and H. Takeuchi, Chitosan-aprotinin coated liposomes for oral peptide delivery: Development, characterisation and *in vivo* evaluation. International Journal of Pharmaceutics, 2009. 370(1-2): p. 26-32.

24. Bennett, E., A.B. Mullen, and V.A. Ferro, Translational modifications to improve vaccine efficacy in an oral influenza vaccine. Methods, 2009. 49(4): p. 322-327.

25. Zhang, N., et al., Lectin-modified solid lipid nanoparticles as carriers for oral administration of insulin. International Journal of Pharmaceutics, 2006. 327(1-2): p. 153-159.

26. Basaran, E., et al., Cyclosporine-A incorporated cationic solid lipid nanoparticles for ocular delivery. Journal of Microencapsulation. 27(1): p. 37-47.

27. Zhang, Z., et al., The characteristics and mechanism of simvastatin loaded lipid nanoparticles to increase oral bioavailability in rats. Int J Pharm. 394(1-2): p. 147-53.

28. Liu, D.H., et al., Enhanced gastrointestinal absorption of N-3-O-toluyl-fluorouracil by cationic solid lipid nanoparticles. Journal of Nanoparticle Research. 12(3): p. 975-984.

29. Tao, Y.Y., et al., Development of mucoadhesive microspheres of acyclovir with enhanced bioavailability. International Journal of Pharmaceutics, 2009. 378(1-2): p. 30-36.

30. Dalvadi, H.P., et al., Development and characterization of controlled release mucoadhesive tablets of captopril to increase the residence time in the gastrointestinal tract. Latin American Journal of Pharmacy, 2011. 30(2): p. 266-272.

31. Patel, J., D. Patel, and J. Raval, Formulation and evaluation of propranolol hydrochloride-loaded carbopol-934p/ethyl cellulose mucoadhesive microspheres. Iranian Journal of Pharmaceutical Research, 2010. 9(3): p. 221-232.

32. Song, H.T., et al., Preparation of the traditional Chinese medicine compound recipe heart-protecting musk pH-dependent gradient-release pellets. Drug Development and Industrial Pharmacy, 2002. 28(10): p. 1261-1273.

33. Kim, J.S., et al., Statistical optimization of tamsulosin hydrochloride controlled release pellets coated with the blend of HPMCP and HPMC. Chemical & Pharmaceutical Bulletin, 2007. 55(6): p. 936-939.

34. Bradford, M.M., Rapid and sensitive method for the quantitation of microgram quantities of protein utilizing the principle of protein-dye binding. Anal. Biochem., 1976(72): p. 248-254.

35. Huyghebaert, N., et al., Evaluation of extrusion/spheronisation, layering and compaction for the preparation of an oral, multi-particulate formulation of viable, hIL-10 producing Lactococcus lactis. European Journal of Pharmaceutics and Biopharmaceutics, 2005. 59(1): p. 9-15.

36. Prieto, S.A., J.B. Mendez, and F.J.O. Espinar, Starch-dextrin mixtures as base excipients for extrusion-spheronization pellets. European Journal of Pharmaceutics and Biopharmaceutics, 2005. 59(3): p. 511-521.

37. Patel, M.M. and A.F. Amin, Design and optimization of colon-targeted system of theophylline for chronotherapy of nocturnal asthma. Journal of Pharmaceutical Sciences, 2011. 100(5): p. 1760-1772.

38. Zhu, X., et al., A novel microsphere with a three-layer structure for duodenum-specific drug delivery. International Journal of Pharmaceutics, 2011. 413(1-2): p. 110-118.

39. Mercier, G.T., et al., Oral immunization of rhesus macaques with adenoviral HIV vaccines using enteric-coated capsules. Vaccine, 2007. 25(52): p. 8687-8701.

40. Ibekwe, V.C., et al., Interplay between intestinal pH, transit time and feed status on the *in vivo* performance of pH responsive ileo-colonic release systems. Pharmaceutical Research, 2008. 25(8): p. 1828-1835.

41. Atyabi, F., et al., The impact of trimethyl chitosan on *in vitro* mucoadhesive properties of pectinate beads along different sections of gastrointestinal tract. Drug Development and Industrial Pharmacy, 2007. 33(3): p. 291-300.

42. Bautzova, T., et al., Bioadhesive pellets increase local 5-aminosalicylic acid concentration in experimental colitis. European Journal of Pharmaceutics and Biopharmaceutics, 2012. 81(2): p. 379-385.

43. Khan, J., et al., Preparation and in-vitro evaluation of different controlled release polymeric matrices containing Ketoprofen. Healthmed, 2010. 4(2): p. 386-392.

44. Liu, F., et al., A novel concept in enteric coating: A double-coating system providing rapid drug release in the proximal small intestine. Journal of Controlled Release, 2009. 133(2): p. 119-124.

45. Zimova, L., et al., The development and *in vivo* evaluation of a colon drug delivery system using human volunteers. Drug Delivery, 2012. 19(2): p. 81-89.

Chapter 4: Development of A pH Sensitive Targeted Oral Release Platform Containing Protein Coated Microcrystals (PCMC)

Abstract

Introduction: Recently, targeted delivery to Peyer's patches has been widely investigated for oral vaccination delivery system. The major advantage of oral vaccination over injection is that it can generate both mucosal and systemic immune response. In this study, we were focusing on developing a pH sensitive targeted oral release platform containing protein coated microcrystals (PCMC), which could be an advantageous platform for future oral vaccination delivery systems. Methods: BSA was used as the model protein and co-precipitated with a protein carrier, DL-valine as protein coated microcrystals (PCMC). PCMC particles were controlled at size between 2-5 μm and coated with enteric coating (Eudragit® S-100). The enteric coated PCMC were then formulated into pellets (wet-granulation/spheronization). Finally, the pellets were coated by another layer of enteric coat (Eudragit® L 30 D-55 and/or Eudragit® F S 30D) for ileum targeted delivery). To further enhance the residence time of the formulation at the targeted site, mucoadhesive polymers, Methocel® K4M, was incorporated into the formulation. Results: PCMC of particle size: 2-10 μm and 95-98% BSA loading: were manufactured. The enteric coated pellets were well protected against gastric fluid (pH 1.2) for at least 2 hours, and started dissolving/disintegrating after 1 hour after adjusting the pH from 1.2 to 7.2, which made the pellets suitable for ileum targeting delivery. Conclusion: Enteric coated pellets with BSA loaded PCMC could be a possible candidate for oral vaccination delivery system, however, further coating condition or protecting

method must be conducted to enhance the stability and prolong the storage period of formulation.

4.1 Introduction

Vaccine immunization is considered one of the most successful public health achievements of the 20th century and has prevented thousands of deaths and illnesses [1]. According to WHO report in 2006, about three-quarters of the world's children received a standard package of childhood vaccines through the WHO/UNICEF Expanded Program on Immunization. These vaccines protected children against diphtheria, tetanus, pertussis, polio, measles and neonatal tuberculosis. The vaccination was estimated to save approximately 3 million lives every year in the world [2]. However, another 3 million lives are still lost to vaccine-preventable diseases, mainly due to the thermal instability of vaccines, which leads to the wastage of half of all supplied vaccines worldwide. Since most currently available vaccines require intravenous (*i.v.)* or subcutaneous (s.c.) delivery of antigens, storage of these vaccines at low temperature (i.e. at 4 °C or below) is required. Therefore, depletion is especially acute in the developing countries, but improper storage has also been reported in temperate countries and in the developed world [3, 4]. Over the past 20 years, numerous studies have assessed the potential of orally delivered antigens on the induction of mucosal and systemic immune responses [5, 6]. In addition, mucosal delivery is the only vaccination route to induce effective B cell class switching and the development of secretory IgA-producing plasma cells [7]. Moreover, mucosal vaccination (delivered via oral or nasal route) has many advantages, including no need for sterile needles [8], a reduced need for trained personnel [9], and the

ability of inducing both mucosal and systematic immunity [10]. However, the major challenge of oral vaccination is the harsh environment of the gastrointestinal tract (GI tract) [11] and the possibility of orally delivered soluble antigens inducing tolerance rather than immunity [12]. Therefore, protection of the antigens or utilization of a carrier system is required.

Most pathogenic microorganisms actually invade through mucosal surface when infecting a subject. In order to protect against such pathogens, induction of the mucosal immune response is required as the critical first-line defense mechanism [13]. An antigen itself, when orally administered, cannot survive through the acidic gastric condition [14] However, when the antigens are bounded to (or loaded into) particular carriers (e.g. biodegradable polymers, such as PLG and PLGA [15, 16]) it is found and proven that the antigens can be uptake and transported over the barrier by M-cells in Peyer's patches (typically, for particles sized less than 5 μm in diameter) [17]. Peyer's patches are a collection of organized lymphoid tissues lining the intestinal tract, which are the most important units of gut-associated lymphoid tissues (GALT). Peyer's patches are the primary induction sites for mucosal immunity, which regulates IgA immunity against orally entered antigens [18].

Although most of the currently available vaccines are administered via the parenteral route, this is associated with several important drawbacks. These drawbacks including: patience compliance [19], higher cost [20], and requirement of low temperature during storage and transportation [21, 22]. In addition, most of the antibodies induced following the used of a parenteral route cannot reach mucosal surfaces where

pathogenic infection takes place [23]. As an alternative, oral vaccination can be a simple and efficient way of inducing both mucosal and systemic immunity [24, 25]. In addition, secretory IgA (sIgA) induced at the mucosal sites can further prevent attachment of bacteria and viruses to mucosa, and neutralize viruses and toxins that can damage the host cells [26].

Other than encapsulation techniques, many other particle-engineering processes have been developed to manufacture micro- or nano-sized particles of poorly soluble drugs, such as spray drying [27, 28], spray-freeze drying [29, 30], spray-freeze-into-liquid [31, 32], precipitation with supercritical fluid [33], ultra-rapid-freezing [34, 35], and controlled precipitation [36, 37]. Size reduction enhances the solubility and bioavailability of the active ingredients, which can contribute to a less fluctuating PK profile [38, 39]. In addition, micro- or nano-structured particles tend to have higher stability and have less storage issues [40, 41]. Multiparticulate drug delivery systems are generally considered to have several advantages compared to a single unit dosage form, including a more predictable gastric transit and a more uniform drug distribution, both contributing to less variance of inter- or intra-individual bioavailability [42]. A combination of nanostructured and multiparticulate drug delivery results in an enhanced dissolution and higher saturation solubility, in comparison to micronized drugs [43]. In addition, nanostructured particles tend to have higher affinity to the inflammatory sites along the gastrointestinal tract [44]. Recently, XstalBio (XstalBio Limited, GLASGOW, U.K.) developed a novel Protein-coated microcrystals particle engineering approach for the formulation of proteins, peptides, DNA/RNA and vaccines [45]. Protein-coated

microcrystals (PCMC) are water-soluble micron-sized particles, which are comprised of a core crystalline material (e.g. amino acid, sugar or salt) on which is coated the therapeutic biomolecule [46]. The advantage of PCMC is that they can be prepared by using a one step process that simultaneously dehydrates these two components and results in the immobilization of the protein on the surface of the carrier, which helps prevent protein degradation during the manufacturing process [47, 48]. The preparation of PCMC involves dissolution of the appropriate crystal-forming carrier together with the given biomolecule in aqueous solution. Rapid dehydration of the two components is facilitated by the addition of the aqueous solution to a water-miscible organic solvent (anti-solvent), resulting in the immediate formation of the PCMC with the biomolecule immobilized on the surface of the crystalline core carrier (via a crystal-lattice mediated self-assembly process). By adjusting the dehydration conditions, particle morphology, protein payload and particle size can be controlled [49]. Potentially a vaccine made of PCMC is of better thermostability, since Parker and co-workers validated that protein-coated micro-crystals (PCMC) are able to improve the thermostability of a model vaccine (adenylate cyclase toxin, CyaA) for intramuscular delivery [50]. The model vaccine, CyaA-PCMC was prepared by co-precipitated of CyaA with L-glutamine as the crystalline materials using the rapid dehydration method. It was reported in the work that following storage as dry powder vaccines at 37 ° C for 2 weeks, the adenylate cyclase activity recovered from the CyaA-PCMC was only marginally reduced.

In order to enhance the oral bioavailability of poor-soluble drugs and/or protein (peptides), a prolonged residence time is required [51]. Mucoadhesive materials are able

to adhere onto the mucus membrane at the gastrointestinal tract, which contributes to a prolonged residence time at the targeted site [52]. The goal of this study was to manufacture a delivery platform that would be capable of carrying a model protein/peptide safely through the stomach and allow it to adhere to a suitable part of the GI tract. Bovine serum albumin (BSA) was chosen as the model protein antigen, which is commonly used as an antigen to induce immune responses in different animal models.

4.2. Materials and methods

4.2.1 Materials

Bovine serum albumin was purchased from Spectrum (Spectrum, Gardena, CA, USA). DL-valine, L-glutamine, and L-glycine were obtained from Sigma (Sigma, St. Louis, MO, USA). Pluronic® F68 and Pluronic® F127 was kindly provided by BASF (BASF Corporation, Florham Park, NJ, USA). Eudragit® FS 30 D, Eudragit® S-100, and Eudragit® L 30 D-55 were kindly donated from Evonik (Evonik Degussa Corporation, Parsippany, NJ, USA). Avicel® PH101 was kindly donated by FMC (FMC Corporation, Philadelphia, Pennsylvania, USA). A Bradford protein assay kit was purchased from Bio-Rad (Bio-Rad Laboratories, Hercules, CA, USA). All the chemicals and solvents used were of analytical grade.

4.2.2 Methods

4.2.2.1 Preparation of PCMC

Protein coated microcrystals in this study were prepared by a simple co-precipitation process. Briefly, a saturated solution of amino acid was prepared at 25 °C (DL-valine: 60

mg/mL; L-glutamine: 40 mg/mL, and L-glycine: 250 mg/mL) as a protein carrier during the co-precipitation process. 25 mg/mL of stock BSA solution was prepared by dissolving lyophilized BSA powders in pH 6.8 phosphate buffer at 25 °C. Both solutions were stored at 4 °C before PCMCs manufacturing or further analysis. In order to optimized the particle size of the PCMC products, BSA stock solution was added into saturated aqueous amino acid solution at the ratio of 1 to 1, 1 to 2, 1 to 3 or 2 to 3 (v/v) to prepare amino acid solution at different % saturation level (Table 4.1) to optimize the precipitation of PCMCs. The mixture solution was mixed for 30 seconds right before the precipitation process. The aqueous mixture solution was then added dropwise to an amino acid saturated anti-solvent (ethanol, propanol, or isopropyl alcohol) through a syringe pump under suitable feeding rate (1, 2, or 5 mL/min) under sonication (Branson Sonifier® S-250A, Branson Ultrasonics, Danbury, CT, USA). The whole mixture was sonicated for 10 minutes at a pulse mode (50% cycle). The precipitated crystals were then obtained by filtration and then dried in the fume hood until a constant weight was obtained. The dry powders were then transferred into HDPE bottles and conducting seal and store in desiccators under room temperature before further use.

Table 4.1: Manufacturing condition of PCMC

PCMC #	Amino acid	Anti-solvent	% saturation of amino acid carrier	Feeding rate of aqueous solution
PCMC 1	DL-valine	Ethanol	80%	1mL/min
PCMC 2	DL-valine	Ethanol	80%	2mL/min
PCMC 3	DL-valine	Ethanol	80%	5mL/min
PCMC 4	DL-valine	Ethanol	60%	1mL/min
PCMC 5	DL-valine	Ethanol	50%	1mL/min
PCMC 6	DL-valine	Propanol	80%	1mL/min
PCMC 7	DL-valine	Propanol	60%	1mL/min
PCMC 8	DL-valine	Propanol	50%	1mL/min
PCMC 9	DL-valine	Isopropyl alcohol	80%	1mL/min
PCMC 10	DL-valine	Isopropyl alcohol	60%	1mL/min
PCMC 11	DL-valine	Isopropyl alcohol	50%	1mL/min
PCMC 12	L-glutamine	Isopropyl alcohol	80%	1mL/min
PCMC 13	L-glutamine	Isopropyl alcohol	60%	1mL/min
PCMC 14	L-glycine	Isopropyl alcohol	80%	1mL/min
PCMC 15	L-glycine	Isopropyl alcohol	60%	1mL/min

4.2.2.2 Physicochemical characteristics of PCMC

4.2.2.2.1 Particle size distribution

A Malvern Zetasizer Nano ZS was used to determine the size distribution of the PCMC by photon correlation spectroscopy (PCS) (, Malvern Instruments Ltd, Worcester, UK).

4.2.2.2.2 Morphology of PCMC

PCMC were fixed onto the SEM specimen stem by carbon tapes and then coated with Pt/Pd using a Cressington 208HR sputter Coater (Cressington Scientific Instruments Ltd, Watford, UK) at 12 mV. The coating thickness was set at 12 nm (estimated coating

thickness). The morphology of PCMCs was then observed using a Zeiss Gemini 1530 scanning electron microscope (Carl Zeiss NTS, LLC, Peabody, MA, USA).

4.2.2.2.3 Loading capacity of bovine serum albumin

The content of BSA in PCMC was determined directly by measuring the protein that was co-precipitated onto the surface of amino acid carriers. The concentration of BSA was determined using Bradford Assay [53]. The loading capacity (LC%) was calculated by using Equation 1:

$$LC\% = \frac{\text{wt. of protein loaded}}{\text{wt. of dried PCMC}} \quad X\ 100 \tag{1}$$

4.2.2.3 Enteric coating of PCMC

After drying, PCMC were then coated with Eudragit® S-100 at two different coating level. Briefly, PCMC were re-suspended with isopropyl alcohol; Eudragit® S-100 was then added to the mixture at 1:2 or 1:5 w/w polymer to BSA/DL-valine ratio to optimize the enteric coat. Eudragit® S-100 was dissolved with constant magnetic stirring at 150 rpm for 30 minutes. The final mixture was then dropped into excess liquid paraffin under continuous agitation at 400 rpm using a RW-16 basic mechanic stirrer (IKA® Works, Inc., Wilmington, NC, USA) overnight to let the solvent (isopropyl alcohol) to completely evaporate. The whole mixture (coated PCMC and liquid paraffin) was left still on benchtop for 1 hour to let the coated PCMC settle down at the bottom of the beaker. The excess amount of liquid paraffin was poured out and dumped. The coated PCMC (with residual liquid paraffin) were then washed with de-ionized water for three

times to get rid off the liquid paraffin. The final particles were harvested by using a Marathon 21K/R centrifuge at 3,000g for 10 minutes (Fisher Scientific, Pittsburgh, PA, USA).

4.2.2.4 Dissolution transit of enteric coated PCMCs

The transit and size change of Eudragit® S-100 coated PCMC was determined using a modified dissolution method. Briefly, 20 mg dried Eudragit® S-100 coated PCMC were weighted and transferred into a glass vial containing 20 mL of heated (37 °C) 0.1N HCl (mimic gastric pH, pH 1.0) or phosphate buffers (mimic pH at lower intestine, pH 7.2). The vial was then placed in an Orbit Environ Shaker shaking incubator (LABLINE, Tripunithura, Kochi, India) and agitated at a constant rate of 150 rpm at 37 °C. At time intervals of 10, 30, 60, 120, and 180 minutes, 0.5 mL aliquots were withdrawn from the sample suspension. The withdrawn sample was then placed (stub via a transfer pipit) and let dry on an SEM specimen prior to SEM imaging.

4.2.2.5 Pellets production

The model API theophylline was used to optimize the pellet manufacturing using an extrusion/spheronisation technique [54]. Briefly, suspensions of PCMC were pre-blended with MCC (Avicel® PH 101), and lactose to a total mixture weight of 250 mg (Table 4.2), for 5 min. Methocel® K4M or Methocel® E15 was added into the mixture and granulated for a further 5 minutes. The mixture was then introduced into a Luwa benchtop granulator (LCI Corporation, Charlotte, NC, USA) and extruded into granules. The granules were then transferred into a Caleva, Model 250 bench-top spheronizer (Caleva Process Solutions LTD, Sturminster Newton, UK) and spheronized into pellets. The pellets were dried in oven overnight at 40 °C. Pellets in the size fraction 1.0-1.5 mm

were separated by U.S. standard sieves (Fisher Scientific, Pittsburgh, PA, USA) and stored in desiccators at room temperature prior to further testing.

Table 4.2: Composition of pellets

Pellet #	API: Theophylline, w/w	Avicel® PH 101, w/w	Kollidon® CL, w/w	Lactose, w/w	Methocel®, K4M, w/w	Methocel®, E15, w/w
Pellet 1	10%	40%	0%	50%	0%	0%
Pellet 2	10%	40%	10%	40%	0%	0%
Pellet 3	10%	40%	10%	30%	0%	10%
Pellet 4	10%	40%	10%	35%	5%	0%

*For BSA (PCMC) loaded pellets, the compositions of pellet 1-4 are exactly the same, except that the API was replaced by BSA/PCMC

Using this method, 250 grams of pellets (as the core) were coated using a Strea-1 (Aeromatic-Fielder, Bubendorf, Switzerland) fluidized-bed coater (bottom set-up and a Wurster column) with an atomized air pressure of 2 bar and an inlet temperature of 45 °C; outlet air temperature of 30 °C. The coating dispersion was stirred continuously during the coating process. The coated weight gain (% w/w, Eudragit® to core pellets ratio) was monitor every 10 minutes, till the final desired weight gain was reached. After coating, the pellets were dried continuously within the fluidized bed at 30 °C for another 10 minutes before transferring to an oven set at 40 °C for 2 hours. The target coating weight gain was set at 5, 10, 15, or 20 %w/w. After the coating conditions were optimized using theophylline-based pellets, BSA/PCMC was introduced into the final pellet formulations to replace theophylline as the API. Briefly, BSA loaded PCMC were re-suspended in IPA and used as the binder solution in the wet-granulation/pelletization

process as previously described. After manufacturing, BCA/PCMC containing pellets were enteric coated in the exactly same manner as we coated the theophylline pellets.

4.2.2.6 Enteric coating of pellets

In order to reduce the waste of BSA, the enteric coating process/condition was first tested with placebo pellets with Theophylline as the active ingredients (in replacement of BSA, while the rest ingredients remained the same as previously described in Section 2.2.6). After manufacturing, the pellets were further coated with an enteric coat (a mixture of Eudragit® FS 30 D/Eudragit® L 30 D-55 to control the release profile) using a previously described fluid-bed coating method [54], and the three different coating solution compositions shown in Table 4.3.

Table 4.3: Composition of enteric coating solutions

Enteric coating 1	Eudragit LD30-55			Eudragit FS 30 D			TEC *			Polysorbate 80 (33% w/w aq.) **			Glyceryl Monostearate		
Coating solution	Total (g)	Dry (g)	/100g	Total (g)	Dry (g)	/100g	Total (g)	Dry (g)	% w/w	Total (g)	Dry (g)	% w/w	Total (g)	Dry (g)	/100g
	21.2	6.4		32	9.6		1.3	1.3	20	1.6	0.5	3.1	1.3	1.3	8.1
Enteric coating 2	Eudragit LD30-55			TEC			Citric Acid			Talc					
Inner coating solution (neutralized to pH 5.6)	Total (g)	Dry (g)	/100g	Total (g)	Dry (g)	% w/w	Total (g)	Dry (g)	% w/w	Total (g)	Dry (g)	% w/w			
	21.0	6.3		0.32	0.32	5	0.95	0.95	15	3.1	3.1	50			
Outer coating solution	Eudragit LD30-55			TEC			Talc								
	Total (g)	Dry (g)	/100g	Total (g)	Dry (g)	% w/w	Total (g)	Dry (g)	% w/w						
	41.67	12.5		1.25	1.25	10	6.25	6.25	50						
Enteric coating 3	Eudragit LD30-55			TEC			Citric Acid			Talc					
Inner coating solution (neutralized to pH 5.6)	Total (g)	Dry (g)	/100g	Total (g)	Dry (g)	% w/w	Total (g)	Dry (g)	% w/w	Total (g)	Dry (g)	% w.w			
	21.0	6.3		0.32	0.32	5	0.95	0.95	15	3.1	3.1	50			
Outer coating solution	Eudragit LD30-55			Eudragit FS 30 D			TEC			Polysorbate 80 (33% w/w aq.)			Glyceryl Monostearate		
	Total (g)	Dry (g)	/100g	Total (g)	Dry (g)	/100g	Total (g)	Dry (g)	% w/w	Total (g)	Dry (g)	% w/w	Total (g)	Dry (g)	% w/w
	21.2	6.4		32	9.6		1.3	1.3	20	1.6	0.5	3.1	1.3	1.3	8.1

*: w/w % ratio related to polymer content.

**: w/w % ratio related to polymer content.

4.2.2.7 In vitro release of BSA loaded pellets

BSA release from coated pellets was determined using a USP paddle dissolution apparatus [55]. Pellets were added to 900 mL pH 1.2, 0.1N HCl and maintained at 37 °C, with the paddle speed set at 100 rpm. At intervals of 10, 30, 60, 90, and 120 minutes, a 5 mL sample was taken from each dissolution vessel and was replaced with the same

volume of pH 1.2, 0.1N. After 2 hours, the testing medium was replaced with 900 mL pH 7.2, phosphate buffer. Additional 5 mL samples were taken at time intervals of 3, 4 and 5 hours. Samples were analyzed using the Bradford assay as previously described in Section 2.2.3. Dissolution tests were repeated six times for all formulations and the mean % BSA released was evaluated.

4.2.2.8. Stability of antigen loaded pellets

After enteric coating, the pellets were stored and protected from light at controlled room temperature for 3 months (25 °C, 60% RH and 40 °C, 75% RH). The formulations were observed for change in physical appearance, color, BSA content and release characteristics monthly.

4.2.3 Statistics

All results were shown as mean ± standard deviation (N=6). Analysis of variance (ANOVA), Turkey's HSD or Wilcoxon test is used to evaluate the results via JMP 7.0 software (JMP, Cary, NC, USA). $p < 0.05$ was considered of significant difference.

4.3 Results and discussion

4.3.1 Particle size, particle size distribution and BSA loading of PCMC

After manufacturing, particle size of each batch of the PCMC formulation was measured using a Mastersizer 2000 to determine D10 , D50, D90 the respective cut-off size of 10, 50%, and 90% by volume, as well as the particle span (span = D50/(D90-D10)) as shown in Table 4.4. In order to obtain a formulation of PCMC with a smaller average particle size (2-5 μm) and lower particle size distribution, several different factors were controlled during the manufacturing process. These factors included: the type of protein carrier (DL-valine, L-glutamine, and L-glycine), the feeding rate of the

BSA/amino acid carrier solution, the type of anti-solvent used (ethanol, n-propanol, and IPA), and % saturation of carrier amino acid solution (80, 66, and 50% saturation). From our results, only DL-valine and L-glutamine were suitable for PCMC manufacturing PCMC made of L-glutamine tended to aggregate together and turned into brittle flakes, instead of fine crystal powders as PCMC made of DL-valine and L-glutamine. PCMC made of L-glycine showed varied particle distribution (particle span >1.7), with particle size larger than 25 μm (D50), which was not fit for oral vaccination delivery system. Particle size of the microparticles is an important parameter in vaccine delivery. In general, particulate systems with a particle size smaller than 10_μm have been shown to improve the immune response significantly, allowing the antigen taken up by the mucosal associated lymphoid tissues (MALTs) [56]. PCMC made of L-glutamine or DL-valine showed a more suitable particle size range for oral vaccination (<10 μm) delivery system. However, PCMC made of DL-valine showed significantly higher % BSA loading ($p<0.05$), compared to PCMC made with L-glutamine (Table 4.4).

Table 4.4: Particle size distribution and BSA loading % of PCMC formulations

PCMC #	D 10 (µm)	D 50 (µm)	D 90 (µm)	Span	Loading %
PCMC 1	2.38	6.67	15.07	1.14	59.12
PCMC 2	8.98	16.78	28.13	1.90	67.23
PCMC 3	4.88	8.89	14.97	1.14	50.21
PCMC 4	3.24	8.50	14.32	1.32	48.34
PCMC 5	4.32	12.21	16.21	1.00	55.02
PCMC 6	2.85	5.32	9.20	1.20	68.21
PCMC 7	4.73	9.43	18.17	1.38	76.32
PCMC 8	3.54	7.93	14.23	1.35	74.10
PCMC 9	2.00	4.60	9.26	1.50	95.32
PCMC 10	2.06	4.15	7.52	1.30	96.23
PCMC 11	2.08	3.70	6.09	1.00	98.07
PCMC 12	2.48	5.55	12.25	1.70	98.92
PCMC 13	1.64	2.93	5.00	1.10	79.80
PCMC 14	7.80	20.51	44.07	1.77	56.96
PCMC 15	8.34	27.30	59.50	1.87	65.27

Therefore, DL-valine was chosen as the final amino acid carrier for preparation of PCMC in the following studies. In addition, we speculated that the type of anti-solvent, the feeding rate (the rate of adding BSA solution into the anti-solvent) and % saturation of the amino acid carrier containing anti-solvent would affect the precipitation process and alter the size and loading % of PCMC products. Under the same manufacturing conditions, particle size of PCMC obtained from different anti-solvents were significantly varied ($p<0.05$.) The rank order of particle size of the three different PCMC products from the smallest to the largest was: PCMC made using IPA as anti-solvent < PCMC made of n-propanol < PCMC made of ethanol. In order to prepare PCMC of proper characteristic for the oral delivery, we used IPA as the antisolvent throughout the following studies. Three feeding rate were used for PCMC preparation, 1, 5, and 10

mL/min. However, both particle size (D50) and particle span showed no significant difference at different feeding rate (particle size: p=0.45; particle span: p=0.11). The concentration level of protein carrier (the amino acids) in the aqueous phase before contacting the antisolvent was critical, since the starting concentration was seen to greatly affect the particle size of PCMC during the precipitation process. The solubility of DL-valine in water at room temperature is 60 mg/mL. Therefore, through out our study, a 60 mg/mL DL-valine aqueous solution represented 100% saturation, while 18 mg/mL and 48 mg/mL DL-valine aqueous solutions represented 30% and 80% saturation, respectively. At 30% (D50, 3.76 μm) and 80% (D50, 2.90 μm) DL-valine saturation, PCMC had a significantly smaller particle size ($p < 0.05$), compared to PCMC prepared at 60% DL-valine saturation (D50, 4.78 μm). At lower DL-valine concentrations (i.e. 30% saturation), less amount of DL-valine was in contact with the antisolvent under a given time and resulted in the formation of smaller precipitated DL-valine (the protein carrier). Therefore, less BSA could be physically precipitated onto the surface, which resulted in the production of smaller PCMC. However, at a much higher saturation level (i.e. 80%), once the carrier (DL-valine) solution was in contact with the antisolvent, a rapid precipitation occurred, resulting in PCMC with even smaller particle size. However, rapid precipitation was a double-edged knife, while particle size of PCMC could be greatly reduced; the amount of BSA that was able to load/precipitate onto the carrier was also hindered. BSA loading (% w/v) was significantly reduced at 80% DL-valine saturation, (79.89% BSA loading), compared to 30% and 60% DL-valine saturation (97.72% and 96.44% BSA loading, respectively) (p=0.024). However, the goal of this study was to manufacture a suitable platform for possible oral vaccination delivery system. In order to achieve this, the particle size of the PCMC should be limited to less than 5 μm. Therefore, the final PCMC manufacturing procedure was set at a BSA feeding rate of 1

mL/min, with 80% saturation DL-valine as the protein carrier and IPA as the anti-solvent in the precipitation process.

4.3.2 Enteric coating of PCMCs

PCMC made by using a combination of BSA and DL-valine was highly water soluble. However, it should be noted that oral vaccination requires antigen containing micro (or nano) particles to be taken up by the M cells at Peyer's patches, followed by the induction of mucosal immune responses [57]. Therefore, the PCMC described in this study were modified by coating with Eudragit® S-100. The main goal of enteric coating was to protect the PCMC from dissolving before they reach the distal small intestine (pH 7.0-7.8), where most of the Peyer's patches are located in man [57]. In order to achieve this, the PCMC must remain intact throughout the stomach (pH 1-2) and the upper intestine (pH 6.0-7.2). PCMC were coated with Eudragit S-100 at varied polymer to BSA/DL-valine ratio (1:2 and 1:5 w/w). After coating, the size of PCMC increased from about 4 μm to approximately 20-25 μm (1:2 w/w coating) and 30-40 μm (1:5 w/w coating). When testing in acidic media to simulate the pH of the stomach (0.1N HCl at pH 1.0), the coated PCMC were observed to remain intact for up to 2 hours in pH 1.0 acidic media (Figure 4.1), which indicated that both coating layers (1:2 or 1:5 w/w, BSA/DL valine: Eudragit® S-100) were able to protect the PCMC *in vitro* acidic condition. We then evaluated the suitability of the Eudragit® S-100 coating in pH 7.2 phosphate buffers to simulate the pH of the small intestine. PCMC coated with a 1:2 w/w (BSA/DL valine: Eudragit® S-100) enteric coat dissolved rapidly with no PCMC particles observed was found after 30 minutes under SEM (data not shown).

Figure 4.1: SEM images of Eudragit® S-100 coated PCMC after testing in SGF: (A) 0 min, 1:2 w/w coating; (B)1 hr, 1:2 w/w coating; (C) 2 hr, 1:2 w/w coating; (D) 0 min, 1:5 w/w coating; (E) 1 hr, 1:5 w/w coating; (F) 2 hr, 1:5 w/w coating.

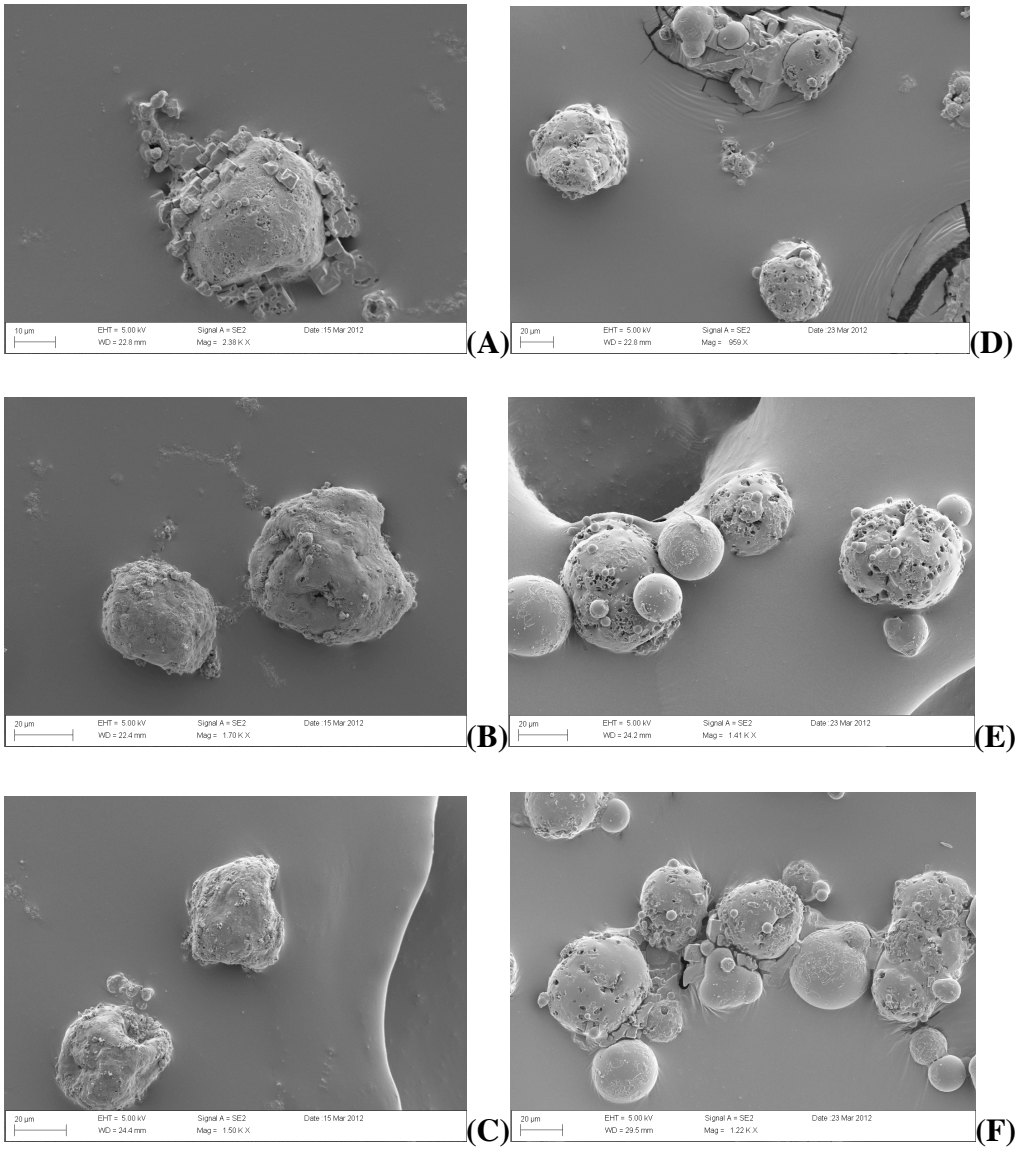

For PCMC coated with a 1:5 w/w (BSA/DL valine: Eudragit® S-100) enteric coat, although the coated layer was gradually eroded at pH 7.2, PCMC particles were still observed, as shown on the isolated SEM images (Figure 4.2) for up to 2 hours. Intestinal

transit from the upper intestine (duodenum) to the lower intestine (ileum) is approximately 1-2 hours (under fasted conditions) with a transit time through the ileum of approximately 1-2 hours [58]. Therefore, in order to design a suitable for targeting the mucosal immunization response at Peyer's patches in the ileum (pH 7-8), the ideal particles type should be eroded/dissolved gradually until the size is less than 5 μm. As indicated above, the 1:5 w/w Eudragit® S-100 coated PCMC were able to remain intact below pH 6.8. In addition, the enteric coating layer of these Eudragit® S-100 coated PCMC was eroded gradually once they were in contact with pH 7.2. The size of these PCMC particles were reduced to a suitable 2 μm size for M cell uptake [24] after 1 hour. Therefore, the transit time and size reduction of these PCMC demonstrated a suitable performance for consideration as an oral vaccination delivery platform.

Figure 4.2: SEM images of Eudragit® S-100 coated PCMC after testing in simulated intestinal fluid: (A)SIF, 30 min, 1:5 w/w coating; (B) SIF, 1 hr, 1:5 w/w coating; (C) SIF, 2 hr, 1:5 w/w.

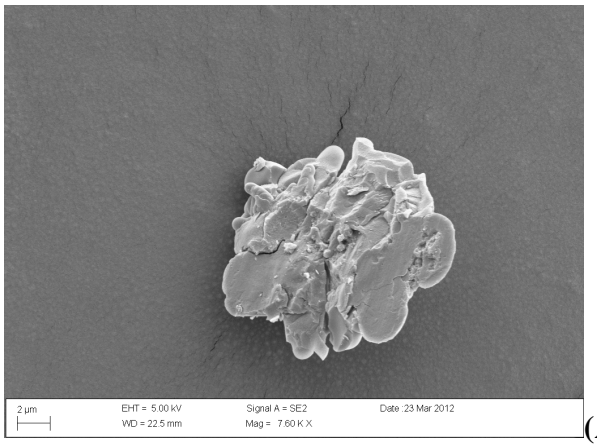

(A)

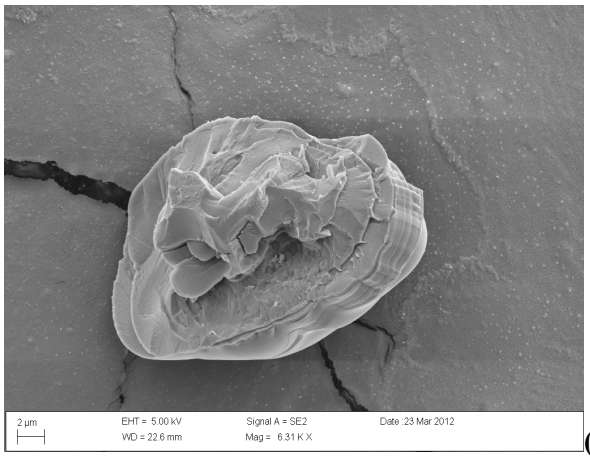

(B)

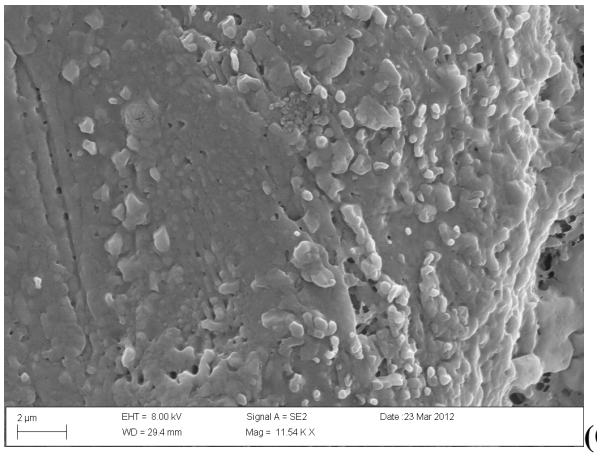

(C)

4.3.7 Pellets production

Granulation/pelletization is widely used in oral drug delivery system [59, 60]. Compared to dry-granulation direct compression (tablets), wet-granulation is more cost-effective and can improve free-flowing properties, homogeneity of the powder ingredients, provides better compressibility, and reduces dust during the processing. In a wet-granulation process, the pharmaceutical active ingredient can be either a dry substance or, be dissolved in a medium as a binder solution, which increases the possibility of optimizing a formulation based on the physicochemical property of its API, compared to direct compression. After wet-granulation, the granules can be further processed for direct compression, or extruded before pelletization. In general, pellets offer the well-known benefits of more uniform release and reproducibility of the formulation. This is due to the *in vivo* dispersion of a multiparticulates system, and the gastrointestinal transit in human body. While the gastric emptying transit time of a single solid tablet might range from 30 minutes to a couple hours, the dispersion of a multiparticulates system starts from the gastric and provide a more reproducible overall transit time. Therefore, in order to produce a more easily to handle pharmaceutical formation, as well as reducing possible damage during the manufacturing process to labile peptides/proteins/antigens (e.g. the model BSA used in these studies) wet-granulation/pelletization techniques were adopted. Eudragit® S-100 coated PCMC were re-suspended in IPA as the API, as well as the binder during the wet-granulation process. MCC (Avicel® PH 101) was used as the filler since it has a well-known advantage of forming an easy moist granulated mass, and generating strong granules on drying [61]. One of the objectives of the present study was to design a pellet based platform that could be capable of targeting the ileum due to a controlled release effect of the Eudragit® S-100 coated PCMC.

4.3.8. Enteric coating of pellets

For ileum targeted drug delivery, it is necessary to overcome relatively long part of GI tract without any drug activity and its stability changes. pH-dependent coating is effective and well known in GI tract targeted drug delivery systems [62, 63]. These systems utilize polymeric carriers that are insoluble in the low pH media of the upper gastrointestinal tract, but dissolve at a higher, near neutral pH of the distal gut. Such polymers will begin to dissolve in the ileum and as such are more appropriately defined as the materials for ileum targeted delivery systems. The pH-dependent approach for ileum drug delivery is based on the pH differences along the gastrointestinal tract with values increasing from about 1 to 2.5 in the stomach through 6.6 in the proximal small bowel to a peak of about 7.5 in the terminal ileum [64]. The mean gastric residence time is considered to be 0.25–2 hours and small intestinal residence time between 3 and 4 hours [65]. These conditions are valid for single solid dosage forms and for fasting state of patients. To provide a rapid disintegration at a desirable time, Kollidon® CL was added during the wet-granulation/pelletization process as an incorporated superdisintegrant. Furthermore, in order to control the releasing time of Eudragit® S-100 coated PCMC and synchronize the releasing time to gastrointestinal transit, three different enteric coating mixtures were evaluated using the model theophylline. . Without superdisintegrant, less than 10% of theophylline was released in 30 minutes; and only about 45% of the drug was released in 1 hour in pH 7.2 phosphate buffers (pellet 1, Figure 4.3A). With 10% w/w Kollidon® CL, more than 95% of the drug was released in 30 minutes; and the drug release was complete in less than one hour in pH 7.2 phosphate buffers (pellet 2, Figure 4.3A). This was appropriate for ileum targeted oral vaccination delivery system, since once the pellets reached ileum, all antigens would be released promptly, rather than miss the target site and be released the lower intestine. In addition,

the Methocel® E15 or Methocel® K4M where incorporated into the fast-disintegrating pellets, to potentially acts as mucoadhesive polymer carriers. By incorporating a mucoadhesive polymer, the pellets (the material following disintegration) have the potential to slow transit at targeted site of the ileum after wetting and prolong the uptake window. However, with 10% w/w Methocel® E15, only less than 25% of the drug was release in 30 minutes in pH 7.2 phosphate buffer (pellet 3, Figure 4.3 A), while nearly 60% of the drug was released in 30 minutes, when 5% w/w Methocel® K4M was used (pellet 4, Figure 4.3 A). The release rate of drug was hindered, because of the gel formation of Methocel®, which formed a matrix system and controlled the drug release through a combination of diffusion/erosion [66].

In order to protect the pellets from the gastric environment, the pellets were coated with proper enteric coat(s). Here we were focusing on controlling the drug release at pH > 7.2 (according to the physiological condition in the ileum). Eudragit® L and S polymers enable targeting specific areas of the intestine. Eudragit® L 30 D-55 dissolves at pH above 5.5, which is excellent for drug delivery at the upper intestine [67]; while Eudragit® FS 30D polymer dissolves at pH above 7.0 and is suitable for drug delivery to colon area [68]. In this study, it was necessary to both prevent drug release at gastric pH, and control drug release gradually in a way that corresponds to drug delivery along the proximal intestine, followed by a rapid release at ileum. To achieve this, three different enteric coating conditions were tested. In coating solution 1, a single layer of a mixture of Eudragit® L 30 D-55 and Eudragit® F S 30D (w/w ratio: 2:3) was coated onto the pellets. No drug was release for up to 2 hours at pH 1.2 (gastric condition), regardless of the type of enteric coating. When applying only 5% w/w (weight gained) Eudragit® L 30 D-55 coating to the pellets, with 10% w/w superdisintegrant, Kollidon® CL, more than 90% of the drug released in just one hour after adjusting the pH from 1.2 to 7.2 (pellet 4, 5%

coating, Figure 3B). When the enteric coating was increased to 10% w/w (weight gained), only about 20% of the drug released in 2 hours after adjusting the pH from 1.2 to 7.2, and nearly 90% of the drug released in 3 hours after adjusting the pH from 1.2 to 7.2 after the (pellet 4, 10% coating, Figure 4.3B). Nevertheless, without superdisintegrant (Kollidon® CL), no drug released for up to 2 hours after adjusting the pH from 1.2 to 7.2, while nearly 90% of the drug released within another hour, regardless enteric coating of 5% or 10% (pellet 1, 5% and 10% coating, Figure 4.3B).

In enteric coating 2, a double-layer coating was applied. The inner coat was composed of Eudragit® L 30 D-55 (while the coating solution was neutralized to pH 5.6). Neutralizing the inner coat would help the rapid release of coated drug, since part of the Eudragit® L 30 D-55 was dissolved during the preparation process of the coating solution. The outer coat was composed of Eudragit® L 30 D-55 and with exactly the same composition as enteric coating 1. With 10% superdisintegrant, Kollidon® CL, nearly 90% of the drug released in less than one hour after the pH was adjusted from 1.2 to 7.2, regardless of the coating level (pellet 4, Figure 4.3D). Without superdisintegrant, Kollidon® CL, about 5% of the drug released while 5% or 10% w/w (weight gained) of the outer coat was applied (with 5% w/w inner coat) in 2 hours at pH 1.2 (pellet 1, 5% inner coat, 5% and 10% outer coat, Figure 4.3C), which showed non-successful enteric coating under gastric condition. When the outer coat was increased to 20% w/w (weight gained), no drug released under gastric condition for up to 2 hours, however, more than 90% of the drug release in less than 2 hours after the pH was adjusted from 1.2 to 7.2 (pellet 1, 5% inner coat, 20% outer coat, Figure 4.3C), which did not fit properly for our ileum targeting delivery system, for that most of the drug would release before it reach ileum. Therefore, neutralization indeed, created a more rapid release of the drug;

however, the drug released too early and would not be suitable for ileum targeting delivery system.

Finally, a third enteric coating composed of a modified outer layer was prepared (enteric coating 3). The inner enteric coat of enteric coating 3 was the same as the inner enteric coat of enteric coating 2. Nevertheless, the outer coat was replaced with a mixture of 1:4 w/w ratio of Eudragit® L 30 D-55 and Eudragit® F S 30D, compared to enteric coating 2. With 10% w/w superdisintegrant, Kollidon® CL and 10% w/w (weight gained) outer enteric coating (5% w/w inner coat), no drug released for up to 2 hours at pH 1.2 (pellet 4, 5% inner coat, 10% outer coat, Figure 4.3E). However, more than 50% of the drug released in just one hour after the pH was adjusted from 1.2 to 7.2. After the outer coat was increased to 20% w/w (weight gained), the drug was protected from releasing for one hour after the pH was adjusted from 1.2 to 7.2, followed by about 90% of the drug released within the following one hour (pellet 4, 5% inner coat, 20% outer coat, Figure 4.3E). This would be advantageous for our ileum targeted formulation, for that the drug was well-protected against gastric condition, and could be further protected for about another hour at pH above 7 (this is parallel to the transit time from duodenum to ileum), followed by prompt release of the drug in less than an hour.

Figure 4.3: Dissolution of enteric coated pellets (API: theophylline): (A) Non-coated pellets; (B) Coating solution 1; (C) and (D) Coating solution 2; (E) Coating solution 3. * N=6, Mean value ± Stdev

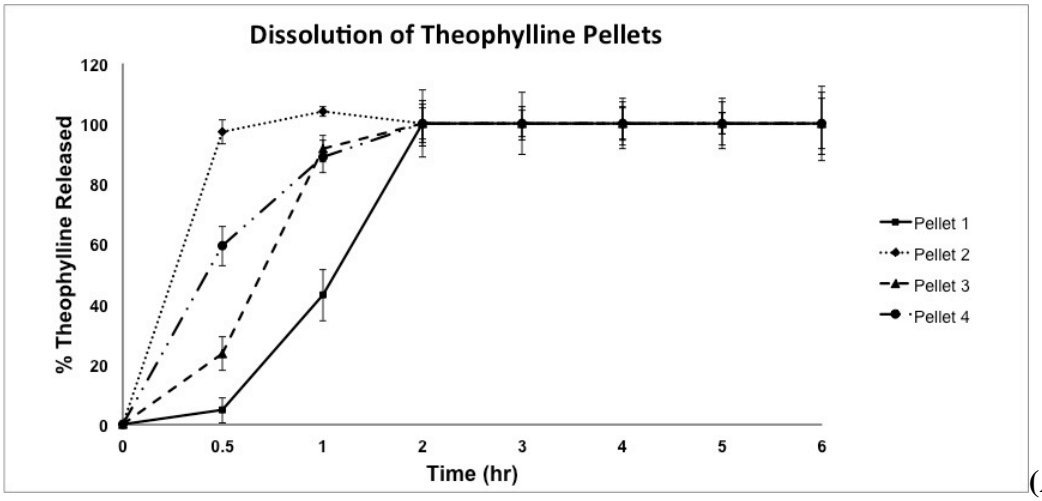

(A)

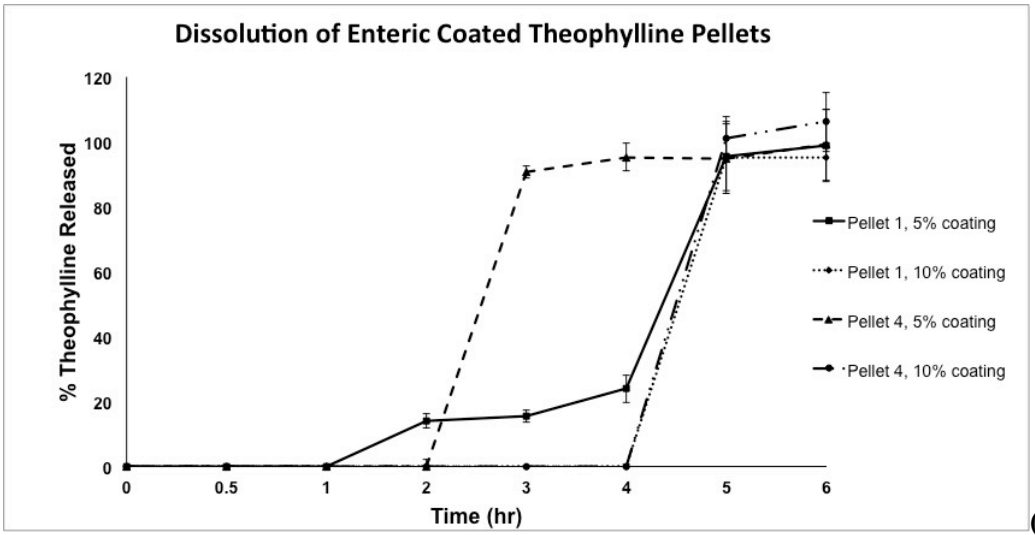

(B)

Figure 4.3 (continued)

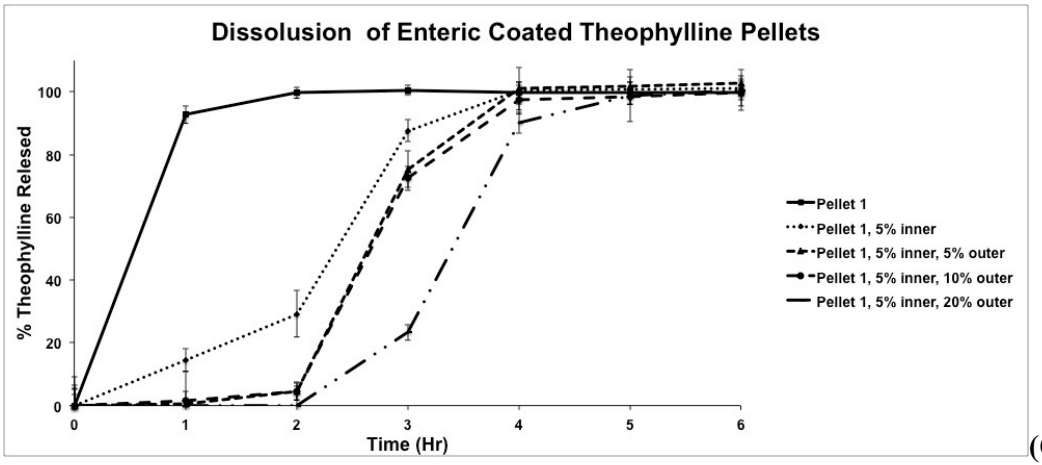

(C)

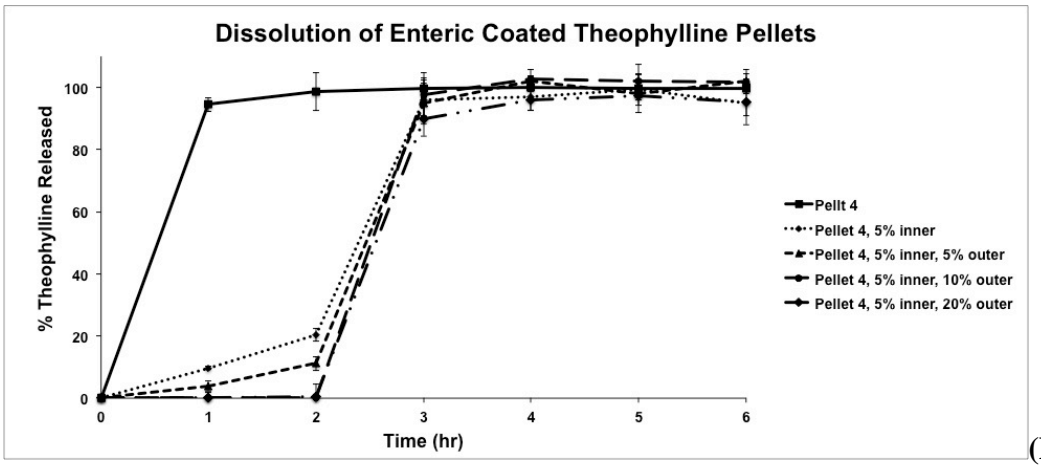

(D)

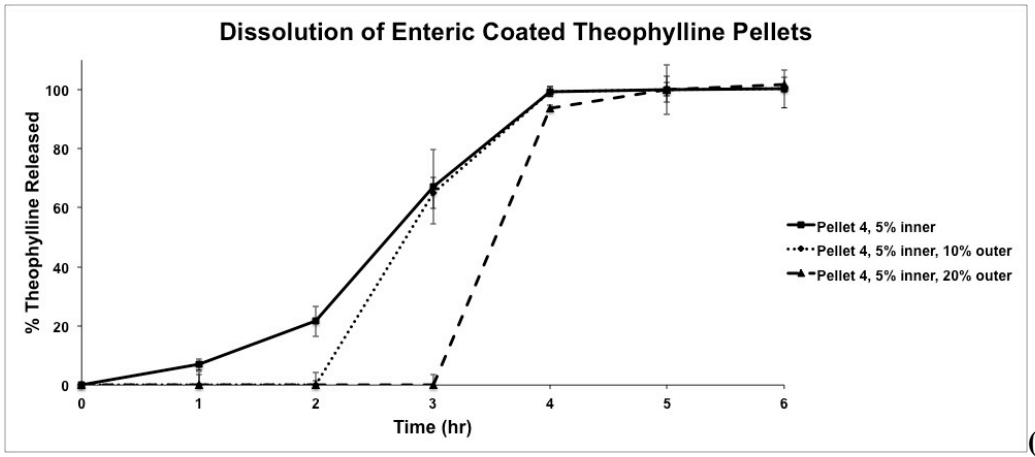

(E)

4.3.9 *In vitro* release of BSA loaded pellets

After the pellet manufacturing process and enteric coating conditions were optimized with theophylline as API, theophylline was replaced with BSA loaded PCMC was as the model protein. The release profile of BSA loaded PCMC containing pellets was similar to the release profile of theophylline as previously described. The major difference was that the release rate of BSA/PCMC was significantly reduced, compared to corresponding theophylline composition using the same coating conditions ($p<0.05$). Following the dissolution pH adjustment 1.2 to 7.2 only about 80% of BSA released in two hours compared to more than 90% of theophylline release under the same conditions (pellets coated with enteric coating 3, Figure 4.4). This was due to the enteric coating of BSA loaded PCMC as previously described. The release of BSA loaded PCMC hindered by the enteric coat (Eudragit® S-100) at intestinal pH, which made the whole delivery system (BSA loaded PCMC in enteric coated pellets) release slower than the theophylline pellets. With this design, we could possibly restricted BSA/PCMC particles release from the pellets after they reach ileum region, thus enhance the possibly of M cell uptake at the targeted site.

Figure 4.4: Dissolution of enteric coated pellets (API: BSA loaded PCMC). * N=6, Mean value ± Stdev

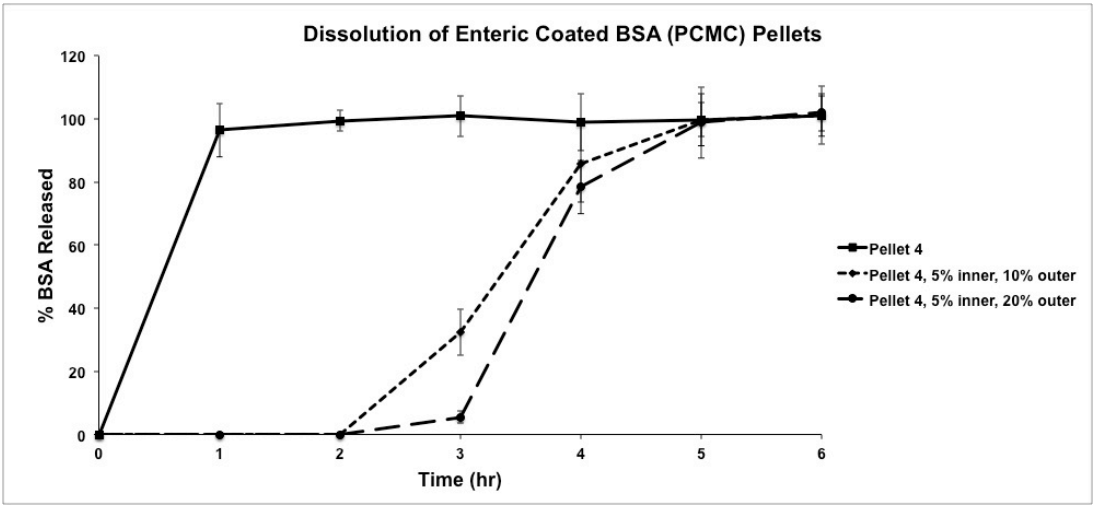

4.3.10 Stability of antigen loaded pellets

BSA/PCMC loaded pellets were stored at 25℃, 60% RH and 40℃, 75% RH for stability test for 3 months. After 3 months, about 45% of BSA released at pH 1.2 under both stability test conditions (Figure 4.5). This might resulted from the burst release of BSA that was diffused from the core to the surface of the enteric coat. In addition, nearly all drug released in one hour after the pH was adjusted from 1.2 to 7.2, which failed our objective of preventing the release of drug for another 1 to 2 hours after the pH was adjusted from 1.2 to 7.2 as previously described. Therefore, our formulation was not successful in the three-month stability tests, and further adjustments must be taken into consideration in the future studies.

Figure 4.5: Dissolution of enteric coated pellets (API: BSA loaded PCMC) after 3 month stability test: (A) 25℃, 60% RH; (B) 40℃, 75% RH. * N=6, Mean value ± Stdev

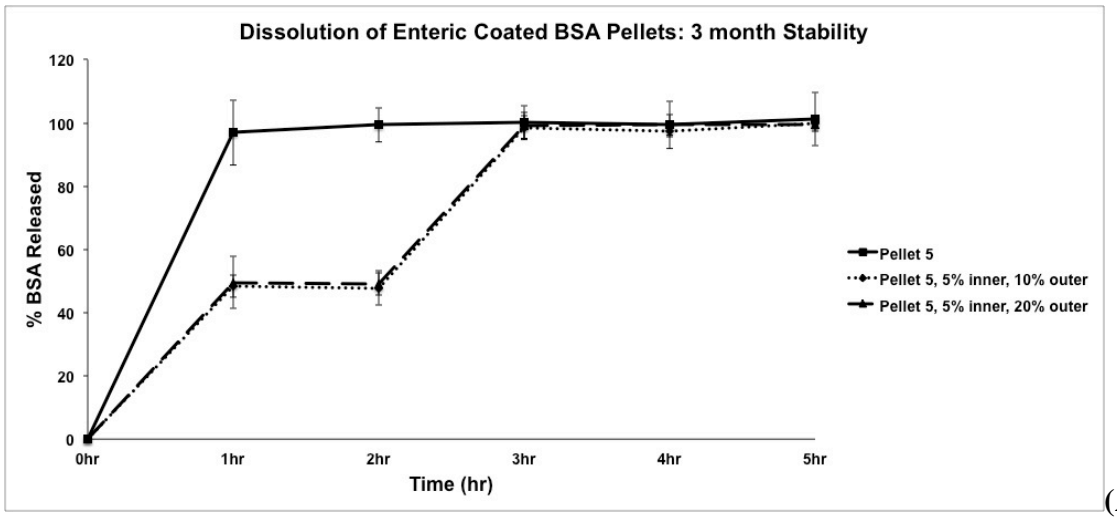

(A)

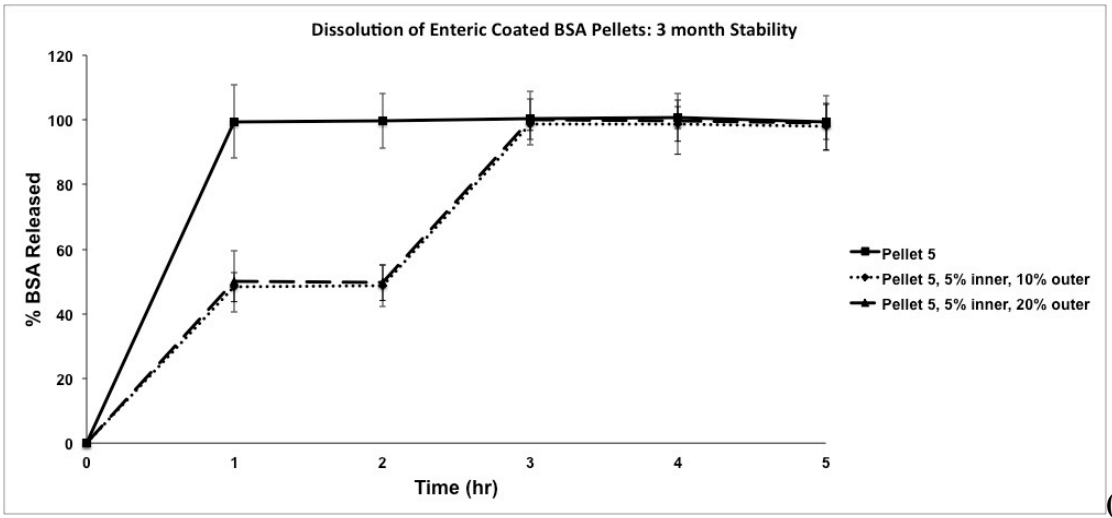

(B)

4.4 Conclusions

In this study, BSA loaded PCMC with high drug loading (95-98%) were manufactured using a simple direct precipitation method. In order to produce PCMC with

specific particle size (less than 2 μm), the manufacturing process was optimized by screening various parameters (i.e. feeding rate of BSA/DL-valine solution and % saturation of DL-valine). Enteric coated pellets with BSA loaded PCMC could be a possible candidate for oral vaccination delivery system, since a protection layer can prevent the drug delivery platform from damage in the gastric pH. A double-layered enteric coating (Eudragit® L 30 D-55 and Eudragit® F S 30D) showed a successful drug releasing profile for ileum-targeted delivery system in our results.

In summary, our study provides proof of successfully manufacturing BSA loading PCMC with particle size fit in the range that is suitable for oral vaccination (< 5 μm). Moreover, we developed a potentially pH sensitive, well-targeted system that could act as a platform for a variety of payloads related to protein/peptide or even antigen delivery to the ileum. Nonetheless, further improvement on the enteric coating property is required to help stabilize the platform for long-term storage processes.

4.5 Reference

1. Ball, R., et al., Statistical, epidemiological, and risk-assessment approaches to evaluating safety of vaccines throughout the life cycle at the food and drug administration. Pediatrics, 2011. 127: p. S31-S38.

2. Barder, O. Vaccines for development. 2006; Available from: http://www.cgdev.org/files/7366_file_Vaccines2.pdf

3. Murdan, S., et al., Immobilisation of vaccines onto micro-crystals for enhanced thermal stability. International Journal of Pharmaceutics, 2005. 296(1-2): p. 117-121.

4. Okeke, I.N., A. Lamikanra, and R. Edelman, Socioeconomic and behavioral factors leading to acquired bacterial resistance to antibiotics in developing countries. Emerging Infectious Diseases, 1999. 5(1): p. 18-27.

5. Shukla, A., B. Singh, and O.P. Katare, Significant systemic and mucosal immune response induced on oral delivery of diphtheria toxoid using nano-bilosomes. British Journal of Pharmacology, 2011. 164(2B): p. 820-827.

6. Yamamoto, M., D.W. Pascual, and H. Kiyono, M cell-targeted mucosal vaccine strategies, in Mucosal Vaccines: Modern Concepts, Strategies, and Challenges, P.A. Kozlowski, Editor. 2012, Springer-Verlag Berlin: Berlin. p. 39-52.

7. Takahashi, E., et al., Oral clarithromycin enhances airway IgA immunity through induction of IgA class switching recombination and B-cell activating factor of the tumor necrosis factor family molecule on mucosal dendritic cells in mice infected with influenza A virus. Journal of Virology, 2012.

8. Lebre, F., et al., Progress towards a needle-free Hepatitis b vaccine. Pharmaceutical Research, 2011. 28(5): p. 986-1012.

9. Azad, N. and Y. Rojanasakul, Vaccine delivery--current trends and future. Curr Drug Deliv., 2006. 3(2): p. 137-46.

10. Chamcha, V., J.R. Scott, and R. Amara, Oral immunization with a recombinant Lactococcus lactis expressing HIV-1 Gag on the tip of the pilus induces strong mucosal immune responses. Retrovirology, 2012. 9(Suppl 2).

11. Garinot, M., et al., PEGylated PLGA-based nanoparticles targeting M cells for oral vaccination. Journal of Controlled Release, 2007. 120(3): p. 195-204.

12. Chehade, M. and L. Mayer, Oral tolerance and its relation to food hypersensitivities. Journal of Allergy and Clinical Immunology, 2005. 115(1): p. 3-12.

13. Kunisawa, J., et al., Characterization of mucoadhesive microspheres for the induction of mucosal and systemic immune responses. Vaccine, 2000. 19(4-5): p. 589-594.

14. Lee, K.A., et al., Acid stability of anti-Helicobacter pyroli IgY in aqueous polyol solution. Journal of Biochemistry and Molecular Biology, 2002. 35(5): p. 488-493.

15. AllaouiAttarki, K., et al., Protective immunity against Salmonella typhimurium elicited in mice by oral vaccination with phosphorylcholine encapsulated in poly(DL-lactide-co-glycolide) microspheres. Infection and Immunity, 1997. 65(3): p. 853-857.

16. Sarti, F., et al., *In vivo* evidence of oral vaccination with PLGA nanoparticles containing the immunostimulant monophosphoryl lipid A. Biomaterials, 2011. 32(16): p. 4052-4057.

17. Wikingsson, L.D. and I. Sjoholm, Polyacryl starch microparticles as adjuvant in oral immunisation, inducing mucosal and systemic immune responses in mice. Vaccine, 2002. 20(27-28): p. 3355-3363.

18. Hashizume, T., et al., Peyer's patches are required for intestinal immunoglobulin A responses to Salmonella spp. Infection and Immunity, 2008. 76(3): p. 927-934.

19. Margolis, K.L., et al., Frequency of adverse reactions to influenza vaccine in the elderly - a randomized, placebo-controlled trial. Jama-Journal of the American Medical Association, 1990. 264(9): p. 1139-1141.

20. Singh, M., et al., Controlled release microparticles as a single dose hepatitis B vaccine: Evaluation of immunogenicity in mice. Vaccine, 1997. 15(5): p. 475-481.

21. Bell, K.N., et al., Risk factors for improper vaccine storage and handling in private provider offices. Pediatrics, 2001. 107(6): p. art. no.-e100.

22. Centers for Disease, C. and Prevention, Guidelines for maintaining and managing the vaccine cold chain. MMWR. Morbidity and mortality weekly report, 2003. 52(42): p. 1023-5.

23. Chalmers, W.S.K., Overview of new vaccines and technologies. Veterinary Microbiology, 2006. 117(1): p. 25-31.

24. Maloy, K.J., et al., Induction of mucosal and systemic immune-responses by immunization with ovalbumin entrapped in poly(lactide-co-glycolide) microparticles. Immunology, 1994. 81(4): p. 661-667.

25. Challacombe, S.J., et al., Enhanced secretory iga and systemic igg antibody-responses after oral immunization with biodegradable microparticles containing antigen. Immunology, 1992. 76(1): p. 164-168.

26. Bowersock, T.L., et al., Oral vaccination with alginate microsphere systems. Journal of Controlled Release, 1996. 39(2-3): p. 209-220.

27. Alhalaweh, A., S. Andersson, and S.P. Velaga, Preparation of zolmitriptan-chitosan microparticles by spray drying for nasal delivery. European Journal of Pharmaceutical Sciences, 2009. 38(3): p. 206-214.

28. Benchabane, S., M. Subirade, and G.W. Vandenberg, Production of BSA-loaded alginate microcapsules: Influence of spray dryer parameters on the microcapsule characteristics and BSA release. Journal of Microencapsulation, 2007. 24(7): p. 647-658.

29. Carrasquillo, K.G., et al., Non-aqueous encapsulation of excipient-stabilized spray-freeze dried BSA into poly(lactide-co-glycolide) microspheres results in release of native protein. Journal of Controlled Release, 2001. 76(3): p. 199-208.

30. Costantino, H.R., et al., Protein spray-freeze drying. Effect of atomization conditions on particle size and stability. Pharmaceutical Research, 2000. 17(11): p. 1374-1383.

31. Yu, Z.S., K.P. Johnston, and R.O. Williams, Spray freezing into liquid versus spray-freeze drying: Influence of atomization on protein aggregation and biological activity. European Journal of Pharmaceutical Sciences, 2006. 27(1): p. 9-18.

32. Engstrom, J.D., et al., Stable high surface area lactate dehydrogenase particles produced by spray freezing into liquid nitrogen. European Journal of Pharmaceutics and Biopharmaceutics, 2007. 65(2): p. 163-174.

33. Meziani, M.J., et al., Protein-protected nanoparticles from rapid expansion of supercritical solution into aqueous solution. Journal of Physical Chemistry B, 2002. 106(43): p. 11178-11182.

34. Yang, W., K.P. Johnston, and R.O. Williams, Comparison of bioavailability of amorphous versus crystalline itraconazole nanoparticles via pulmonary administration in rats. European Journal of Pharmaceutics and Biopharmaceutics, 2010. 75(1): p. 33-41.

35. Overhoff, K.A., et al., Solid dispersions of itraconazole and enteric polymers made by ultra-rapid freezing. International Journal of Pharmaceutics, 2007. 336(1): p. 122-132.

36. Matteucci, M.E., et al., Highly supersaturated solutions from dissolution of amorphous itraconazole microparticles at ph 6.8. Molecular Pharmaceutics, 2009. 6(2): p. 375-385.

37. Rogers, T.L., et al., Development and characterization of a scalable controlled precipitation process to enhance the dissolution of poorly water-soluble drugs. Pharmaceutical Research, 2004. 21(11): p. 2048-2057.

38. Poggi, G., et al., Transhepatic arterial chemoembolization with oxaliplatin-eluting microspheres (oem-tace) for unresectable hepatic tumors. Anticancer Research, 2008. 28(6B): p. 3835-3842.

39. Johnson, B.A., A synopsis of the pharmacological rationale, properties and therapeutic effects of depot preparations of naltrexone for treating alcohol dependence. Expert Opinion on Pharmacotherapy, 2006. 7(8): p. 1065-1073.

40. Wang, Y., et al., Preparation and stability study of norfloxacin-loaded solid lipid nanoparticle suspensions. Colloids and Surfaces B-Biointerfaces, 2012. 98: p. 105-111.

41. Kanthamneni, N., et al., Enhanced stability of horseradish peroxidase encapsulated in acetalated dextran microparticles stored outside cold chain conditions. International Journal of Pharmaceutics, 2012. 431(1-2): p. 101-110.

42. Dey, N.S., S. Majumadar, and M.E.B. Rao, Multiparticulate drug delivery systems for controlled release. Tropical Journal of Pharmaceutical Research, 2008. 7(3): p. 1067-1075.

43. Kumar, M.P., Y.M. Rao, and S. Apte, Formulation of nanosuspensions of albendazole for oral administration. Current Nanoscience, 2008. 4(1): p. 53-58.

44. Jung, T., et al., Biodegradable nanoparticles for oral delivery of peptides: is there a role for polymers to affect mucosal uptake? European Journal of Pharmaceutics and Biopharmaceutics, 2000. 50(1): p. 147-160.

45. Murdan, S., et al., Vaccine-coated microcrystals: Enhanced thermal stability of diphtheria taxoid. Journal of Pharmacy and Pharmacology, 2003. 55 (Supplement): p. 71-72.

46. Lyle, C., J. Vos, and B.D. Moore, Formulation of hyaluronidase as a temperature-stable dry powder using protein-coated micro-crystals (PCMC). Journal of Pharmacy and Pharmacology, 2006. 58: p. A72-A72.

47. Wu, J.C., et al., Activity, stability and enantioselectivity of lipase-coated microcrystals of inorganic salts in organic solvents. Biocatalysis and Biotransformation, 2009. 27(5-6): p. 283-289.

48. Konig, C., et al., Development of a pilot-scale manufacturing process for protein-coated microcrystals (PCMC): Mixing and precipitation - Part I. European Journal of Pharmaceutics and Biopharmaceutics, 2012. 80(3): p. 490-498.

49. Moore, B.D., et al., Isolation of recombinant proteins from culture broth by co-precipitation with an amino acid carrier to form stable dry powders. Biotechnology and Bioengineering, 2010. 106(5): p. 764-773.

50. Khosravani, A., et al., Formulation of the adenylate cyclase toxin of Bordetella pertussis as protein-coated microcrystals. Vaccine, 2007. 25(22): p. 4361-4367.

51. Tao, Y.Y., et al., Development of mucoadhesive microspheres of acyclovir with enhanced bioavailability. International Journal of Pharmaceutics, 2009. 378(1-2): p. 30-36.

52. Sugihara, H., et al., Effectiveness of submicronized chitosan-coated liposomes in oral absorption of indomethacin. Journal of Liposome Research, 2012. 22(1): p. 72-79.

53. Lozzi, I., et al., Interferences of suspended clay fraction in protein quantitation by several determination methods. Analytical Biochemistry, 2008. 376(1): p. 108-114.

54. Song, H.T., et al., Preparation of the traditional Chinese medicine compound recipe heart-protecting musk pH-dependent gradient-release pellets. Drug Development and Industrial Pharmacy, 2002. 28(10): p. 1261-1273.

55. Kim, J.S., et al., Statistical optimization of tamsulosin hydrochloride controlled release pellets coated with the blend of HPMCP and HPMC. Chemical & Pharmaceutical Bulletin, 2007. 55(6): p. 936-939.

56. Eldridge, J.H., et al., Biodegradable and biocompatible poly(dl-lactide-co-glycolide) microspheres as an adjuvant for staphylococcal enterotoxin-b toxoid which enhances the level of toxin-neutralizing antibodies. Infection and Immunity, 1991. 59(9): p. 2978-2986.

57. Stertman, L., E. Lundgren, and I. Sjoholm, Starch microparticles as a vaccine adjuvant: Only uptake in Peyer's patches decides the profile of the immune response. Vaccine, 2006. 24(17): p. 3661-3668.

58. Dvorackova, K., et al., Coated hard capsules as the pH-dependent drug transport systems to ileo-colonic compartment. Drug Development and Industrial Pharmacy, 2011. 37(10): p. 1131-1140.

59. Huyghebaert, N., et al., Evaluation of extrusion/spheronisation, layering and compaction for the preparation of an oral, multi-particulate formulation of viable, hIL-10 producing Lactococcus lactis. European Journal of Pharmaceutics and Biopharmaceutics, 2005. 59(1): p. 9-15.

60. Prieto, S.A., J.B. Mendez, and F.J.O. Espinar, Starch-dextrin mixtures as base excipients for extrusion-spheronization pellets. European Journal of Pharmaceutics and Biopharmaceutics, 2005. 59(3): p. 511-521.

61. Rabiskova, M., et al., Microcrystalline cellulose in oral dosage forms. Chemicke Listy, 2007. 101(1): p. 70-77.

62. Patel, M.M. and A.F. Amin, Design and optimization of colon-targeted system of theophylline for chronotherapy of nocturnal asthma. Journal of Pharmaceutical Sciences, 2011. 100(5): p. 1760-1772.

63. Zhu, X., et al., A novel microsphere with a three-layer structure for duodenum-specific drug delivery. International Journal of Pharmaceutics, 2011. 413(1-2): p. 110-118.

64. Mercier, G.T., et al., Oral immunization of rhesus macaques with adenoviral HIV vaccines using enteric-coated capsules. Vaccine, 2007. 25(52): p. 8687-8701.

65. Ibekwe, V.C., et al., Interplay between intestinal pH, transit time and feed status on the *in vivo* performance of pH responsive ileo-colonic release systems. Pharmaceutical Research, 2008. 25(8): p. 1828-1835.

66. Khan, J., et al., Preparation and in-vitro evaluation of different controlled release polymeric matrices containing Ketoprofen. Healthmed, 2010. 4(2): p. 386-392.

67. Liu, F., et al., A novel concept in enteric coating: A double-coating system providing rapid drug release in the proximal small intestine. Journal of Controlled Release, 2009. 133(2): p. 119-124.

68. Zimova, L., et al., The development and *in vivo* evaluation of a colon drug delivery system using human volunteers. Drug Delivery, 2012. 19(2): p. 81-89.

Chapter 5: *In Vitro* Evaluation of Mucoadhesive Formulations

Abstract

Purpose. To evaluate the mucoadhesive properties of different formulations using an adjustable ramp and an artificial biorelavent gel layer. Methods. Various formulation types (i.e. lyophilized powders, films, pellets, and tablets) were manufactured to include the known mucoadhesive polymers: chitosan, alginate, HPMC (Methocel® K4M), or Carbopol® 974P (CP974P). Biorelevant gels comprised of agar and porcine mucin were prepared, and placed in a specially made holder on top of a constant temperature water-circulating system. Each mucoadhesive polymer containing formulation was applied onto the gel to adhere in a horizontal position for 1 minute. The test apparatus could be adjusted to any selected preset angle perpendicular to the horizontal plane, and a biorelavent wash medium was allowed to flow down the face of the experimental ramp at a preset rate (1, 2 or 5 mL/min). Visual progression of the test samples was observed and the quantity of test article remaining on the biorelevant ramp was assessed to quantify the relative *in vitro* mucoadhesiveness. The results were compared to an equivalent test using excised porcine intestine that replaced the synthetic biorelevant gel layer. Additionally, the data was compared to that of a previously reported rotating cylinder test method using the excised porcine tissues. To further compare the relative mucoadhesiveness of the biorelevant gel and the excised porcine intestine a texture analyzer was used to determine a force of adhesion profile with both materials. Results. The retention time of different mucoadhesive polymer containing formulations on the biorelevant gel ramp varied

significantly ($p<0.05$) in all cases. For all formulation types, HPMC (Methocel® K4M) showed the most promising mucoadhesion property (the longest retention time on the biorelevant gel ramp or excised porcine intestine), followed by Carbopol® 974P (CP974P), alginate, and chitosan. In addition, results from our biorelevant gel and from porcine intestine were comparable when using both the flowing ramp method and the tensile strength method ($p<0.05$). In addition, although the retention time of the test formulation (mucoadhesive tablets, 7mm in diameter) increased significantly on the porcine intestine, compared to the biorelevant gel ($p<0.05$), the adhesive rank order among the mucoadhesive polymers remained the same (HPMC (Methocel® K4M) > Carbopol® 974P (CP974P) > alginate). Conclusions. The *in vitro* ramp with biorelevant gel was able to evaluate the mucoadhesiveness of various polymer-containing formulations. Parameters under the control of the operator include the composition and inclination of the biorelevant gel layer, and the rate of biorelevant media washing over the test area. With this flexibility of operating conditions, the apparatus could be adjusted to parallel the varying physiological conditions along the gastrointestinal tract, as well as other potentially mucoadhesive sites in man. Furthermore, the *in vitro* test described in these studies works to reduce the burden on animal testing for high throughput screening purposes.

5.1 Introduction

"Bioadhesion" refers to the interactions between bioadhesive material (either natural or synthetic polymers) and the substrates (surface of biological cell membrane). Theories of bioadhesion have been well documented, including the wetting theory, the

diffusion theory, the electronic theory and the absorption theory [1]. Briefly, bioadhesive polymers are first wetted and absorb water, which allows the polymers to swell and further approach the biological cell membrane (Wetting theory). Once the polymers are in contact with the substrate, the polymer chains start to diffuse into the biological cell membrane. These diffused polymer chains entangle with the glycoprotein chains in the biological cell membrane (Diffusion theory), where numerous interactions between the two materials are then built-up (e.g. hydrogen bonding, electrostatic interactions, van Der Waals force, and covalent binding) (Electronic and absorption theory). These interactions provide the adhesive property of the polymers and enable a prolonged retention time of the polymers on the adhered substrates.

Bioadhesive drug delivery systems are designed to adhere onto different biological cell membranes, such as the buccal membrane [2], nasal cavity [3], vaginal membrane [4], and the mucus membrane lining along gastrointestinal tract (GI tract) [5, 6]. Satishbabu and co-worked prepared a bilaminated buccoadhesive film comprised of sodium alginate and atenolol with or without Carbopol® 974P. In an *in vitro* mucoadhesion study, both of the bilaminated films were able to remain staying on porcine buccal tissues for up to 48 hours. In addition, bilaminated films with Carbopol® 974P showed a higher hydration rate (better swelling property and higher viscosity due to the physicochemical property of the polymer), which contributed to a well-controlled and delayed release pattern of the drug [7]. Mohammadi-Samanni et al. demonstrated the use of hydroxypropylmethyl cellulose (HMPC, or Hypromellose), sodium carboxy methyl cellulose (NaCMC), and Carbopol® 974P (CP974P) for buccal adhesive tablets. The

composition of these polymers controls not only the period of adhesion, but also the release profile of the active ingredients used in the study. For the buccal adhesive tablets comprised of HPMC 500 mPas, the increase in the ratio of CP974P/HPMC or CP974P/NaCMC reduces the release rate of prednisolone, which is suitable for a controlled prednisolone release in 4-6 hours. However the increase in the ration of CP974P/NaCMC reduces the adhesiveness of the buccoadhesive tablets. Therefore, tablets made of HOMC 500 mPas and Cp974P are more suitable for controlled mucoadhesive prednisolone delivery in the buccal cavity [8].

The term "mucoadhesion" is used when adhesion is associated with the mucous membrane surfaces lining certain regions of the gastrointestinal tract including the stomach [6], intestine [9], and colon [5]. There has been increasing interest in the study of mucoadhesive drug delivery system. One of the main potential advantages of mucoadhesive formulations is the prolonged retention time and enhanced bioavailability. [10, 11]. It has been well proposed that a mucoadhesive formulation can minimize first-pass effect and provide long-term drug delivery [12]. A suitable mucoadhesive polymer should be inert, non-toxic, biodegradable and biocompatible. In addition, these polymers are generally hydrophilic, being able to absorb water and able to form a gel-like network easily after water absorption. After hydration, the macromolecular chains of mucoadhesive polymer diffused into the mucus membrane and entangled with the mucus glycoproteins (mucins). Such associated network then contributed to numerous interactions between the mucoadhesive polymer and mucins, including hydrogen bonding, van Del Waal's interactions, even covalent bonding, which provide firm

adhesion forces that allow the polymers retain on the substrate [1]. Mucoadhesive polymers can be either naturally originated, (e.g. sodium alginate [13], pectin [14], and chitosan [15] or synthetic / semi-synthetic, (e.g. HPMC [16], CP 974P [17], NaCMC [18] and some thiolated polymers.

Several feasible methods have been proposed to evaluate the mucoadhesiveness of different dosage forms *in vitro*. These include tensile test [19], everted-gut method [20], rotating cylinder method [21], and flowing test method [22]. Investigating mucoadhesive property through modified tensile tests was well documented. A rheometer is a good apparatus for evaluating mucoadhesive strength by measuring the maximum detachment force between the adhering analytes (mucoadhesive polymer containing formulation in a tablet or a disc form) and mucin films (or excised gastrointestinal membrane from animal models) [23]. The use of a rheometer in mucoadhesive strength monitoring is easy, feasible, and straightforward. Other similar methods include modified tensile strength test, [24] shear stress test [25], or studies using modified texture analyzer [26] have also been brought out.

"Everted intestine sacs" method [27-30] was also wildly used for mucoadhesion studies. Briefly, test animal intestine (e.g. rats or pigs) were harvested fresh and cut into smaller sections. Each section was everted to expose the mucus membrane and filled up with test medium. The everted sacs were then immersed into a medium containing mucoadhesion formulations (e.g. nano- or microparticles). Over a period of time, the amount of particles attached onto the everted sac was quantified and thus a relative mucoadhesiveness could be obtained. In a variation on this method, the rotating cylinder

method requires that the everted intestines be fixed onto a USP dissolution cylinder (or paddle). Here the test formulation (e.g. tablets or multiparticles) is affixed onto the everted intestinal tissue before immersion into a test medium. During the emersion period the basket/paddle is rotated at a set speed (usually 50 to 100 rpm) for a controlled period of time. Finally, the relative mucoadhesiveness of the test formulation can be obtained by evaluating the amount of material remaining on the everted intestinal tissues.

"Flowing test" is another approach for mucoadhesive strength measuring came up in the late 90's [31, 32]. In short, "Flowing test" is done by the creation of an apparatus mimicking the *in vivo* condition, in which a piece of mucus membrane or fresh excited gastrointestinal membrane lining tissue is prepared and placed on a thermal-controlled (regarding to the body temperature) slant (set at certain angle), gastric simulated fluid is flushing down the slant continuously at constant rate, while the mucoadhesive polymer containing analytes are applied and adhere on to the membrane film. Therefore, the retention time of the analytes and the amount of analytes on the film can be measured and quantified easily [33]. In addition, different *in vivo* mucus turnover rates at different region of GI tract might be paralleled by adjusting the flow rate of the specific simulated GI test medium, which is a useful variable when compared to other published *in vitro* methods.

However, all the methods introduced above need freshly excised tissue or part of the gastrointestinal tract from life animals. In recent year, laws that mandate **replacement** alternatives, **reduction** alternatives, and **refinement** alternatives (**the Three Rs**) in scientific research have been passed in the United Kingdom, Germany, the Netherlands,

the United States, and the European Union over the past decade. Therefore, our objective of this work is to perform an easily controlled, reproducible and straightforward *in vitro* estimation for evaluating mucoadhesive property of different formulations, while avoiding the need to sacrifice animals at the same time. We developed our own *in vitro* method by using a biorelevant gel (an agar/mucin mixture) as our test platform for mucoadhesion tests, which is in concord with "**Replacement** alternatives" in the **Three Rs** for the animal welfare. In this current study, various formulation types (powders, films, pellets, and tablets) were applied onto this platform and their retention time (transit on the test platform), as well as drug release profile could be monitored. Additionally, in order to investigate the correlation between using our biorelevant gel and using porcine intestinal mucus membrane as the mucoadhesion test material, the relative mucoadhesiveness of tablets on a biorelevant gel and excised porcine intestine was compared using both a modified *in vitro* mucoadhesion test with a texture analyzer and a modified *in vitro* rotating cylinder method.

5.2 Materials and methods

5.2.1 Materials

We purchased theophylline, Carbopol® 974P (CP974P) and porcine mucins from Spectrum (Spectrum, Gardena, CA, USA). Hypromellose (HPMC, Methocel® K4M) was obtained from Dow Chemical (Dow Chemical, Midland, Michigan, USA). Sodium Alginate and chitosan (medium molecular grade) was purchased from Sigma (Sigma, St. Louis, MO, USA). Avicel® PH101 was kindly provided by Asahi (Asahi, Tokyo, Japan).

5.2.2 Methods

5.2.2.1 Preparation of lyophilized powder

Theophylline and selected polymers (HPMC, Methocel® K4M, CP974P, sodium alginate, or chitosan) were dissolved in deionized water (dH_2O) overnight in 1:2 ratios (final concentration, 0.5% w/w theophylline and 1% w/w polymer). The final solution was frozen at -70 °C and then lyophilized for 2 days using a benchtop freeze dryer (Virtis, Gardiner, New York USA). After lyophilization, the samples were transferred into glass vials, sealed, and stored in desiccators at room temperature until needed.

5.2.2.2 Preparation of mucoadhesive polymer containing films

Alginate or HPMC containing films were prepared by dissolving 2% w/w (1: 1 ratio) polymer and theophylline 2% w/w in dH_2O overnight. The solution was then poured into a 15 x 15 cm^2 polytetrafluroethylene (PTFE) mold and dried at 60 °C for 5 hours. Following the casting and drying steps the films were carefully peeled off from the PTFE molds and cut into 2 x 1 cm^2 rectangular pieces for the *in vitro* mucoadhesion test.

5.2.2.3 Preparation of pellets

Polymer containing pellets were prepared via wet granulation and spheronization (Table 5.1). Before mixing, all ingredients were sieved through a US standard sieve (mesh No. 30). Each blend was dry mixed for 2 minutes using a two-blade impeller. Deionized water (15 mL) was added into the mixture and granulated for 5 minutes. The mixture was then transferred to a bench-top granulator (Luwa Benchtop Granulator, LCI Corporation, Charlotte, NC, USA) for extrusion as granules. The granules were then transferred into a bench-top spheronizer (Caleva, Model 250, Caleva Process Solution

LTD, UK) and spheronized into pellets. The pellets were dried in oven overnight at 60 °C and stored in desiccators at room temperature until needed.

Table 5.1: Composition of mucoadhesive tablets (w/w %)

Formulation, %	Avicel® PH101	Lactose	Theophylline	Mg stearate	Talc	Chitosan	Carbopol® 974P	Sodium Alginate	Methocel®, K4M
Chitosan	29	20	10	0.5	0.5	40			
Carbopol 974P	29	20	10	0.5	0.5		40		
Alginate	29	20	10	0.5	0.5			40	
HPMC, K4M	29	20	10	0.5	0.5				40
Control	29	60	10	0.5	0.5				

5.2.2.4 Preparation of tablets

The composition of varies tablets with mucoadhesive polymers were listed in Table 5.2.

Table 5.2: Composition of mucoadhesive polymer containing pellets (w/w %)

Formulation, %	Avicel® PH101	Yellow Lake	Theophylline	Chitosan	Carbopol® 974P	Sodium Alginate	Methocel®, K4M
Chitosan	55.5	0.4	14.7	29.4			
Carbopol 974P	55.5	0.4	14.7		29.4		
Alginate	55.5	0.4	14.7			29.4	
HPMC, K4M	55.5	0.4	14.7				29.4
Control	84.9	0.4	14.7				

Before mixing, all ingredients were sieved through an US standard sieve (mesh No. 30). Methocel® K4M, sodium alginate, and Carbopol® 974P (Spectrum, Gardena, CA)

were selected as polymers for matrix tablet preparation. Avicel® PH101, each polymer, talc, and theophylline were mixed for 20 minutes in a V-shape blender. Magnesium stearate was then added before a further mixing for 5 minutes. The tablet mixture was compressed into either 7 mm or 10 mm diameter tablets by direct compression using a rotary tablet press (Stokes, Dual Pressure Press Model 2, PA, USA). All tablets were controlled at the same hardness of 5kp.

5.2.2.5 Preparation of artificial gel for the in vitro mucoadhesion test:

Biorelavent gels for *in vitro* mucoadhesion test were prepared fresh before each test. Agar (2 g) was dissolved into deionized water (100 mL) and heated up in a microwave for 2 minutes, at 700-Watt power. The agar gel solution (2% w/v) was then poured into a PTFE mold (15 cm in length and 3 cm in width, Figure 5.1). The gels were left on a benchtop at room temperature for cooling (30 minutes). Another biorelevant gel was prepared by the same method as previous described, but comprised of 1or 2% (w/v) porcine mucins with 1 or 2% (w/v) agar.

Figure 5.1: Preparation of artificial gels. (A) A 4% w/v mucin suspension was first mixed with a heated solution of 4% w/v agar to make a final mixture of 2% mucin and 2% agar. (B) The mixture was then cooled down and poured into the Teflon mold to form the final gel for mucoadhesion test.

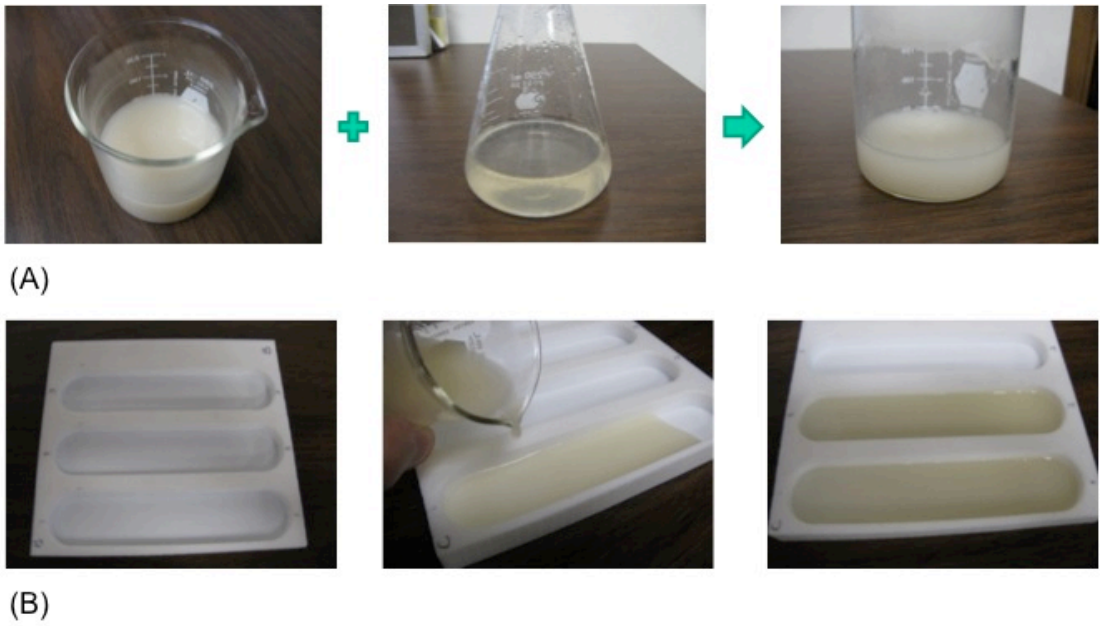

5.2.2.6 In vitro mucoadhesion test: Flowing ramp

5.2.2.6.1 Powders and films

A biorelevant gel was first attached onto a 500 mL incubation flask using double-sided tape and then placed at an angular elevation of 40 degree (adjustable). The incubation flask was filled with circulating water at 45 °C by a water bath and a sink water pump to maintain the surface temperature of the biorelevant gel at 37 °C. A plastic cover was then put onto the flask (covering the whole biorelevant gel) to keep the system at 37°C (all temperature was verified using an infrared thermometer (Fisher Scientific, Pittsburgh, PA, USA). Simulated gastric fluid (SGF) or simulated intestinal fluid (SIF) was allowed to flow down from the top of the biorelevant gel using a reservoir that was

powered by a peristaltic pump (Q-400, Watson Marlow, Wilmington, MA, USA) at a constant rate (adjustable). At the beginning of each mucoadhesion test, a sample (250 mg of prepared powders or 250 mg of prepared films) was applied directly onto the biorelevant gel at a specific starting point (shown in Figure 5.2) and set for 5 minutes to equilibrium the temperature to 37°C. All samples were hydrated before the test. Deionized water at37 °C (200 μL) was immediately applied onto each sample using a transfer pipette, for a 30 second hydrated period. In each test, SGF (or SIF) was set to flow at a starting point (0.5 cm above the sample position). Photos of the test samples were taken by digital camera (Casio EX-Z40, Casio, Shibuya, Tokyo, Japan); also, 1 mL of SGF (or SIF) eluent samples were collected at 30, 60, 120, 180, and 240 minutes.

Figure 5.2: *In vitro* mucoadhesion test ramp. The prepared gel was attached onto a plastic flask by double-sided tape. The flask was filled with water and circulated with a water bath to maintain the system temperature at 37◦C. The whole gel area was covered by a plastic thermal cover to avoid moisture lost and maintain the system temperature.

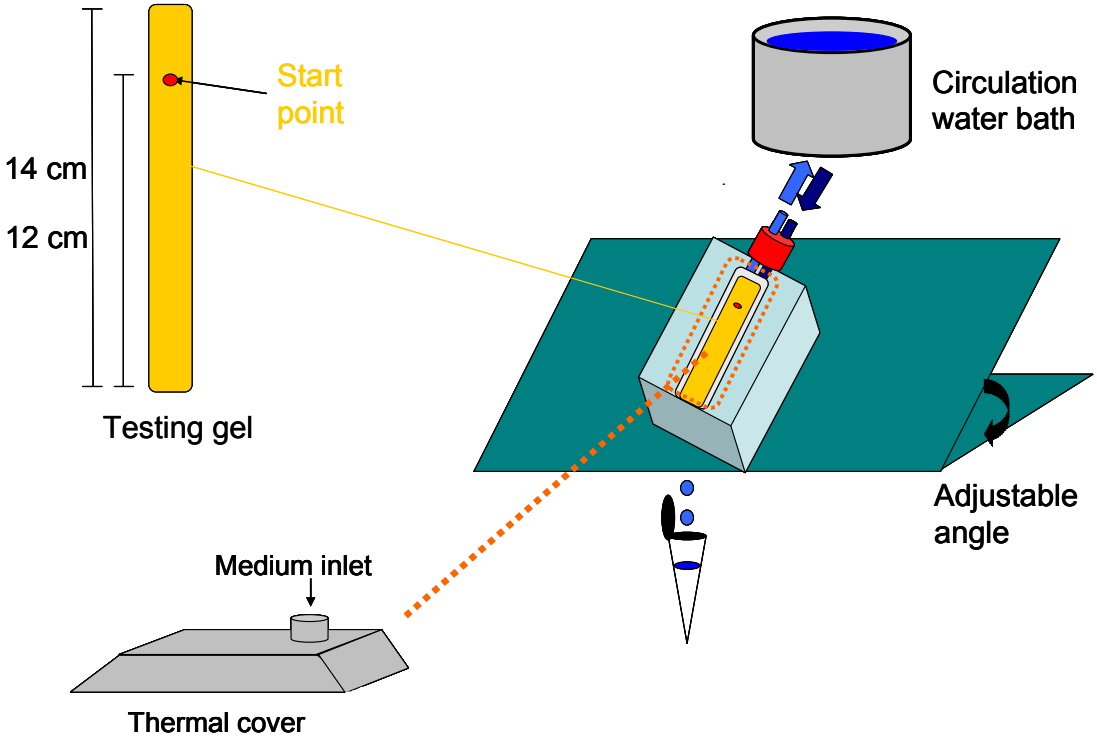

An aliquot (200 μL) of the collected eluent samples was placed into a 96-well culture plate (BD Falcon Microplate, Germany) and analyzed by a *UV* detector at 270 nm. All measurements were carried out in triplicate and drug release was calculated retrospectively following completion of drug release (drug loading and the total drug released from a tablet after complete dissolution were measured and found the same).

5.2.2.6.2 Tablets

The inclined mucoadhesion platform was set-up as previously described. A tablet was put on the biorelevant gel and a force of 20 N was applied onto the tablet for 30

seconds to hold the tablet at the starting position. 200 μL deionized water (37 °C) was immediately applied onto the each sample using a transfer pipette. The tablet was then allowed to be hydrated for 30 seconds. In each test, SGF (or SIF) was set to flow at a starting point (0.5 cm above the sample position). All sample collecting and analyzing methods were the same as described in the methods description for powders or films. The flow rate of SGF (or SIF) was controlled at 1, 2, or 5 ml/min.

5.2.2.6.3 Pellets

For each test, 50 pellets were applied onto the gel with 200 μL deionized water at 37 °C for hydration, and allowed to remain at a horizontal position for 1 minute. All sample collecting and analyzing methods were the same as described in the methods description for powders or films.

5.2.2.7 In vitro mucoadhesion test: Tablet and porcine intestinal mucus membrane

Pig intestines were obtained from freshly excised animals at a local slaughterhouse (Taylor Meat, Taylor, TX, USA) and stored in 37 °C normal saline during transportation. Before each mucoadhesion test, the pig intestines were cut into sections of 15 cm in length, and remaining intestinal content residues were flushed out using pH 6.8 phosphate buffer. The intestine tissue was then cut open and attached onto a 500 mL culture flask, with the surface of the porcine intestine being maintained as smooth as possible. A 10 mm diameter tablet was applied onto the porcine intestinal mucus membrane, and a force of 20N was applied onto the tablet for 30 seconds before the mucoadhesion test started.

Photos were taken at 0.5, 1, 2, 3, and 4 hours. . All sample collecting and analyzing methods were the same as described in the methods description for powders or films.

5.2.2.8 In vitro mucoadhesion test: Rotating cylinder method

In order to validate our objective of using artificial get as a replacement of animal tissue for *in vitro* mucoadhesion test, the differences of mucoadhesion property of various mucoadhesive tablets between the biorelevant gel and pig intestine were conducted via a modified rotating cylinder method. Polymer containing or control tablets (10 mm in diameter, manufactured as previously described) were attached onto freshly excised intestinal porcine mucosa (or 2% mucin, 2% agar biorelevant gel), which was been adhered onto a stainless-steel cylinder (diameter 4 cm; height 5. cm; apparatus 4-cylinder, USP) by cyanoacrylate glue. Thereafter, the cylinder was placed in the dissolution apparatus according to the USP, entirely immersed with 900 mL of pH 6.8 phosphate buffer at 37 °C and agitated with 100 rpm (Figure 5.3). The detachment of the test tablets was determined within an observation time of up to 4 hours.

Figure 5.3: *In vitro* mucoadhesion test: Rotating cylinder method. Two different test substrates were used to compare the mucoadhesion property between the test material and mucoadhesive polymer containing tablets: (A) Pig intestinal mucus membrane (a layer of everted porcine intestine was adhered/wrapped a disc of artificial gel (2% mucin, 2% agar, 7mm in diameter), (B) Artificial gel.

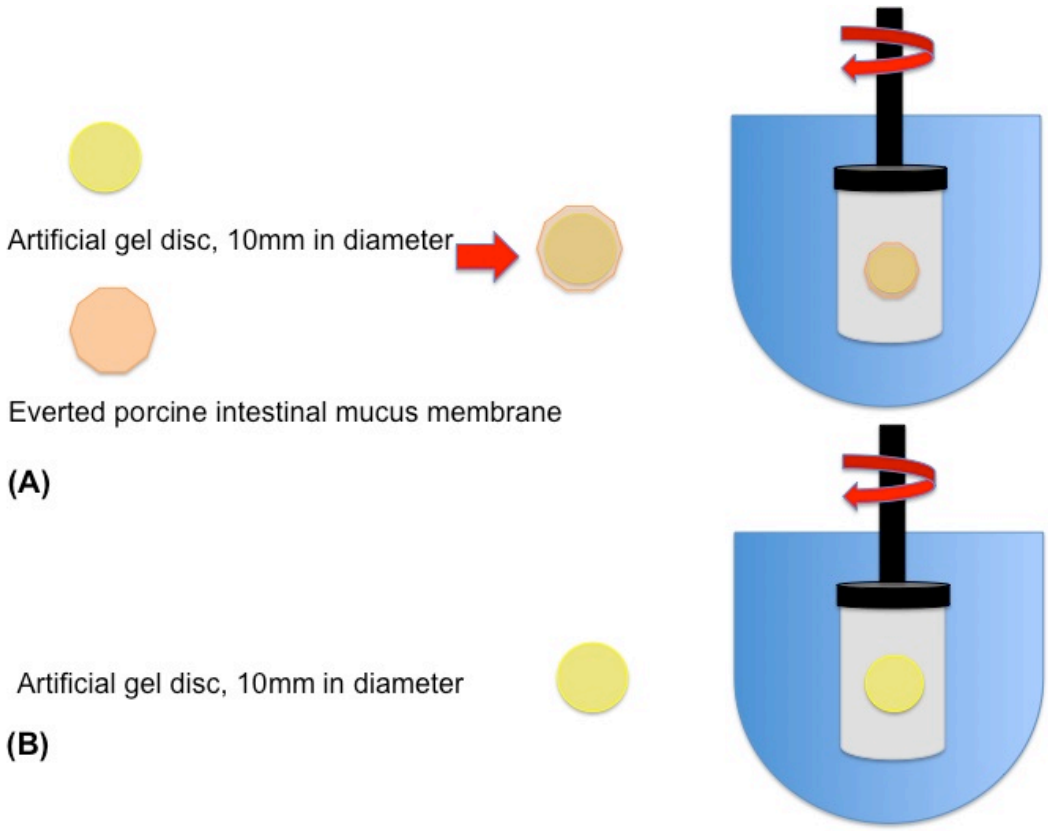

5.2.2.9 In vitro mucoadhesion test: Texture Analyzer

To further quantify the adhesive property of the mucoadhesive tablets and validate that whether it is feasible to use our biorelevant gel as a replacement for life animal tissue (from GI tract). A modified *in vitro* mucoadhesion test using TA.XT*Plus* Texture Analyzer (Texture Technology, Scarsdale, NY, USA) was conducted [10, 26]. Briefly, mucoadhesion was evaluated by means of a tensile test, where the measurement of

maximum detachment force (Fmd) or work of adhesion (Wad) required for detach the test tablet from a piece of biorelevant gel or pig intestinal mucus membrane, after an initial period of intimate contact, is indicative of the mucoadhesion property. The force involved in the detachment process was measured by a TA-XT2 texture analyzer under the adhesive mode. Immediately before the mucoadhesive measurements, biorelevant gel or freshly excised porcine intestinal mucus membrane were rinsed with deionized water (37 °C), and mounted onto the instrument clamp and immersed into 600 mL pH 6.8 phosphate buffer (37 °C) for 10 minutes. A test tablet was attached onto a plastic probe (cylindrical, 15 mm diameter) by means of double-sided carbon tape. The contact region of either the artificial get or pig intestinal mucus membrane was kept as smooth as possible and the contact area was larger than the diameter of the test tablet to avoid test errors. Each group of test tablets (attached on the probe) was then immersed in the test fluid for a hydration period of 10, 30 or 60 seconds. The probe was then lowered at a speed of 1 cm per minute until it touched the biorelevant gel surface or porcine mucus membrane surface. A contact force of 0.05N was applied for 30 seconds. Subsequently, probe was brought to its initial position at a speed of 0.5 mm/min. and F_{md} and W_{ad} were measured automatically by the software provided with the texture analyzer.

5.2.3 Statistics

All biorelevant gel related tests where repeated (n=6), and tests using pig intestine were repeated less (n=3) due to the limited access to animal tissues. All results were analyzed by statistic software, SAS JMP 7.0 (Student's t Test, Tukey HSD, and /or ANCOVA).

5.3 Results and discussion

5.3.1 Biorelavent Gel

Before setting up the *in vitro* mucoadhesion test device, several different gelling materials were tested and screened for the most appropriate material for our study. 1, 2, or 5% (w/v) of porcine mucin suspension was prepared and the viscosity of each suspension was measured using a rheometer (AR2000ex rheometer, TA Instrument, New Castle, DE, USA). As the mucins content in each suspension increased, the viscosity also increased (Table 5.3). However, when the mucins content reached 5% w/v, the final product of the biorelevant gel became soft and was not able to form a stable gel subsequent mucoadhesion testing. Therefore, a 2% mucins (w/v) solution was selected as the final biorelevant gel throughout the study. Alginate, Carbopol® 974P, Methocel® K4M, and agar were tested as the gel forming material after the final mucins content was decided (2% w/v). Several biorelevant gel forming mixtures were prepared and their viscosity was measured using a rheometer (Table 5.3). Although a mixture composed of 2% Methocel® K4M (w/v) and 2% mucins (w/v) showed the highest viscosity (766.32±12.12 cp), the mixture was not able to form a stable gel after cooling down to room temperature; therefore, agar was selected as the gel forming material in this study, and the final biorelevant gel prepared for the *in vitro* mucoadhesion test was made of 2% w/v mucins and 2% w/v agar.

Table 5.3: Summary of the viscosity test of screening the artificial gel forming material

Gel forming mixture	Viscosity (cp), at 25°C
Mucin 1%	1.19 ± 0.11
Mucin 2%	2.32 ± 0.17
Mucin 5%	6.01 ± 0.30
Mucin 1%, agar 0.5%	100.94 ± 7.14
Mucin 2%, agar 0.5%	464.02 ± 18.41
Mucin 2%, agar 1%	527.02 ± 9.12
Mucin 2%, agar 2%	Gel formed at 35°C, not able to measure the viscosity
Mucin 2%, alginate 2%	184.81 ± 13.57
Mucin 2%, Carbopol 974P 2%	286.61 ± 12.37
Mucin 2%, Methocel®K4M 2%	766.32 ± 12.12

5.3.2 *In vitro* mucoadhesion test: Biorelevant gel inclined mucoadhesion platform

5.3.2.1. Lyophilized powder

As a preliminary study, we used a biorelevant gel composed of only 2% w/w agar as our prototype test gel for our *in vitro* mucoadhesion test ramp. In the test with either simulated intestinal fluid or simulated gastric fluid, HPMC (Methocel® K4M) and Carbopol® 974P showed promising mucoadhesion properties by displaying an increased retention time on our test gel slant ($p<0.05$, Student's t Test). However, sodium alginate containing sample showed similar increased retention time when tested with simulated gastric fluid (Figure 5.4A), but this lasted less than 30 minutes when simulated intestinal fluid was used (Figure 5.4B**).** Chitosan containing samples were surprisingly found top have no adhesive properties when using agar as a substrate, this is in contrast to previous study with other experimental designs [6, 9]. This lack of adhesion could be due to the

fact that the lyophilized powders dissolve more rapidly in both simulated gastric fluid and simulated intestinal fluid, a consequence of the large surface area and overall porosity of the samples which was evidenced by SEM imaging, compare to alginate, HPMC (Methocel® K4M) and Carbopol® 974P (data not shown). Previous studies have indicated that microcrystalline chitosan does not demonstrate an *in vitro in vivo* correlation in terms of mucoadhesive properties [5], demonstrating that further investigation is required for this material. Modified chitosans, such as thiolated chitosan have been shown to have good mucoadhesion of therapeutic ingredients in many *in vitro* studies [34].

Figure 5.4: % Retention of lyophilized mucoadhesive polymer containing powders (A): Test media: SGF; flow rate: 1mL/min; artificial gel: 2% mucin; angle: 30 degree; (B):Test media: SIF; flow rate: 1mL/min; artificial gel: 2% mucin; angle: 30 degree). * N=6, Mean value ± Stdev

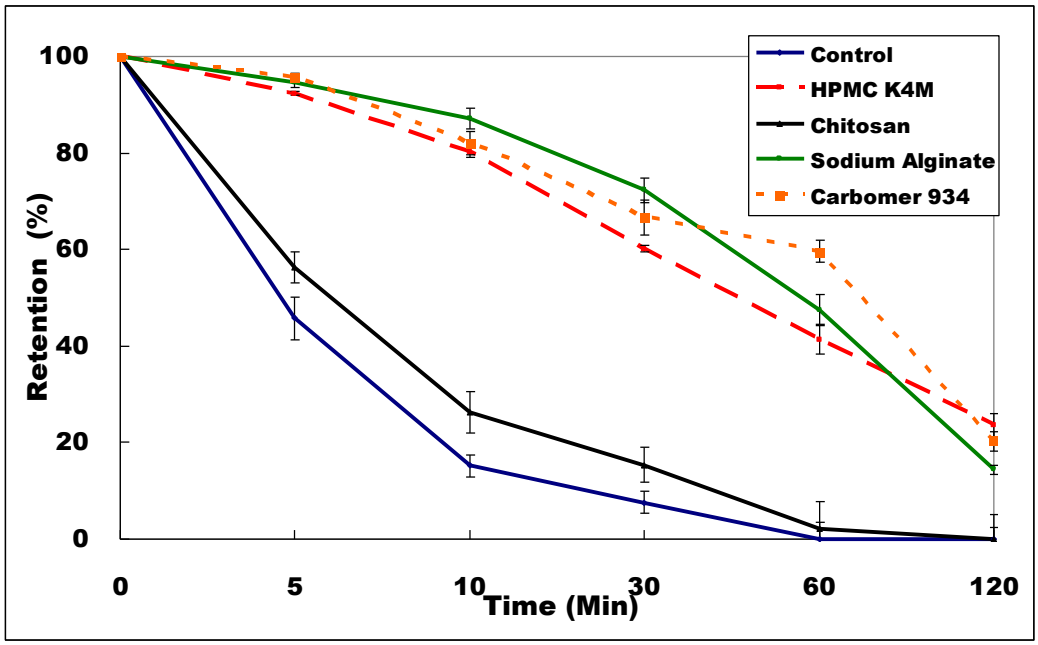

(A)

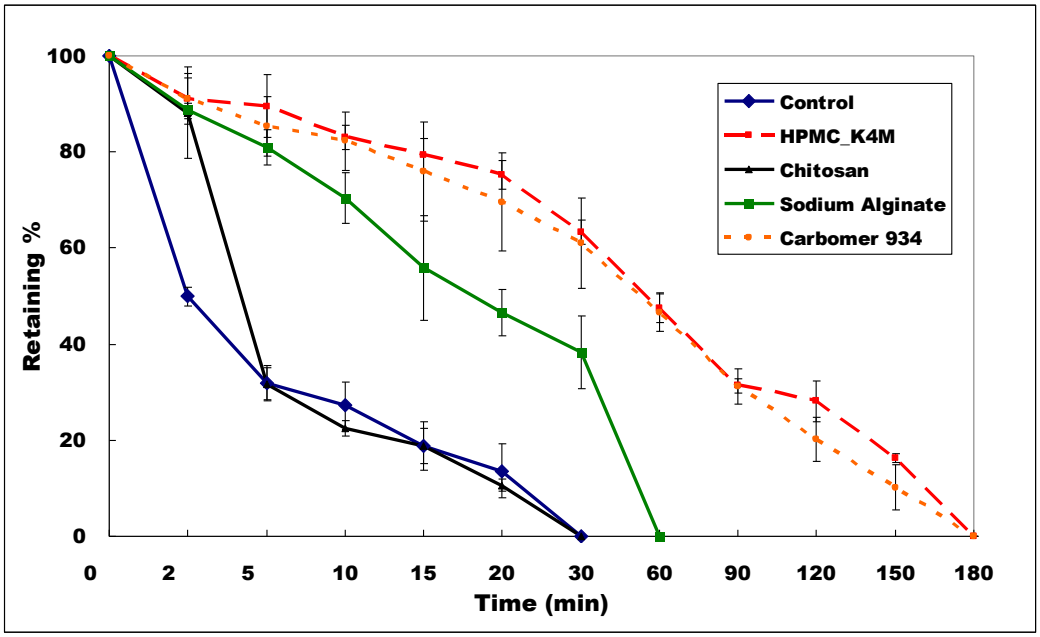

(B)

To further investigate the modified test apparatus, different composition of the test gels were compared. The 2% w/v agar gel was replaced with a 2% w/v agar and 2% w/v mucins gel mixture for our test device. Lyophilized samples containing selected polymers had a statistically significant longer retention time on the biorelevant gel with both agar and mucin compared to the agar alone ($p < 0.05$) (Figure 5.4 and 5.5), implying that the interaction between agar and mucin might be a more suitable tool for a future *in vitro* mucoadhesion test by allowing for a greater formulation discrimination time. Therefore, a biorelevant gel composed of 2% mucin and 2% agar might be able to parallel current *in vitro* mucoadhesion tests, where animal tissues are required.

Figure 5.5: % Retention of lyophilized mucoadhesive polymer containing samples (Test medium: SIF, flow rate: 1mL/min; artificial gel: 2% w/w agar and 2% mucin; angle: 30 degree). * N=6, Mean value ± Stdev

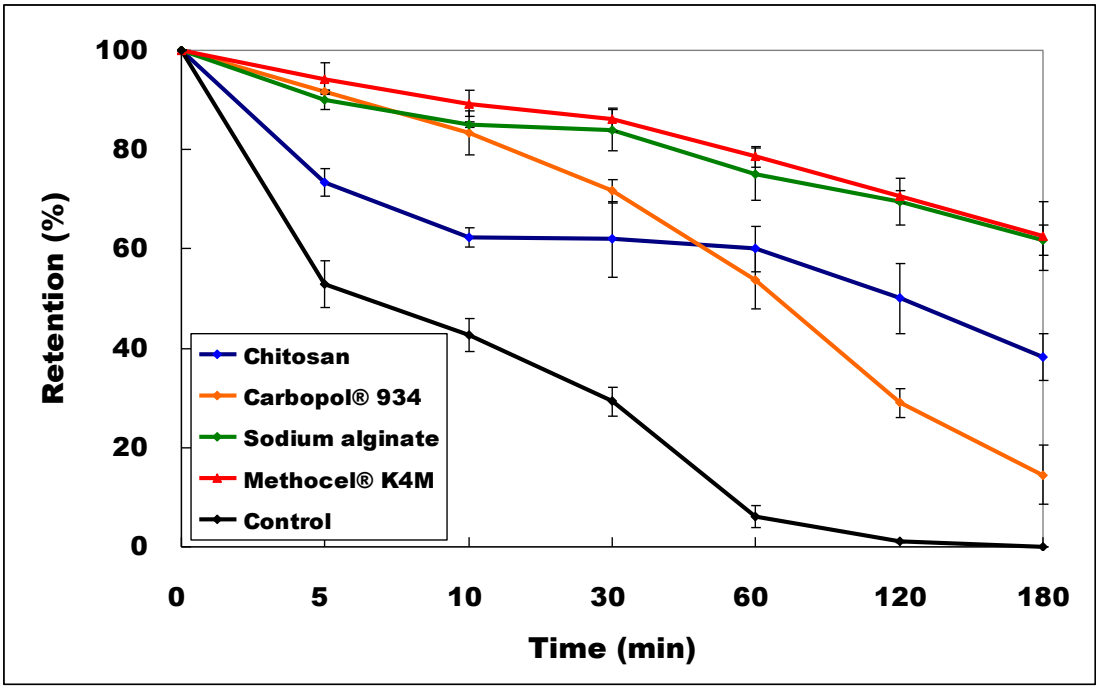

5.3.3.2 Mucoadhesive polymer containing films

Similar trends were found when test polymer containing films under the same condition (2% w/v mucin: 2% w/v agar biorelevant gel, flow rate: 1 mL/min). No significant difference was found between two test mediums, SGF and SIF ($p>0.05$, Student's t Test). Films made of HPMC or sodium alginate showed significant longer retention time on the test gel ramp ($p<0.0001$, Student's t Test), compared to the control film. And after 180 minutes the HPMC containing film showed an increased retention time on the test gel ramp compared to the film containing sodium alginate ($p<0.05$, Student's t Test). However, contrary to the lyophilized sample, the retention time of films composed of sodium alginate showed no significant difference, compared to the HPMC containing film ($p>0.05$), regardless of whether SGF or SIF was used as the flowing media (Figure 5.6)**.** Each film itself was seen to dissolve much slower than was observed with the corresponding lyophilized powders. For each film during the testing phase, thorough wetting followed by adhesion enabled each film to stick on the gel ramp for a longer period of time, compared to the corresponding lyophilized powders.

Figure 5.6: % Retention of mucoadhesive polymer containing films: (A): Test medium: SGF, flow rate: 2mL/min; artificial gel: 2% mucin, 2% agar; angle: 30 degree; (B): Test medium: SIF; flow rate: 2mL/min; artificial gel: 2% mucin, 2% agar; angle: 30 degree). * N=6, Mean value ± Stdev

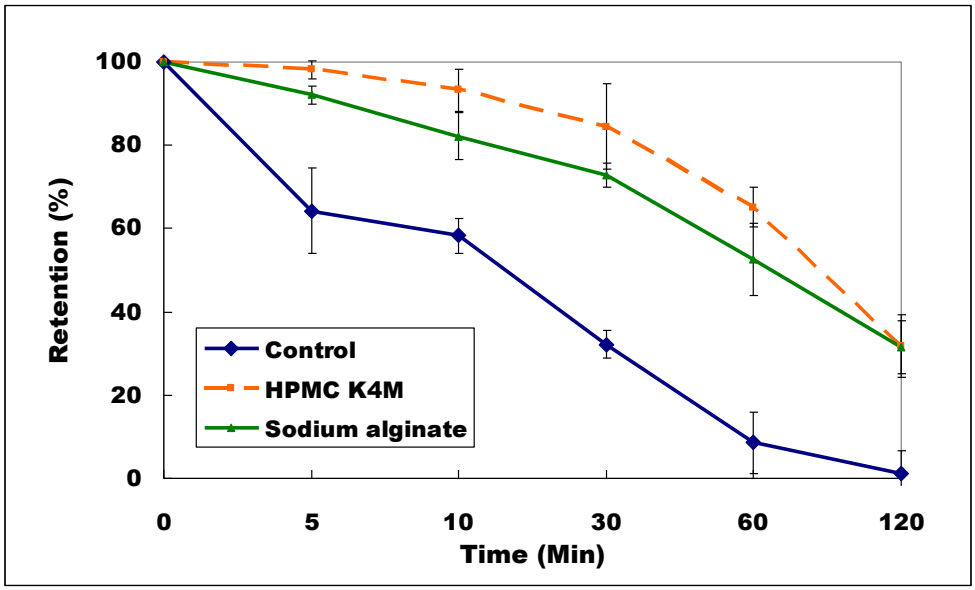

(A)

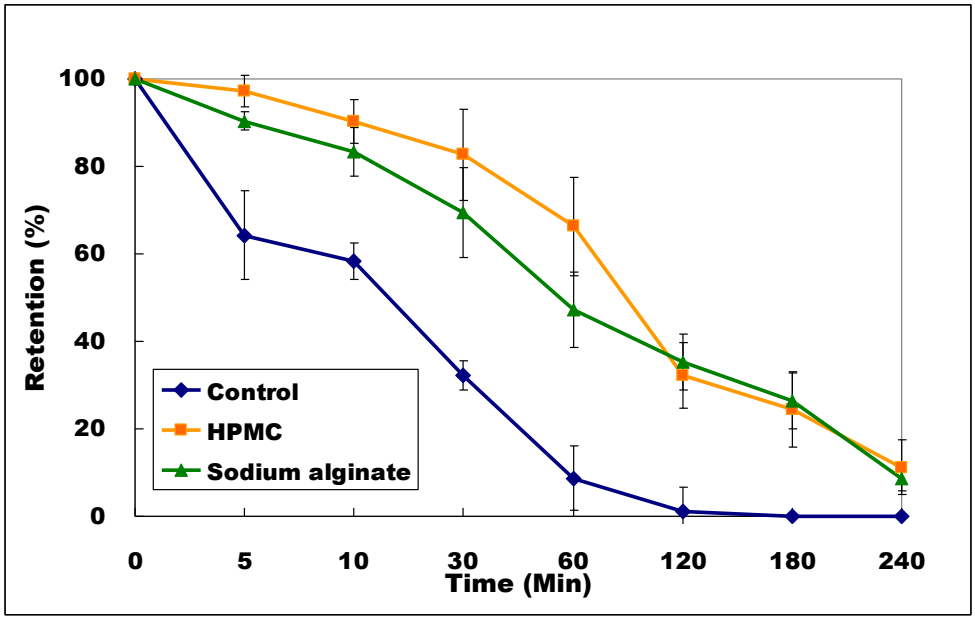

(B)

5.3.3.3 Polymer containing pellets

At a flow rate of 1 mL/min all pellets stayed on the gel throughout the 4-hour test period. As the flow rate doubled up to 2 mL/min, pellets containing HPMC or Carbopol absorbed water quickly to cause swelling in the first 10-30 minutes. This enabled the pellets to attach more firmly onto the gel, supporting the same observations obtained for the polymer containing powders or films, described above. At a constant flow rate of 2 mL/min, pellets containing sodium alginate or chitosan remained on the gel ramp for 2 hours and 3 hours, respectively. Control pellets were flushed down from the gel ramp in less than 1.5 hours (Figure 5.7 and 5.8).

Figure 5.7*: In vitro* mucoadhesion test of mucoadhesive polymer containing pellets (Test medium: SIF; flow rate: 2mL/min; artificial gel: 2% mucin, 2% agar; angle: 40 degree).

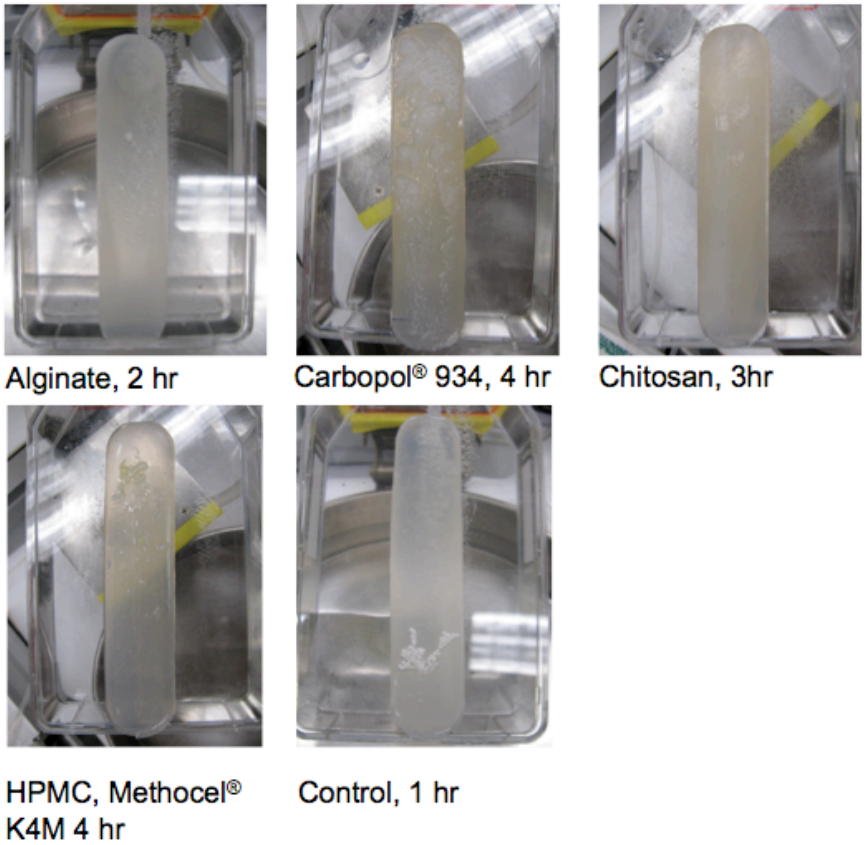

When the flow rate was increased to 5 mL/min, only HPMC and Carbopol containing pellets were able to remain attached to the gel ramp for up to 2 hours, with all the other pellets being washed down the test ramp in less than 1.5 hours (control pellets: 5 minutes; chitosan pellets: 30 minutes; alginate pellets: 1.5 hours) (Figure 5.8).

Figure 5.8: % Retention of pellets; (A): Test medium: SIF; flow rate: 2mL/min; artificial gel: 2% mucin, 2% agar; angle: 40 degree; (B): Test medium: SIF; flow rate: 5mL/min; artificial gel: 2% mucin, 2% agar; angle: 40 degree. * N=6, Mean value ± Stdev

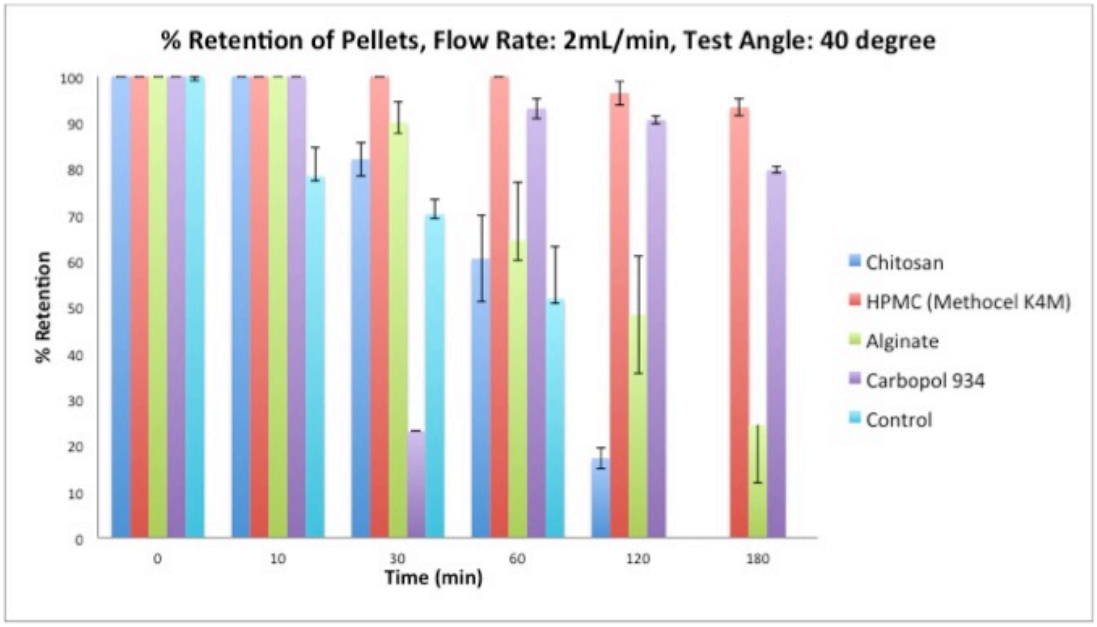

(A)

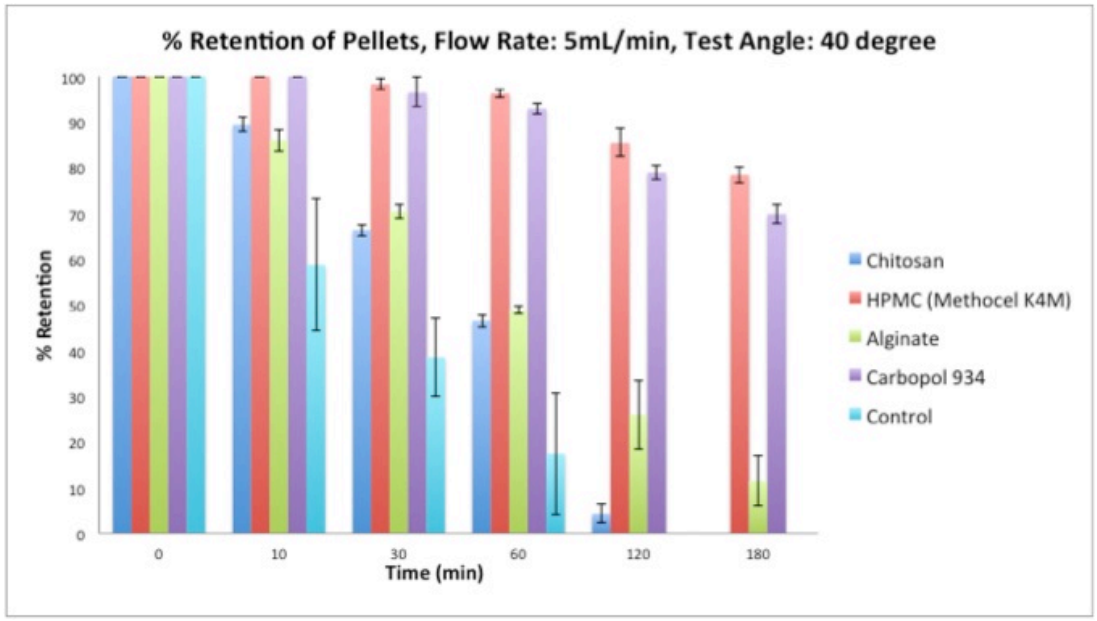

(B)

The adhesiveness of each polymer formulation was greatly affected by the flow rate of the simulated GI tract medium. It is well documented that the he thickness of the mucus gel and its turnover rate varies along the GI tract [35, 36]. For example previous studies have shown that in a rat model, mucus secretion rate was significantly higher in the jejunum (1.1 ±0.5 μg glucose equivalent/min*cm^2) than in the colon (0.5±0.2 μg glucose equivalent/min*cm^2 [37]. It is highly likely that the adhesiveness of a given mucoadhesive formulation would be influenced differently at particular regions of the GI tract. Using the test method described in this study for the *in vitro* biorelevant gel ramp, different *in vivo* mucus turnover rates at different region of GI tract might be paralleled by adjusting the flow rate of the specific simulated GI test medium, a useful variable when compared to other published *in vitro* methods.

5.3.3.4 Polymer containing tablets

Similar trends to those found with the lyophilized samples and films were found seen with the polymer containing matrix tablets. HPMC, sodium alginate, and Carbopol enhanced the retention time of tablets for more than 4 hours at a continuous flow SIF of 1 mL/min. However, significant differences were seen after 120 minutes, for each tablet with a SIF flow rate set at 2 mL/min. Both HPMC and Carbopol displayed better retention than sodium alginate ($p<0.05$, Tukey HSD). When comparing the control tablet with the HPMC containing tablets, a significant difference ($p<0.05$) was observed at 120 minutes (flow rate: 2 mL/min). At 2 hours, the control tablet was completely disintegrated and was not able to attach onto the gel ramp; while a tablet containing 40% HPMC maintained its initial starting position on the artificial mucous ramp for at least 4 hours. Even with a change in ramp elevation, from 20 to 40 degrees adjacent to the

horizontal plane, no significant change in movement was seen ($p>0.05$, Student's t Test) (Figure 5.9).

Figure 5.9: % Retention of mucoadhesive polymer containing tablets; (A): Test medium: SIF; flow rate: 1mL/min; artificial gel: 2% mucin, 2% agar; angle: 20 degree; (B): Test medium: SIF; flow rate: 1mL/min; artificial gel: 2% mucin, 2% agar; angle: 40 degree. * N=6, Mean value ± Stdev

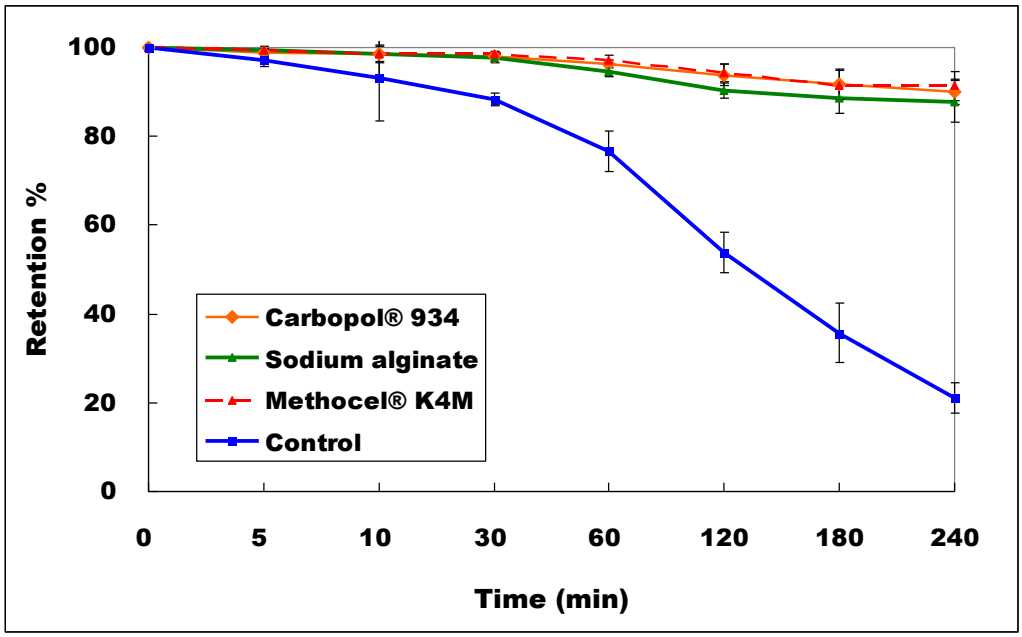

(A)

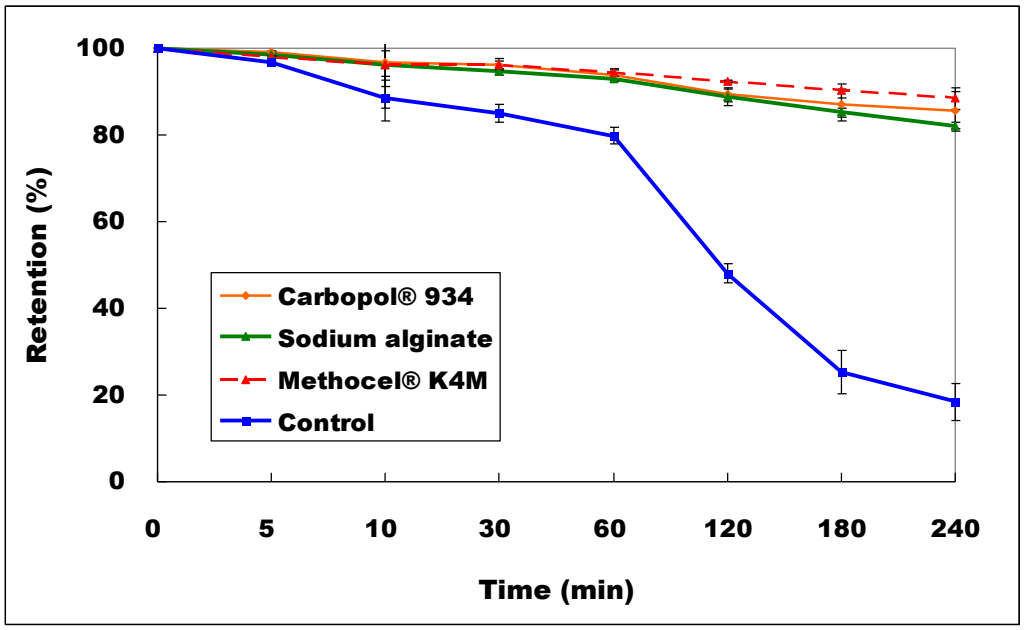

(B)

The flow rate (1 ml/min and 2 ml/min) can significantly affect the retention of our test tablets, except for tablets composed of HPMC ($p<0.05$, Student's t Test) (Figure 5.9A and 5.10), which can be further applied to the study that needs to be carried out at different flowing speed to mimic different sections of the GI tract of living animals.

Figure 5.10: % Retention of mucoadhesive polymer containing tablets (Test medium: SIF; flow rate: 2mL/min; artificial gel: 2% mucin, 2% agar; angle: 40 degree). * N=6, Mean value ± Stdev

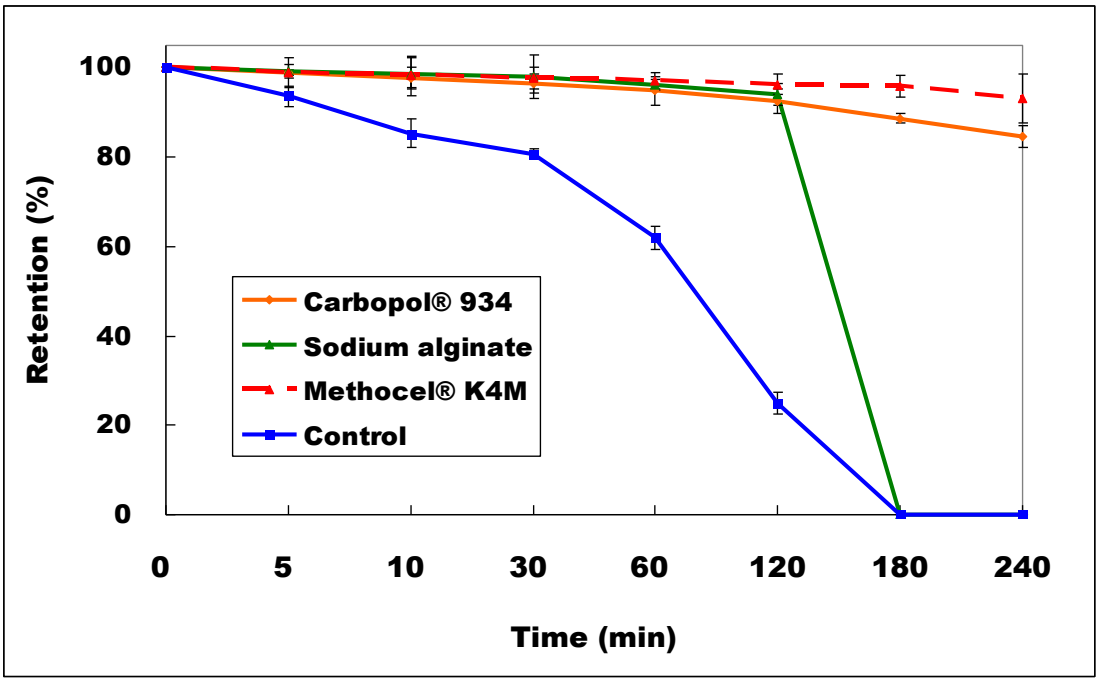

In addition, when the flowing rate of test medium was further increased to 5 mL/min, only tablets made of HPMC (Methocel® K4M) (Figure 5.11) and Carbopol® 974P could still hold on to the gel ramp for more than 4 hours, while tablet with sodium alginate can only stay on the gel for about 45 minutes (data not shown).

Figure 5.11: Pictures taken at specific time points during the *in vitro* mucoadhesion test. Sample: 10mm, 40% w/w Methocel®, K4M tablet; test media: SIF; flow rate: 5mL/min (A. 0 minute; B. 30 minutes; C. 2 hours; D. 3 hours).

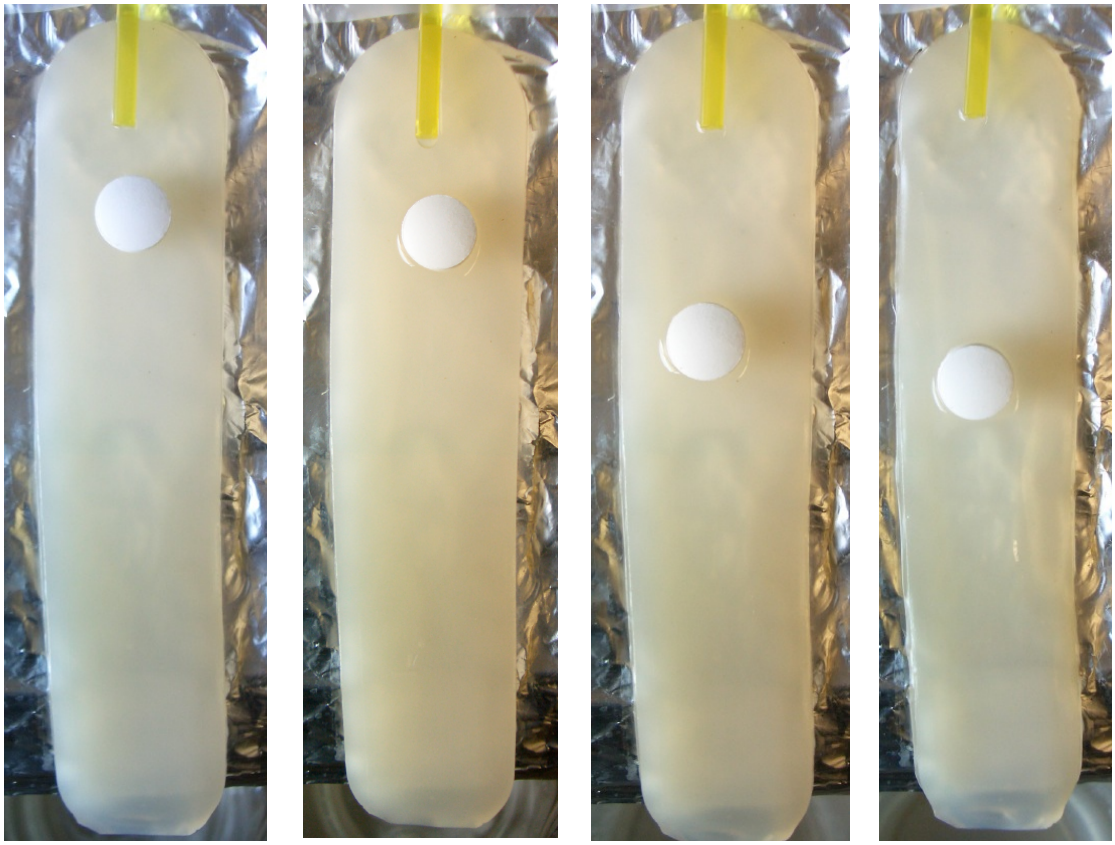

(A) **(B)** **(C)** **(D)**

In summary, the rank order for tablet mucoadhesion was found to be HPMC > Carbopol > sodium alginate. Both HPMC and Carbopol containing tablets showed a prolonged retention time that could potentially be exploited to enhance local absorption of a drug at a particular region of the GI tract.

The increased retention time of all the tablet formulation compared with the other studied formulation types is a direct result of the more rapid wetting and water absorption properties, whereby tablets were observed to wet and absorb the simulated GI fluids

within the first 1-2 minutes, enabling the tablets to adhere firmly onto the artificial mucous gel layer.

The different retention times of polymer containing tablets at various flow rates is shown in Figure 5.12. Since physiological conditions vary in different sections of the GI tract, a given orally administered formulation encounters changing conditions during GI transit (e.g. varied propagating rate from the stomach to the lower small intestine or colon) This varying propagation rate may be due to different flow rates of the physiological fluid or even varying gravitational influences related to patient/gut orientation. Using the adjustable components of by our *in vitro* biorelevant gel flowing ramp, it is possible to monitor mucoadhesive property of a given formulation at conditions to parallel different sections of the GI tract *in vitro* (i.e. media flow rate of the testing medium and/or testing angle).

Figure 5.12: Retention time of different mucoadhesive polymer containing tablets under varied flow rate. * N=6, Mean value ± Stdev

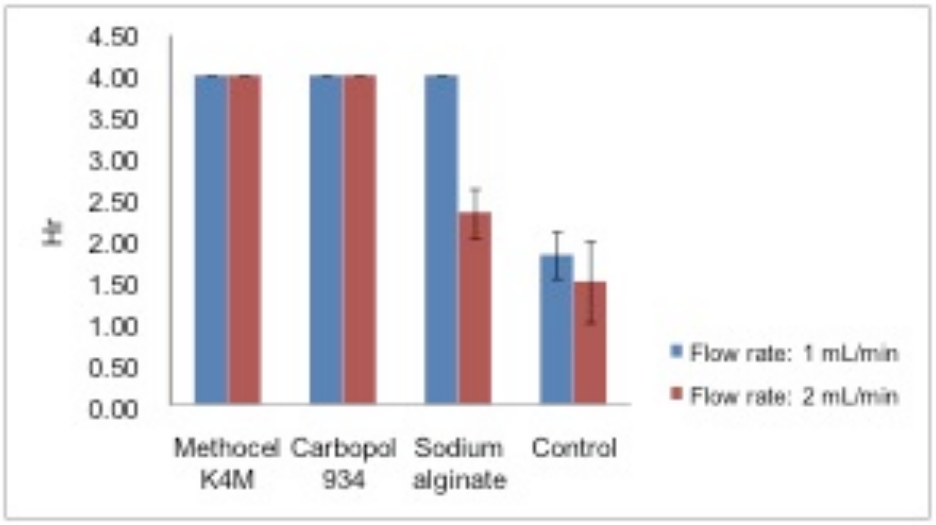

Furthermore, when using porcine intestine as test material, a slight increase, but not significant ($p>0.05$) retention time was found with the HPMC and Carbopol containing tablets, compared to using the biorelevant gel (2% mucin, 2% agar) as test material. However, chitosan containing tablets showed an increased retention time on the porcine intestine, compared to that on the biorelevant gel ($p<0.05$). This is likely that the polymer chains of chitosan were able to diffuse and entangle with the glycoprotein chains of the porcine intestinal mucus membrane, which provide the adhesion force between each other. However, although the biorelevant gel was made of 2% mucin content, after the gelling process, the accessibility of glycoprotein chains from mucin was highly hindered; which limited the diffusion and entanglement of polymer chains between mucin glycoprotein; therefore, greatly reduced the adhesion force. Unlike chitosan, HPMC and Carbopol have a greater propensity to uptake substantial quantities of water [38]. It is well documented that both HPMC and Carbopol swell and form gel network after hydration [39, 40], while chitosan swells rapidly, but requires ionic or covalent cross-linking with basic salts to generate a gel network after hydration [41]. Therefore, in our study, tablets made of only 40% chitosan disintegrated rapidly and then spread along the biorelevant gel during the mucoadhesion test; while tablets made with 40% HPMC or Carbopol swelled and formed a gel network at the surface of the biorelevant gel to enable an increased retention time on the gel ramp.

5.3.3.5 Polymer containing tablet test using excised porcine intestine

To validate our results using biorelevant gel as a potential replacement of animal tissues for *in vitro* mucoadhesion test, freshly excised porcine intestines were obtained and tested with mucoadhesive polymer containing tablets as comparison. The % retention of test tablet is shown in Figure 5.13. The results from porcine intestine were in

agreement with the results from the biorelevant gel (2% mucin, 2% agar). Both HPMC and Carbopol containing tablets were able to stay onto the porcine intestine ramp for more than 4 hours. Alginate containing tablets were able to stay adhered to the ramp for up to 3 hours.

Figure 5.13: % Retention of mucoadhesive polymer containing tablets (Test medium: SIF; flow rate: 2mL/min; test angle: 30 degree), (A) Artificial gel, 2% mucin, 2% agar; (B) Porcine intestine. * N=6, Mean value ± Stdev

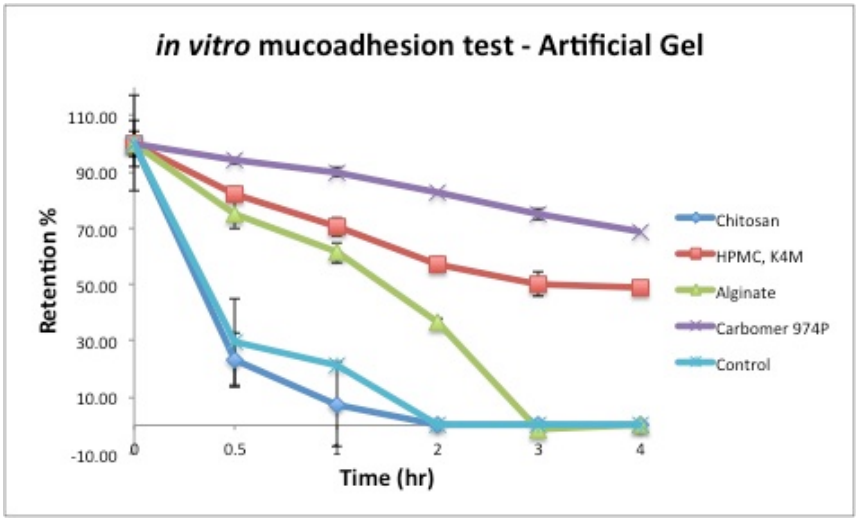

(A)

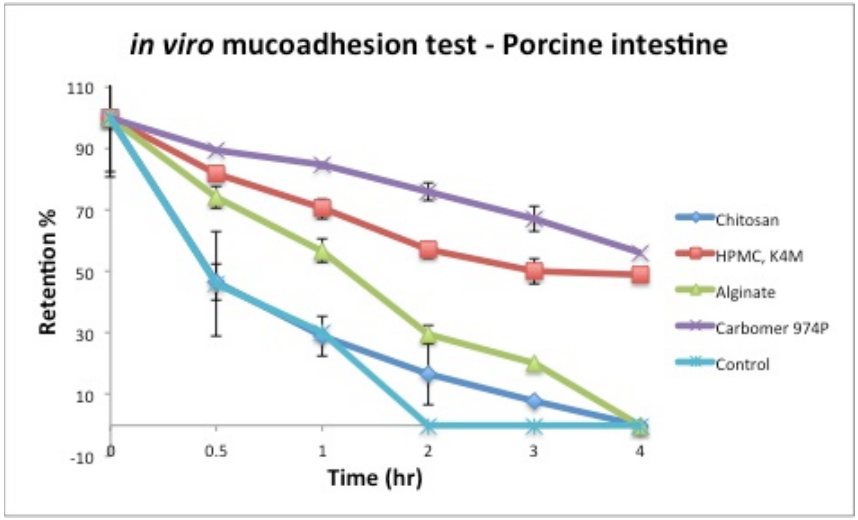

(B)

Furthermore, when using porcine intestine as test material, a slight increase, but not significant ($p>0.05$) retention time was found with the HPMC and Carbopol containing tablets, compared to using the biorelevant gel (2% mucin, 2% agar) as test material. However, chitosan containing tablets showed an increased retention time on the porcine intestine, compared to that on the biorelevant gel ($p<0.05$). This is likely that the polymer chains of chitosan were able to diffuse and entangle with the glycoprotein chains of the porcine intestinal mucus membrane, which provide the adhesion force between each other. However, although the biorelevant gel was made of 2% mucin content, after the gelling process, the accessibility of glycoprotein chains from mucin was highly hindered; which limited the diffusion and entanglement of polymer chains between mucin glycoprotein; therefore, greatly reduced the adhesion force. Unlike chitosan, HPMC and Carbopol have a greater propensity to uptake substantial quantities of water [38]. It is well documented that both HPMC and Carbopol swell and form gel network after hydration [39, 40], while chitosan swells rapidly, but requires ionic or covalent cross-linking with basic salts to generate a gel network after hydration [41]. Therefore, in our study, tablets made of only 40% chitosan disintegrated rapidly and then spread along the biorelevant gel during the mucoadhesion test; while tablets made with 40% HPMC or Carbopol swelled and formed a gel network at the surface of the biorelevant gel to enable an increased retention time on the gel ramp.

5.3.4 *In vitro* mucoadhesion test: Rotating cylinder

Mucoadhesion is a complex phenomenon that can be influenced by numerous physicochemical circumstances. Clearly one of these is the electrostatic force. The chemical nature of the cell surface and mucin causes negative charges at physiological pH, and so positively charged molecules interact with them. The mucoadhesive

properties of neutral HPMC polymers and anionic Carbomers are based on other physicochemical processes, such as hydrogen bonding and van der Waal's interactions [42]. A USP dissolution apparatus modified rotating cylinder method is well documented to evaluate and compare mucoadhesive properties among different mucoadhesive polymers, such as, PAA, pectin, thiolated-chitosan and thiolated-PAA. Of the polymer tablets tested, both HPMC and Carbopol containing tablets showed significant prolonged adhesion times on the biorelevant gel made of 2% mucin and 2% agar, when compared to the gel made of only 2% agar ($p<0.05$). This was in agreement with the previous observations determined using the *in vitro* ramp test. Chitosan tablets disintegrated rapidly when immersed in the dissolution medium, therefore, its mucoadhesive property could not be evaluated using this method. In addition, the adhesion time of HPMC (Methocel® K4M), Carbopol® 974P and alginate tablet on the everted porcine intestine mucus membrane was more than 8-, 5-, and 4-fold increased, respectively, in comparison to on the 2% mucin, 2% agar biorelevant gel (Figure 5.14).

Figure 5.14: *In vitro* mucoadhesion test: Rotating cylinder, (A) 2% agar; (B) 2% mucin, 2% agar; (C) porcine intestine. * N=6, Mean value ± Stdev

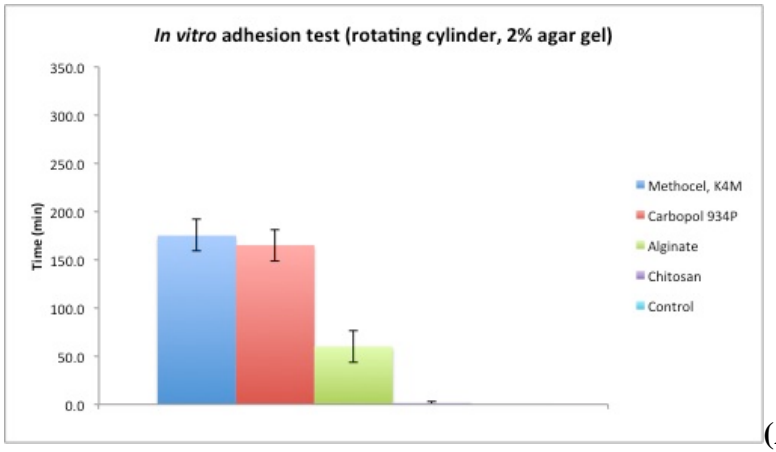

(A)

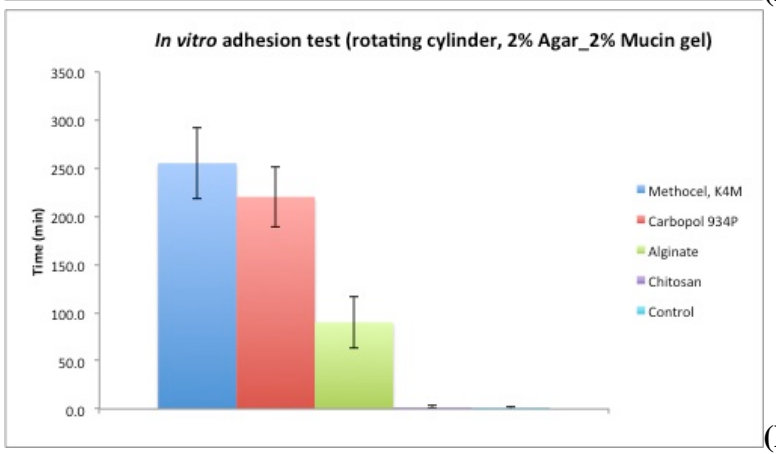

(B)

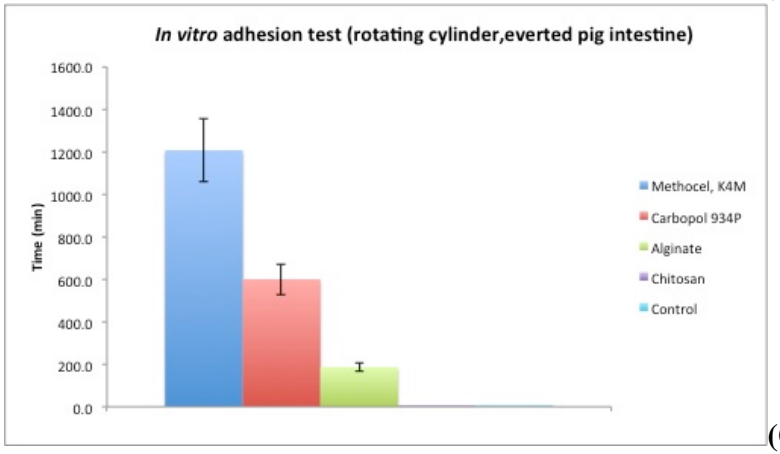

(C)

5.3.5 *In vitro* mucoadhesion test: Texture Analyzer

Orally delivered dosage forms reach the GI tract in a wetted state [26], and so each of the test tablets were pre-hydrated before starting the tensile test. The pre-hydration time was set at 10, 30, or 60 seconds. However, it was determined that 10 seconds was too short to allow a tablet to fully wet, and 60 seconds was deemed to cause certain tablets to disintegrate before adhesion could take place (i.e. the control and alginate tablets). Therefore, the final pre-hydration time selected was a compromise of 30 seconds.

Data from tensile test showed a significant difference ($p<0.05$) in the behavior (both Force of Detachment and Work of Adhesion) of either the HPMC or Carbopol containing tablets with respect to the control tablets. The analysis of mucoadhesive power by the detachment force and the adhesion work allowed for a better characterization of the interactions between mucoadhesive polymers and substrate material (i.e. the mucus membrane) according to findings from other studies on the bioadhesive drug delivery systems. The maximum force of detachment (Fmd) for either HPMC or Carbopol mucoadhesion was significantly higher (Figure 5.15) than for either the alginate or the control groups ($p<0.05$), regardless whether the 2% w/w mucin: 2% w/w agar biorelevant gel or porcine intestine was used as the tablet attachment substrate. This was in concordance with both the results from the *in vitro* ramp and rotating cylinder methods. The work of adhesion (Wad), using the experimental conditions described above showed that adhesion values of HPMC and Carbopol were always greater than those for the alginate or the control groups (Figure 5.15) ($p<0.05$). Additionally it was observed that

both Fmd and Wad showed an increase, but not statistically significant, when the biorelevant gel was replaced by porcine intestine as the test substrate material, which is in accordance to what we found from the *in vitro* ramp study.

Figure 5.15: Tensile test of mucoadhesive polymer containing tablets, (A) on 2% mucin, 2% agar artificial gel; (B) porcine intestinal mucus membrane. * N=6, Mean value ± Stdev

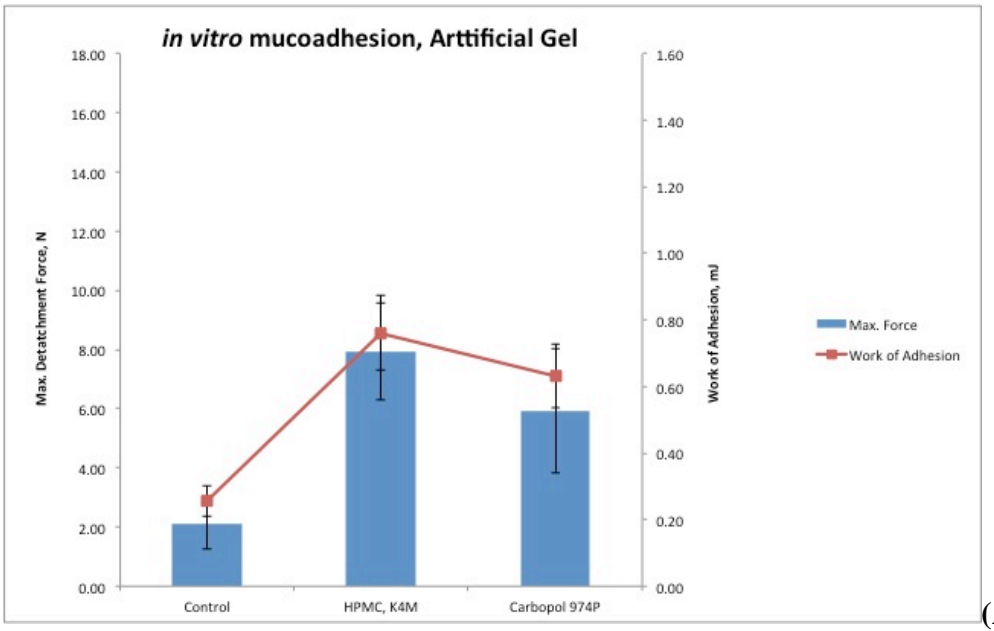

(A)

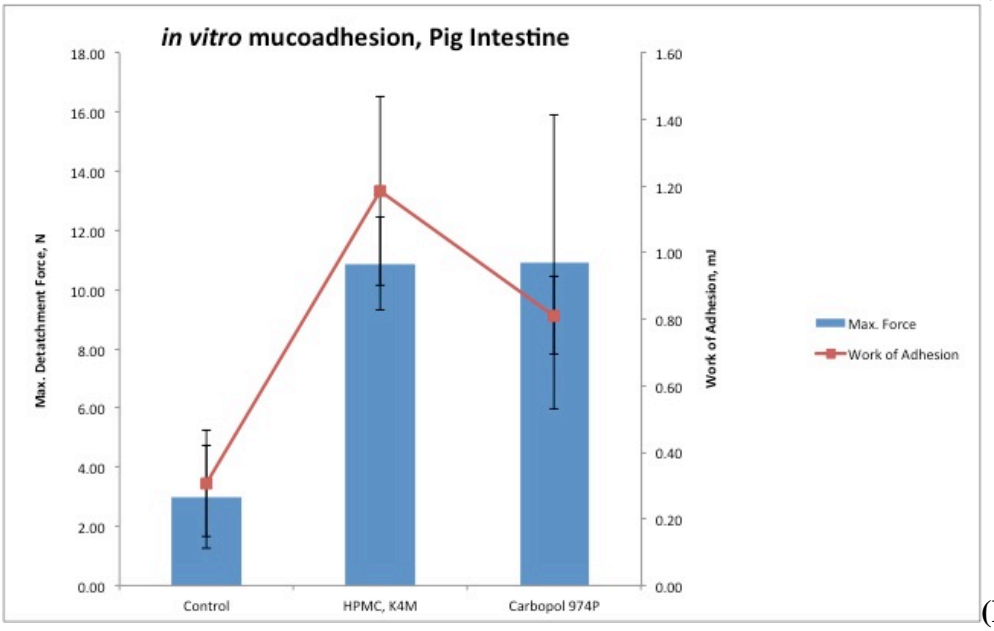

(B)

5.4 Conclusions

The *in vitro* biorelevant gel flowing ramp developed in this study may be used to investigate the mucoadhesive properties of polymers and provide an *in vitro* rank order for study. It is anticipated that this may reduce the burden of testing animals future proposed mucoadhesive studies. Among the mucoadhesive polymers tested in the study, HPMC (Methocel® K4M) showed best mucoadhesive property, followed by Carbopol® 974P, and sodium alginate. This is anticipated that this may reduce the burden of test animals future proposed mucoadhesive studies. Moreover, we proved that, the *in vitro* biorelevant gel flowing ramp we developed is capable of investigating the mucoadhesive properties of different dosage forms, including powders, pellets, and tablets. The device could further be adapted to mimic physiological conditions at different sections of the gastrointestinal tract by adjusting the flow rate, device angle, and the testing medium applied. Most important of all, it is anticipated that the biorelevant gel is able to replace animal tissues in *in vitro* mucoadhesion and reduces the burden of test animals in *in vitro* mucoadhesion test, which is in concord with the 3R's of animal welfare.

5.5 Reference

1. Dodou, D., P. Breedveld, and P.A. Wieringa, Mucoadhesives in the gastrointestinal tract: revisiting the literature for novel applications. European Journal of Pharmaceutics and Biopharmaceutics, 2005. 60(1): p. 1-16.

2. Kamel, R., A. Mahmoud, and G. El-Feky, Double-phase hydrogel for buccal delivery of tramadol. Drug Development and Industrial Pharmacy, 2012. 38(4): p. 468-483.

3. Belgamwar, V.S., et al., Design and development of nasal mucoadhesive microspheres containing tramadol HCl for CNS targeting. Drug Delivery, 2011. 18(5): p. 353-360.

4. Pereira, R.R.D. and M.L. Bruschi, Vaginal mucoadhesive drug delivery systems. Drug Development and Industrial Pharmacy, 2012. 38(6): p. 643-652.

5. Varum, F.J.O., et al., Mucoadhesive platforms for targeted delivery to the colon. International Journal of Pharmaceutics, 2011. 420(1): p. 11-19.

6. Pund, S., et al., Gastroretentive delivery of rifampicin: *In vitro* mucoadhesion and *in vivo* gamma scintigraphy. International Journal of Pharmaceutics, 2011. 411(1-2): p. 106-112.

7. Satishbabu, B.K. and B.P. Srinivasan, Preparation and Evaluation of Buccoadhesive Films of Atenolol. Indian Journal of Pharmaceutical Sciences, 2008. 70(2): p. 175-179.

8. Mohammadi-Samani, S., R. Bahri-Najafi, and G. Yousefi, Formulation and *in vitro* evaluation of prednisolone buccoadhesive tablets. Farmaco (Lausanne), 2005. 60(4): p. 339-344.

9. Dunnhaupt, S., et al., Distribution of thiolated mucoadhesive nanoparticles on intestinal mucosa. International Journal of Pharmaceutics, 2011. 408(1-2): p. 191-199.

10. Hagerstrom, H. and K. Edsman, Interpretation of mucoadhesive properties of polymer gel preparations using a tensile strength method. Journal of Pharmacy and Pharmacology, 2001. 53(12): p. 1589-1599.

11. Chowdary, K.P.R. and Y.S. Rao, Mucoadhesive microspheres for controlled drug delivery. Biological & Pharmaceutical Bulletin, 2004. 27(11): p. 1717-1724.

12. Varum, F.J.O., et al., An investigation into the role of mucus thickness on mucoadhesion in the gastrointestinal tract of pig. European Journal of Pharmaceutical Sciences, 2010. 40(4): p. 335-341.

13. Md, S., et al., Gastroretentive drug delivery system of acyclovir-loaded alginate mucoadhesive microspheres: Formulation and evaluation. Drug Delivery, 2011. 18(4): p. 255-264.

14. Bigucci, F., et al., Pectin-based microspheres for colon-specific delivery of vancomycin. Journal of Pharmacy and Pharmacology, 2009. 61(1): p. 41-46.

15. Makhlof, A., Y. Tozuka, and H. Takeuchi, Design and evaluation of novel pH-sensitive chitosan nanoparticles for oral insulin delivery. European Journal of Pharmaceutical Sciences, 2011. 42(5): p. 445-451.

16. Pandey, S., et al., Formulation and in-vitro evaluation of bilayered buccal tablets of carvedilol. Indian Journal of Pharmaceutical Education and Research, 2010. 44(3): p. 259-266.

17. Adhikary, A. and P.R. Vavia, Bioadhesive ranitidine hydrochloride for gastroretention with controlled microenvironmental pH. Drug Development and Industrial Pharmacy, 2008. 34(8): p. 860-869.

18. Chary, R.B.R., G. Vani, and Y.M. Rao, *In vitro* and *in vivo* adhesion testing of mucoadhesive drug delivery systems. Drug Development and Industrial Pharmacy, 1999. 25(5): p. 685-690.

19. Jackson, S.J. and A.C. Perkins, *In vitro* assessment of the mucoadhesion of cholestyramine to porcine and human gastric mucosa. European Journal of Pharmaceutics and Biopharmaceutics, 2001. 52(2): p. 121-127.

20. Cattani, V.B., et al., Lipid-core nanocapsules restrained the indomethacin ethyl ester hydrolysis in the gastrointestinal lumen and wall acting as mucoadhesive reservoirs. European Journal of Pharmaceutical Sciences, 2010. 39(1-3): p. 116-124.

21. Bernkop-Schnurch, A., et al., Preparation and characterisation of thiolated poly(methacrylic acid)-starch compositions. European Journal of Pharmaceutics and Biopharmaceutics, 2004. 57(2): p. 219-224.

22. Le Ray, A.M., et al., Development of a "continuous-flow adhesion cell" for the assessment of hydrogel adhesion. Drug Development and Industrial Pharmacy, 1999. 25(8): p. 897-904.

23. Mortazavi, S.A. and J.D. Smart, An investigation of some factors influencing the in-vitro assessment of mucoadhesion. International Journal of Pharmaceutics, 1995. 116(2): p. 223-230.

24. Park, H. and J.R. Robinson, Mechanisms of mucoadhesion of poly(acrylic acid) hydrogels. Pharmaceutical Research, 1987. 4(6): p. 457-464.

25. Smart, J.D., I.W. Kellaway, and H.E.C. Worthington, An *in vitro* investigation of mucosa-adhesive materials for use in controlled drug delivery. Journal of Pharmacy and Pharmacology, 1984. 36(5): p. 295-299.

26. Thirawong, N., et al., Mucoadhesive properties of various pectins on gastrointestinal mucosa: An *in vitro* evaluation using texture analyzer. European Journal of Pharmaceutics and Biopharmaceutics, 2007. 67(1): p. 132-140.

27. Santos, C.A., et al., Correlation of two bioadhesion assays: the everted sac technique and the CAHN microbalance. Journal of Controlled Release, 1999. 61(1-2): p. 113-122.

28. Santos, C.A., et al., Evaluation of anhydride oligomers within polymer microsphere blends and their impact on bioadhesion and drug delivery *in vitro*. Biomaterials, 2003. 24(20): p. 3571-3583.

29. Takeuchi, H., et al., Mucoadhesive properties of carbopol or chitosan-coated liposomes and their effectiveness in the oral administration of calcitonin to rats. Journal of Controlled Release, 2003. 86(2-3): p. 235-242.

30. Miyazaki, Y., et al., Evaluation of mucoadhesion for dextran derivatives in solid state. Yakuzaigaku, 2002. 62(1): p. 14-22.

31. Kakoulides, E.P., J.D. Smart, and J. Tsibouklis, Azocrosslinked poly(acrylic acid) for colonic delivery and adhesion specificity: *in vitro* degradation and preliminary *ex vivo* bioadhesion studies. Journal of Controlled Release, 1998. 54(1): p. 95-109.

32. Patel, M.M., et al., Mucin/poly(acrylic acid) interactions: A spectroscopic investigation of mucoadhesion. Biomacromolecules, 2003. 4(5): p. 1184-1190.

33. Smart, J.D., et al., The retention of C-14-labelled poly(acrylic acids) on gastric and oesophageal mucosa: an *in vitro* study. European Journal of Pharmaceutical Sciences, 2003. 20(1): p. 83-90.

34. Baloglu, E., et al., *In vitro* evaluation of mucoadhesive vaginal tablets of antifungal drugs prepared with thiolated polymer and development of a new dissolution technique for vaginal formulations. Chemical & Pharmaceutical Bulletin, 2011. 59(8): p. 952-958.

35. Smart, J.D., The basics and underlying mechanisms of mucoadhesion. Advanced Drug Delivery Reviews, 2005. 57(11): p. 1556-1568.

36. Varum, F.J.O., et al., Mucoadhesion and the gastrointestinal tract. Critical Reviews in Therapeutic Drug Carrier Systems, 2008. 25(3): p. 207-258.

37. Rubinstein, A. and B. Tirosh, Mucus gel thickness and turnover in the gastrointestinal-tract of the rat - response to cholinergic stimulus and implication for mucoadhesion. Pharmaceutical Research, 1994. 11(6): p. 794-799.

38. Villalobos, R., P. Hernandez-Munoz, and A. Chiralt, Effect of surfactants on water sorption and barrier properties of hydroxypropyl methylcellulose films. Food Hydrocolloids, 2006. 20(4): p. 502-509.

39. Bajwa, G.S., et al., Microstructural imaging of early gel layer formation in HPMC matrices. Journal of Pharmaceutical Sciences, 2006. 95(10): p. 2145-2157.

40. Tamburic, S. and D.Q.M. Craig, An investigation into the rheological, dielectric and mucoadhesive properties of poly(acrylic acid) gel systems. Journal of Controlled Release, 1995. 37(1-2): p. 59-68.

41. Moura, M.J., et al., *In situ* forming chitosan hydrogels prepared via ionic/covalent co-cross-linking. Biomacromolecules, 2011. 12(9): p. 3275-3284.

42. Carvalho, F.C., et al., Mucoadhesive drug delivery systems. Brazilian Journal of Pharmaceutical Sciences, 2010. 46(1): p. 1-17.

Chapter 6: Size Discrimination in Rat and Mouse Gastric Emptying

Abstract

Objectives: To investigate the relationship between particle size and gastric emptying in rodents using radiolabeled insoluble polymethyl methacrylate (PMMA) microcapsules/beads. Methods: PMMA microcapsules (50–500 μm) and beads (0.5–3 mm) loaded with technetium-99m diethylene triamine pentaacetic acid (^{99m}Tc-DTPA) were administered to ICR mice or Sprague Dawley (SD) rats by oral gavage (n=6 in each testing group). Gamma scintiscans were acquired initially following administration and then at hourly intervals to 4 hours. Results: Scintiscans revealed that the smallest PMMA microcapsules (50-100 μm) or beads (0.5-1 mm) were impeded in the stomach and emptied slower in both rodent species. In mice, no significant difference in gastric emptying was found with microcapsules between 100 to 300 μm in diameter (p=0.25). In rats, beads with diameters of 2-3 mm stayed in the stomach for up to 4 hours. Conclusions: Gastric emptying in both ICR mice and SD rats was remarkably influenced by particle size. However, the cut-off emptying size in ICR mice could not be determined, due to the limitation of current available dosing method (the largest particle that could be administered via oral gavage was 300 μm)The cut-off emptying size in SD rats was between 1.5 to 2 mm. Therefore, particles with a diameter greater than 2 mm should not be used for gastric emptying studies of intact particles in SD rats, as their emptying is retarded in the stomach.

6.1 Introduction

The rate of gastric emptying is a key concern for oral drug administration and its potential impact on drug bioavailability and/or localized therapies in the gastrointestinal (GI) tract [1-3]. The gastric emptying rate is dependent on both physiological variables [4] and pharmaceutical factors [5]. Physiological variables include the fed or fasted state of a testing subject, health/disease status [6], and the dosing time in relation to the interdigestive migrating myoelectric current (IMMC) [5]. Pharmaceutical factors include size, shape and the density of oral solid dosage forms. In a monogastric species, the gastric emptying rate of an oral dosage form can be altered by its size, shape, as well as density, and the varied gastric emptying rate, which is related to the sieving property of the pylorus [5]. Martinez et al. further indicated that particles larger than 2-3 mm in diameter were not able to pass freely to the duodenum, inferring that particles larger than this range are retained in the stomach for continued attrition and size reduction due to gastric motility [5]. Additionally, in a canine model under fasted state, particles less than 1 mm in diameter take approximately 0.5 hours to empty the stomach, while particles of 5-10 mm in diameter empty following 1.5 hours [7]. In humans, particle of diameters between 3-7 mm can pass through the pylorus freely, although particles larger than this range and up to 16 mm have been shown to pass through the stomach and reach the small intestine when administered with water. [5]. In addition to size and density of the given formulation, the composition of food can also alter the gastric emptying rate. In general, foods with high fat or high carbohydrate content display a longer gastrointestinal emptying time [8]. The gastric emptying rate was prolonged in the fed state of beagle

dogs when compared to a fasted state, irrespective of the administered particle sizes in the study [7].

The relationship between particle size and the rodent stomach pylorus are currently not fully understood *in vivo*. It is widely accepted that the pylorus of monogastric animals performs a sieving function during the postprandial state, allowing passage of liquid chyme and small particles into the duodenum but retaining larger particles, during each contraction [5, 8]. The larger particles are propelled to the back of the stomach (at which point their size may be reduced) until they can pass into the small intestine [5]. Therefore, the gastric emptying time of larger particles would be delayed until suitable attrition has occurred; compared to smaller particles. Thus, it may be assumed that different particle sizes would have differing gastric emptying rates. In the case of a rodent, orally administered insoluble matter is generally masticated to a smaller size, and can pass through the pyloric sphincter to the intestine. However, when considering intact particles and their passage through the stomach it is potentially very useful to understand to what extent size exclusion may be present in the applicable rodent models.

Gamma scintigraphy is one of the most useful techniques for mapping gastrointestinal transit [9, 10]. A solid oral dosage form can be mixed with a gamma emitting radionuclide to monitor gastrointestinal transit in animal or human subjects [11, 12]. After the administration of a radionuclide such as technetium-99m (^{99m}Tc), the test subject is monitored via a gamma camera. In addition, gastric emptying rate and/or gastrointestinal transit can be further investigated by biodistribution analysis, which was

based on subsequent analysis of the obtained images (region of interest ROI) from the test animals [13].

The length, volume and diameter of the stomach and intestine of several laboratory animals (e.g. beagle dog, pig, and rabbit) as well as that of the human were previously investigated [14]. The cut-off size at the pyloric sphincter of some larger laboratory animals and humans was also validated, but this had not been determined for the smaller rodent models. As part of this investigation, the maximum particle size that could potentially pass through the pyloric sphincter intact for mice and rats was initially estimated according to their relative body mass by extrapolating from other larger laboratory animals. In this study, it was hypothesized that by administering inert, non-disintegrable PMMA microcapsules/beads with an incorporated radiopharmaceutical, ^{99m}Tc-diethylene triamine pentaacetic acid (^{99m}Tc-DTPA) to rodents (mice and rats), the gastric emptying rate and size discriminating ability of the pyloric sphincter in these rodent species could be evaluated using gamma scintigraphy.

6.2 Materials and Methods

6.2.1 Materials

Poly(vinyl alcohol) (PVA) 80%, poly(methyl methacrylate) (PMMA) (MW 120,000), benzoyl peroxide (reagent grade, >98%), 4, N,N-trimethylaniline, and sodium acetate were obtained from Sigma (Sigma Aldrich, St. Louis, MO, USA). Methyl methacrylate (MMA), ferrous ammonium sulfate, dichloromethane, and 1,10-phenanthroline was purchased from Spectrum (Spectrum Chemical, Brunswick, NJ, USA). Hydroxylamine hydrochloride, 97% was obtained from Acros (Acros Organics,

New Jersey, NJ, USA). ^{99m}Tc-DTPA was obtained from GE Healthcare Radiopharmacy (GE Healthcare Radiopharmacy, San Antonio, TX, USA). All the other reagents used were analytical grade (Sigma Aldrich, St. Louis, MO, USA).

6.2.2. Preliminary PMMA Microcapsule/Bead Size Selection

To avoid using an excessive amount of the radioactive isotope, ferrous ammonium sulfate (ferrous ammonium complex) was used as a model compound instead of ^{99m}Tc-DTPA to estimate loading efficiency of the microcapsules/beads. The loading efficiency value was used to estimate the amount of radionuclide needed for encapsulation in the subsequent animal study.

Based on the validated body mass and pylorus diameter of rabbits and beagle dogs from literature [14], the pylorus cut-off size for mice and rats was estimated to be 250 μm and 2 mm, respectively (Table 6.1). Following this estimation, three particle size ranges were selected for each animal model (Table 6.2). Sizes were selected *ad hoc* with the assumption that the largest particles in both animal models would stay in the stomach throughout the test period, and that the mid-sized range would be approximately at the size limit for gastric emptying.

Table 6.1: Body mass and pylorus diameter of common laboratory animals and human

Animal	Body mass	Pylorus diameter	
Human	70 kg	5 cm	
Pig	25-35 kg	2.5-3.5 cm	
Beagle dog	10-12 kg	1 cm	
Rhesus Monkey	5-10 kg	1.2-2 cm	
Animal	Body mass	Pylorus diameter	Estimated pylorus diameter
Mouse	20-30 g	Not determined	250 μm
Rat	250-350 g	Not determined	2 mm

Table 6.2: Particle sizes of PMMA microcapsules/beads received by 36 rodents of the study

Group	Formulation	Number of Animals
1. Mice-Small	50-100 μm microcapsules with model material	6 mice
2. Mice-Medium	100-250 μm microcapsules with model material	6 mice
3. Mice-Large	250-500 μm microcapsules with model material	6 mice
4. Rat-Small	0.5-1 mm beads with model material	6 rats
5. Rat-Medium	1-2 mm beads with model material	6 rats
6. Rat-Large	2-3 mm beads with model material	6 rats

6.2.3 Manufacture of PMMA Microcapsules/Beads

To prepare beads of different size ranges, two manufacturing methods were used. Solvent evaporation microencapsulation was used to prepare microcapsules ranging from 50 to 500 μm. For mice study, three size ranges were prepared: 50-100 μm, 100-250 μm, and 250-500 μm. Microencapsulation functioned well to prepare PMMA particles below 500 μm; however, PMMA particles larger than this size range could not be manufactured using this method. Attempts at microencapsulation at sizes >500 μm resulted in either ruptured particles, or particles with irregular shapes. Therefore, surface polymerization using methyl methacrylate monomer was chosen to prepare PMMA beads above 500 μm

in the study (ranging from 0.5 to 3 mm). PMMA bead sizes prepared for the rat study were: 0.5-1 mm, 1-2 mm, and 2-3 mm in diameter.

6.2.3.1. Preparation of Microcapsules: Solvent Evaporation Microencapsulation

Microcapsules with diameters <500 μm were prepared using a solvent evaporation method, as previously described in the literature [15]. Briefly, an inner aqueous phase was made by dissolving an appropriate amount of PVA, dependent on the required particle size (2% w/v for microcapsules size of 50-100 μm and 100-250 μm, and 6% w/v for microcapsules size of 250-500 μm) in de-ionized water. After the PVA was fully dissolved, ferrous ammonium sulfate was dissolved to make a 0.07 M ferrous ammonium solution (as the inner aqueous phase). The oil phase was obtained by dissolving 5% w/w PMMA in dichloromethane (DCM). To initiate encapsulation, the aqueous phase was added into the organic phase, followed by 2 minutes with gentle shaking by hand to make a W/O emulsion. Each W/O emulsion was then poured into 2% w/w PVA solution (outer aqueous phase), with continuous agitation by an RW-16 basic overhead mechanical stirrer (IKA® Works, Inc., Wilmington, NC, USA) at speeds ranging from 100 rpm to 600 rpm (dependent on the desired particle size; 200 rpm for microcapsules between 250-500 μm; 600 rpm for microcapsules between 50-100 μm) to form the final W/O/W emulsions. After 30 minutes, an additional 100 mL of 0.5% w/w PVA solution was added to further stabilize and solidify the microcapsules. After microencapsulation, each mixture was centrifuged at 5,000 rpm for 5 minutes. The microcapsules were then washed with de-ionized water 3 times to remove the non-

encapsulated ferrous ammonium complex and residual PVA. All microcapsules were oven dried (60°C) and weighed before measuring the % encapsulation efficiency (%EE).

6.2.3.2. Bead Preparation: Surface Polymerization

Briefly, 0.5 g of benzoyl peroxide (as the initiator) was added to 10 mL methyl methacrylate (MMA, liquid) and stirred till fully dissolved (as the organic phase). Simultaneously, 0.07 M ferrous ammonium aqueous phase was prepared with 6% w/w PVA. The two phases were combined with gentle agitation using a plastic rod (1:10, aqueous:organic). The catalyst, 0.2 mL 4, N, N-trimethylaniline was then added using a transfer pipette, with continued gentle agitation, to make a W/O emulsion [16]. A low agitation speed (< 150 rpm) was maintained to ensure that the W/O droplets stayed at the surface of the solution for the polymerization procedure to occur (no higher than 150 rpm). After the beads were formed, the whole mixture was agitated at 200 rpm for another 30 minutes to further stabilize and solidify the PMMA beads. Unlike solvent evaporation microencapsulation, a wide range (250 μm – 4 mm in diameter) of PMMA beads can be obtained from a single batch using the surface polymerization process. All PMMA beads were then dried in an oven overnight at 60°C. After drying, the PMMA beads were sieved and separated using US standard sieves (three size ranges: 0.5-1, 1-2, and 2-3 mm) and weighted before measuring %EE.

6.2.4 Loading Efficiency of Ferrous Ammonium Sulfate

The ferrous content was detected using 1, 10-phenanthroline (orthophenanthroline) as previously described in the literature [17]. To measure the encapsulation efficiency of

ferrous ammonium sulfate loaded PMMA microcapsules/beads, 10 mL of DCM was first added to dissolve 500 mg of microcapsules/beads. The mixture was then transferred into a 50 mL tube and the aqueous reagents were added (the ferrous ammonium sulfate partitioned into the aqueous phase). The total ferrous content was determined using spectrophotometry at a wavelength of 508 nm as previously described.

6.2.5 99mTc-DTPA PMMA Loading

On each day of the animal dosing, a fresh batch of ^{99m}Tc-DTPA was received from the radiopharmacy. The activity of each batch of ^{99m}Tc-DTPA (1 mL solution in syringe) was measured using a dose calibrator (Atomlab 100, Biodex, Shirley, NY, USA) and recorded both immediately upon receipt to the facility, and directly following PMMA bead/microcapsule manufacture just prior to dosing (Table 6.3). Microcapsules for the mice studies were obtained by solvent evaporation microencapsulation as previously described, while beads for the rat studies were manufactured by surface polymerization. Both methods were performed exactly in the same way as previously described, except that the radionuclide, ^{99m}Tc-DTPA, was used in replacement for ferrous ammonium sulfate.

Table 6.3: Radioactivity of ^{99m}Tc-DTPA sample received and dosed to animals

Batch/Animals	Initial radioactivity of ^{99m}Tc-DTPA received (mCi)	Final radioactivity per batch (mCi)	Radioactivity dosed per animal (μCi)
Microcapsules, Mice			
50-100 μm	194	2.03	90
100-250 μm	192	72	280
250-500 μm	195	9.9	170
^{99m}Tc-DTPA solution	53	53	260
Beads, Rat			
0.5-1 mm	35	60.4	10
1-2 mm	48		11
2-3 mm	40	3.6	12
^{99m}Tc-DTPA solution	48	48	250

6.2.6 Particle Size Analysis

Particle sizes for the microcapsules used in the mouse study (50-100 μm, 100-250 μm, and 250-500 μm) were determined using a Malvern Mastersizer 2000 (Malvern Instruments Ltd, Worcestershire, UK). D(50) values (median particle size) and particle span was measured to evaluate the size and uniformity of the microcapsules. For the rat study, the diameter of large beads was evaluated using a micrometer (Starrett, Athol, MA, USA). For each batch of the PMMA beads, all beads were separated using a series of laboratory test sieves (500 μm, 1 mm, and 2 mm) (VWR International, LLC, Batavia, IL, USA). The beads were then oven-dried and weighted to calculate the percentage size distribution of beads in each batch.

6.2.7 SEM Morphology of PMMA Microcapsules

Dried microcapsules (for the mice study) were fixed on to stainless steel SEM pin stub specimen mounts via double-sided carbon tape. Samples were then coated with gold particles before SEM imaging. Morphology and size of the microcapsules were evaluated using SEM imaging (LEO 1530 Scanning electron microscope, Carl Zeiss SMT Ltd, Germany).

6.2.8 Percentage Encapsulation Efficiency (%EE)

The encapsulation efficiency (%) was calculated by the following equation:

$$\text{Encapsulation efficiency (\%)} = \frac{\text{Fe (or } ^{99m}\text{Tc-DTPA) loaded}}{\text{Total Fe (or } ^{99m}\text{Tc-DTPA)}} \text{ X } 100\ (\%) \qquad \text{- Eq. (1)}$$

6.2.9 Oral Administration

All animal-handling procedures followed the guidance/regulation of Institutional Animal Care and use Committee Review (IACUC) at the University of Texas Health Science Center in San Antonio (UTHSCSA). Male ICR mice (25-30 g) and male Sprague-Dawley rats (250-300 g) were housed and maintained on a normal rodent chow diet with free access to water at the UTHSCSA facility. Male animals were selected, as growth curves for each species are less variable than that of the female animals. A total of 24 mice and 24 rats were used in this study. Each rodent species was randomly divided into 4 groups (each species had 3 different groups corresponding to 3 different microcapsule/bead size ranges, and an additional group dosed with a ^{99m}Tc-DTPA

solution as a positive control) (Table 2). All animals were fasted overnight prior to administration of microcapsules/beads, to avoid any possible food effects of gastric emptying in the study. After the microcapsules were obtained, aqueous suspensions were prepared for mice administration (activities for each particle dose were measured for all test animals). Compositions were administered to mice as a suspension via oral gavage (approximately 40 μCi per animal), followed by oral gavage with 0.3 mL of water (to aid passage of each formulation in the stomach). All animals were left to rest for 10 minutes prior to imaging.

For the rat study, individual beads were dry-blotted using Kimwipes® and filled into size 9 mini capsules (Torpac Inc., Fairfield, NY, USA) before dosing (30-40 beads, 4 beads and 3 beads per capsule, for 0.5-1 mm, 1-2 mm and 2-3 mm bead size ranges respectively). A single capsule was administered to each animal (approximately 10 μCi) using a Torpac® mini capsule dosing syringe (Torpac Inc., Fairfield, NY, USA), followed by administration of 0.3 mL water via oral gavage. All animals were left to rest for 10 minutes prior to scintigraphic imaging.

6.2.10 Gamma Scintigraphy

Scintigraphic images were used for determining the effect that the pylorus may have on size cut-off and gastrointestinal transit time. Additionally, biodistribution of ^{99m}Tc-DTPA in different sections of the gastrointestinal tract was also evaluated as confirmation of the scintigraphy results.

The animals were anesthetized by continuous inhalation of 1-3% isoflurane (Vedco, St. Joseph, MO, USA) in pure oxygen using an anesthesia inhalation unit

(Bickford, Wales Center, NY, USA) at intervals of 10 minutes, 1, 2, 3, and 4 hours. {A 4-hour scintiscan period was determined based on the finding from literature reviews. The gastric emptying time of rats and mice under fasted state is between 30-60 minutes and 60-90 minutes, respectively [18, 19]}. The mice and rats were placed in the prone position on the scanner bed. All limbs of the rodents were affixed lightly to the side of a suitably sized rodent cradle, using surgical tape to keep the animals motionless during the scanning process. A standard amount of ^{99m}Tc in an Eppendorf® tube was placed beside the animal in the camera field of view, acting as an anatomical marker. The 140 keV±20% window gamma rays emitted by ^{99m}Tc were imaged using dual head gamma cameras equipped with high-resolution parallel hole collimators (FLEX® Pre-Clinical Platform, Gamma Media Ideas, Northridge, CA, USA). At the predetermined time intervals, anterior and posterior images were acquired for 5 minutes. Radioactivity at esophagus, stomach and intestines of the testing animal were obtained from the scintiscans.

6.2.11 Biodistribution Study

After acquisition of the 4-hour images, the animals were euthanized using deep isoflurane followed by cervical dislocation. Following euthanasia, blood was withdrawn by performing a cardiac puncture procedure. Esophagus, stomach, intestine and cecum were collected, weighed and counted in automated gamma counter (Wallac Wizard 1470 Gamma Counter, PerkinElmer, Waltham, MA, USA) for biodistribution analysis.

6.2.12 Data processing

The scintigraphic images of the animals were displayed and quantified by ASIPro VM (Siemens Medical Systems, Knoxville, TN). A region of interest (ROI) was overlaid on the images for the esophagus, stomach, and intestines to obtain the quantified ROI (qROI) from the images. Counts were recorded in each region and the percentage of counts in the region compared with whole body counts was determined.

6.2.13 Statistics

All results are shown as mean ± standard deviation (n = 6). Analysis of variance (ANOVA) and Turkey-Kramer HSD was used to evaluate all the results via JMP 7.0 software (JMP, Cary, NC, USA). A significant difference was considered when $p < 0.05$.

6.3. Results

6.3.1 Preliminary PMMA Microcapsule/Bead Size Selection

Solvent evaporation microencapsulation was used to prepare PMMA microcapsules for all the mouse study size ranges. Particle size, span and encapsulation efficiency of each microcapsule group are shown in Table 6.4. To prepare larger beads for the rat study, surface polymerization was used**.** Since monomer polymerization occurred in an aqueous environment, we were able to control particle size by adjusting the applied agitation. Here PMMA beads of various sizes were produced in a single batch. Following preparation and drying, the beads were separated and their size distributions were evaluated. Encapsulation efficiencies were evaluated. Both methods produced uniform and spherical particles (the approximate particle size span of the

microcapsules was between 1-1.3). The results of each batch were consistent and reproducible.

Table 6.4: Characteristics of PMMA microcapsules/beads used for animal study

Batch/Animals	Initial radioactivity of ^{99m}Tc-DTPA received (mCi)	Final radioactivity per batch (mCi)	Radioactivity dosed per animal (µCi)
Microcapsules, Mice			
50-100 µm	194	2.03	90
100-250 µm	192	72	280
250-500 µm	195	9.9	170
^{99m}Tc-DTPA solution	53	53	260
Beads, Rat			
0.5-1 mm	35	60.4	10
1-2 mm	48		11
2-3 mm	40	3.6	12
^{99m}Tc-DTPA solution	48	48	250

6.3.2 Particle Size Analysis

Particle size and span of ferrous ammonium sulfate loaded PMMA microcapsules (from the preliminary test) were investigated using a Malvern Mastersizer 2000 (Malvern Instruments Ltd, Worcestershire, UK). The mean ± SD of D(50) values (referred to median particle size) for small, medium, and large microcapsules were 81.27±10.43, 194.75±12.76, and 375.96±39.9 μm, respectively. The mean particle size spans were 0.86, 1.14, and 1.23, respectively for the small, medium, and large microcapsules. After a 3-day decay period, particle size and particle span of ^{99m}Tc-DTPA loaded PMMA microcapsules were investigated as previously described. Particle size range and span

were measured and compared to the desired particle size ranges designed at the beginning of the study (Table 4). The mean ± SD of D(50) values (median particle size) of the small, medium, and large radionucleoids loaded PMMA microcapsules were 88.91±9.89, 144.75±12.76 and 405.95±39.92 μm, respectively. The mean particle size spans were 1.09, 1.33, and 1.12, for particle sizes of 50-100 μm, 100-250 μm, and 250-500 μm, respectively. In addition, for both ferrous ammonium sulfate and ^{99m}Tc-DTPA loaded PMMA microcapsules, particle size distributions of all three sized microcapsules matched the intended study design.

For the rat study, individual beads were dry-blotted using Kimwipes®. PMMA beads were first sieved using US standard sieves with appropriate size opening and separated. The actual size of the PMMA beads was measured by a micrometer and recorded in Table 4 (N=20). The actual size of the beads was in the same particle ranges as required.

6.3.3 99mTc-DTPA PMMA Loading

After confirming that the particle size, shape, and uniformity of the particles loaded with ferrous ammonium sulfate were reproducible, solvent evaporation microencapsulation was used to prepare microcapsules for the mouse study and surface polymerization was selected to obtain beads for the rat study. After allowing ^{99m}Tc decay for 3 days due to radioactive handling safety concerns (The half-life of ^{99m}Tc is 6 hours.10 half-lives are required for the material to return to background radioactivity levels.), particle size of the microcapsules/beads was measured. No significant difference in size was found compared to the preliminary ferrous PMMA loading (student's t test, p

>0.05). The encapsulation efficiency was 8%, 5%, and 6% for small (50-100 μm), medium (100-250 μm), and large (250-500 μm) microcapsules, respectively (Table 6.4). Encapsulation efficiencies of the PMMA beads for the rats were between 2-11% (Table 6.4).

^{99m}Tc-DTPA loaded microcapsules were further investigated using SEM. The small and medium particles displayed a spherical shape, while some of the large particles displayed a slightly irregular shape (Figure 6.1B-6.1C). However, all particles were within the required size ranges as preliminary ammonium ferrous sulfate loading test (Figure 6.1).

Figure 6.1: SEM images of 99mTc-DTPA loaded microcapsules for the mice study. (A) Small microcapsules, 50-100 μm; (B) Medium microcapsules, 100-250 μm; (C) Large microcapsules, 250-500 μm.

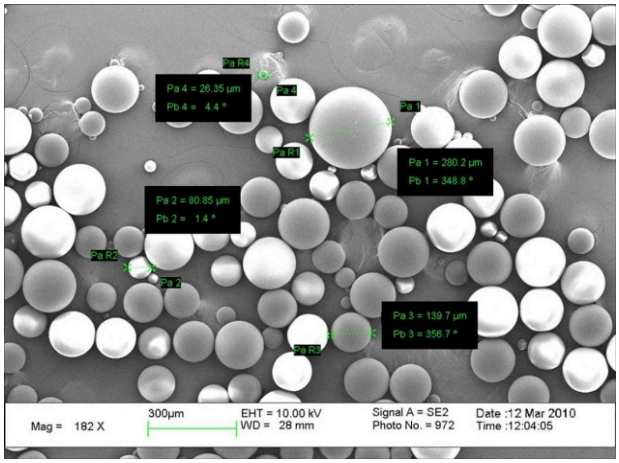

(A)

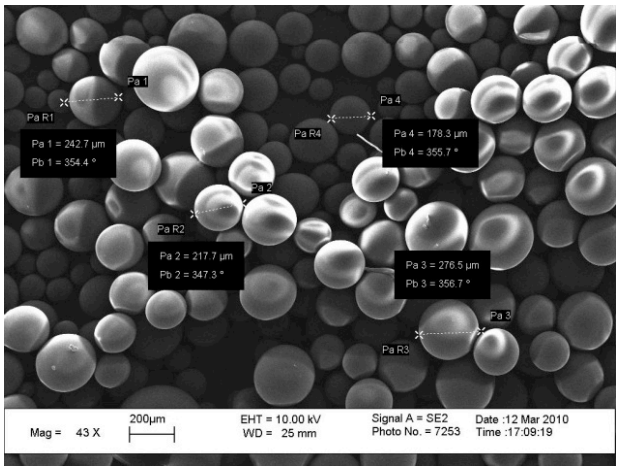

(B)

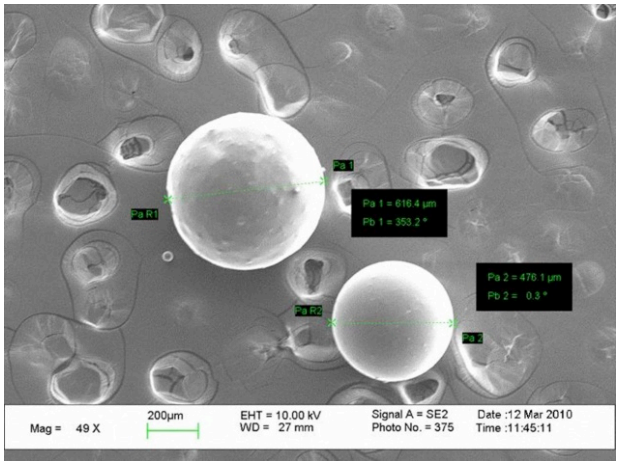

(C)

6.3.4 Gamma Scintigraphy

Gamma scintigraphy for different sized microcapsules/beads was performed in mice and rats in order to determine the potential influence of the particle size cut-off imparted by the pyloric sphincter of the stomach. When the mice were dosed with a ^{99m}Tc-DTPA solution (as the positive control), the scintigraphic images immediately showed localized ^{99m}Tc-activity in the stomach (Figure 6.2A). ^{99m}Tc-DTPA solutions emptied from the stomach quickly (less than 10 minutes post-administration). Scintiscan images showed ^{99m}Tc-activity in the intestine in less than 2 hours (Figure 6.2B-6.2C). From the images obtained, it was observed that the majority of ^{99m}Tc-DTPA solutions reached the lower intestine as rapidly as 2 hours (Figure 6.2D). After dosing with the small microcapsules (50-100 μm), scintiscans showed maximum ^{99m}Tc-activity in the stomach after 10 minutes (Figure 6.2E), which was identical to the control group. However, high ^{99m}Tc-activity was found in the stomach even up to 4 hours after dosing (Figure 6.2F-6.2G), which suggested that the 50-100 μm microcapsules were trapped in the stomach for a longer period of time, compared to the positive control. In addition, for the mice dosed with medium (100-250 μm) and large (250-500 μm) sized microcapsules, particles started emptying the stomach in less than 1 hour (Figure 6.2J and 6.2N) and most of the particles reached the intestine in less than 4 hours (Figure 6.2L and 6.2P) as shown in the scintiscans.

Similar results were shown in the rats dosed with ^{99m}Tc-DTPA solution (positive control), indicated that all ^{99m}Tc-labeled beads reached the stomach after administration (Figure 6.3). Since a size 9 gelatin mini capsule was used as a carrier to deliver the beads

into the rats, the rapidly dissolved gelatin capsule was sometimes observed to stick onto the esophagus shortly after dosing, as shown in the appropriate scintiscans (Figure 6.3E, 6.3I, and 6.3M). From the scintiscans, both small (0.5-1 mm) and medium (1-2 mm) beads were able to empty the stomach intact; however, although not significantly different, the gastric emptying time of the small beads trended longer than the medium beads (Figure 6.3G and 6.3K). In addition, more small beads remained in the stomach throughout the 4 hours study period, compared to the medium beads (Figure 6.3H and 6.3L). The scintigraphy images indicated that 1 or 2 (out of the total of 3 beads loaded per capsule) of the large beads (2-3 mm) remained in the stomach throughout the 4 hour scanning period (Figure 6.3P), which was further validated by CPM quantification at each section along the GI tract. For those rats dosed with beads sized 2-3 mm, CPM at the stomach was significantly higher, compared to those rats dosed with the other two larger sized PMMA beads ($p < 0.05$). This indicated that beads sized 2-3mm stayed in the stomach significantly longer than beads <2 mm, and were not able to pass through the rat pylorus intact for at least 4 hours.

Figure 6.2: Scintiscans of the mice dosed with ^{99m}Tc-DTPA solution or ^{99m}Tc-DTPA containing PMMA microcapsules up to 4 h. Yellow arrow: Standard marker. Radioactivity is represented in rainbow scale, red: highest intensity, purple: lowest intensity. Image 2(A)-3(D): ^{99m}Tc-DTPA solution, 0, 1, 2, and 4 h; image 2(E)-3(H): small PMMA microcapsules, 0, 1, 2, and 4 h; image 2(I)-3(L): medium PMMA microcapsules, 0, 1, 2, and 4 h; and image 2(M)-2(P): Large PMMA microcapsules, 0, 1, 2, and 4 h.

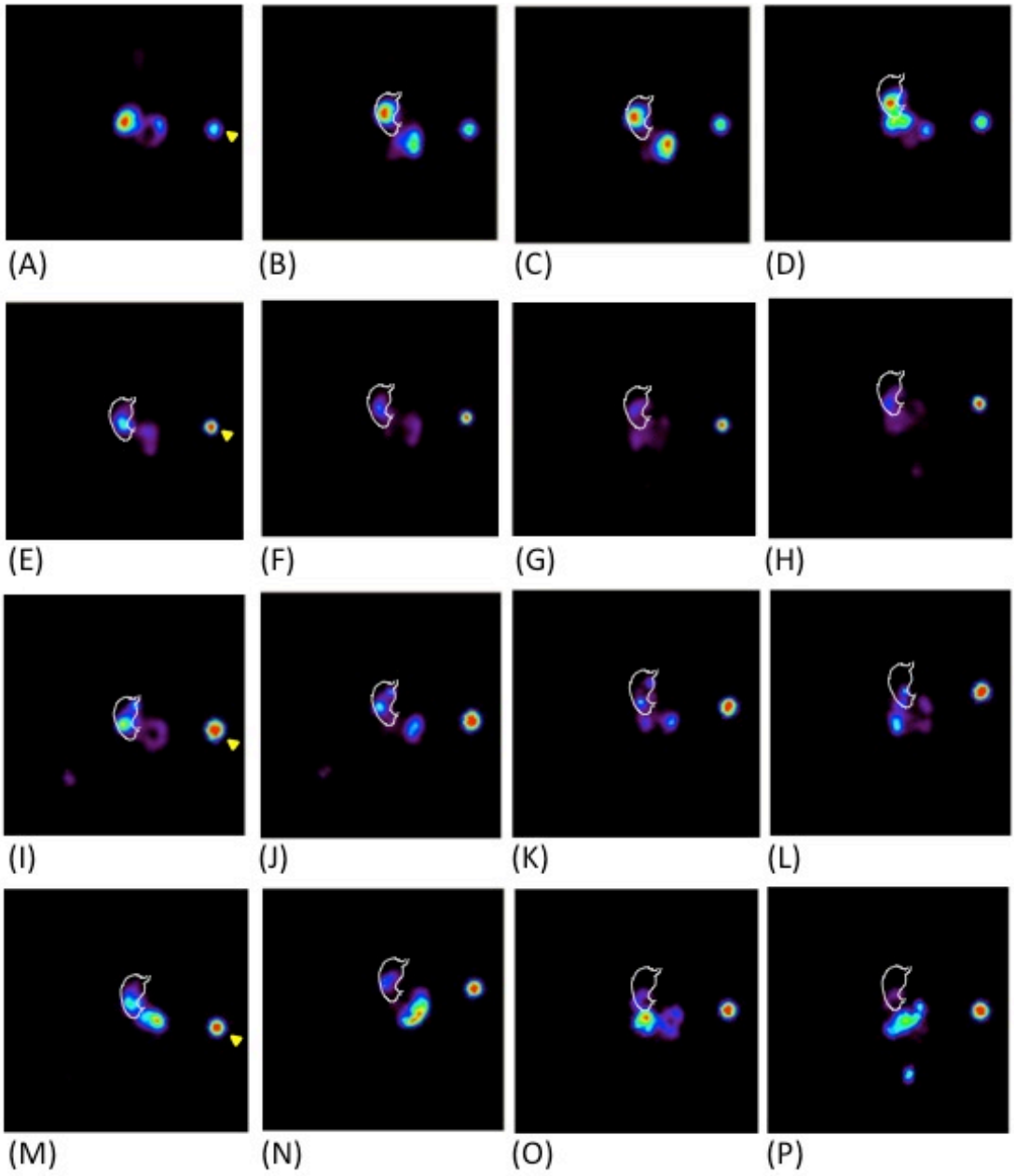

Similar results were shown in the rats dosed with ^{99m}Tc-DTPA solution (positive control), indicated that all ^{99m}Tc-labeled beads reached the stomach after administration (Figure 6.3). Since a size 9 gelatin mini capsule was used as a carrier to deliver the beads into the rats, the rapidly dissolved gelatin capsule was sometimes observed to stick onto the esophagus shortly after dosing, as shown in the appropriate scintiscans (Figure 6.3E, 6.3I, and 6.3M). From the scintiscans, both small (0.5-1 mm) and medium (1-2 mm) beads were able to empty the stomach intact; however, although not significantly different, the gastric emptying time of the small beads trended longer than the medium beads (Figure 6.3G and 6.3K). In addition, more small beads remained in the stomach throughout the 4 hours study period, compared to the medium beads (Figure 6.3H and 6.3L). The scintigraphy images indicated that 1 or 2 (out of the total of 3 beads loaded per capsule) of the large beads (2-3 mm) remained in the stomach throughout the 4 hour scanning period (Figure 6.3P), which was further validated by CPM quantification at each section along the GI tract. For those rats dosed with beads sized 2-3 mm, CPM at the stomach was significantly higher, compared to those rats dosed with the other two larger sized PMMA beads ($p < 0.05$). This indicated that beads sized 2-3mm stayed in the stomach significantly longer than beads <2 mm, and were not able to pass through the rat pylorus intact for at least 4 hours.

Figure 6.3: Scintiscans of the rat dosed with ^{99m}Tc-DTPA solution or ^{99m}Tc-DTPA containing PMMA beads up to 4 h. Yellow arrow: Standard marker. Radioactivity is represented in rainbow scale, red: highest intensity, purple: lowest intensity. Image 3(A)-3(D): ^{99m}Tc-DTPA solution, 0, 1, 2, and 4 h; image 3(E)-3(H): small PMMA beads, 0, 1, 2, and 4 h; image 3(I)-3(L): medium PMMA beads, 0, 1, 2, and 4 h; and image 3(M)-3(P): Large PMMA beads, 0, 1, 2, and 4 h.

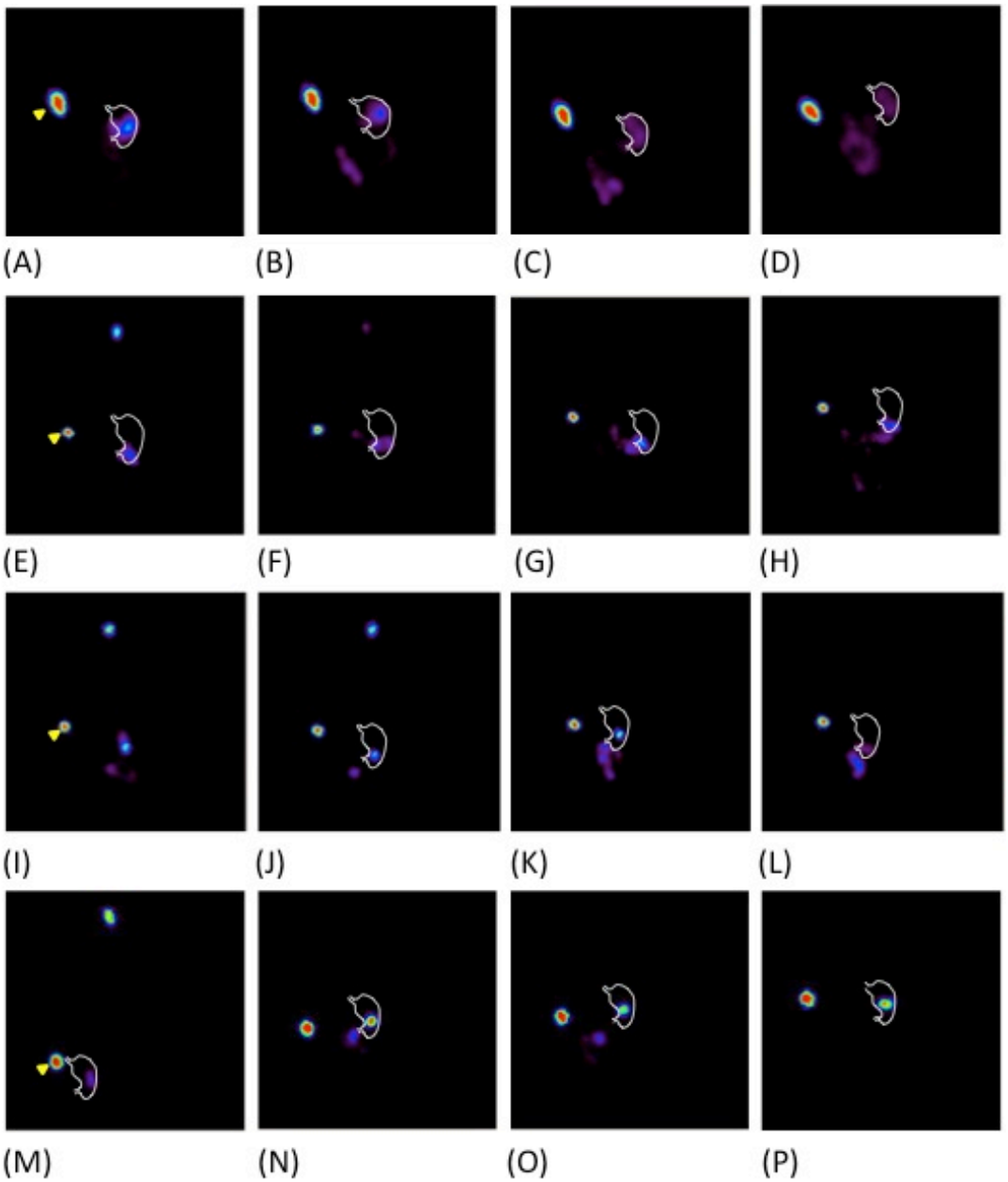

6.3.5 Quantified ROI Images

To further confirm the ROI collected from scintigraphy, quantitative ROI (qROI) data was investigated. The qROI was used to back up the images and provided a pattern of the movement of the particles. The total body Tc-99m radioactivity of each test animal was obtained and represented as "Whole Body Radioactivity". Tc-99m radioactivity at each part of the gastrointestinal tract (esophagus, stomach, or intestines) was also obtained and converted to a ratio of Tc-99m radioactivity at each part to total body radioactivity (e.g. % Esophagus/Whole Body). Figure 6.4 represents the Tc-99m radioactivity along the mouse gastrointestinal tract at 0, 1, 2, and 4 hours, respectively (Mean ± SD). Tc-99m radioactivity showed no significant difference at the mouse esophagus at all time points, regardless of the administered microcapsules size. In the mouse stomach at 4 hours (last time point), the smallest microcapsules (50-100 μm) showed significantly higher Tc-99m radioactivity, compared to the medium and large microcapsules ($p=0.0023$ and 0.0007, respectively). Moreover, at the mouse intestines at 2 and 4 hours, the smallest microcapsules (50-100 μm) showed significantly lower Tc-99m radioactivity, compared to the medium and large microcapsules ($p=0.0389$). Figure 6.5 represents the Tc-99m radioactivity along the rat gastrointestinal tract at 0, 1, 2, and 4 hours, respectively (Mean ± SD). At the earlier test time points (0 and 1 hour), the largest beads (2-3 mm) showed significantly higher Tc-99m radioactivity at the rat esophagus, compared to the small and medium size beads ($p=0.0155$ and 0.0043, respectively). At the rat stomach at 1 hour, the smallest and largest beads showed significantly higher Tc-99m radioactivity, compared to the medium size beads ($p=0.0023$). However, from the qROI, at 2 and 4 hours, the small beads showed significantly lower Tc-99m radioactivity, compared to medium and large beads ($p=0.021$ and 0.003, respectively). At the rat intestines, medium size beads (1-2 mm) showed

significantly higher Tc-99m radioactivity at 1 hour, compared to the small and large size beads (p=0.0027). In addition, at 2 and 4 hours, both small and medium beads showed significantly higher Tc-99m radioactivity at the rat intestines, compared to the large size beads (p=0.001 and 0.0478, respectively). The qROI results were therefore consistent with the scintigraphy images obtained from both the mice and the rats.

Figure 6.4: Quantified ROIs in mouse esophagus, stomach, and intestine at: (A) 10 min, (B) 1 h, (C) 2 h, and (D) 4 h. The Tc-99m radioactivity was represented as % at each area related to the whole body radioactivity, 1 means a total of 100% Tc-99m activity. *: With statistically significant difference (p<0.05). * N=6, Mean value ± Stdev

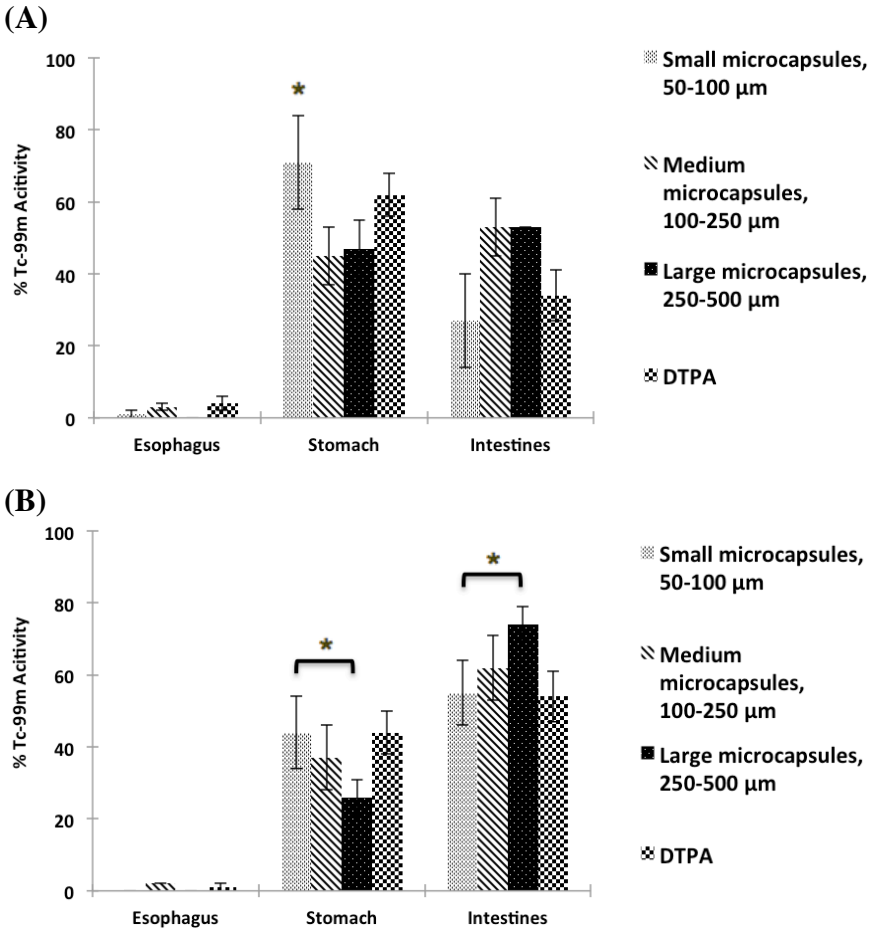

Figure 6.4 (continued)

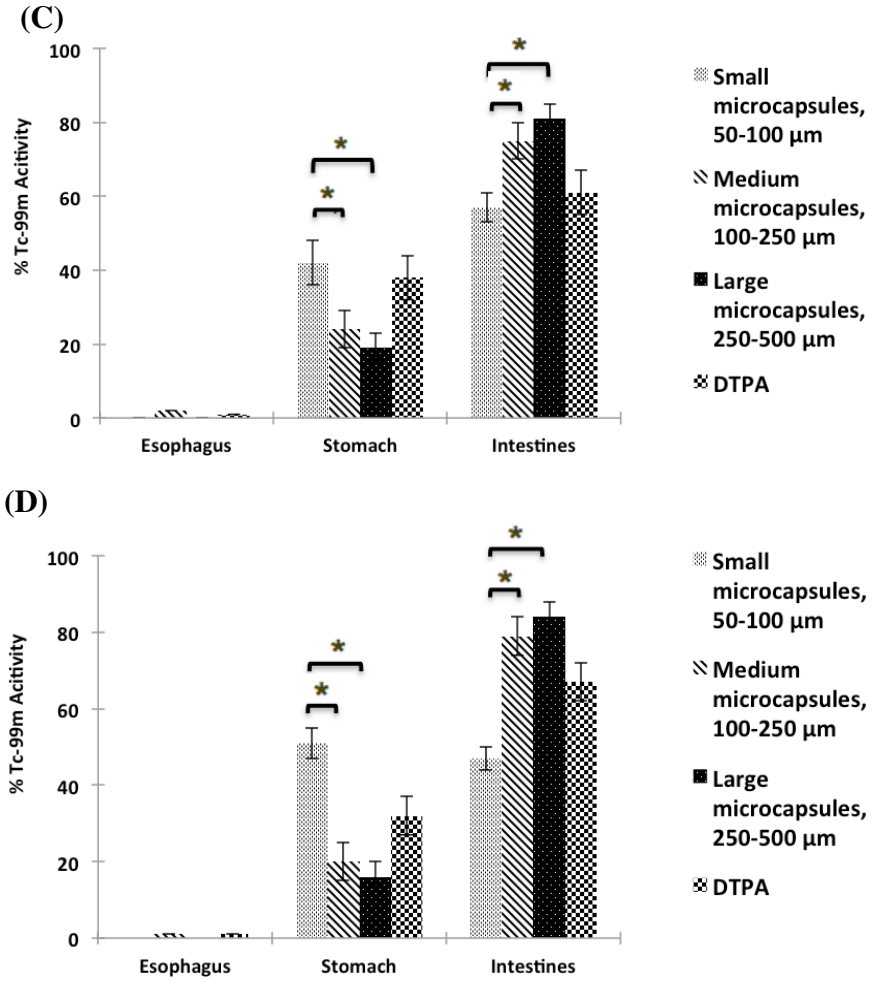

Figure 6.5 represents the Tc-99m radioactivity along the rat gastrointestinal tract at 0, 1, 2, and 4 hours, respectively (Mean ± SD). At the earlier test time points (0 and 1 hour), the largest beads (2-3 mm) showed significantly higher Tc-99m radioactivity at the rat esophagus, compared to the small and medium size beads ($p=0.0155$ and 0.0043, respectively). At the rat stomach at 1 hour, the smallest and largest beads showed significantly higher Tc-99m radioactivity, compared to the medium size beads ($p=0.0023$). However, from the qROI, at 2 and 4 hours, the small beads showed

significantly lower Tc-99m radioactivity, compared to medium and large beads (p=0.021 and 0.003, respectively). At the rat intestines, medium size beads (1-2 mm) showed significantly higher Tc-99m radioactivity at 1 hour, compared to the small and large size beads (p=0.0027). In addition, at 2 and 4 hours, both small and medium beads showed significantly higher Tc-99m radioactivity at the rat intestines, compared to the large size beads (p=0.001 and 0.0478, respectively). The qROI results were therefore consistent with the scintigraphy images obtained from both the mice and the rats.

Figure 6.5: Quantified ROI in rat esophagus, stomach, and intestine at: (A) 10 min, (B) 1 h, (C) 2 h, and (D) 4 h. The Tc-99m radioactivity was represented as % at each area related to the whole body radioactivity, 1 means a total of 100% Tc-99m activity. *: With statistically significant difference (p<0.05). * N=6, Mean value ± Stdev

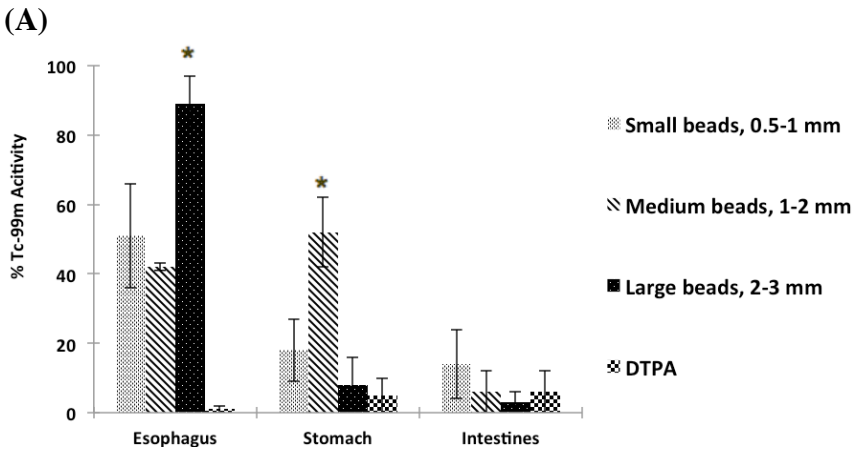

Figure 6.5 (continued)

(B)

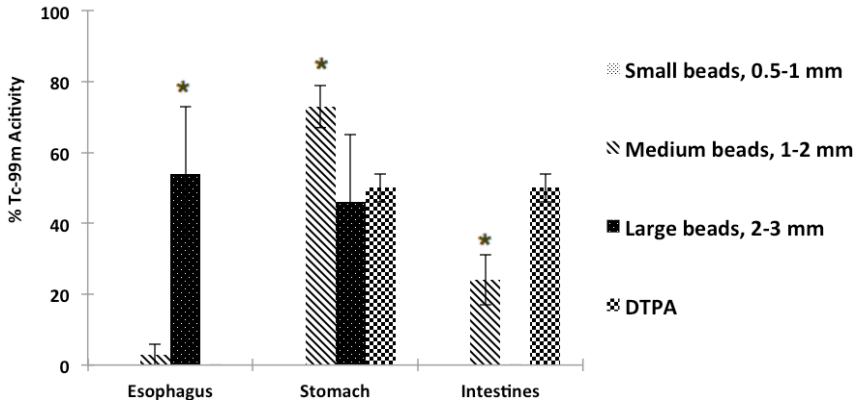

(C)

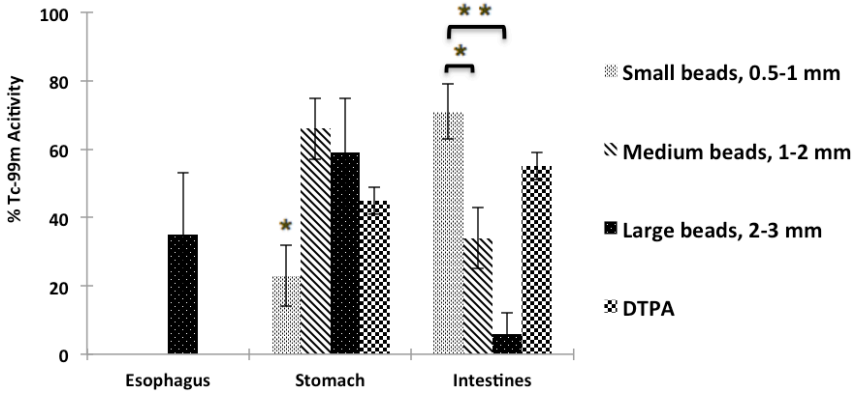

(D)

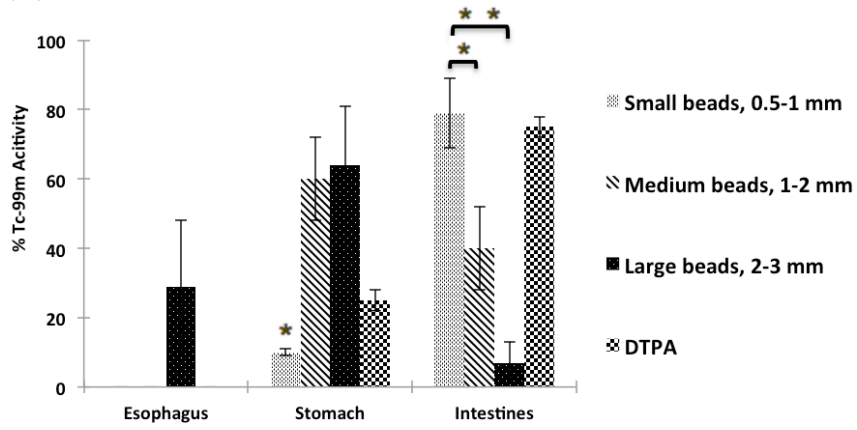

6.3.6 Biodistribution

Following the imaging portion of the study, the radioactivity in different sections along the gastrointestinal tract of the test animals was evaluated. Blood, esophagus, stomach, intestine, and cecum from the test animals were harvested and collected separately into scintillation vials. The activity of each of the tissues was measured using a gamma counter to determine the biodistribution of the ^{99m}Tc-DTPA-loaded formulations. The radioactivity was quantified and represented in terms of "Count per Minute" (CPM), higher CPM represented higher radioactivity in a specific organ (which indicated that more ^{99m}Tc-DTPA labeled substances were remained in that area). The counts obtained from the blood and esophagus samples were below the limit of detection (compared to the ^{99m}Tc-DTPA standard marker used during the scintiscan) and were subsequently rejected for use in the biodistribution analysis. The counting results were converted into "count-per-minute in different organs" (CPM/Organ) and "percentage of ^{99m}Tc-DTPA dosed remaining in different organs" (% ^{99m}Tc-DTPA/Organ).

When comparing the mice dosed with medium microcapsules (sized 100-250 μm) to the mice dosed with large microcapsules (sized 250-500 μm), no significant difference was found in the stomach (CPM/stomach: p=0.0617, % ^{99m}Tc-DTPA/stomach: p=0.1597) or in the cecum (CPM/cecum: p=0.1953, % ^{99m}Tc-DTPA/cecum: p=0.0661) (Figure 6.6). In addition, no significant difference was observed in the mouse intestine throughout the 4-hour study period among the three different microcapsule size groups (p=0.3083, 0.1615, 0.1407, 0.4848, and 0.303, at 10 minutes, 1, 2, 3, and 4 hours after administration, respectively). From the intestinal results, CPM of the mice dosed with

small microcapsules (50-100 μm) was significantly lower compared with the other two sized microcapsules (p=0.0052), which suggested that the gastric emptying of particles at sizes between 50-100 μm was impeded, compared to the other two microcapsule sizes. However, from the scintigraphy images, it was clear that all three sized microcapsules were ultimately able to pass through the pyloric sphincter, in spite of differences observed in the emptying rate in the mice.

Figure 6.6: Biodistribution of ^{99m}Tc-DTPA loaded microcapsules in mice (Mean ± SD). Percentage of ^{99m}Tc-DTPA dosed in each specific organ. *: With statistically significant difference (p<0.05). * N=6, Mean value ± Stdev

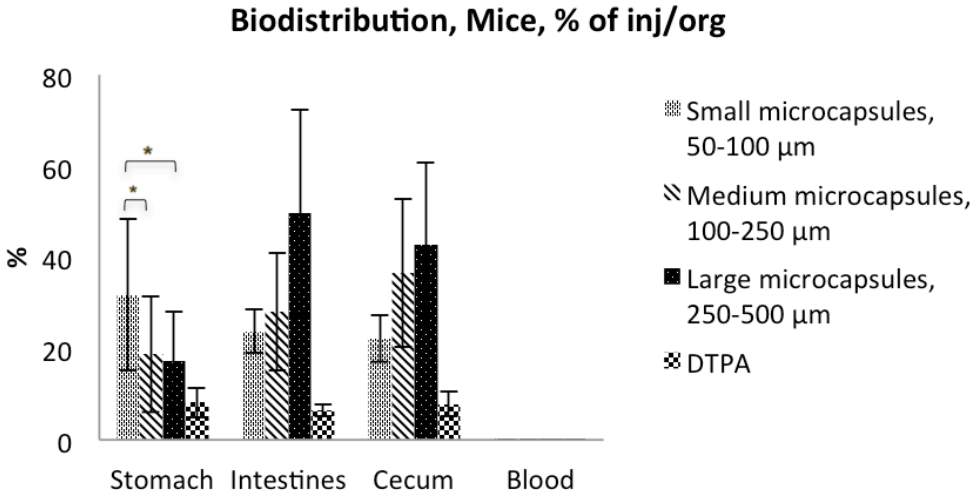

When the rat was dosed with medium sized beads (1-2 mm), CPM/intestine and % ^{99m}Tc-DTPA/intestine were significantly higher (p=0.0469 and 0.0112, respectively), compared to the animal dosed with the other two sized beads. This implied that particles sized 1-2 mm passed through the rat pylorus faster than particles either <1 mm or >2 mm. On the other hand, CPM/stomach and % ^{99m}Tc-DTPA/stomach were significantly higher (p<0.05) in the rats dosed with either small (0.5-1 mm) or large (2-3 mm) beads,

compared to the animals dosed with medium beads (1-2 mm) (Figure 6.7). In addition, when the rats were dosed with small and large beads, CPM/Cecum and % ^{99m}Tc-DTPA/Cecum were significantly lower (p=0.0396 and 0.02, respectively), compared to the animals that were administered with medium beads. These observations indicated that particles <1 mm were delayed in the rat stomach and would be emptied out slower (compared to particles between 1-2 mm), while beads >2 mm are unlikely to be able to pass through the rat pyloric sphincter intact.

Figure 6.7: Biodistribution of 99mTc-DTPA loaded beads in rats (Mean ± SD). Percentage of 99mTc-DTPA dosed in each specific organ. *: With statistically significant difference (p<0.05). * N=6, Mean value ± Stdev

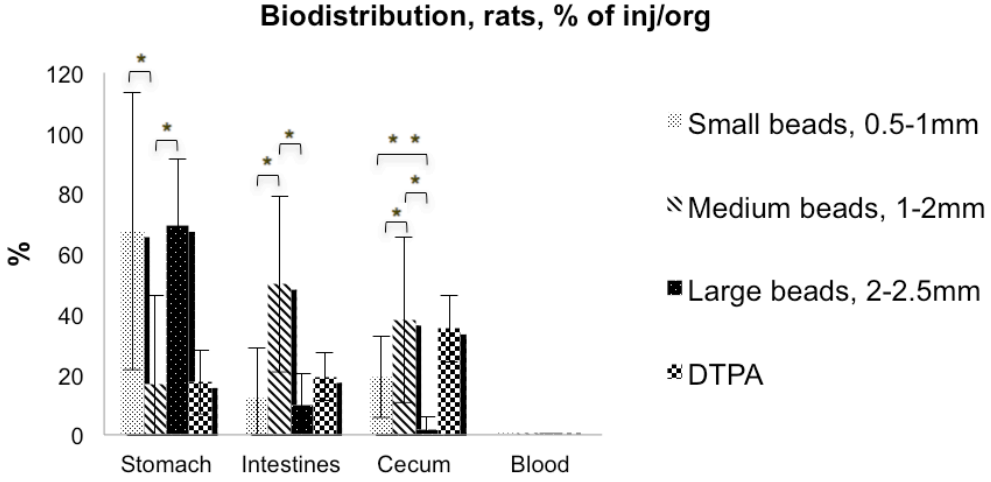

6.4 Discussion

Our objective was to evaluate the relationship between particle size and gastric emptying in small rodents using gamma scintigraphy. Particles at the size ranges tested were either prepared by solvent evaporation or surface polymerization. Integrity of the particles was confirmed prior to the study no rupturing was found in particles prepared by

solvent evaporation microencapsulation, as a result of the manufacturing process. Particle shape, size, span, and encapsulation efficiency were reproducible; therefore, both solvent evaporation emulsification and surface polymerization were both demonstrated to be appropriate methods for preparing uniform PMMA microcapsules/beads. SEM evaluation of preliminary ferrous loaded and ^{99m}Tc-DTPA loaded particles indicated that respective microcapsule/beads were of identical size and shape, indicating the effectiveness of substitution with the ferrous sulfate to allow for processing/formulation optimization without using a radioactivity during the development process. Microcapsule and bead sizes could be well controlled by altering the surfactant content (%PVA) and/or agitation speed. Furthermore, microparticles/beads were effectively prepared to be the exact size ranges as were purposed in the estimation of pylorus cut-off size in mice and rats as extrapolated from the existing literature (Section 2.2 above). (Table 6.1)

The estimated cut-off size at the pyloric sphincter of mice and rats was determined to be 250 μm and 2 mm, respectively. Therefore, it was assumed that particles above those specific sizes would remain in the stomach during the scintigraphy study. However, in the mice all sizes of microcapsules emptied over the course of the study. One limiting factor when dosing the mice with an oral gavage is an upper limit of using 18-gauge gavage needle (which is the largest size recommended for mice dosing due to physical concerns). Subsequently a concern was realized in that microcapsules at the upper size range were found to stick in the gavage tube. As a consequence, we confirmed retrospectively that only particles less than approximately 300 μm were actually delivered to the animals during oral gavage. It should be considered that it is not even

practically possible or ethical for mice to be dosed using conventional methods with particles greater than about 300 μm, due to practical constraints imposed by the use of an 18-gauge gavage tube.

Previous work has shown that smaller particles (or dosage forms) empty from the stomach faster than larger particles [20, 21]. We also investigated the effect of particle size on gastric emptying rate in this study. However, compared to the medium and large microcapsules, the gastric emptying rate of the small microcapsules was remarkably delayed. From the scintiscans, we found that many of the small microcapsules remained in the stomach even after 3 hours, while most of the medium and large microcapsules passed through the pyloric sphincter in approximately 2 hours.

All PMMA microcapsules reached the lower intestine after 4 hours (Figure. 6.3), regardless of the size of the particles. It was anticipated that the largest size microcapsules/beads would not empty from stomach as quickly as the smallest size microcapsules, before the study in both rodent models. However, it was found that in the mouse study, all medium and large microcapsules reached intestine and cecum after approximately the same transit time. Since the maximum particles dosed to the mice were approximately 300 μm, it can be concluded that in the mouse model used, the PMMA microcapsule size has no effect on the gastric emptying rate, when the particle size was between 100 and 300 μm.

A similar trend of gastric emptying was observed in the rat study. The medium size beads (1-2 mm) passed through the pyloric sphincter to the intestine and then reached the cecum significantly faster than the other two size groups (from the results shown in both

the biodistribution and scintiscan images). From the scintiscans, gastrointestinal transit of the smallest beads (0.5-1 mm) was found to be similar to that of the largest beads (2-3 mm), except in fact that the smallest beads were able to empty the stomach, while the largest beads were trapped in the stomach. Therefore, above a certain particle size range (1 mm in the SD rats and 100 μm in the ICR mice), gastric emptying time of intact particles increases with increasing particle size, provided that the particles are able to pass through the pyric sphincter. On the other side, gastric emptying was prolonged if the particles were below this size range. This may due to the rough surface or the mucosal folds in the stomach of these two rodent species [22, 23] impeded the smallest particles from passing through the stomach, which was found similarly in healthy human subjects by Podczeck and co-workers [24]. Moreover, after the small beads emptied from the stomach, no significant differences in CPM were observed when comparing the intestine to the cecum, suggesting that the particles were only hindered in the stomach, rather than the other regions along the lower GI tract.

Mucoadhesion is a process by which mucoadhesive polymers contact and attach on to the mucus membrane, which can attribute to a prolonged residence time in the nasal, buccal, vaginal, and gastrointestinal tract [25, 26]. PMMA is inert, non-dissolvable, well known and is therefore, an ideal carrier polymer for a drug delivery system. In this study, PMMA carriers were prepared using microencapsulation/surface polymerization. Although the mucoadhesive property of PMMA is not fully confirmed or conducted, it is possible that the these PMMA microcapsules/beads were able to adhere onto the mucous membrane lining the GI tract via hydrogen bonding [27], which led to an extended

residence time, especially considering what was observed for the scintiscans in the gastric region of the mouse model. However, it may be assumed that the retention of small microcapsules (50-100μm) in the gastric region (mouse) was more likely due to microcapsule impedance in the mucosal folds in the stomach, rather than mucoadhesive property of PMMA microcapsules. This is because the prolonged residence time that occurred at the gastric region when the smallest microcapsules were administered to the mouse only, but not in the small intestine or lower intestine area. Further studies must be conducted to confirm whether PMMA is mucoadhesive.

By observing the scintiscans, it can be clearly seen that 1 or 2 out of the total 3 administrated beads in the largest bead size group (2-3 mm) stayed in the rat stomach throughout the 4 hours study (Figure. 6.4). Although about 30% radioactivity (from the biodistribution data) was found in the esophagus of 2-3 mm PMMA beads dosed SD rats, as we stated earlier, the "hot spot" at the esophagus we found on the scintiscans at 1 hour was from the residues of the dissolving gelatin capsule, not the PMMA beads. These radioactive residues of the gelatin capsules contributed to the high radioactivity reading at esophagus, even at 4hour. However, from the scintiscans, we could not find the "hot-spot" at esophagus, which in concords with our arguments. Therefore, we did not consider the delayed gastric emptying was resulted from the stuck of beads at esophagus in our study. Moreover, CPM/Organ is remarkably lower in intestine and cecum in the rats dosed with large beads, compared to the animals dosed with the other two smaller size beads. These results are consistent with our hypothesis that inert particles ranging from 2-3 mm in diameters fitted well for evaluating the cut-off size at the pyloric

sphincter of the rats. In rats, non-disintegrating, non-dissoluble particles larger than 2-3 mm in diameter are retained in the stomach. Therefore, we conclude that PMMA beads larger than approximately 3 mm could not pass through the pyloric sphincter intact in a rat, which is close to the initial estimation of the pylorus cut-off size in this animal model.

Since oral gavage is commonly used to administer solid dosage forms to the laboratory animal [28], it could be of critical importance to understand whether the formulation could reach the proximal or distal intestine intact, especially if it contains acid labile components. In other words, when evaluating an enteric-coated solid oral dosage form in rodent models, there exists the possibility that the given formulation could be retarded (with prolonged transit time) in the gastric area, with no possibility of leaving the stomach in a timely fashion. This scenario of prolonged gastric retention could make the formulation fail to elicit the desired effect at the target site(s) in the GI tract. To avoid this issue, we have successfully defined the particle cut-off size and gastric sieving property in the Sprague Dawley rats investigated. In summary, for oral dosage forms designed for the Sprague Dawley rat model using oral gavage, it is not advisable to administer particles above 3 mm, as it is unlikely that these particles could pass through the stomach.

It should be noted that although we confirmed that gastric emptying rate is dependent on the particle size of the administered dosage forms in mice, we were not able to define the specific pyloric cut-off size for the ICR mice investigated. However, we have determined that the maximum particle size that can be feasibly administered in ICR mice is limited to the upper limit of gavage feeding tube gauge. Moreover, the larger

particles (250-300 μm in diameter) administered could be emptied from the gastric by ICR mice.

6.5 Conclusions

In this study, we conclude that the cut-off size at the pyloric sphincter in Sprague Dawley rats (body weight 250-300 g) is approximately 3 mm, and the cut-off size for stomach emptying in ICR mice is limited only by the upper limit of feasible dosing (300 μm) method. Additionally, particle size was found to significantly alter gastric emptying rates in both rodent species investigated. This information is valuable for designing preclinical rodent testing studies, especially for oral drug delivery systems designed for lower intestine targeting, or when investigating acid labile compounds for oral drug delivery systems.

6.6 References

1. Piao, J., et al., Development of novel mucoadhesive pellets of metformin hydrochloride. Archives of Pharmacal Research, 2009. 32(3): p. 391-397.

2. Sahasathian, T., N. Praphairaksit, and N. Muangsin, Mucoadhesive and Floating Chitosan-coated Alginate Beads for the Controlled Gastric Release of Amoxicillin. Archives of Pharmacal Research, 2010. 33(6): p. 889-899.

3. Sajeesh, S. and C.P. Sharma, Mucoadhesive hydrogel microparticles based on poly (methacrylic acid-vinyl pyrrolidone)-chitosan for oral drug delivery. Drug Delivery, 2011. 18(4): p. 227-235.

4. Amidon, G.L., G.A. Debrincat, and N. Najib, Effects of gravity on gastric-emptying, intestinal transit, and drug absorption. Journal of Clinical Pharmacology, 1991. 31(10): p. 968-973.

5. Martinez, M.N. and M.G. Papich, Factors influencing the gastric residence of dosage forms in dogs. Journal of Pharmaceutical Sciences, 2009. 98(3): p. 844-860.

6. Loreno, M., et al., Gastric clearance of radiopaque markers in the evaluation of gastric emptying rate. Scandinavian Journal of Gastroenterology, 2004. 39(12): p. 1215-1218.

7. Cilurzo, F., et al., Characterization and physical stability of fast-dissolving microparticles containing nifedipine. European Journal of Pharmaceutics and Biopharmaceutics, 2008. 68(3): p. 579-588.

8. Cecil, J.E., J. Francis, and N.W. Read, Comparison of the effects of a high-fat and high-carbohydrate soup delivered orally and intragastrically on gastric emptying, appetite, and eating behaviour. Physiology & Behavior, 1999. 67(2): p. 299-306.

9. McGirr, M.E.A., et al., The use of the InteliSite (R) Companion device to deliver mucoadhesive polymers to the dog colon. European Journal of Pharmaceutical Sciences, 2009. 36(4-5): p. 386-391.

10. Nafee, N.A., et al., Mucoadhesive delivery systems. II. Formulation and in-vitro/in-vivo evaluation of buccal mucoadhesive tablets containing water-soluble drugs. Drug Development and Industrial Pharmacy, 2004. 30(9): p. 995-1004.

11. Bennink, R.J., et al., Validation of gastric emptying scintigraphy in mice. Gastroenterology, 2002. 122(4): p. T1298.

12. Breiter, N. and T. Sassy, Development of methods for measuring the gastric-emptying time of liquid and solid test meals in rats. Arzneimittel-Forschung/Drug Research, 1993. 43-1(6): p. 694-698.

13. Jain, S.K., G.P. Agrawal, and N.K. Jain, A novel calcium silicate based microspheres of repaglinide: *In vivo* investigations. Journal of Controlled Release, 2006. 113(2): p. 111-116.

14. Kararli, T.T., Comparison of the gastrointestinal anatomy, physiology, and biochemistry of humans and commonly used laboratory-animals. Biopharmaceutics & Drug Disposition, 1995. 16(5): p. 351-380.

15. Morello, A.P., R. Burrill, and E. Mathiowitz, Preparation and characterization of poly(methyl methacrylate) - iron (III) oxide microparticles using a modified solvent evaporation method. Journal of Microencapsulation, 2007. 24(5): p. 476-491.

16. Duguet, E., et al., PMMA encapsulation of alumina particles through aqueous suspension polymerisation processes. Macromolecular Symposia, 2000. 151: p. 365-370.

17. Bokra, Y., Spectrophotometric study of complexes of ferrous ion with orthophenanthroline and some of its derivatives. Bulletin De La Societe Chimique De France, 1972(12): p. 4483-4489.

18. Forster, E.R., et al., Gastric-emptying in rats - role of afferent neurons and cholecystokinin. American Journal of Physiology, 1990. 258(4): p. G552-G556.

19. Schwarz, R., et al., Gastrointestinal transit times in mice and humans measured with Al-27 and F-19 nuclear magnetic resonance. Magnetic Resonance in Medicine, 2002. 48(2): p. 255-261.

20. Sugito, K., et al., Gastric-emptying rate of drug preparations .3. Effects of size of enteric micro-capsules with mean diameters ranging from 0.1 to 1.1 mm in man. Chemical & Pharmaceutical Bulletin, 1992. 40(12): p. 3343-3345.

21. Keely, S., et al., *In vitro* and *ex vivo* intestinal tissue models to measure mucoadhesion of poly (methaerylate) and N-trimethylated chitosan polymers. Pharmaceutical Research, 2005. 22(1): p. 38-49.

22. Lee, E.R., et al., Division of the mouse gastric-mucosa into zymogenic and mucous regions on the basis of gland features. American Journal of Anatomy, 1982. 164(3): p. 187-&.

23. Mersereau, W.A. and E.J. Hinchey, Role of gastric-mucosal folds in formation of focal ulcers in the rat. Surgery, 1982. 91(2): p. 150-155.

24. Podczeck, F., et al., The influence of non-disintegrating tablet dimensions and density on their gastric emptying in fasted volunteers. Journal of Pharmacy and Pharmacology, 2007. 59(1): p. 23-27.

25. Bravo-Osuna, I., et al., Mucoadhesion mechanism of chitosan and thiolated chitosan-poly(isobutyl cyanoacrylate) core-shell nanoparticles. Biomaterials, 2007. 28(13): p. 2233-2243.

26. Casadei, M.A., et al., Biodegradable and pH-sensitive hydrogels for potential colon-specific drug delivery: Characterization and *in vitro* release studies. Biomacromolecules, 2008. 9(1): p. 43-49.

27. Nikonenko, N.A., I.A. Bushnak, and J.L. Keddie, Spectroscopic Ellipsometry of Mucin Layers on an Amphiphilic Diblock Copolymer Surface. Applied Spectroscopy, 2009. 63(8): p. 889-898.

28. Bando, H. and J.W. McGinity, Relationship between drug dissolution and leaching of plasticizer for pellets coated with an aqueous Eudragit ((R)) S100 : L100 dispersion. International Journal of Pharmaceutics, 2006. 323(1-2): p. 11-17.

Chapter 7: Dissertation Conclusion

Most currently available vaccines require intravenous (i.v.) or subcutaneous (s.c.) delivery of antigens. Over the past 20 years, numerous studies have assessed the potential of orally delivered antigens on the induction of mucosal and systemic immune responses. In addition, mucosal delivery is the only vaccination route to induce effective B cell class switching and the development of secretory IgA-producing plasma cells. Moreover, mucosal vaccination (delivered via oral or nasal route) has many advantages, including no need for sterile needles, a reduced need for trained personnel, and the ability of inducing both mucosal and systematic immunity. However, the major challenge of oral vaccination is the harsh environment of the gastrointestinal tract and the possibility of orally delivered soluble antigens inducing tolerance rather than immunity. Therefore, protection of the antigens or utilization of a carrier system is required. Our goal was to develop a mucoadhesive, oral vaccination delivery system designed to target Peyer's patches in the ileum. In order to achieve that, we started by investigating the possibility of preparing particles of various sizes using W/O/W solvent evaporation method. The particle size (uniformity and particle span), loading efficiency, and drug releasing profile are evaluated. From the animal study, we conclude that the cut-off size at the pyloric sphincter in Sprague Dawley rats (body weight 250-300 g) was approximately 3 mm, and the cut-off size for stomach emptying in ICR mice was limited only by the upper limit of feasible dosing (300 μm) method. Additionally, particle size was found to significantly alter gastric emptying rates in both rodent species investigated. This information is valuable for designing preclinical rodent testing studies, especially for oral drug delivery

systems designed for lower intestine targeting, or when investigating acid labile compounds for oral drug delivery systems.

In addition, since an increased residence time of a given formulation at the targeted site tends to enhance both absorption and bioavailability of a drug, our second goal was to coat or employ mucoadhesive polymers into the carrier system. To do so, we first developed our own *in vitro* mucoadhesion testing device as an evaluation tool. Adhesion properties of matrix tablet and pellets (made of potentially mucoadhesive polymers. Methocel® K4M, Carbopol® 934, chitosan, and sodium alginate were investigated using our testing device. The mucoadhesive property of several polymers, HPMC (Methocel® K4M), Carbopol® 974P and sodium alginate were studied using a novel *in vitro* test ramp. Both HPMC (Methocel® K4M) and Carbopol® 974P containing formulation showed significantly prolonged retention time. The increased retention time could potentially enhance local absorption of the drug in the GI tract.

The *in vitro* test ramp developed in this study may be used to investigate the mucoadhesive properties of polymers and provide a rank order for study. Among the mucoadhesive polymers tested in the study, HPMC (Methocel® K4M) showed best mucoadhesive property, followed by Carbopol® 974P, and sodium alginate. We proved that, the *in vitro* flowing test ramp we developed was capable of investigating the mucoadhesive properties of different dosage forms, including powders, pellets, and tablets, providing a rank order of mucoadhesion property. The device could further be adapted to mimic physiological conditions at different sections of the gastrointestinal tract by adjusting the flow rate, device angle, and the testing medium applied. Most

important of all, it is anticipated that the biorelevant gel is able to replace animal tissues in *in vitro* mucoadhesion and reduces the burden of test animals in *in vitro* mucoadhesion test, which is in concord with the 3R's of animal welfare.

Mucosal immunity is stimulated by administration of antigen directly on the mucosal site where an infection occurs. Antigen is processed by mucosa-associated lymphoid tissue (MALT) in inductive sites where plasma cell precursors are induced. Gut associated lymphoid tissue (GALT) is one of the major MALT. Peyer's Patches of GALT are responsible for antigen uptake. Peyer's patches are collections of lymphoid tissue containing B and T lymphocytes, as well as macrophages. Antigens are taken up via endocytosis by the Microfold cells (M cells) at the Peyer's patches. Particles less than 5 μm could be transferred to the draining lymph nodes and spleen to stimulate both a mucosal and systemic immune response after uptake by the M cells. Therefore, we prepared two nano- and microstructured antigen carrying system composed of solid lipid nanoparticles (SLNs) or protein coated microcrystals (PCMC) with bovine serum albumin (BSA) as the model antigen. The two delivery systems were design to target to the ileum and uptake at Peyer's patches. To further enhance the contact time of the delivery system at the epithelium (at ileum), mucoadhesive polymers (Methocel® K4M and Methocel® E15) were incorporated into the two delivery systems. The mixture was granulated and spheronized into pellets (1-1.5 mm in diameter). The pellets were then enteric coated with a mixture of Eudragit® F S 30 D/Eudragit® L 30 D-55 to prevent from gastric damage and control the release of BSA at pH above 7.2.

Enteric coated pellets with BSA loaded PCMC could be a possible candidate for oral vaccination delivery system, however, further coating condition or protecting method must be conducted to enhance the stability and prolong the storage period of formulation. BSA was successfully loaded into SLNs with Gelucire® 50/13 as the lipid matrix. The particle size of SLNs we manufactured was in the proper range for oral vaccine delivery systems. With proper enteric coating, the release of BSA/SLNs loaded pellets could be well-controlled for targeted delivery to ileum. However, further studies must be conducted to enhance the encapsulation efficiency % of BSA and assure the stability of the formulation for long-term storage.

Bibliography

Adhikary, A. and P.R. Vavia, Bioadhesive ranitidine hydrochloride for gastroretention with controlled microenvironmental pH. Drug Development and Industrial Pharmacy, 2008. 34(8): p. 860-869.

Ahire, V.J., et al., Chitosan microparticles as oral delivery system for tetanus toxoid. Drug Development and Industrial Pharmacy, 2007. 33(10): p. 1112-1124.

Alhalaweh, A., S. Andersson, and S.P. Velaga, Preparation of zolmitriptan-chitosan microparticles by spray drying for nasal delivery. European Journal of Pharmaceutical Sciences, 2009. 38(3): p. 206-214.

AllaouiAttarki, K., et al., Protective immunity against Salmonella typhimurium elicited in mice by oral vaccination with phosphorylcholine encapsulated in poly(DL-lactide-co-glycolide) microspheres. Infection and Immunity, 1997. 65(3): p. 853-857.

Alpar, H.O., et al., Biodegradable mucoadhesive particulates for nasal and pulmonary antigen and DNA delivery. Advanced Drug Delivery Reviews, 2005. 57(3): p. 411-430.

Amidon, G.L., G.A. Debrincat, and N. Najib, Effects of gravity on gastric-emptying, intestinal transit, and drug absorption. Journal of Clinical Pharmacology, 1991. 31(10): p. 968-973.

Arap, M.A., Phage display technology - Applications and innovations. Genetics and Molecular Biology, 2005. 28(1): p. 1-9.

Atyabi, F., et al., The impact of trimethyl chitosan on *in vitro* mucoadhesive properties of pectinate beads along different sections of gastrointestinal tract. Drug Development and Industrial Pharmacy, 2007. 33(3): p. 291-300.

Azad, N. and Y. Rojanasakul, Vaccine delivery--current trends and future. Curr Drug Deliv., 2006. 3(2): p. 137-46.

Bajwa, G.S., et al., Microstructural imaging of early gel layer formation in HPMC matrices. Journal of Pharmaceutical Sciences, 2006. 95(10): p. 2145-2157.

Baloglu, E., et al., In vitro evaluation of mucoadhesive vaginal tablets of antifungal drugs prepared with thiolated polymer and development of a new dissolution technique for vaginal formulations. Chemical & Pharmaceutical Bulletin, 2011. 59(8): p. 952-958.

Bando, H. and J.W. McGinity, Relationship between drug dissolution and leaching of plasticizer for pellets coated with an aqueous Eudragit ((R)) S100 : L100 dispersion. International Journal of Pharmaceutics, 2006. 323(1-2): p. 11-17.

Barder, O. Vaccines for development. 2006; Available from: http://www.cgdev.org/files/7366_file_Vaccines2.pdf

Basaran, E., et al., Cyclosporine-A incorporated cationic solid lipid nanoparticles for ocular delivery. Journal of Microencapsulation. 27(1): p. 37-47.

Baudner, B.C., et al., Modulation of immune response to group C meningococcal conjugate vaccine given intranasally to mice together with the LTK63 mucosal

adjuvant and the trimethyl chitosan delivery system. Journal of Infectious Diseases, 2004. 189(5): p. 828-832.
Bautzova, T., et al., Bioadhesive pellets increase local 5-aminosalicylic acid concentration in experimental colitis. European Journal of Pharmaceutics and Biopharmaceutics, 2012. 81(2): p. 379-385.
Beier, R. and A. Gebert, Kinetics of particle uptake in the domes of Peyer's patches. American Journal of Physiology-Gastrointestinal and Liver Physiology, 1998. 275(1): p. G130-G137.
Belgamwar, V.S., et al., Design and development of nasal mucoadhesive microspheres containing tramadol HCl for CNS targeting. Drug Delivery, 2011. 18(5): p. 353-360.
Bell, K.N., et al., Risk factors for improper vaccine storage and handling in private provider offices. Pediatrics, 2001. 107(6): p. art. no.-e100.
Benchabane, S., M. Subirade, and G.W. Vandenberg, Production of BSA-loaded alginate microcapsules: Influence of spray dryer parameters on the microcapsule characteristics and BSA release. Journal of Microencapsulation, 2007. 24(7): p. 647-658.
Bennett, E., A.B. Mullen, and V.A. Ferro, Translational modifications to improve vaccine efficacy in an oral influenza vaccine. Methods, 2009. 49(4): p. 322-327.
Bennink, R.J., et al., Validation of gastric emptying scintigraphy in mice. Gastroenterology, 2002. 122(4): p. T1298.
Berner, V.K., M.E. Sura, and K.W. Hunter, Conjugation of protein antigen to microparticulate beta-glucan from Saccharomyces cerevisiae: a new adjuvant for intradermal and oral immunizations. Applied Microbiology and Biotechnology, 2008. 80(6): p. 1053-1061.
Bernkop-Schnurch, A., et al., Preparation and characterisation of thiolated poly(methacrylic acid)-starch compositions. European Journal of Pharmaceutics and Biopharmaceutics, 2004. 57(2): p. 219-224.
Bhattacharjee, S., et al., Cytotoxicity and cellular uptake of tri-block copolymer nanoparticles with different size and surface characteristics. Particle and Fibre Toxicology, 2012. 9.
Bigucci, F., et al., Pectin-based microspheres for colon-specific delivery of vancomycin. Journal of Pharmacy and Pharmacology, 2009. 61(1): p. 41-46.
Bokra, Y., Spectrophotometric study of complexes of ferrous ion with orthophenanthroline and some of its derivatives. Bulletin De La Societe Chimique De France, 1972(12): p. 4483-4489.
Borges, O., et al., Evaluation of the immune response following a short oral vaccination schedule with hepatitis B antigen encapsulated into alginate-coated chitosan nanoparticles. European Journal of Pharmaceutical Sciences, 2007. 32(4-5): p. 278-290.
Bowersock, T.L., et al., Oral vaccination with alginate microsphere systems. Journal of Controlled Release, 1996. 39(2-3): p. 209-220.

Bradford, M.M., Rapid and sensitive method for the quantitation of microgram quantities of protein utilizing the principle of protein-dye binding. Anal. Biochem., 1976(72): p. 248-254.
Brandtzaeg, P., Molecular and cellular aspects of the secretory immunoglobulin system. Apmis, 1995. 103(1): p. 1-19.
Brandtzaeg, P., Mucosal immunity: induction, dissemination, and effector functions. Scandinavian Journal of Immunology, 2009. 70(6): p. 505-515.
Bravo-Osuna, I., et al., Mucoadhesion mechanism of chitosan and thiolated chitosan-poly(isobutyl cyanoacrylate) core-shell nanoparticles. Biomaterials, 2007. 28(13): p. 2233-2243.
Breiter, N. and T. Sassy, Development of methods for measuring the gastric-emptying time of liquid and solid test meals in rats. Arzneimittel-Forschung/Drug Research, 1993. 43-1(6): p. 694-698.
Brewer, J.M., et al., Lipid vesicle size determines the Th1 or Th2 response to entrapped antigen. Journal of Immunology, 1998. 161(8): p. 4000-4007.
Carrasquillo, K.G., et al., Non-aqueous encapsulation of excipient-stabilized spray-freeze dried BSA into poly(lactide-co-glycolide) microspheres results in release of native protein. Journal of Controlled Release, 2001. 76(3): p. 199-208.
Carvalho, F.C., et al., Mucoadhesive drug delivery systems. Brazilian Journal of Pharmaceutical Sciences, 2010. 46(1): p. 1-17.
Casadei, M.A., et al., Biodegradable and pH-sensitive hydrogels for potential colon-specific drug delivery: Characterization and in vitro release studies. Biomacromolecules, 2008. 9(1): p. 43-49.
Cattani, V.B., et al., Lipid-core nanocapsules restrained the indomethacin ethyl ester hydrolysis in the gastrointestinal lumen and wall acting as mucoadhesive reservoirs. European Journal of Pharmaceutical Sciences, 2010. 39(1-3): p. 116-124.
Cecil, J.E., J. Francis, and N.W. Read, Comparison of the effects of a high-fat and high-carbohydrate soup delivered orally and intragastrically on gastric emptying, appetite, and eating behaviour. Physiology & Behavior, 1999. 67(2): p. 299-306.
Centers for Disease, C. and Prevention, Guidelines for maintaining and managing the vaccine cold chain. MMWR. Morbidity and mortality weekly report, 2003. 52(42): p. 1023-5.
Chablani, L., S.A. Tawde, and M.J. D'Souza, Spray-dried microparticles: a potential vehicle for oral delivery of vaccines. Journal of Microencapsulation, 2012. 29(4): p. 388-397.
Challacombe, S.J., et al., Enhanced secretory iga and systemic IgG antibody-responses after oral immunization with biodegradable microparticles containing antigen. Immunology, 1992. 76(1): p. 164-168.
Chalmers, W.S.K., Overview of new vaccines and technologies. Veterinary Microbiology, 2006. 117(1): p. 25-31.

Chamcha, V., J.R. Scott, and R. Amara, Oral immunization with a recombinant Lactococcus lactis expressing HIV-1 Gag on the tip of the pilus induces strong mucosal immune responses. Retrovirology, 2012. 9(Suppl 2).

Channarong, S., et al., Development and evaluation of chitosan-coated liposomes for oral DNA vaccine: The improvement of Peyer's patch targeting using a polyplex-loaded liposomes. Aaps Pharmscitech, 2011. 12(1): p. 192-200.

Chary, R.B.R., G. Vani, and Y.M. Rao, In vitro and *in vivo* adhesion testing of mucoadhesive drug delivery systems. Drug Development and Industrial Pharmacy, 1999. 25(5): p. 685-690.

Chehade, M. and L. Mayer, Oral tolerance and its relation to food hypersensitivities. Journal of Allergy and Clinical Immunology, 2005. 115(1): p. 3-12.

Chen, F., et al., In vitro and *in vivo* study of N-trimethyl chitosan nanoparticles for oral protein delivery. International Journal of Pharmaceutics, 2008. 349(1-2): p. 226-233.

Chowdary, K.P.R. and Y.S. Rao, Mucoadhesive microspheres for controlled drug delivery. Biological & Pharmaceutical Bulletin, 2004. 27(11): p. 1717-1724.

Cilurzo, F., et al., Characterization and physical stability of fast-dissolving microparticles containing nifedipine. European Journal of Pharmaceutics and Biopharmaceutics, 2008. 68(3): p. 579-588.

Coppi, G. and V. Iannuccelli, Alginate/chitosan microparticles for tamoxifen delivery to the lymphatic system. International Journal of Pharmaceutics, 2009. 367(1-2): p. 127-132.

Costantino, H.R., et al., Protein spray-freeze drying. Effect of atomization conditions on particle size and stability. Pharmaceutical Research, 2000. 17(11): p. 1374-1383.

Cui, F.D., et al., Preparation and in vitro evaluation of pH, time-based and enzyme-degradable pellets for colonic drug delivery. Drug Development and Industrial Pharmacy, 2007. 33(9): p. 999-1007.

Dalvadi, H.P., et al., Development and characterization of controlled release mucoadhesive tablets of captopril to increase the residence time in the gastrointestinal tract. Latin American Journal of Pharmacy, 2011. 30(2): p. 266-272.

De Aizpurua, H.J. and G.J. Russell-Jones, Oral vaccination identification of classes of proteins that provoke an immune response upon oral feeding. Journal of Experimental Medicine, 1988. 167(2): p. 440-451.

Della Porta, G., et al., Bacteria microencapsulation in PLGA microdevices by supercritical emulsion extraction. Journal of Supercritical Fluids, 2012. 63: p. 1-7.

Devriendt, B., et al., Crossing the barrier: Targeting epithelial receptors for enhanced oral vaccine delivery. Journal of Controlled Release, 2012. 160(3): p. 431-439.

Dewit, M.A. and E.R. Gillies, A Cascade Biodegradable Polymer Based on Alternating Cyclization and Elimination Reactions. Journal of the American Chemical Society, 2009. 131(51): p. 18327-18334.

Dey, N.S., S. Majumadar, and M.E.B. Rao, Multiparticulate drug delivery systems for controlled release. Tropical Journal of Pharmaceutical Research, 2008. 7(3): p. 1067-1075.
Dodou, D., P. Breedveld, and P.A. Wieringa, Mucoadhesives in the gastrointestinal tract: revisiting the literature for novel applications. European Journal of Pharmaceutics and Biopharmaceutics, 2005. 60(1): p. 1-16.
D'Souza, B., et al., Oral microparticulate vaccine for melanoma using M-cell targeting. Journal of Drug Targeting, 2012. 20(2): p. 166-173.
Duguet, E., et al., PMMA encapsulation of alumina particles through aqueous suspension polymerisation processes. Macromolecular Symposia, 2000. 151: p. 365-370.
Dunnhaupt, S., et al., Distribution of thiolated mucoadhesive nanoparticles on intestinal mucosa. International Journal of Pharmaceutics, 2011. 408(1-2): p. 191-199.
Dupeyron, D., et al., Protein delivery by enteric copolymer nanoparticles. Journal of Dispersion Science and Technology, 2009. 30(8): p. 1188-1194.
Dvorackova, K., et al., Coated hard capsules as the pH-dependent drug transport systems to ileo-colonic compartment. Drug Development and Industrial Pharmacy, 2011. 37(10): p. 1131-1140.
Eldridge, J.H., et al., Biodegradable and biocompatible poly(dl-lactide-co-glycolide) microspheres as an adjuvant for staphylococcal enterotoxin-b toxoid which enhances the level of toxin-neutralizing antibodies. Infection and Immunity, 1991. 59(9): p. 2978-2986.
Eldridge, J.H., et al., Controlled vaccine release in the gut-associated lymphoid-tissues .1. Orally-administered biodegradable microspheres target the Peyer's patches. Journal of Controlled Release, 1990. 11(1-3): p. 205-214.
Engstrom, J.D., et al., Stable high surface area lactate dehydrogenase particles produced by spray freezing into liquid nitrogen. European Journal of Pharmaceutics and Biopharmaceutics, 2007. 65(2): p. 163-174.
Faubion, W.A. and C. Fiocchi, Gut immunity and inflammatory bowel disease, in Pediatric Inflammatory Bowel Disease. 2008, Springer US. p. 15.
Fievez, V., et al., Targeting nanoparticles to M cells with non-peptidic ligands for oral vaccination. European Journal of Pharmaceutics and Biopharmaceutics, 2009. 73(1): p. 16-24.
Flower, D.R. and Y. Perrie, Immunomic discovery of adjuvants and candidate subunit Vaccines: Springer.
Forster, E.R., et al., Gastric-emptying in rats - role of afferent neurons and cholecystokinin. American Journal of Physiology, 1990. 258(4): p. G552-G556.
Garinot, M., et al., PEGylated PLGA-based nanoparticles targeting M cells for oral vaccination. Journal of Controlled Release, 2007. 120(3): p. 195-204.
Garnier, B., et al., Development of a Platform of Antibody-Presenting Liposomes. Biointerphases, 2012. 7(1-4).
Gavini, E., et al., Development of solid nanoparticles based on hydroxypropyl-beta-cyclodextrin aimed for the colonic transmucosal delivery of diclofenac sodium. Journal of Pharmacy and Pharmacology, 2011. 63(4): p. 472-482.

Giudice, E.L. and J.D. Campbell, Needle-free vaccine delivery. Advanced Drug Delivery Reviews, 2006. 58(1): p. 68-89.

Gullberg, E., et al., Identification of cell adhesion molecules in the human follicle-associated epithelium that improve nanoparticle uptake into the Peyer's patches. Journal of Pharmacology and Experimental Therapeutics, 2006. 319(2): p. 632-639.

Hagerstrom, H. and K. Edsman, Interpretation of mucoadhesive properties of polymer gel preparations using a tensile strength method. Journal of Pharmacy and Pharmacology, 2001. 53(12): p. 1589-1599.

Hanson, L.A., et al., Breast-feeding, a complex support system for the offspring. Pediatrics International, 2002. 44(4): p. 347-352.

Hashizume, T., et al., Peyer's patches are required for intestinal immunoglobulin A responses to Salmonella spp. Infection and Immunity, 2008. 76(3): p. 927-934.

He, P., S.S. Davis, and L. Illum, In vitro evaluation of the mucoadhesive properties of chitosan microspheres. International Journal of Pharmaceutics, 1998. 166(1): p. 75-88.

Heritage, P.L., et al., Oral administration of polymer-grafted starch microparticles activates gut-associated lymphocytes and primes mice for a subsequent systemic antigen challenge. Vaccine, 1998. 16(20): p. 2010-2017.

Hird, T.R. and N.C. Grassly, Systematic review of mucosal immunity induced by oral and inactivated Poliovirus vaccines against virus shedding following oral Poliovirus challenge. Plos Pathogens, 2012. 8(4).

Holmgren, J. and C. Czerkinsky, Mucosal immunity and vaccines. Nature Medicine, 2005. 11(4): p. S45-S53.

Hsu, L.W., et al., Elucidating the signaling mechanism of an epithelial tight-junction opening induced by chitosan. Biomaterials, 2012. 33(26): p. 6254-6263.

Hu, Y., T.M. Yang, and X.M. Hu, Novel polysaccharides-based nanoparticle carriers prepared by polyelectrolyte complexation for protein drug delivery. Polymer Bulletin, 2012. 68(4): p. 1183-1199.

Huang, Y.Y., T.W. Chung, and T.W. Tzeng, A method using biodegradable polylactides polyethylene glycol for drug release with reduced initial burst. International Journal of Pharmaceutics, 1999. 182(1): p. 93-100.

Hussain, N., V. Jaitley, and A.T. Florence, Recent advances in the understanding of uptake of microparticulates across the gastrointestinal lymphatics. Advanced Drug Delivery Reviews, 2001. 50(1-2): p. 107-142.

Huyghebaert, N., et al., Evaluation of extrusion/spheronisation, layering and compaction for the preparation of an oral, multi-particulate formulation of viable, hIL-10 producing Lactococcus lactis. European Journal of Pharmaceutics and Biopharmaceutics, 2005. 59(1): p. 9-15.

Ibekwe, V.C., et al., Interplay between intestinal pH, transit time and feed status on the *in vivo* performance of pH responsive ileo-colonic release systems. Pharmaceutical Research, 2008. 25(8): p. 1828-1835.

Jackson, S.J. and A.C. Perkins, In vitro assessment of the mucoadhesion of cholestyramine to porcine and human gastric mucosa. European Journal of Pharmaceutics and Biopharmaceutics, 2001. 52(2): p. 121-127.

Jain, S., et al., Mannosylated niosomes as adjuvant-carrier system for oral genetic immunization against Hepatitis B. Immunology Letters, 2005. 101(1): p. 41-49.

Jain, S., et al., Nanocarriers for transmucosal vaccine delivery. Current Nanoscience, 2011. 7(2): p. 160-177.

Jain, S.K., G.P. Agrawal, and N.K. Jain, A novel calcium silicate based microspheres of repaglinide: *In vivo* investigations. Journal of Controlled Release, 2006. 113(2): p. 111-116.

Johnson, B.A., A synopsis of the pharmacological rationale, properties and therapeutic effects of depot preparations of naltrexone for treating alcohol dependence. Expert Opinion on Pharmacotherapy, 2006. 7(8): p. 1065-1073.

Jung, T., et al., Biodegradable nanoparticles for oral delivery of peptides: is there a role for polymers to affect mucosal uptake? European Journal of Pharmaceutics and Biopharmaceutics, 2000. 50(1): p. 147-160.

Kakoulides, E.P., J.D. Smart, and J. Tsibouklis, Azocrosslinked poly(acrylic acid) for colonic delivery and adhesion specificity: in vitro degradation and preliminary *ex vivo* bioadhesion studies. Journal of Controlled Release, 1998. 54(1): p. 95-109.

Kamel, R., A. Mahmoud, and G. El-Feky, Double-phase hydrogel for buccal delivery of tramadol. Drug Development and Industrial Pharmacy, 2012. 38(4): p. 468-483.

Kaneko, H., et al., Oral DNA vaccination promotes mucosal and systemiciImmune responses to HIV envelope glycoprotein. Viology, 2000. 267(1): p. 9.

Kang, M.L., C.S. Cho, and H.S. Yoo, Application of chitosan microspheres for nasal delivery of vaccines. Biotechnology Advances, 2009. 27(6): p. 857-865.

Kanthamneni, N., et al., Enhanced stability of horseradish peroxidase encapsulated in acetalated dextran microparticles stored outside cold chain conditions. International Journal of Pharmaceutics, 2012. 431(1-2): p. 101-110.

Kararli, T.T., Comparison of the gastrointestinal anatomy, physiology, and biochemistry of humans and commonly used laboratory-animals. Biopharmaceutics & Drug Disposition, 1995. 16(5): p. 351-380.

Keely, S., et al., In vitro and *ex vivo* intestinal tissue models to measure mucoadhesion of poly (methaerylate) and N-trimethylated chitosan polymers. Pharmaceutical Research, 2005. 22(1): p. 38-49.

Khan, J., et al., Preparation and in-vitro evaluation of different controlled release polymeric matrices containing Ketoprofen. Healthmed, 2010. 4(2): p. 386-392.

Khosravani, A., et al., Formulation of the adenylate cyclase toxin of Bordetella pertussis as protein-coated microcrystals. Vaccine, 2007. 25(22): p. 4361-4367.

Kim, J.S., et al., Statistical optimization of tamsulosin hydrochloride controlled release pellets coated with the blend of HPMCP and HPMC. Chemical & Pharmaceutical Bulletin, 2007. 55(6): p. 936-939.

Ko, Y.T. and U. Bickel, Liposome-encapsulated polyethylenimine/oligonucleotide polyplexes prepared by reverse-phase evaporation technique. Aaps Pharmscitech, 2012. 13(2): p. 373-378.
Konig, C., et al., Development of a pilot-scale manufacturing process for protein-coated microcrystals (PCMC): Mixing and precipitation - Part I. European Journal of Pharmaceutics and Biopharmaceutics, 2012. 80(3): p. 490-498.
Kotze, A.F., et al., Chitosan for enhanced intestinal permeability: Prospects for derivatives soluble in neutral and basic environments. European Journal of Pharmaceutical Sciences, 1999. 7(2): p. 145-151.
Krishnamachari, Y., P. Madan, and S.S. Lin, Development of pH- and time-dependent oral microparticles to optimize budesonide delivery to ileum and colon. International Journal of Pharmaceutics, 2007. 338(1-2): p. 238-247.
Kuklin, N., et al., Induction of mucosal immunity against herpes simplex virus by plasmid DNA immunization. Journal of Virology, 1997. 71(4): p. 8.
Kumar, M.P., Y.M. Rao, and S. Apte, Formulation of nanosuspensions of albendazole for oral administration. Current Nanoscience, 2008. 4(1): p. 53-58.
Kunisawa, J., et al., Characterization of mucoadhesive microspheres for the induction of mucosal and systemic immune responses. Vaccine, 2000. 19(4-5): p. 589-594.
Lameiro, M.H., et al., Encapsulation of adenoviral vectors into chitosan-bile salt microparticles for mucosal vaccination. Journal of Biotechnology, 2006. 126(2): p. 152-162.
Larhed, A., et al., Starch microparticles as oral vaccine adjuvant: Antigen-dependent uptake in mouse intestinal mucosa. Journal of Drug Targeting, 2004. 12(5): p. 289-296.
Le Ray, A.M., et al., Development of a "continuous-flow adhesion cell" for the assessment of hydrogel adhesion. Drug Development and Industrial Pharmacy, 1999. 25(8): p. 897-904.
Lebre, F., et al., Progress towards a needle-free Hepatitis b vaccine. Pharmaceutical Research, 2011. 28(5): p. 986-1012.
Lee, E.R., et al., Division of the mouse gastric-mucosa into zymogenic and mucous regions on the basis of gland features. American Journal of Anatomy, 1982. 164(3): p. 187-&.
Lee, K.A., et al., Acid stability of anti-Helicobacter pyroli IgY in aqueous polyol solution. Journal of Biochemistry and Molecular Biology, 2002. 35(5): p.
Li, X.Y., et al., Chitosan-alginate microcapsules for oral delivery of egg yolk immunoglobulin (IgY): Effects of chitosan concentration. Applied Biochemistry and Biotechnology, 2009. 159(3): p. 778-787.
Li, X.Y., et al., Preparation of alginate coated chitosan microparticles for vaccine delivery. Bmc Biotechnology, 2008. 8.
Liu, D.H., et al., Enhanced gastrointestinal absorption of N-3-O-toluyl-fluorouracil by cationic solid lipid nanoparticles. Journal of Nanoparticle Research. 12(3): p. 975-984.

Liu, F., et al., A novel concept in enteric coating: A double-coating system providing rapid drug release in the proximal small intestine. Journal of Controlled Release, 2009. 133(2): p. 119-124.
Liu, F., et al., A novel concept in enteric coating: A double-coating system providing rapid drug release in the proximal small intestine. Journal of Controlled Release, 2009. 133(2): p. 119-124.
Liu, M.X., et al., Anti-inflammatory effects of triptolide loaded poly(D,L-lactic acid) nanoparticles on adjuvant-induced arthritis in rats. Journal of Ethnopharmacology, 2005. 97(2): p. 219-225.

Longbottom, D. and M. Livingstone, Vaccination against chlamydial infections of man and animals. Veterinary Journal, 2006. 171(2): p. 263-275.

Loreno, M., et al., Gastric clearance of radiopaque markers in the evaluation of gastric emptying rate. Scandinavian Journal of Gastroenterology, 2004. 39(12): p. 1215-1218.

Lozzi, I., et al., Interferences of suspended clay fraction in protein quantitation by several determination methods. Analytical Biochemistry, 2008. 376(1): p. 108-114.

Lycke, N., Recent progress in mucosal vaccine development: potential and limitations. Nature Reviews Immunology, 2012. 12(8): p. 592-605.

Lyle, C., J. Vos, and B.D. Moore, Formulation of hyaluronidase as a temperature-stable dry powder using protein-coated micro-crystals (PCMC). Journal of Pharmacy and Pharmacology, 2006. 58: p. A72-A72.

Mainardes, R.M., N.M. Khalil, and M.P.D. Gremiao, Intranasal delivery of zidovudine by PLA and PLA-PEG blend nanoparticles. International Journal of Pharmaceutics, 2010. 395(1-2): p. 266-271.

Makhlof, A., Y. Tozuka, and H. Takeuchi, Design and evaluation of novel pH-sensitive chitosan nanoparticles for oral insulin delivery. European Journal of Pharmaceutical Sciences, 2011. 42(5): p. 445-451.

Maloy, K.J., et al., induction of mucosal and systemic immune-responses by immunization with ovalbumin entrapped in poly(lactide-co-glycolide) microparticles. Immunology, 1994. 81(4): p. 661-667.

Mann, J.F.S., et al., Lipid vesicle size of an oral influenza vaccine delivery vehicle influences the Th1/Th2 bias in the immune response and protection against infection. Vaccine, 2009. 27(27): p. 3643-3649.

Mann, J.F.S., et al., Optimisation of a lipid based oral delivery system containing A/Panama influenza haemagglutinin. Vaccine, 2004. 22(19): p. 2425-2429.

Margolis, K.L., et al., Frequency of adverse reactions to influenza vaccine in the elderly - a randomized, placebo-controlled trial. Jama-Journal of the American Medical Association, 1990. 264(9): p. 1139-1141.

Martinez, M.N. and M.G. Papich, Factors influencing the gastric residence of dosage forms in dogs. Journal of Pharmaceutical Sciences, 2009. 98(3): p. 844-860.

Mata, E., et al., Enhancing immunogenicity to PLGA microparticulate systems by incorporation of alginate and RGD-modified alginate. European Journal of Pharmaceutical Sciences, 2011. 44(1-2): p. 32-40.

Matteucci, M.E., et al., Highly supersaturated solutions from dissolution of amorphous itraconazole microparticles at ph 6.8. Molecular Pharmaceutics, 2009. 6(2): p. 375-385.
McClean, S., et al., Binding and uptake of biodegradable poly-DL-lactide micro- and nanoparticles in intestinal epithelia. European Journal of Pharmaceutical Sciences, 1998. 6(2): p. 153-163.
McGirr, M.E.A., et al., The use of the InteliSite (R) Companion device to deliver mucoadhesive polymers to the dog colon. European Journal of Pharmaceutical Sciences, 2009. 36(4-5): p. 386-391.
Md, S., et al., Gastroretentive drug delivery system of acyclovir-loaded alginate mucoadhesive microspheres: Formulation and evaluation. Drug Delivery, 2011. 18(4): p. 255-264.
Meng, J.N., T.F. Sturgis, and B.B.C. Youan, Engineering tenofovir loaded chitosan nanoparticles to maximize microbicide mucoadhesion. European Journal of Pharmaceutical Sciences, 2011. 44(1-2): p. 57-67.
Mercier, G.T., et al., Oral immunization of rhesus macaques with adenoviral HIV vaccines using enteric-coated capsules. Vaccine, 2007. 25(52): p. 8687-8701.
Mersereau, W.A. and E.J. Hinchey, Role of gastric-mucosal folds in formation of focal ulcers in the rat. Surgery, 1982. 91(2): p. 150-155.
Meziani, M.J., et al., Protein-protected nanoparticles from rapid expansion of supercritical solution into aqueous solution. Journal of Physical Chemistry B, 2002. 106(43): p. 11178-11182.
Mishra, N., et al., Recent advances in mucosal delivery of vaccines: role of mucoadhesive/biodegradable polymeric carriers. Expert Opinion on Therapeutic Patents, 2010. 20(5): p. 661-679.
Mitragotri, S., Immunization without needles. Nature Reviews Immunology, 2005. 5(12): p. 905-916.
Miyazaki, Y., et al., Evaluation of mucoadhesion for dextran derivatives in solid state. Yakuzaigaku, 2002. 62(1): p. 14-22.
Mohammadi-Samani, S., R. Bahri-Najafi, and G. Yousefi, Formulation and in vitro evaluation of prednisolone buccoadhesive tablets. Farmaco (Lausanne), 2005. 60(4): p. 339-344.
Moore, B.D., et al., Isolation of recombinant proteins from culture broth by co-precipitation with an amino acid carrier to form stable dry powders. Biotechnology and Bioengineering, 2010. 106(5): p. 764-773.
Morello, A.P., R. Burrill, and E. Mathiowitz, Preparation and characterization of poly(methyl methacrylate) - iron (III) oxide microparticles using a modified solvent evaporation method. Journal of Microencapsulation, 2007. 24(5): p. 476-491.
Mortazavi, S.A. and J.D. Smart, An investigation of some factors influencing the in-vitro assessment of mucoadhesion. International Journal of Pharmaceutics, 1995. 116(2): p. 223-230.

Moura, M.J., et al., *In situ* forming chitosan hydrogels prepared via ionic/covalent co-cross-linking. Biomacromolecules, 2011. 12(9): p. 3275-3284.
Moyle, P.M., et al., Mucosal immunisation: Adjuvants and delivery systems. Current Drug Delivery, 2004. 1(4): p. 385-396.
Murdan, S., et al., Immobilisation of vaccines onto micro-crystals for enhanced thermal stability. International Journal of Pharmaceutics, 2005. 296(1-2): p. 117-121.
Murdan, S., et al., Vaccine-coated microcrystals: Enhanced thermal stability of diphtheria taxoid. Journal of Pharmacy and Pharmacology, 2003. 55 (Supplement): p. 71-72.
Muzzarelli, R.A.A., Human enzymatic activities related to the therapeutic administration of chitin derivatives. Cellular and Molecular Life Sciences, 1997. 53(2): p. 131-140.
Nafee, N.A., et al., Mucoadhesive delivery systems. II. Formulation and in-vitro/in-vivo evaluation of buccal mucoadhesive tablets containing water-soluble drugs. Drug Development and Industrial Pharmacy, 2004. 30(9): p. 995-1004.
Nayak, B., et al., Formulation, characterization and evaluation of rotavirus encapsulated PLA and PLGA particles for oral vaccination. Journal of Microencapsulation, 2009. 26(2): p. 154-165.
Neutra, M.R., et al., Transport of membrane-bound macromolecules by m-cells in follicle-associated epithelium of rabbit Peyer's patch. Cell and Tissue Research, 1987. 247(3): p. 537-546.
Nikonenko, N.A., I.A. Bushnak, and J.L. Keddie, Spectroscopic ellipsometry of mucin layers on an amphiphilic diblock copolymer surface. Applied Spectroscopy, 2009. 63(8): p. 889-898.
Nograles, N., et al., Formation and characterization of pDNA-loaded alginate microspheres for oral administration in mice. Journal of Bioscience and Bioengineering, 2012. 113(2): p. 133-140.
Okeke, I.N., A. Lamikanra, and R. Edelman, Socioeconomic and behavioral factors leading to acquired bacterial resistance to antibiotics in developing countries. Emerging Infectious Diseases, 1999. 5(1): p. 18-27.
Okhamafe, A.O., et al., Modulation of protein release from chitosan-alginate microcapsules using the pH-sensitive polymer hydroxypropyl methylcellulose acetate succinate. Journal of Microencapsulation, 1996. 13(5): p. 497-508.
Ouadahi, S., et al., Liposomal formulations for oral immunotherapy: In-vitro stability in synthetic intestinal media and in-vivo efficacy in the mouse. Journal of Drug Targeting, 1998. 5(5): p. 365-378.
Overhoff, K.A., et al., Solid dispersions of itraconazole and enteric polymers made by ultra-rapid freezing. International Journal of Pharmaceutics, 2007. 336(1): p. 122-132.
Oyarzun-Ampuero, F.A., et al., Chitosan-coated lipid nanocarriers for therapeutic applications. Journal of Drug Delivery Science and Technology, 2010. 20(4): p. 259-265.

Pandey, S., et al., Formulation and in-vitro evaluation of bilayered buccal tablets of carvedilol. Indian Journal of Pharmaceutical Education and Research, 2010. 44(3): p. 259-266.

Park, H. and J.R. Robinson, Mechanisms of mucoadhesion of poly(acrylic acid) hydrogels. Pharmaceutical Research, 1987. 4(6): p. 457-464.

Patel, J., D. Patel, and J. Raval, Formulation and evaluation of propranolol hydrochloride-loaded carbopol-934p/ethyl cellulose mucoadhesive microspheres. Iranian Journal of Pharmaceutical Research, 2010. 9(3): p. 221-232.

Patel, M.M. and A.F. Amin, Design and optimization of colon-targeted system of theophylline for chronotherapy of nocturnal asthma. Journal of Pharmaceutical Sciences, 2011. 100(5): p. 1760-1772.

Patel, M.M., et al., Mucin/poly(acrylic acid) interactions: A spectroscopic investigation of mucoadhesion. Biomacromolecules, 2003. 4(5): p. 1184-1190.

Patil, S.B. and K.K. Sawant, Development, optimization and in vitro evaluation of alginate mucoadhesive microspheres of carvedilol for nasal delivery. Journal of Microencapsulation, 2009. 26(5): p. 432-443.

Peppas, N.A., K.M. Wood, and J.O. Blanchette, Hydrogels for oral delivery of therapeutic proteins. Expert Opinion on Biological Therapy, 2004. 4(6): p. 881-887.

Pereira, R.R.D. and M.L. Bruschi, Vaginal mucoadhesive drug delivery systems. Drug Development and Industrial Pharmacy, 2012. 38(6): p. 643-652.

Perlman, M.E., et al., Development of a self-emulsifying formulation that reduces the food effect for torcetrapib. International Journal of Pharmaceutics, 2008. 351(1-2): p. 15-22.

Piao, J., et al., Development of novel mucoadhesive pellets of metformin hydrochloride. Archives of Pharmacal Research, 2009. 32(3): p. 391-397.

Podczeck, F., et al., The influence of non-disintegrating tablet dimensions and density on their gastric emptying in fasted volunteers. Journal of Pharmacy and Pharmacology, 2007. 59(1): p. 23-27.

Poggi, G., et al., Transhepatic arterial chemoembolization with oxaliplatin-eluting microspheres (oem-tace) for unresectable hepatic tumors. Anticancer Research, 2008. 28(6B): p. 3835-3842.

Prieto, S.A., J.B. Mendez, and F.J.O. Espinar, Starch-dextrin mixtures as base excipients for extrusion-spheronization pellets. European Journal of Pharmaceutics and Biopharmaceutics, 2005. 59(3): p. 511-521.

Prior, S., et al., In vitro phagocytosis and monocyte-macrophage activation with poly(lactide) and poly(lactide-co-glycolide) microspheres. European Journal of Pharmaceutical Sciences, 2002. 15(2): p. 197-207.

Pund, S., et al., Gastroretentive delivery of rifampicin: In vitro mucoadhesion and *in vivo* gamma scintigraphy. International Journal of Pharmaceutics, 2011. 411(1-2): p. 106-112.

Rabiskova, M., et al., Microcrystalline cellulose in oral dosage forms. Chemicke Listy, 2007. 101(1): p. 70-77.

Rajapaksa, T.E., et al., Claudin 4-targeted protein incorporated into PLGA nanoparticles can mediate M cell targeted delivery. Journal of Controlled Release, 2010. 142(2): p. 196-205.
Ren, J.M., et al., PELA microspheres loaded H-pylori lysates and their mucosal immune response. World Journal of Gastroenterology, 2002. 8(6): p. 1098-1102.
Rogers, T.L., et al., Development and characterization of a scalable controlled precipitation process to enhance the dissolution of poorly water-soluble drugs. Pharmaceutical Research, 2004. 21(11): p. 2048-2057.
Rubinstein, A. and B. Tirosh, Mucus gel thickness and turnover in the gastrointestinal-tract of the rat - response to cholinergic stimulus and implication for mucoadhesion. Pharmaceutical Research, 1994. 11(6): p. 794-799.
Ryan, E.J., L.M. Daly, and K.H.G. Mills, Immunomodulators and delivery systems for vaccination by mucosal routes. Trends in Biotechnology, 2001. 19(8): p. 293-304.
Sahasathian, T., N. Praphairaksit, and N. Muangsin, Mucoadhesive and floating chitosan-coated alginate beads for the controlled gastric release of Amoxicillin. Archives of Pharmacal Research, 2010. 33(6): p. 889-899.
Sajeesh, S. and C.P. Sharma, Mucoadhesive hydrogel microparticles based on poly (methacrylic acid-vinyl pyrrolidone)-chitosan for oral drug delivery. Drug Delivery, 2011. 18(4): p. 227-235.
Salamat-Miller, N. and T.P. Johnston, Current strategies used to enhance the paracellular transport of therapeutic polypeptides across the intestinal epithelium. International Journal of Pharmaceutics, 2005. 294(1-2): p. 201-216.
Sandri, G., et al., The role of chitosan as a mucoadhesive agent in mucosal drug delivery. Journal of Drug Delivery Science and Technology, 2012. 22(4): p. 275-284.
Santos, C.A., et al., Correlation of two bioadhesion assays: the everted sac technique and the CAHN microbalance. Journal of Controlled Release, 1999. 61(1-2): p. 113-122.
Santos, C.A., et al., Evaluation of anhydride oligomers within polymer microsphere blends and their impact on bioadhesion and drug delivery in vitro. Biomaterials, 2003. 24(20): p. 3571-3583.
Sarti, F., et al., *In vivo* evidence of oral vaccination with PLGA nanoparticles containing the immunostimulant monophosphoryl lipid A. Biomaterials, 2011. 32(16): p. 4052-4057.
Satishbabu, B.K. and B.P. Srinivasan, Preparation and evaluation of buccoadhesive films of Atenolol. Indian Journal of Pharmaceutical Sciences, 2008. 70(2): p. 175-179.
Schultz-Cherry, S. and J.C. Jones, Influenza Vaccines: The good, the bad, and the eggs, in Advances in Virus Research, Vol 77, K. Maramorosch, A.J. Shatkin, and F.A. Murphy, Editors. 2010, Elsevier Academic Press Inc: San Diego. p. 63-84.
Schwarz, R., et al., Gastrointestinal transit times in mice and humans measured with Al-27 and F-19 nuclear magnetic resonance. Magnetic Resonance in Medicine, 2002. 48(2): p. 255-261.

Severino, P., et al., Biodegradable Synthetic Polymers: Raw-Materials and Production Methods of Microparticles for Drug Delivery and Controlled Release. Polimeros-Ciencia E Tecnologia, 2011. 21(4): p. 286-292.
Shalaby, W.S.W., Development of oral vaccines to stimulate mucosal and systemic immunity - barriers and novel strategies. Clinical Immunology and Immunopathology, 1995. 74(2): p. 127-134.
Shukla, A., B. Singh, and O.P. Katare, Significant systemic and mucosal immune response induced on oral delivery of diphtheria toxoid using nano-bilosomes. British Journal of Pharmacology, 2011. 164(2B): p. 820-827.
Singh, M., et al., Controlled release microparticles as a single dose hepatitis B vaccine: Evaluation of immunogenicity in mice. Vaccine, 1997. 15(5): p. 475-481.
Singh, P., et al., Cholera toxin B subunit conjugated bile salt stabilized vesicles (bilosomes) for oral immunization. International Journal of Pharmaceutics, 2004. 278(2): p. 379-390.
Smart, J.D., et al., The retention of C-14-labelled poly(acrylic acids) on gastric and oesophageal mucosa: an in vitro study. European Journal of Pharmaceutical Sciences, 2003. 20(1): p. 83-90.
Smart, J.D., I.W. Kellaway, and H.E.C. Worthington, An in vitro investigation of mucosa-adhesive materials for use in controlled drug delivery. Journal of Pharmacy and Pharmacology, 1984. 36(5): p. 295-299.
Smart, J.D., The basics and underlying mechanisms of mucoadhesion. Advanced Drug Delivery Reviews, 2005. 57(11): p. 1556-1568.
Smith, G.P., Filamentous fusion phage - novel expression vectors that display cloned antigens on the virion surface. Science, 1985. 228(4705): p. 1315-1317.
Song, H.T., et al., Preparation of the traditional Chinese medicine compound recipe heart-protecting musk pH-dependent gradient-release pellets. Drug Development and Industrial Pharmacy, 2002. 28(10): p. 1261-1273.
Spahn, T.W. and T. Kucharzik, Modulating the intestinal immune system: the role of lymphotoxin and GALT organs. Gut, 2004. 53(3): p. 456-465.
Stertman, L., E. Lundgren, and I. Sjoholm, Starch microparticles as a vaccine adjuvant: Only uptake in Peyer's patches decides the profile of the immune response. Vaccine, 2006. 24(17): p. 3661-3668.
Sugihara, H., et al., Effectiveness of submicronized chitosan-coated liposomes in oral absorption of indomethacin. Journal of Liposome Research, 2012. 22(1): p. 72-79.
Sugito, K., et al., Gastric-emptying rate of drug preparations .3. Effects of size of enteric micro-capsules with mean diameters ranging from 0.1 to 1.1 mm in man. Chemical & Pharmaceutical Bulletin, 1992. 40(12): p. 3343-3345.
Sunoqrot, S., et al., Temporal control over cellular targeting through hybridization of folate-targeted dendrimers and PEG-PLA nanoparticles. Biomacromolecules, 2012. 13(4): p. 1223-1230.
Swaminathan, J. and C. Ehrhardt, Liposomal delivery of proteins and peptides. Expert Opinion on Drug Delivery, 2012. 9(12): p. 1489-1503.

Tabata, Y., Y. Inoue, and Y. Ikada, Size effect on systemic and mucosal immune responses induced by oral administration of biodegradable microspheres. Vaccine, 1996. 14(17-18): p. 1677-1685.

Takahashi, E., et al., Oral clarithromycin enhances airway IgA immunity through induction of IgA class switching recombination and B-cell activating factor of the tumor necrosis factor family molecule on mucosal dendritic cells in mice infected with influenza A virus. Journal of Virology, 2012.

Takami, T. and Y. Murakami, Development of PEG-PLA/PLGA microparticles for pulmonary drug delivery prepared by a novel emulsification technique assisted with amphiphilic block copolymers. Colloids and Surfaces B-Biointerfaces, 2011. 87(2): p. 433-438.

Takeuchi, H., et al., Mucoadhesive properties of carbopol or chitosan-coated liposomes and their effectiveness in the oral administration of calcitonin to rats. Journal of Controlled Release, 2003. 86(2-3): p. 235-242.

Tamaddon, A.M., F. Hosseini-Shirazi, and H.R. Moghimi, Preparation of oligodeoxynucleotide encapsulated cationic liposomes and release study with models of cellular membranes. Daru-Journal of Pharmaceutical Sciences, 2007. 15(2): p. 61-70.

Tamburic, S. and D.Q.M. Craig, An investigation into the rheological, dielectric and mucoadhesive properties of poly(acrylic acid) gel systems. Journal of Controlled Release, 1995. 37(1-2): p. 59-68.

Tao, Y.Y., et al., Development of mucoadhesive microspheres of acyclovir with enhanced bioavailability. International Journal of Pharmaceutics, 2009. 378(1-2): p. 30-36.

Tawde, S.A., et al., Formulation and evaluation of oral microparticulate ovarian cancer vaccines. Vaccine, 2012. 30(38): p. 5675-5681.

Thirawong, N., et al., Mucoadhesive properties of various pectins on gastrointestinal mucosa: An in vitro evaluation using texture analyzer. European Journal of Pharmaceutics and Biopharmaceutics, 2007. 67(1): p. 132-140.

Torche, A.M., et al., *Ex vivo* and *in situ* PLGA microspheres uptake by pig ileal Peyer's patch segment. International Journal of Pharmaceutics, 2000. 201(1): p. 15-27.

Tsai, M.L., et al., The storage stability of chitosan/tripolyphosphate nanoparticles in a phosphate buffer. Carbohydrate Polymers, 2011. 84(2): p. 756-761.

Van der Lubben, I.M., et al., Chitosan microparticles for mucosal vaccination against diphtheria: oral and nasal efficacy studies in mice. Vaccine, 2003. 21(13-14): p. 1400-1408.

Varum, F.J.O., et al., An investigation into the role of mucus thickness on mucoadhesion in the gastrointestinal tract of pig. European Journal of Pharmaceutical Sciences, 2010. 40(4): p. 335-341.

Varum, F.J.O., et al., Mucoadhesion and the gastrointestinal tract. Critical Reviews in Therapeutic Drug Carrier Systems, 2008. 25(3): p. 207-258.

Varum, F.J.O., et al., Mucoadhesive platforms for targeted delivery to the colon. International Journal of Pharmaceutics, 2011. 420(1): p. 11-19.

Venkatesan, N. and S.P. Vyas, Polysaccharide coated liposomes for oral immunization - development and characterization. International Journal of Pharmaceutics, 2000. 203(1-2): p. 169-177.

Villalobos, R., P. Hernandez-Munoz, and A. Chiralt, Effect of surfactants on water sorption and barrier properties of hydroxypropyl methylcellulose films. Food Hydrocolloids, 2006. 20(4): p. 502-509.

Wang, D.A., et al., Liposomal oral DNA vaccine (mycobacterium DNA) elicits immune response. Vaccine, 2010. 28(18): p. 3134-3142.

Wang, Y., et al., Preparation and stability study of norfloxacin-loaded solid lipid nanoparticle suspensions. Colloids and Surfaces B-Biointerfaces, 2012. 98: p. 105-111.

Werle, M. and H. Takeuchi, Chitosan-aprotinin coated liposomes for oral peptide delivery: Development, characterisation and *in vivo* evaluation. International Journal of Pharmaceutics, 2009. 370(1-2): p. 26-32.

Wikingsson, L.D. and I. Sjoholm, Polyacryl starch microparticles as adjuvant in oral immunisation, inducing mucosal and systemic immune responses in mice. Vaccine, 2002. 20(27-28): p. 3355-3363.

Wu, J.C., et al., Activity, stability and enantioselectivity of lipase-coated microcrystals of inorganic salts in organic solvents. Biocatalysis and Biotransformation, 2009. 27(5-6): p. 283-289.

Yamamoto, M., D.W. Pascual, and H. Kiyono, M cell-targeted mucosal vaccine strategies, in Mucosal Vaccines: Modern Concepts, Strategies, and Challenges, P.A. Kozlowski, Editor. 2012, Springer-Verlag Berlin: Berlin. p. 39-52.

Yang, W., K.P. Johnston, and R.O. Williams, Comparison of bioavailability of amorphous versus crystalline itraconazole nanoparticles via pulmonary administration in rats. European Journal of Pharmaceutics and Biopharmaceutics, 2010. 75(1): p. 33-41.

Yeh, P.Y., H. Ellens, and P.L. Smith, Physiological considerations in the design of particulate dosage forms for oral vaccine delivery. Advanced Drug Delivery Reviews, 1998. 34(2-3): p. 123-133.

Yin, L.C., et al., Drug permeability and mucoadhesion properties of thiolated trimethyl chitosan nanoparticles in oral insulin delivery. Biomaterials, 2009. 30(29): p. 5691-5700.

Yoo, M.K., et al., Targeted delivery of chitosan nanoparticles to Peyer's patch using M cell-homing peptide selected by phage display technique. Biomaterials, 2010. 31(30): p. 7738-7747.

Yu, Z.S., K.P. Johnston, and R.O. Williams, Spray freezing into liquid versus spray-freeze drying: Influence of atomization on protein aggregation and biological activity. European Journal of Pharmaceutical Sciences, 2006. 27(1): p. 9-18.

Zhang, N., et al., Lectin-modified solid lipid nanoparticles as carriers for oral administration of insulin. International Journal of Pharmaceutics, 2006. 327(1-2): p. 153-159.

Zhang, Z., et al., The characteristics and mechanism of simvastatin loaded lipid nanoparticles to increase oral bioavailability in rats. Int J Pharm. 394(1-2): p. 147-53.

Zhou, F. and M.R. Neutra, Antigen delivery to mucosa-associated lymphoid tissues using liposomes as a carrier. Bioscience Reports, 2002. 22(2): p. 355-369.

Zhu, X., et al., A novel microsphere with a three-layer structure for duodenum-specific drug delivery. International Journal of Pharmaceutics, 2011. 413(1-2): p. 110-118.

Zimova, L., et al., The development and *in vivo* evaluation of a colon drug delivery system using human volunteers. Drug Delivery, 2012. 19(2): p. 81-89. 1. Ball, R., et al., Statistical, epidemiological, and risk-assessment approaches to evaluating safety of vaccines throughout the life cycle at the food and drug administration. Pediatrics, 2011. 127: p. S31-S38.

Zimova, L., et al., The development and *in vivo* evaluation of a colon drug delivery system using human volunteers. Drug Delivery, 2012. 19(2): p. 81-89.

Vita

Shih-Fan Jang was born on September 16, 1980 in Taipei, Taiwan to Mr. Syuan-Ming Jang and Mrs. Chien-Chih Yu. After completing his high school in Taipei at Taipei Municipal Chien Kuo High School (CKHS), he entered National Taiwan University (NTU) and received his professional degree in Biochemistry. During the following years he served as Second Lieutenant, in The Army of Republic of China, Taiwan (Oct. 2003 ~ May 2005). After that he worked as a research assistant in Dr. Wuh-Liang, Whu's lab, National Taiwan University Hospital, Taipei. During that year, he was focusing on the study of newborn metabolic diseases, such as PKU, and Pompe's disease. In fall 2006, he attended graduate school in College of Pharmacy at The University of Texas at Austin having Dr. Jason T. McConville as an advisor. During his graduate study, he has been a TA in several pharmacy related coursed for the Pharm. D. students, including Pharmacokinetics and Physical Chemistry for many years. He was also once a Graduate Research Assistant in the Drug Dynamics Institute, Therapeutex, (College of Pharmacy, University of Texas at Austin), and was specialized for analysis including: Rheometer, Dissolution station, Texture analyzer, and Particle seizer. In 2010, he took an internship at an Austin based pharmaceutical company, Enavail LLC for 4 months. As a graduate student he has authored 4 publications which have been submitted to and/or published in many leading journals, presented 6 abstracts describing his research at national.

Permanent address (or email): jangsf6916@utexas.edu

This dissertation was typed by the author.